LOS ANGELES PUBLIC LIBRARY

SCIENCE & TECHNOLOGY

NOV 30 1959

ARS JOURNAL

A PUBLICATION OF THE AMERICAN ROCKET SOCIETY

FORMERLY JET PROPULSION

BIND

SURVEY ARTICLE

Recent Advances in Ramjet Combustion . . . . . Gordon L. Dugger 819

CONTRIBUTED ARTICLES

Theory of Particle Combustion at High Pressures . . . . . D. B. Spalding 828

Vaporization of Propellants in Rocket Engines . . . . . Richard J. Priem and Marcus F. Heidmann 836

Composite Trajectories Yielding Maximum Coasting Apogee Velocity . . . . . Stanley Ross 843

Earth-Period (24-Hr) Satellites . . . . . J. H. Hutcheson 849

Dynamic Analysis of a Nuclear Rocket Engine System . . . . . Bernard R. Felix and Richard J. Bohl 853

TECHNICAL NOTES

Applicability of Euler's Dynamical Equations to Rocket Motion . . . . . James W. Ellis and Charles W. McArthur 863

Some Extensions of the Hohmann Transfer Maneuver . . . . . T. N. Edelbaum 864

Comparison of Minimum Energy Paths and Apogee Designation Paths . . . Wayne Tempelman 865

New Ion Source for Propulsion of Space Vehicles . . . . . C. D. Moak, H. E. Banta, J. W. Johnson and R. F. King 868

Solubility of Air, N_2 and O_2 in n-Propyl Nitrate . . . . . Adolph B. Amster and Joseph B. Levy 870

Magnetogasdynamic Flow Regimes . . . . . Ching-Shi Liu and Ali Bulent Cambel 871

DEPARTMENTS

Technical Comments 874 New Patents 882

Book Reviews 878 Technical Literature Digest 885

November 1959 Volume 29 Number 11

all you need

to store NITROGEN TETROXIDE

is a rocket

This liquid-fuel oxidizer needs no refrigeration, causes no freeze-ups

As an oxidizer for liquid fuels, Nitrogen Tetroxide has even more to recommend it than its high performance (99% of theoretical I_v, hypergolic at low altitude). The ease with which it can be stored and handled offers another major advantage.

N_2O_4 requires no refrigeration, no high-pressure vessels. It is noncorrosive, can be stored indefinitely in plain carbon steel tanks at the launching site or right in the rocket itself. And it's ready when it's needed—there are no freeze-ups in valves and motors with N_2O_4.

Availability: excellent. Allied is a major producer of Nitrogen Tetroxide, can ship immediately in cylinders or tank car lots. Allied also produces ammonia, ethylene oxide and methanol for the rocket industry. Write for technical or other information you desire on any of these products.

For specifications and local offices, see our insert in Chemical Materials Catalog, pages 435-442 and in Chemical Week Buyers Guide, pages 35-42.

BASIC TO AMERICA'S PROGRESS

Allied Chemical

NITROGEN DIVISION
Dept. NT 5 12 4, 40 Rector Street, New York 6, N. Y.

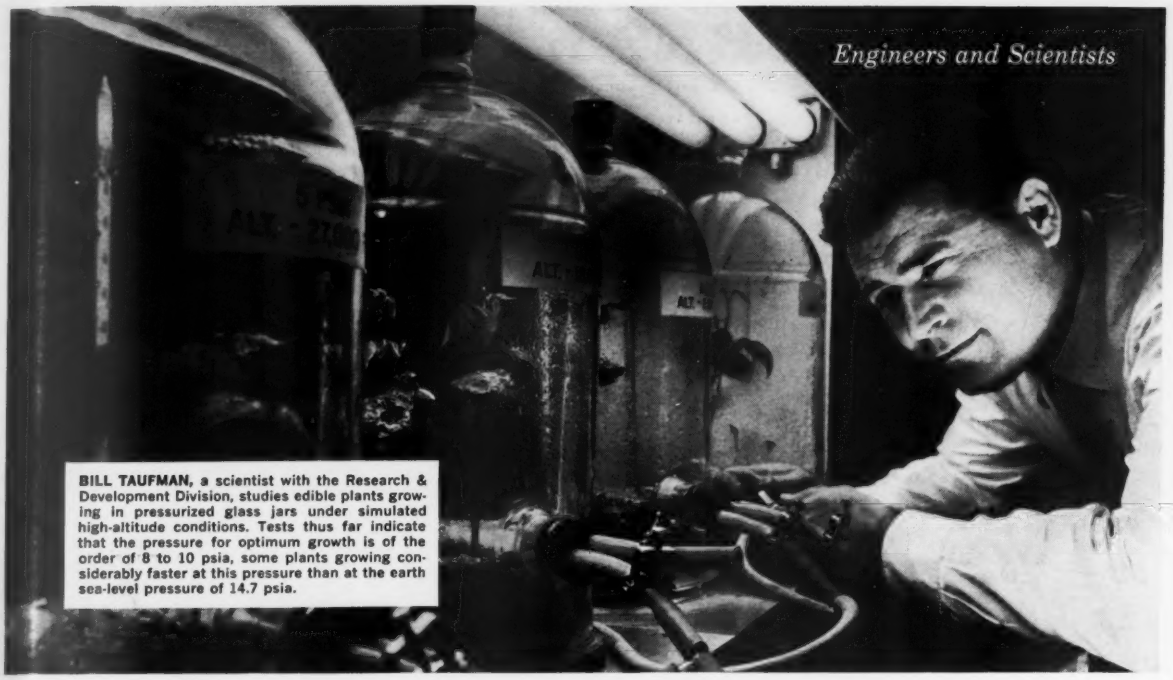

BILL TAUFMAN, a scientist with the Research & Development Division, studies edible plants growing in pressurized glass jars under simulated high-altitude conditions. Tests thus far indicate that the pressure for optimum growth is of the order of 8 to 10 psia, some plants growing considerably faster at this pressure than at the earth sea-level pressure of 14.7 psia.

HOTHOUSE ON THE MOON

Studies in low-pressure plant growth for lunar application... just one of the unique programs for engineers and scientists at REPUBLIC AVIATION

An example of the scope of Republic's investigations into every ramification of space exploration is a study to determine the lowest pressure level which will permit normal plant growth. The project is part of an Air Force program to judge the feasibility of a moon base. Another aspect of the study seeks to find the effect of zero gravity on plant growth. Although zero gravity cannot be created on the earth, the potential problems were indicated when plants subjected to negative g, or up-side-down growth, showed only one-half the development of normally grown plants.

Every facet of flight technology, from advanced aircraft design and space vehicle propulsion systems to computer-based trajectory studies for planetary reconnaissance probes, is being explored in Republic's Research and Development program. Distinguished advances have already been made in space guidance concepts, in plasma and nuclear propulsion systems, in radiation physics, in new materials and processing techniques, and in prototype development of hardware (as an example: hydraulic systems that operate reliably up to 1500F.)

These programs will be intensified with the completion – early next year – of Republic's new $14 million Research and Development Center. As the date draws near, staff expansion for these modern facilities is creating in-at-the-beginning career opportunities for senior engineers and scientists capable of sophisticated thinking in theoretical and experimental research. Republic invites qualified individuals to discuss how they can make material contributions to advancing the state of the art.

Opportunities In All Areas of Flight Technology

Electronics
Inertial Guidance & Navigation
Digital Computer Development
Systems Engineering
Information Theory
Telemetry-SSB Technique
Doppler Radar • Countermeasures
Radome & Antenna Design
Microwave Circuitry & Components
Receiver & Transmitter Design
Airborne Navigational Systems
Jamming & Anti-Jamming
Miniaturization — Transistorization
Ranging Systems • Propagation Studies
Ground Support Equipment
Infrared & Ultra-violet Techniques

Thermo, Aerodynamics
Theoretical Gasdynamics
Hyper-Velocity Studies
Astronautics Precision Trajectories
Airplane/Missile Performance
Air Load and Aeroelasticity
Stability and Controls
Flutter & Vibration
Vehicle Dynamics & System Designs
High Altitude Atmosphere Physics
Re-entry Heat Transfer
Hydromagnetics

Plasma Propulsion
Plasma Physics
Gaseous Electronics
Hypersonics and Shock Phenomena
Hydromagnetics
Physical Chemistry
Combustion and Detonation
Instrumentation
High Power Pulse Electronics

Nuclear Propulsion & Radiation Phenomena
Nuclear Weapons Effects
Radiation Environment in Space
Nuclear Power & Propulsion Applications
Nuclear Radiation Laboratories

Send resume in confidence to: Mr. George R. Hickman, Engineering Employment Mgr., Dept. 10L

REPUBLIC AVIATION

Farmingdale, Long Island, New York

ARS JOURNAL

A PUBLICATION OF THE AMERICAN ROCKET SOCIETY

FORMERLY JET PROPULSION

EDITOR — Martin Summerfield

ASSOCIATE TECHNICAL EDITOR — Irvin Glassman

MANAGING EDITOR — Barbara Nowak

ASSISTANT EDITOR — Julie Hight

ART EDITOR — John Culin

ASSOCIATE EDITORS

J. George Adashko, *Russian Supplement;* **Ali Bulent Cambel,** *Northwestern University, Book Reviews;* **Charles J. Mundo Jr.,** *American Bosch Arma Corporation, Electronics;* **M. H. Smith,** *Princeton University, Technical Literature Digest*

CONTRIBUTOR

George F. McLaughlin

ADVERTISING AND PROMOTION MANAGER

William Chenoweth

ADVERTISING PRODUCTION MANAGER

Walter Brunke

ADVERTISING REPRESENTATIVES

New York
D. C. Emery and Associates
400 Madison Ave., New York, N. Y.
Telephone: Plaza 9-7460

Los Angeles
James C. Galloway and Co.
6535 Wilshire Blvd., Los Angeles, Calif.
Telephone: Olive 3-3223

Chicago
Jim Summers and Associates
35 E. Wacker Dr., Chicago, Ill.
Telephone: Andover 3-1154

Detroit
R. F. Pickrell and Associates
318 Stephenson Bldg., Detroit, Mich.
Telephone: Trinity 1-0790

Boston
Robert G. Melendy
17 Maugus Ave., Wellesley Hills, Mass.
Telephone: Cedar 5-6503

Pittsburgh
John W. Foster
239 4th Ave., Pittsburgh, Pa.
Telephone: Atlantic 1-2977

American Rocket Society

500 Fifth Avenue, New York 36, N. Y.

Founded 1930

OFFICERS

President	John P. Stapp
Vice-President	Howard S. Seifert
Executive Secretary	James J. Harford
Treasurer	Robert M. Lawrence
Secretary and Asst. Treasurer	A. C. Slade
General Counsel	Andrew G. Haley
Director of Publications	Irwin Hersey

BOARD OF DIRECTORS

Terms expiring on dates indicated

James R. Dempsey	1961	Simon Ramo	1960
Alfred J. Eggers Jr.	1959	H. W. Ritchey	1959
Krafft Ehricke	1959	William L. Rogers	1959
Samuel K. Hoffman	1960	David G. Simons	1961
J. Preston Layton	1960	John L. Sloop	1961
A. K. Oppenheim	1961	Martin Summerfield	1959
William H. Pickering	1961	Wernher von Braun	1960
	Maurice J. Zucrow 1960		

TECHNICAL COMMITTEE CHAIRMEN

Lawrence S. Brown, Guidance and Navigation
Milton U. Clauser, Magnetohydrodynamics
Herbert L. Karsch, Logistics and Operations
William H. Dorrance, Hypersonics
Herbert Friedman, Instrumentation
George Gerard, Structures and Materials
Milton Greenberg, Physics of the Atmosphere and Space
Stanley V. Gunn, Nuclear Propulsion
Andrew G. Haley, Space Law and Sociology
Samuel Herrick, Astrodynamics
Maxwell W. Hunter, Missiles and Space Vehicles
David B. Langmuir, Ion and Plasma Propulsion
Y. C. Lee, Liquid Rockets
Max Lowy, Communications
Richard A. Schmidt, Test Facilities and Support Equipment
Paul E. Sandorff, Education
William B. Shippen, Ramjets
John L. Sloop, Propellants and Combustion
Ivan E. Tuhy, Solid Rockets
Stanley C. White, Human Factors and Bio-Astronautics
George F. Wislicenus, Underwater Propulsion
Abe M. Zarem, Power Systems

Scope of ARS JOURNAL

This Journal is devoted to the advancement of astronautics through the dissemination of original papers disclosing new scientific knowledge and basic applications of such knowledge. The sciences of astronautics are understood here to embrace selected aspects of jet and rocket propulsion, space flight mechanics, high-speed aerodynamics, flight guidance, space communications, atmospheric and outer space physics, materials and structures, human engineering, overall system analysis, and possibly certain other scientific areas. The selection of papers to be printed will be governed by the pertinence of the topic to the field of astronautics, by the current or probable future significance of the research, and by the importance of distributing the information to the members of the Society and to the profession at large.

Information for Authors

Manuscripts must be as brief as the proper presentation of the ideas will allow. Exclusion of dispensable material and conciseness of expression will influence the Editor's acceptance of a manuscript. In terms of standard-size double-spaced typed pages, a typical maximum length is 22 pages of text (including equations), 1 page of references, 1 page of abstract and 12 illustrations. Fewer illustrations permit more text, and vice versa. Greater length will be acceptable only in exceptional cases.

Short manuscripts, not more than one-quarter of the maximum length stated for full articles, may qualify for publication as Technical Notes or Technical Comments. They may be devoted to new developments requiring prompt disclosure or to comments on previously published papers. Such manuscripts are usually published within a few months of the date of receipt.

Sponsored manuscripts are published occasionally as an ARS service to the industry. A manuscript that does not qualify for publication, according to the above-stated requirements as to subject, scope or length, but which nevertheless deserves widespread distribution among jet propulsion engineers, may be printed as an extra part of the Journal or as a special supplement, if the author or his sponsor will reimburse the Society for actual publication costs. Estimates are available on request. Acknowledgment of such financial sponsorship appears as a footnote on the first page of the article. Publication is prompt since such papers are not in the ordinary backlog.

Manuscripts must be double spaced on one side of paper only with wide margins to allow for instructions to printer. Include a 100 to 200 word abstract. State the authors' positions and affiliations in a footnote on the first page. Equations and symbols may be handwritten or typewritten; clarity for the printer is essential. Greek letters and unusual symbols should be identified in the margin. If handwritten, distinguish between capital and lower case letters, and indicate subscripts and superscripts. References are to be grouped at the end of the manuscript and are to be given as follows: For journal articles: authors first, then title, journal, volume, year, page numbers; for books: authors first, then title, publisher, city, edition and page or chapter numbers. Line drawings must be clear and sharp to make clear engravings. Use black ink on white paper or tracing cloth. Lettering should be large enough to be legible after reduction. Photographs should be glossy prints, not matte or semi-matte. Each illustration must have a legend; legends should be listed in order on a separate sheet.

Manuscripts must be accompanied by written assurance as to security clearance in the event the subject matter lies in a classified area or if the paper originates under government sponsorship. Full responsibility rests with the author.

Submit manuscripts in duplicate (original plus first carbon, with two sets of illustrations) to the Editor, Martin Summerfield, Professor of Aeronautical Engineering, Princeton University, Princeton, N. J. Preprints of papers presented at ARS national meetings are automatically considered for publication.

ARS JOURNAL is published monthly by the American Rocket Society, Inc. and the American Interplanetary Society at 20th & Northampton Sts., Easton, Pa., U. S. A. Editorial offices: 500 Fifth Ave., New York 36, N. Y. Price: $12.50 per year, $2.00 per single copy. Second-class mail privileges authorized at Easton, Pa. This publication is authorized to be mailed at the special rates of postage prescribed by Section 132.122. Notice of change of address should be sent to the Secretary, ARS, at least 30 days prior to publication. Opinions expressed herein are the authors and do not necessarily reflect the views of the Editors or of the Society.

© Copyright 1959 by the American Rocket Society, Inc.

EXCELCO

Builders of more large, thin wall, high strength solid propellant rocket engine cases and nozzles for development purposes than any other company in America.

RV-A-10 SERGEANT
AIR FORCE—RE-ENTRY—X-17
POLARIS—RE-ENTRY—X-36
JUPITER JR. JUPITER SR.
POLARIS O POLARIS A
POLARIS A-1 POLARIS A-2
NIKE HERCULES NIKE ZEUS
MINUTEMAN PERSHING

AND MANY OTHER CLASSIFIED PROJECTS

A small experienced organization geared to handle your development and prototype requirements for static and flight tests in the shortest possible time.

Call or write

EXCELCO DEVELOPMENTS

MILL STREET • PHONE 101
SILVER CREEK, NEW YORK

The Log of the Navy's Polaris

1958 In January, just a year after the Navy had announced its pl for a Fleet Ballistic Missile, the first Polaris test vehicle was su cessfully fired. Firings continued throughout 1958. By Septemb the test vehicles were close to the final configuration of the Polari

1959 Operations Skycatch and Peashooter tested methods for ejecting the Polaris... Operations Pop-up and Fishhook tested a submerged launcher. In August, a Polaris test vehicle was launched from the deck of the USS Observation Island.

1960 The Polaris is scheduled for active duty in late 1960. Each of the Navy's nuclear subs will carry 16. Lockheed is prime contractor and missile system manager of a team that includes Aerojet-General, General Electric, and Westinghouse.

LOCKHEED

MISSILES AND SPACE DIVISION

MISSILE RESEARCH & DEVELOPMENT • BALLISTIC MISSILE SYSTEMS MANAGEMENT
ROCKETRY • ULTRASONIC AERODYNAMICS • SPACE INVESTIGATIONS • NUCLEAR PHYSICS
ADVANCED ELECTRONICS • HIGH-SPEED AUTOMATIC DATA REDUCTION
RAMJET PROPULSION TESTING

FROM LAGRANGIAN TO LIFT-OFF

Sometimes forgotten during the thundering ascent of a space probe rocket are months of meticulous analysis, engineering and planning. The staff of Space Technology Laboratories is now engaged in a broad program of space research for the Air Force, the National Aeronautics and Space Administration and the Advanced Research Projects Agency under the direction of the Air Force Ballistic Missile Division. For space probe projects STL provides the total concept approach, including preliminary analysis, sub-system development, design, fabrication, testing, launch operations and data evaluation. The total task requires subtle original analysis in many fields as well as sound technical management.

The STL technical staff brings to this space research the talents which have provided system engineering and technical direction since 1954 to the Air Force Ballistic Missile Program. Major missile systems currently in this program are Atlas, Titan, Thor and Minuteman.

The scope of STL's responsibilities offers creative engineers, physicists and mathematicians unusual opportunities to see their ideas tested in working hardware. Inquiries are invited regarding staff openings in the areas of Advanced Systems Analysis, Rocket Propulsion, Space Flight Mechanics, Dynamics, Structural Analysis, and Aerodynamics.

Space Technology Laboratories, Inc.

P. O. Box 95004, Los Angeles 45, California

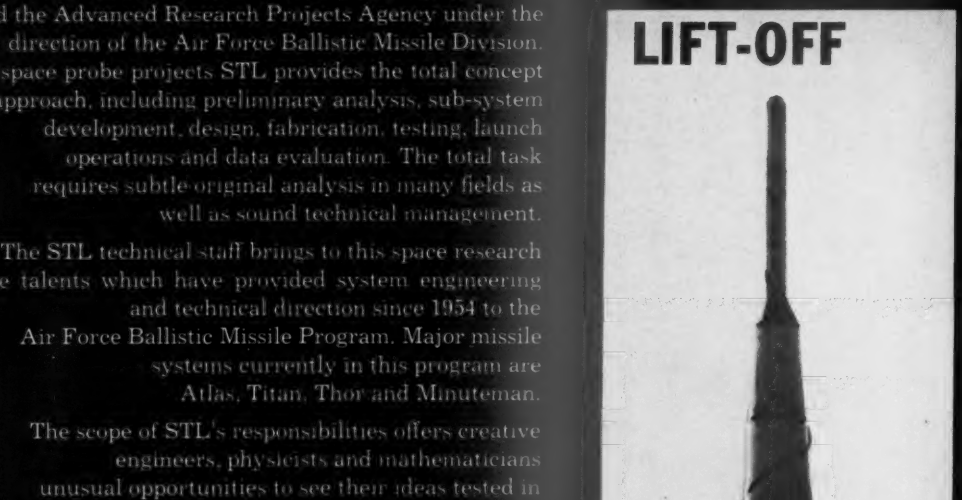

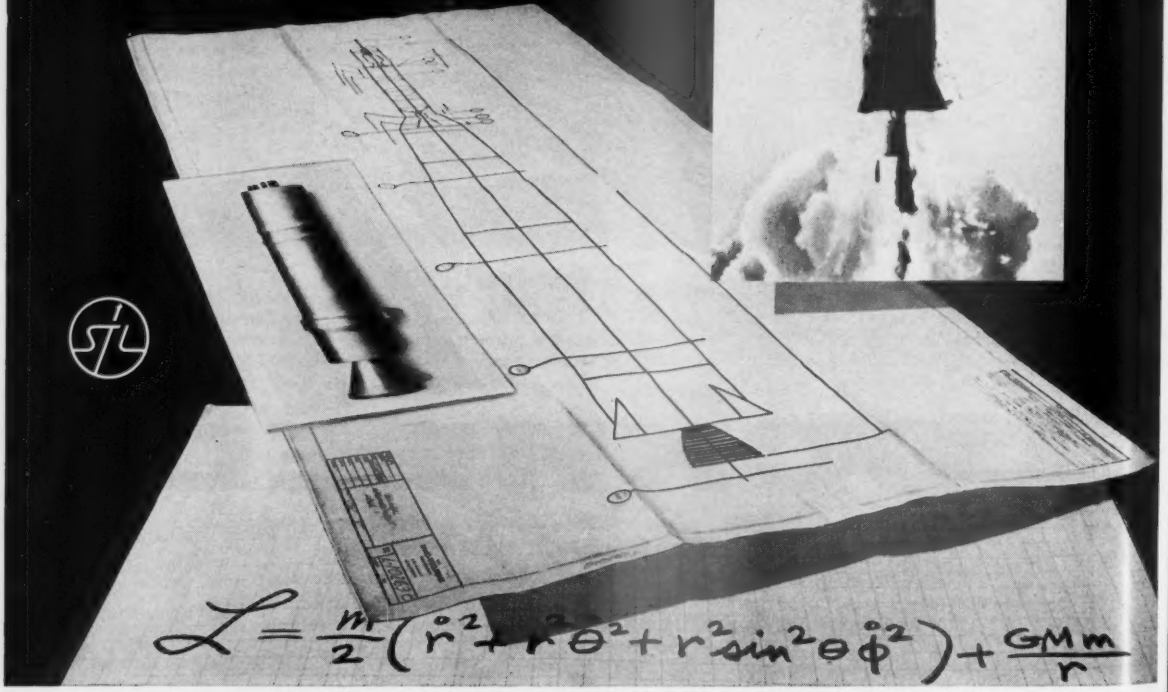

Recent Advances in Ramjet Combustion

GORDON L. DUGGER

The Johns Hopkins University
Silver Spring, Md.

The author is project supervisor for hydrocarbon combustor development and research on advanced ramjet engines at Applied Physics Laboratory. After receiving his B.Ch.E. and M.S.E degrees from the University of Florida, he joined the Lewis Laboratory in 1947. Most of his work there was related to fundamental combustion research and particularly to flame velocity and stability. This research resulted in numerous papers and his Ph.D. thesis in 1953 for Case Institute of Technology in chemical engineering. In 1954 Dr. Dugger joined the staff of the International Minerals and Chemical Corp. in Florida, where he worked until coming to APL in 1957.

ADVANCES in ramjet combustion or, more broadly, ramjet propulsion, are likely to have a considerable impact on our way of life in coming years. Today, ramjets are in use only in guided missiles, small helicopters and a few research airplanes. But the quest for speed in terrestrial transport has not ended with the recently introduced commercial jet transports or the Mach 2 military planes. Already the aircraft companies are looking forward to supersonic transports (1).[1] Predictions of hypersonic airbreathing aircraft appear frequently, e.g. (2,3), and ramjet propulsion will undoubtedly be used in such aircraft.

When one considers the time required for passengers to get to and from airports, or the time required to assemble and load and then unload and deploy military personnel and material, there appears to be no great advantage in reducing transport time below an hour or two. Such transport times—for intercontinental distances—are within the reach of airbreathing aircraft, but do call for speeds of Mach 3 and higher. A Mach 7 transport could make a nonstop flight of 6000 nautical miles in 2 hr. The ramjet engine would be at its best in this flight speed range. A slight extension of present technology indicates that the ramjet will reach its greatest overall efficiency somewhere in the range Mach 6 to Mach 8 (2,4). This means that direct operating costs for hypersonic aircraft using ramjets for high speed phases of flight will probably be no greater and may be smaller than those of the subsonic craft of today (3). Nuclear ramjets are currently under study and should have a place in a second generation of supersonic terrestrial transports. However, as long as our petroleum reserves hold up, the kerosene-fueled ramjet probably will be prevalent, and beyond that, it is likely that hydrogen or some other chemical fuel will be burned with air to supply the energy for supersonic and hypersonic ramjets.

Scope and Background

Interpreted literally, the title of this paper might be expected to restrict the following review and discussion to recent work directly applicable to current ramjet engines. However, a broader viewpoint is taken for the following reasons.

On the one hand, there have been no significant changes in the ramjet engineer's understanding and application of combustion principles in engine design in the last few years, but rather a general refinement and drawing together of loose ends in the scientist's picture of how combustible mixtures are prepared, how heat and mass are transferred in a flame, and how—more empirically here—flames are stabilized in high velocity (subsonic) streams. The basic concepts and engineering practice are much the same as they were a few years ago, and the actual design and production of a particular ramjet engine to fill a particular mission is still a matter of engineering judgment and compromise. Furthermore, design and combustion performance details on recently developed ramjet engines, such as those for the current and advanced versions of the surface-to-air missile Talos (developed by the Applied Physics Laboratory of the Johns Hopkins University for the U. S. Navy and produced by Bendix as prime contractor) and Bomarc (produced by Boeing for the U. S. Air Force, using Marquardt engines), fall within the realm of classified information, so that they cannot be specifically disclosed here.

On the other hand, many papers have appeared in recent years which are not related to current engines but do foretell future ramjet applications. Of particular interest are reports of successful experiments with stabilized detonation waves and with external combustion and theoretical papers which show the potential benefits of supersonic combustion for hypersonic airbreathing vehicles. In order to determine whether such unconventional combustion schemes promise advances in ramjet propulsion, the combustion process must be considered in context as part of a propulsion system. The scope of the present paper is therefore extended to include a review and discussion of experiments and analyses related to unconventional ramjet systems which are likely to find application in airbreathing vehicles within the next decade.

For those readers who have not followed the ramjet literature closely, some of the survey papers and documents which have appeared during recent years should be mentioned briefly as providing a background for subsequent sections of the present paper.

Avery (5) succinctly reviewed ramjet history and progress up to 1955 and described the basic operating principles, relative performance and advantages of ramjets to Mach 4, and current and foreseen applications of ramjets as of that date. He updated this picture and extended his considerations into the hypersonic regime in classified papers in 1958 and 1959 (unclassified titles listed as (6 and 7)). Hawthorne (8) wrote a well-referenced review of the aerodynamic problems of aircraft engines, which includes the aerodynamic aspects of combustion, in 1957. Morris (9) briefly outined the 1958 ramjet state-of-art. Emmons (10) reviewed the nature and problems of combustion as an aeronautical science. Brief general reviews of ramjet combustion, trends, fuel systems, diffusers

Received Oct. 2, 1959.

[1] Numbers in parentheses indicate References at end of paper.

and future prospects appeared in ASTRONAUTICS, April 1959 (11). Weber (4) discussed several unconventional ramjet concepts, including supersonic combustion, external burning, jet lift, fuel-rich operation, oxygen recombination and nuclear power.

Leduc (12), Daum (13), and Roy (14) have reviewed the notable French accomplishments in jet propulsion. Particularly interesting are their demonstrations of the use of ramjets in manned aircraft. Leduc's first ramjet powered airplane was completely designed in 1939! Its combustion chamber was huge, and its overall efficiency was quite low, but its little-acclaimed first flight in 1949 is likely to take on greater historial importance in future years when ramjets finally achieve their deserved place in powerplants for manned aircraft. The Daum paper covers in some detail the major design features and accomplishments of the Nord Griffon airplanes, which have so ably demonstrated the advantages of a combined turbojet-ramjet (or turboramjet) powerplant for supersonic aircraft. The combined engine consists of a turbojet in parallel with a ramjet, with a common inlet and with air flow division phased gradually from pure turbojet at takeoff to pure ramjet at Mach 2. The great advantage of paralleling the two engines between common inlet and exhaust lies in the way their air flow and thrust coefficient vs. Mach number characteristics complement each other at supersonic speeds; the ramjet's air flow and thrust coefficient increase as the turbojet's decrease, so that the combined thrust coefficient remains nearly constant at supersonic speeds. An important corollary advantage of this characteristic is that less geometry variation in inlet and exhaust is required for optimum performance of the combination than would be required for either alone. Thus an engine comprising a small, relatively inexpensive and easily serviced turbojet inside a lightweight ramjet can produce more thrust per pound with less sensitivity to flight speed and to angle of attack or yaw than can the best and most complicated turbojets. The speed limitation of a turboramjet will depend upon the thermal protection system provided for the "swallowed" turbojet; Mach 4 appears to be a very reasonable goal, and a Mach 5 turboramjet would appear to be more practical than the Mach 5 turbojets with afterburners which have been proposed (1). Roy (14) considers conventional ramjets to be practical to Mach 6 and is a proponent of the detonative ramjet.

Probert (15) and Jamison (16,17) presented fine reviews of British ramjet progress, ramjet applications in missiles, such as the Bloodhound, and expected future performance trends and applications. Jamison strongly supports the turboramjet for supersonic (around Mach 3) transport aircraft.

Among the books on combustion and jet propulsion, the following works may be cited. A 259-page report entitled "Basic Considerations in the Combustion of Hydrocarbon Fuels with Air" by the NACA Lewis staff (18), quite thoroughly covers that subject through 1955. Zucrow revised his text on jet propulsion with a two-volume series published in 1958 (19), and includes chapters on ramjets (20); both of these are good as introductory textbook references on ramjet engine principles, but neither presents much information on ramjet combustion nor seriously considers speeds beyond Mach 4. A Russian book on ramjets appeared in 1958 (21); although it quotes heavily from American work, it is an impressive volume, and its publication indicates their strong interest and technological capabilities in the field. A book on ramjet technology by the staff of the Applied Physics Laboratory and various contributors under the Bumblebee program is to be published in 1960 (22). The books resulting from the biannual Combustion Symposia, e.g., (23,24), contain many valuable papers on combustion, flames and flame stabilization which bear on ramjet combustion problems, as do the proceedings of the AGARD Combustion and Propulsion Panel Meetings, e.g., (25,26). Other valuable texts on combustion which have appeared in recent years or will appear shortly include (27) through (30).

Basic Information on and Interpretation of Combustion Processes

In the jet engines of today, heat addition is accomplished in the combustor by a number of overlapping physical and chemical steps, which might broadly be called atomization (and initial distribution) of fuel, vaporization of fuel, mixing of fuel and air, stabilization of flame through provision of recirculation zones from which hot, burned gas can pilot the main flame, flame spreading, mixing of hot gas with cooling air (if any), and reassociation of dissociatied species as the gas cools by expansion in a supersonic nozzle. As combustor inlet conditions change due to flight schedule, or combustor hardware is changed to best suit the requirements of a particular engine for a particular vehicle's mission or missions, the relative importance of the various steps listed above may shift. Breitwieser (11) gives a good overall exposition of the nature, interactions and changing roles of these processes in ramjet combustors, but a few specific references and comments are in order here.

The literature on atomization and evaporation and combustion of droplets and sprays is growing rapidly (see papers in (23) and reference lists therein). Weiss and Worsham's (31) results on atomization in high velocity streams show that for simple tubes or pressure-atomizing nozzles the *relative* velocity between fuel and air has an overwhelming effect on drop size, which masks lesser effects of nozzle size, injection pressure and air stream density. Most fuel injectors are oriented contrastream for this reason. Air-atomizing nozzles are more effective than simple tubes or pressure types, but at relative velocities approaching 1000 fps any nozzle will produce a mean drop diameter of less than 20 μ (petroleum wax at 300 F). Agoston et al. (32) and others (33) show that data on the evaporation of drops are usually correlated by semi-empirical equations, of the type introduced by Frössling, as follows.

For evaporation with relative gas motion in the absence of combustion or large temperature differences, diffusion controls the rate

$$\frac{dm}{dt} = C_1 \frac{dD^2}{dt} = -C_2(1 + 0.3\ Re^{1/2}Sc^{1/3})$$

Foster and Ingebo (34) found that when temperature difference between drop and air was large, spray evaporation rate varied with $\Delta T^{0.28}$.

For the evaporation of burning droplets (or droplet burning rate), heat transfer controls the rate, and the above equation is altered simply by the replacement of $Sc^{1/3}$ by $Pr^{1/3}$. Bolt and Saad (35) measured burning rates of freely falling drops of hydrocarbon at 1500 F and found that most of the heat transfer required for evaporation had to come from conduction and convection rather than radiation. Since both evaporation ahead of the burning region and droplet burning occur in ramjets, and these are mixed up with fuel-air mixing by turbulent transport as well as by molecular (diffusional) transport, the picture is indeed a complicated one.

The physical picture of the flame stabilization process has been delineated rather clearly in recent years. There is general agreement that recirculation zones are established; in "baffle" combustors, these zones are in the wakes behind the baffles, whereas in "can" combustors, they fall behind the metal which separates the air (or mixture) admission holes. The wake behind a baffle is somewhat wider than the baffle and several times as long. Hot, nearly completely burned gases (average wake temperature is about 90 per cent of adiabatic flame temperature (36)), recirculate in regular eddies, which are parallel to the burned gas at the wake boundary and opposite in direction in the wake core. Turbulent transfer of heat and mass occurs between fresh gas and wake at the boundary. The critical parameter for flame stabilization can usually be explained in terms of reaction kinetics of approximately second order. See (36) in light of (37), or (38).

The ignition delay concept of flame stabilization proposed by Marble and Zukoski (36) may be expressed quite simply: If the fresh gas, moving at velocity V_2 past the transfer region at the boundary, does not reach its effective ignition temperature by the time it reaches the end of the recirculation zone of length L, then the main body of the flame will blow out

$$\tau V_2/L > 1, \text{ flame stable}$$

$$\tau V_2/L \leq 1, \text{ flame blows out}$$

The delay time τ required to reach the effective ignition temperature is a chemical factor which is a function only of chemical properties of the mixture, i.e., varies with fuel type, oxygen concentration and fuel-air equivalence ratio; has Arrhenius-type temperature dependence and varies inversely with pressure (37,39). The ignition delay concept can be used to predict lean screech limits (large amplitude, stable transverse oscillations) in combustion ducts (36); it is found that $\tau a/h$ is constant in a given system, where a is acoustic velocity and h is transverse duct dimension. The wake length and the relationship between V_2 and approach velocity V_1 are characteristic of a given flameholder-duct system. Wright (40) finds that for flat-plate flameholders

$$(V_1)_{bo} = \left(\frac{V_1}{V_2}\right)\left(\frac{L}{d}\right)\left(\frac{d}{h}\right)\left(\frac{h}{\tau}\right) \simeq \left(\frac{\sqrt{d/h}}{C_1 + C_2\, d/h}\right)\left(\frac{h}{\tau}\right)$$

where h is duct height and d is flameholder width. This formula predicts that maximum blowoff velocity will be found for $d/h = C_1/C_2 = 0.35$ for flat plates or 0.56 for cylinders.

Weiss, Rohrer and Longwell (38) present evidence that reaction rate is the controlling factor, based on an excellent correlation of lean blowout equivalence ratios for various fuels and flameholders with those for spherical reactor blowout at a loading factor equal to that for lean blowout of isooctane with the same flameholders. (They did not find as good correlation with an ignition delay criterion using Mullins' data (37) or with a laminar flame velocity criterion based on Spalding's (41) proposal that $V_{bo} \sim dpU_f^2$.) The spherical reactor experiment was invented by Longwell (42) following papers by Longwell et al. (43) and Avery and Hart (44) describing flame stabilization and combustor heat release rates for cases limited by chemical kinetics of near homogeneous reacting mixtures. Most of the results indicate overall or "global" reaction kinetics of approximately 1.8 order, so that for a given fuel and temperature the loading factor, in terms of air weight flow rate divided by reactor volume and by pressure to the 1.8 power, is a function of fuel-air ratio. For hydrocarbons, a "global activation energy" of 42 to 45 kcal/g-mole is indicated (45). Other interesting results (46) from spherical reactors support the premise that reaction rate controls, but suggest that the pressure exponent may vary with fuel type or with feed injection momentum (mixing effects are not completely eliminated). Williams (47) points out that Khramtsov's (48) turbulent flame results show that the feed rate per unit volume of turbulent flame zone is also proportional to $p^{1.8}$.

Weiss et al. (38) also studied the effect of heat loss from the recirculation zone to the wall of a rectangular can-type combustor on blowout loading factor for the combustor. In one case an independently variable, annular cooling air flow surrounded a metal can; in the other, the can walls were made of insulating firebrick. In the metal can, heat losses averaged 20 per cent of the heat liberation rate; in the latter, only 6 per cent. Such a decrease in heat loss (14 per cent difference) would be expected to reduce blowout loading factor for a given fuel-air ratio by a factor of 4, but the observed factor was only 2. The authors concluded that in a jet engine application it would be better to make use of available space to increase recirculation zone volume rather than to insulate a smaller recirculation zone volume.

Hottel et al. (49) have studied rod-stabilized flames in volatile fuel sprays with the flameholder wetted to varying degrees by fuel. For wetted flameholders, part of the fuel in the recirculation zone comes from vaporization of the fuel on the flameholder, so that heat transfer between the recirculation zone and the wetted flameholder plays an important part in the establishment of stability limits.

Various studies of the propagation of confined (stabilized inside ducts) and unconfined (above Bunsen burners) turbulent flames through prevaporized, premixed gases have shed considerable light on the part of laminar flame velocity (most turbulent flame velocity correlations involve U_f), intensity of approach stream turbulence (50,51), shear regions between burned and unburned gases and flame generated turbulence (51,52,53), pressure (48) and temperature effects (related to temperature effects on laminar flame velocity and approach stream Reynolds number (18)), and acoustic disturbances (53). Blackshear's tests (53) indicated that significant increases in turbulent flame velocity could be obtained with the introduction of transverse velocity gradients by means of "benign" acoustic disturbances (92 db, serious damage to hardware occurs at 200 db). This corresponds to the frequent observation that combustion efficiency goes up when a ramjet "screeches." Blackshear suggested that improvements in engine combustion efficiency might result from putting whistles on the flameholders or making the combustor wall wavy.

Basic information on heat and mass transfer in flames and on transport properties at high temperatures is still of importance in ramjet combustion because turbulent flame velocity—or flame spreading rate in a combustor—is related to laminar flame velocity (or at least to the way in which fresh mixture is burned at a local interface or in a pocket or an eddy) and to the more basic thermal and molecular diffusion rates as well as the momentum transfer rate. Fristrom and Westenberg (54) have done some excellent work in unraveling the mysteries of laminar flame front structure. From recent measurements on a low pressure methane-oxygen flame, Fristrom et al. (55) hope to get at the high temperature reaction kinetics. Such experimental information on reaction kinetics at flame temperatures would permit a much more accurate assessment of the problem of dissociation in combustion chambers and degree of recombination to be expected in supersonic nozzles, which is of major importance to ramjet (or rocket) thrust obtained with the high combustion temperatures associated with hypersonic flight. However, the reaction rates could not be determined from flame front structure experiments without knowledge of transport properties at high temperatures; the work of Walker and Westenberg (56) makes a valuable contribution to this field. Transport properties may also be important in detonations (57).

Advantages and Disadvantages of Higher Temperatures

The variable which has the greatest impact on both the ramjet heat addition process and the overall ramjet design is temperature. The inlet air temperature to a conventional ramjet combustor is some large fraction of the inlet total temperature, which is a function of ambient temperature, flight Mach number and effective specific heat ratio

$$T_{ac} \approx 0.95\, T_{t_\infty}$$

$$T_{t_\infty} \approx T_\infty \left(1 + \frac{\bar{\gamma} - 1}{2} M_\infty^2\right)$$

The combustor inlet air temperature which might be encountered by a typical engine on a typical flight program is illustrated by curve A in Fig. 1. The external skin temperature for the same aircraft, for areas 1 ft or more from leading edges, might follow curve B. For a ramjet burning kerosene, the temperature of the combustion products might fall between curves C and C′, depending on whether the engine follows a

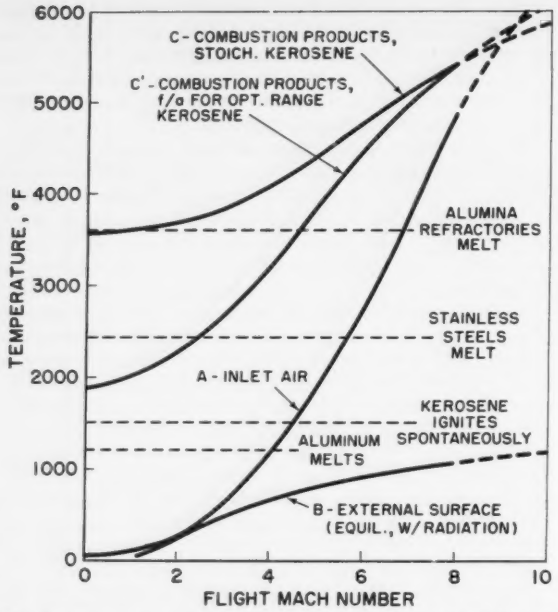

Fig. 1 Temperatures which may be typical in ramjet engines at supersonic and hypersonic speeds. (Altitude assumed to increase with Mach number to maintain constant free stream dynamic pressure of 350 pfsa)

maximum thrust fuel schedule (near stoichiometric fuel-air ratio) or a maximum range fuel schedule (optimized for minimum specific fuel consumption; fuel-air ratio increases with speed until stoichiometric is reached near Mach 7).[2] Approximate melting points of a few structural materials are shown for reference.

Let us consider first the trends in conventional ramjet combustor design brought about by the increasing inlet air temperature with flight speed. The ramjets (and turbojets) in use today operate at speeds below Mach 3 and encounter combustor inlet air temperatures in the range 200 to 800 F. In order to obtain high combustion efficiency, the fuel must be injected some distance upstream of the flameholding point to allow time for vaporization and mixing, and a sheltered region must be provided for flameholding, as discussed in the previous section. Such flameholders have appreciable drag (see for example, Wright's results (40), which are quite conservative with respect to full-scale engine practice). Flame spreading rates are moderate, so that a tailpipe length of 2 to 4 ft must be provided between flameholder and exhaust nozzle.

Engines now under development for speeds of Mach 3 to 5 are entering the spontaneous ignition regime. The flameholder can be moved closer to the fuel injector, because vaporization rates are considerably higher. Less blockage or burner drag is required to achieve the same flame stability, and less tailpipe length is required for efficient combustion, because both blowoff velocity and flame spreading rate increase as power functions of inlet temperature. The maximum space heating rate for a lean hydrocarbon-air mixture in a well-stirred reactor increases by an order of magnitude when the inlet temperature is doubled (45).

Some possibilities for the virtual elimination of burner hardware drag in higher speed ramjets are seen in aerodynamic flameholding and flame spreading techniques and recessed geometry experiments. Various experiments have shown that flames in small ducts can be stabilized by opposed jets (58) or transverse fluid sheets (59), even at mild inlet temperatures, and it has been shown that stabilization still occurs through the formation of recirculation zones. Bertin and Salmon (60) described "aerodynamic combustion" studies culminated by flying-test-bed tests in a full-scale turbojet afterburner (45 per cent thrust augmentation on 6600-lb thrust turbojet). Their basic concept is to speed up the flame spreading process by using transverse air jets within the recirculation zone behind a gutter-type flameholder; the air jets force the rapid turbulent spreading of active centers from the recirculation zone into the fresh mixture. (In the full-scale tests, they also injected a small fraction of the total fuel behind the gutter.) Their preliminary tests in a 7-in. pipe had shown that tailpipe length required to produce 85 per cent combustion efficiency could be cut in half by bleeding $2\frac{1}{2}$ per cent of the inlet air through the jet flame spreader. Such aerodynamic flameholders and/or flame spreaders may find use in higher speed ramjets, because stabilization and rapid flame spreading will require only very small (if any) piloting or recirculation zones. Fluid jets or sheets could issue from the burner walls, from an otherwise required streamlined centerbody, such as a diffuser plug, or from the vicinity of smaller than usual flameholders. Or, the flame could be stabilized by the recessed geometry technique (61), in which a recirculation zone is established in a cavity in the engine wall (e.g., at the base of the ramjet diffuser centerbody) rather than by placing an otherwise unnecessary drag-producing obstruction in the main stream.

However, the simplification of the conventional ramjet combustor hardware requirements from the performance standpoint will be compromised by two major problems as flight speeds enter the hypersonic regime, say, speeds above Mach 5. One problem is the problem of containing the high temperature gases without seriously compromising engine weight or performance, and the other is the loss in temperature rise attainable in the combustion chamber. In current ramjets, the tailpipe and exhaust nozzle are often protected by passing a film of the relatively cool combustor inlet air between the tailpipe and an interior metal liner or "cooling shroud." At hypersonic flight speeds this will no longer be feasible, because the temperature of the combustor inlet air will be too high. Some small gains can be made by internal insulation of the tailpipe and nozzle with ceramics (62), or by the use of "refractory metals," such as molybdenum or columbium alloys, but it is obvious that elaborate, forced cooling systems would soon be required. Further discussion of the structural problems associated with hypersonic conventional ramjets is beyond the scope of this paper, but unconventional combustion systems which will relieve this problem are discussed in later sections.

The effect of flight speed on the temperature rise due to combustion is seen by comparing either curve C or C′ with curve A in Fig. 1. As the flight speed and inlet air temperature increase, less temperature rise is obtained for a given energy addition, because more and more of the energy is being absorbed by dissociation of the combustion products. That is, the static enthalpy of the "burned" gas represents a larger fraction of the stagnation enthalpy, so that there is a smaller conversion of potential chemical energy to kinetic energy *in the combustor*. As noted previously, part of the dissociation energy will be recovered in the exit nozzle. Moreover, even if there were no further change in the chemical composition of the burned gas leaving the combustor, part of the energy absorbed by dissociation would still be useful, because for the partially dissociated gas both the specific heat ratio and the molecular weight are lower, and a reduction in either of these increases air specific impulse and exit stream thrust obtained with a given burned gas temperature. Nevertheless, the loss in engine thrust due to dissociation will be felt more and more as flight speed increases in the hypersonic range.

[2] Both the stoichiometric curve C and the minimum SFC curve C′ are estimated for an aircraft following a moderate, constant dynamic pressure trajectory of $q_\infty = 350$ psfa, with a diffuser kinetic energy efficiency of 0.94, giving combustion chamber pressures of the order of 1 to 10 atm.

Ways to Circumvent the Effect of T_{t_∞} on ΔT_t

The reduction in combustor temperature rise with increased flight speed can be mitigated by using fuels which form stable products of combustion, for example, fuels containing metals which form stable oxides not subject to dissociation. A further gain will be made if the stable products appear in a condensed phase, that is, as small droplets or fine powderlike particles, so that an exothermic phase change releases more heat in the combustor; again, oxides of metals provide examples. Another type of tailored fuel would be one which would dissociate or react to give a burned gas of lower molecular weight and hence higher specific thrust for a given temperature rise.

On the subject of fuels which form metallic oxides, Olson and Setze (63) discuss the advantages and problems of the use of high energy fuels (borohydrides or organoborohydrides) and fuels containing magnesium or aluminum. The high energy fuels have higher heats of combustion and higher flame temperatures than hydrocarbon fuels. This means that for a given thrust level, a lower fuel-air ratio is required, so that for a given fuel weight, the aircraft using high energy fuel will have a considerably greater range. The familiar Breguet range equation may be written (for moderate speeds)

$$R = h_c \eta_e \frac{L}{D} \ln \left[\frac{1}{1 - (W_f/W_g)} \right]$$

where

h_c = heat of combustion of the fuel
η_e = overall engine efficiency
L/D = lift to drag ratio
W_f = weight of fuel consumed in cruise
W_g = gross weight at beginning of cruise

It is seen that h_c first enters directly, but, even more important for very long ranges, the lower fuel consumption rate permitted with higher h_c keeps the gross weight from increasing as quickly; that is, it puts a restraining leash on "longer range means more fuel means more structure means more fuel, etc." An example for aircraft carrying 45,000-lb useful payloads is cited: For 6000-mile range the plane using kerosene (JP-4) would weigh 450,000 lb compared to 212,000 lb for a similar but smaller plane using a high energy fuel with a 40 per cent higher h_c.

Aside from the heat of combustion advantage, the borohydride fuels are attractive due to their very high flame velocities and very wide stability limits. The maximum laminar flame velocity of pentaborane is 22 fps, compared to 9 fps for hydrogen measured by the same method at the same conditions (64), and less than 2 fps for propane. As noted in an earlier section, flame spreading rate is related to laminar flame velocity U_f, and space heating rate (loading factor) is roughly correlated with U_f^2; it becomes apparent then that much smaller recirculation zones are required for flame stabilization with the borohydride fuel, and that good combustion efficiencies could be achieved in much shorter combustion chambers. Berl and Renich (65) review the available unclassified information on the combustion of boron hydrides through July 1958. Breisacher et al. (66) report studies on the structure of laminar flames of borohydrides and borohydride-hydrocarbon mixtures. In the flames of the borohydride-hydrocarbon mixed fuels, the borohydride is always oxidized first; the hydrocarbon may only be cracked and partially oxidized if the borohydride flame is lean, or it may burn in a second luminous reaction zone following a hotter (nearer stoichiometric) borohydride reaction zone. The wide flammability limits and low ignition temperatures of these fuels—as well as of metal alkyls, such as aluminum trimethyl, boron triethyl, etc. (67, 68), and mixed metal hydrides, such as aluminum borohydride (68)—suggest that they could also be used as igniter or piloting fuels to widen the operating limits of jet engines using a hydrocarbon fuel as the primary energy source. (External combustion of such fuels in supersonic air streams is discussed later.) However, these same combustion properties, plus toxicity, are disadvantages from the safety standpoint.

It should be pointed out that the heat of condensation of B_2O_3 usually represents a large part of the heat of combustion advantage of a borohydride fuel over a hydrocarbon fuel. This means that if temperatures are too high to obtain the condensed phase in the combustor, one must again rely on the lower temperatures in the supersonic nozzle to bring about the condensation before the vapor leaves the region in which it can influence the pressure field of the engine. If condensation does not occur within the pressure field of the engine, as much as two thirds of the high energy fuel's heat advantage may be lost, depending on its boron and hydrogen contents (63). Of course, condensation offers problems too; if B_2O_3 condenses on relatively cool engine hardware, it forms unwanted deposits. If particle size is too large, the heat of condensation may not be effectively transferred to the gas. Olson and Setze (63) described studies of particle growth and deposition.

The metals magnesium and aluminum do not have high heats of combustion, but due to their high densities (compared to liquids) and high stoichiometric fuel-air ratios, they do look attractive on the basis of short range, high thrust applications, because they can add a lot of heat per pound of inlet air. For this reason, the burning properties of the metals, and particularly the properties of slurries of magnesium in JP-4 fuel, have been studied (63). A 50 per cent slurry of fine Mg particles (1μ) in JP-4 gave a combustion efficiency one third higher (0.8^+ vs. 0.6) than JP-4 alone in a 19-in. long tailpipe.

As noted above, at high flight speeds and high combustion temperatures, the products of "combustion" of hydrocarbon fuels will be highly dissociated in the combustion chamber and must recombine in the exit nozzle if all of the potential chemical energy is to be converted to kinetic energy; this also applies to condensation of metallic oxides in the case of high energy fuels. Little is known about high temperature kinetics and recombination rates, even at fixed conditions; in supersonic nozzles the problem is compounded by rapid changes in pressure, temperature and velocity, which in turn depend both on the changing properties (γ and molecular weight) of the gas mixture and on the design of the nozzle. Unfortunately, pressure decreases much more rapidly than temperature, and velocity is increasing at the same time. When more is learned about the kinetics, it may be possible to tailor the nozzle (perhaps by adding more slowly diverging sections at points where favorable changes would occur) to obtain higher efficiency. Meanwhile, some very interesting work is noted in which the situation has been turned around—a diverging reactor, or supersonic nozzle, may be used to determine the kinetics of a simple reaction—work such as Wegener (69) has done for $2\ NO_2 \rightleftarrows N_2O_4$.

Use of Unconventional Engines for Hypersonic Speeds

An interesting proposal for a ramjet capable of flight speeds from supersonic all the way to Mach 18 or 20 has been advanced by Breitwieser and Morris (see (4)). Their proposed "fuel-rich ramjet," is not limited to stoichiometric fuel flows, but is deliberately operated at higher and higher equivalence ratios as flight speed increases. Although fuel specific impulse falls rapidly as equivalence ratio is increased, it remains higher than rocket specific impulses, and an adequate accelerative thrust margin is provided to speeds of the order of Mach 20. Advantages cited for such a system are:

1 Rich operation means lower burned gas temperatures and less dissociation.

2 Varying fuel rate can be used to match inlet and exit flows in a simple fixed geometry system.

3 The large fuel flows can be used for cooling the engine and possibly the airframe as well.

Another approach to higher propulsive efficiencies at very

high speeds is to diffuse the inlet air only to some moderate supersonic velocity before adding the heat (2,4,70). Such an engine might be called a supersonic combustion ramjet or SCRJ (Fig. 2). Heat addition to a supersonic stream results in a decrease in Mach number. The ideal supersonic engine performance would be obtained by adding just enough heat to reduce the Mach number to unity and then expanding the gas supersonically without ever taking a strong shock loss. In other words, the desired heat addition level would determine the desired combustor inlet Mach number. For any given heat addition level at any given flight speed, the highest static temperature reached in the supersonic combustion engine would be 10 to 12 per cent lower than that obtained with the same heat addition in subsonic flow. This 10 to 12 per cent reduction in static temperature is very important insofar as reducing dissociation is concerned. The higher total pressure loss due to fuel-air mixing and heat addition in supersonic rather than subsonic flow would be compensated (to some degree dependent on M_∞) by a lower total pressure loss in the diffuser. Analyses suggest that the gain due to lesser dissociation (and at high M_∞, lesser overall total pressure loss) may make this engine superior to a conventional engine at Mach numbers higher than 7 or 8 (2,4,70). Thrust augmentation of ramjet engines by afterburning in the supersonic nozzle may prove to be another valuable application of supersonic combustion, in that it would provide a means for increasing ramjet thrust without affecting the diffuser performance (4).

A modification to the latter approach is the detonative or

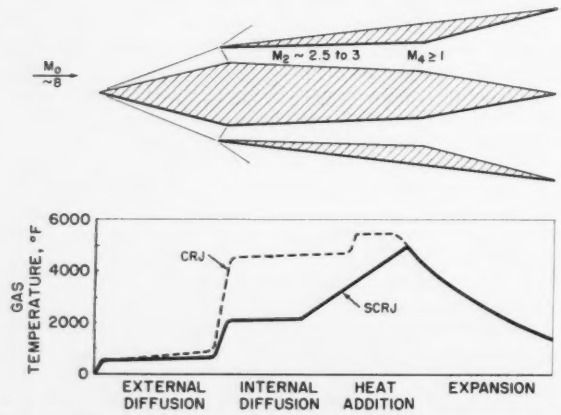

Fig. 2 The supersonic combustion ramjet (SCRJ) as discussed in (70) and (2). The reduction in static temperatures in diffuser and combustion chamber, as compared to temperatures which would be experienced in a conventional ramjet (CRJ), means less dissociation in the burned gas

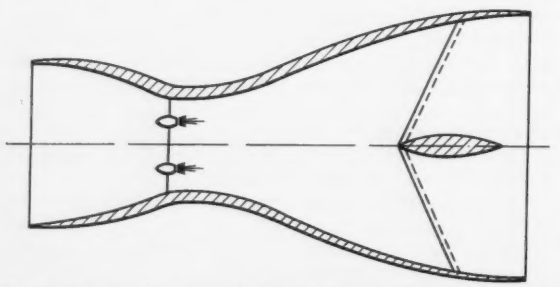

Fig. 3 The standing wave (detonative) ramjet (SWRJ), with an oblique detonation wave stabilized by a streamlined centerbody, as proposed in (71)

standing wave engine, which might be designated SWRJ. See Fig. 3, after (71). Fuel would be added to a supersonic stream ahead of a strong shock wave held stationary by the duct geometry with the heat release occurring behind the wave. Roy (72) proposed such an engine in 1946. Nicholls et al. (73) and Gross et al. (57,74,75) have demonstrated stabilized detonation waves in hydrogen-air streams at Mach numbers in the range 2 to 5. Most of Gross' fascinating experiments were done with hydrogen addition upstream of a Mach-reflected normal shock. The latter was obtained by placing opposing wedges on the top and bottom walls of a two-dimensional, slightly divergent test section of a nominal Mach 3 tunnel (Fig. 4a). The geometry was chosen so that oblique waves from the wedges generated a normal wave at the center of the tunnel. Hydrogen, introduced through a small streamlined injector just upstream of the nozzle throat, diffused through the air as it was swept toward the test section. At air stagnation temperatures of approximately 1860 R and higher, the resulting mixture ignited behind the shock system and caused the plane wave to move forward and become larger in vertical dimension. Even though the fuel concentration profile was far from flat ahead of the shock, the shock itself remained rather flat. The extent of the location and size change was directly related to the fuel injection rate and inversely related to temperature. This was interpreted as suggesting that Q/c_pT_1, the dimensionless "Damköhler second parameter," where Q is heat added and T_1 is static temperature before the shock, plays an important role in characterizing detonation waves.

An ignition "hysteresis" effect was found (57,75): After ignition at high air stagnation temperature, the air stagnation temperature could be lowered to as little as 860 R (static temperature at Mach 3, 310 R, or −150 F) before ignition ceased, and the normal wave regressed to its "no-burning" position. The extent of the hysteresis effect, which was also related to Q/c_pT_1, was purported to imply that transport mechanisms within the wave are important once the combustion has been initiated, thus supporting the theoretical work of Hirschfelder et al. (76), but denying the assumption of zero transport properties in the von Neumann-Zeldovich type of analysis which separates shock wave and chemical reaction. Supporting evidence that no ordinary "ignition delay" time was involved was obtained by superimposing Schlieren and sodium emission (from injected NaCl) photographs, which showed that combustion began in less than 5 microsec. By using a dual fuel injection system, exothermal waves of hydrogen, methane and air were also stabilized. Pure methane-air waves were never successfully stabilized, but it was believed that careful experimentation would reveal combinations of conditions conducive to their stabilization. Oblique detonation waves were also produced with hydrogen by using a single wedge. Ignition hysteresis was observed in all cases.

Nicholls et al. (73) did their experiments with a small, underexpanded, free jet, which produced a Mach reflected shock in the expanding jet at a local Mach number of 3.5 to 6.2 (Fig. 4b). Their experiments, chronologically ahead of Gross, indicated an ignition delay of the order of 25 microsec with a stagnation temperature of ~2150 R, an M_1 of ~5, and roughly double the stagnation pressure Gross used. Contrary to Gross, Nicholls contends that the separation of shock and combustion, and the corresponding ignition delay are real; perhaps at some later date an explanation will be found which ties together the apparently incompatible results from these different experimental techniques and experimental conditions. This same group also did an analysis (71) for a detonative engine as sketched in Fig. 3. They estimated the stagnation pressure loss for the mixing of the fuel with the supersonic air stream ahead of the oblique detonation wave. The estimated mixing loss was reasonable, 10 to 20 per cent, but it was based on the assumption that no oblique shocks were caused by the fuel injectors. This problem of getting the fuel into the supersonic stream without shock losses—which applies also

to the SCRJ previously discussed—is likely to provide the greatest obstacle in the course of demonstrating the calculated potential performance of detonative or supersonic combustion ramjets.

Various estimates have been made for the performance potentials of these engines compared to conventional ramjets (2,4,14,57,70,71). Fig. 5 compares overall engine efficiencies estimated for SCRJ and SWRJ with those for a conventional ramjet (CRJ) and a turbojet. Ramjets are superior to turbojets for flight speeds above Mach 3 or 3.5. The conventional ramjet probably will reach its maximum efficiency at some speed between Mach 6 and Mach 8, depending upon the efficiencies of the various engine components. The supersonic combustion ramjet may surpass the conventional ramjet for speeds greater than the CRJ's maximum efficiency speed, and the detonative or standing wave ramjet will follow slightly behind the SCRJ due to its shock loss. The curves for Fig. 5, except for the "optimistic" CRJ curve, are taken from (2); the CRJ curve is based on a higher diffuser kinetic energy efficiency (0.94 compared to 0.90) and higher combustor total pressure recovery (0.96 compared to 0.86). All curves are based on the use of kerosene fuel on an approximately optimum fuel schedule for an aircraft following a moderate, constant dynamic pressure trajectory (q_∞ = 350 psfa). Dynamic equilibrium is assumed in all cases for the burned gas expansion—an optimistic assumption—but the favorable effect of centrifugal lift at high speed, which would serve to increase range, is not included in efficiency estimates.

External Burning Experiments Point to Still Higher Speeds

The previous discussion pointed out ways to extend the performance barrier due to combustor temperature rise, but an equally important problem is that of the large structural cooling requirement imposed by the staggering temperatures encountered in the diffuser, combustor and exit nozzle at flight speeds above Mach 6. Either supersonic combustion ramjets or standing wave ramjets would have a smaller diffuser cooling requirement than a conventional ramjet due to the lower heat transfer rate per unit area with supersonic flow (70). The combustor and nozzle areas for the standing wave ramjet may be much smaller than those for a conventional ramjet (14,71) which may further reduce overall cooling requirement. An SCRJ would have a lower heat transfer rate per unit area in the heat addition region than a subsonic combustion engine (70), but more area would be required. (Lower temperature means lower reaction rate; coupled with higher velocity this means at least an order of magnitude increase in combustion chamber length, which in turn means more area for heat transfer.) It is difficult to estimate, therefore, whether the combustor cooling requirement would be greater or smaller.

A better way to push back the structural temperature limitation on ramjet engine flight speed might be to turn the engine inside out, so that all of the compression-heat addition-expansion cycle is carried out on external surfaces, which are free to radiate to the atmosphere. Thus the all-external engine (ERJ) is simply a supersonic wing beneath which mass and heat are added by injecting fuel into the supersonic air stream. The addition of mass and heat beneath a wing causes the supersonic air stream reaching the heat addition region to be deflected away from the wing, and increases lift in much the same way that an increased angle of attack would increase lift. If the heat or mass addition is concentrated under the rear part of the wing (Fig. 6, after Weber (4)), where the increase in surface pressure will serve to reduce drag, then the maximum lift to drag ratio may be increased by a factor of 2 or more (77,78). If the pressure rise under the rearward-facing surface is great enough, the "wing" will have a net thrust, and it becomes a "propulsive wing" or "engine." Luidens and Flaherty (79) estimate that a simple wedge airfoil of small thickness to chord ratio and large rear to fore angle ratio could become more efficient than a conventional ramjet engine plus wings at speeds greater than about Mach 8. Since the major part of the burned gas expansion force goes into lift rather than thrust, lift to drag ratio and thrust specific impulse cannot be separated for an overall engine efficiency comparison, such as Fig. 5. The comparison of Luidens and Flaherty is made on the basis of a range parameter $L/\dot{Q}$, where $\dot{Q} = \dot{w}_f h_c$. For constant velocity cruise with thrust

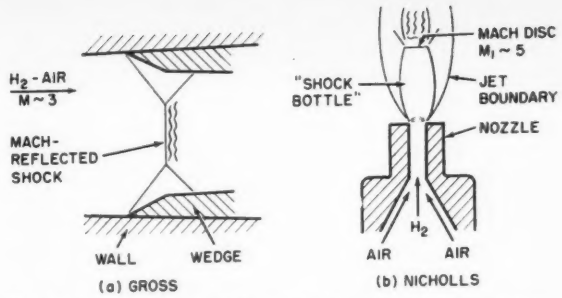

Fig. 4 Experimental techniques for obtaining standing detonation waves, as reported in (75) and (73)

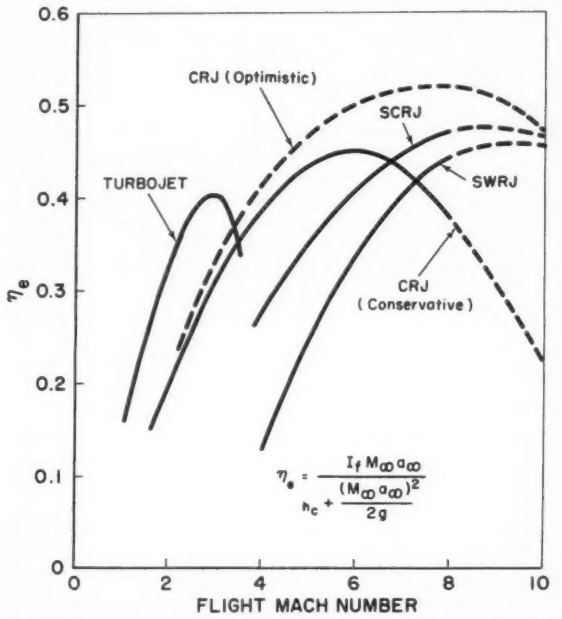

Fig. 5 Comparison of overall engine efficiencies estimated for various airbreathing engines

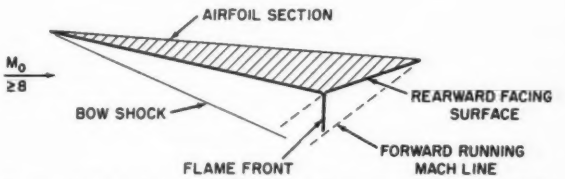

Fig. 6 Sketch of a "propulsive wing," or external ramjet (ERJ), after (79)

equal to drag, this parameter, for a given h_c, is proportional to $I_f L/D$.

Dorsch et al. (78,80,81) have conducted some interesting experiments on external burning. Their results for the combustion of aluminum borohydride under a two-dimensional supersonic wing in Mach 2.5 and 3.0 air streams (78) appear to agree reasonably well with the "conservative" curve of Luidens and Flaherty (79) for a propulsive wing with concentrated heat addition. Dorsch et al. (78) show that their results are also in reasonable agreement with the predictions of a linearized theory and a graphical method. This agreement between experiment and theory at low Mach numbers might be optimistically interpreted to mean that the prediction (79) of external ramjet superiority to conventional ramjet plus wing for $M_\infty \geq 8$ may be realized, and that the same propulsive wing or ERJ will be superior in fuel economy to chemical rockets to $M_\infty \geq 12$. Dorsch et al. have burned, or attempted to burn, several other pyrophoric fuels in a Mach 2.5 air stream (81). Gross has also demonstrated burning in a supersonic boundary layer with hydrogen injection (75).

Concluding Remarks

Combustion science and ramjet engineering technology have reached a stage such that efficient ramjet engines can be designed and produced for vehicles with flight speeds up to the threshold of the hypersonic regime. The higher temperatures associated with hypersonic flight speeds will have a considerable impact on both combustor temperature rise and overall engine design, but various approaches are envisioned for overcoming or bypassing these obstacles. For conventional engines with subsonic combustion, it may be possible to tailor a fuel to mitigate the deleterious effect of low combustor temperature rise on thrust. The thrust obtained from any hypersonic ramjet engine will depend in large measure on the effectiveness of recombination reactions and/or favorable phase changes in the supersonic flow in the exhaust nozzle. With more information on the kinetics of these changes (which appears to be forthcoming), it may be possible to tailor the nozzle to obtain higher thrust.

Supersonic (SCRJ), detonative (SWRJ), or external combustion (ERJ) engines may be employed for flight at Mach numbers above about 8. The crossover points obtained from performance estimates are of course strongly dependent on the assumptions used to make the estimates, but the trends indicated by comparisons such as Fig. 5 are probably realistic, provided that the promise of early experiments with the various combustion systems at low Mach numbers holds up to hypersonic Mach numbers. In any event, these recent combustion experiments and aerothermodynamic analyses have suggested several ways in which ramjet propulsion might be used to power hypersonic airbreathing vehicles in coming years.

Nomenclature

a = acoustic velocity, fps
C = constant
c_p = specific heat at constant pressure, Btu/lb-R
D = drop diameter
d = flameholder width (characteristic dimension), ft
h = duct height, ft
h_c = heat of combustion for fuel, ft-lb/lb
I_f = fuel specific impulse, gross thrust divided by fuel rate, lb/lb/sec ($3600/I_f$ = SFC)
L = length of recirculation zone, ft
L/D = lift to drag ratio
M_∞ = flight (free stream) Mach number
m = mass
Pr = Prandtl number
p = absolute pressure, atm or psfa
Q = heat added, Btu/lb
$\dot{Q}$ = heat addition rate, Btu/sec
q_∞ = dynamic pressure of free stream, $\gamma M_\infty^2/2$, psfa
R = range, ft
Re = Reynolds number
Sc = Schmidt number
T_{ac} = static temperature of air at inlet to combustion, R
ΔT_t = total temperature rise in combustor, R
$T_{t\infty}$ = total (stagnation) temperature of free stream, R
T_1 = static temperature before shock, R
T_∞ = static temperature of free stream, R
t = time
U_f = laminar flame velocity, fps
V = velocity, fps
V_1 = reference velocity upstream of flameholder, fps
V_2 = velocity of fresh gas mixture past wake, fps
W_f = weight of fuel consumed during cruise, lb
W_g = gross weight of aircraft at beginning of cruise, lb
$\dot{w}_f$ = fuel flow rate, lb/sec
$\bar{\gamma}$ = effective ratio of specific heats during compression, R
η_e = overall engine efficiency, ft-lb work/ft-lb input
τ = ignition delay time, sec

References

1 "Supersonic Transports (Proceedings)," presented at IAS 27th Annual Meeting, New York, N. Y., Jan. 26–29, 1959, S.M.F. fund paper no. FF-20.

2 Dugger, G. L., "A Future for Hypersonic Ramjets," Astronautics, vol. 3, no. 4, 1959, p. 38.

3 Cornog, R., "Some Economic Aspects of Hypersonic Flight," ARS Journal, vol. 29, no. 10, Part 1, Oct. 1959, pp. 706–715.

4 Weber, R. J., "A Survey of Hypersonic Ramjet Concepts," ARS preprint no. 875–59.

5 Avery, W. H., "Twenty-Five Years of Ramjet Development," Jet Propulsion, vol. 25, 1955, p. 604.

6 Avery, W. H., "Status and Future of Ramjet Propulsion," presented at IAS Meeting, St. Louis, Mo., May 12, 1959. *Confidential; unclassified title.*

7 Avery, W. H., Dugger, G. L. and Walker, J. H., "Prospects and Design Considerations for Hypersonic Flight," presented at IAS National Flight Propulsion Meeting, Cleveland, Ohio, March 5–6, 1959. *Confidential; unclassified title.*

8 Hawthorne, W. R., "Some Aerodynamic Problems of Aircraft Engines," *J. Aeron. Sci.*, vol. 24, 1957, p. 713.

9 Morris, B. T., "Ramjets," Astronautics, vol. 3, 1958, p. 60.

10 Emmons, H. W., "Combustion—An Aeronautical Science," *J. Aero/Space Sci.*, vol. 25, 1958, p. 730.

11 Breitwieser, R., "Ramjet Combustion," Astronautics, vol. 3, no. 4, 1959, p. 44; Perchonok, E., "Ramjet Trends," p. 40; Muhlfelder, L., "Ramjet Fuel-Air Control," p. 42; Pearce, R. B., Jr., "Supersonic Ramjet Diffuser Design," p. 46; also ref. 2.

12 Leduc, R., "Early Work and Latest Realizations With Ramjet Engines," Jet Propulsion, vol. 27, no. 1, Jan. 1957, pp. 64–67.

13 Daum, N., "The Griffon Aircraft and the Future of the Turbo-Ram-Jet Combination in the Propulsion of Supersonic Aeroplanes," Twelfth Louis Blériot Lecture, *J. Royal Aeron. Soc.*, vol. 63, 1959, p. 327.

14 Roy, M., "Propulsion Supersonique par Turboreacteurs et par Statoreacteurs," presented at First International Congress in the Aero. Sciences, Madrid, Spain, Sept. 8–13, 1958. Preprinted by Permagon Press, London.

15 Probert, R. P., "Ram-Jets," *J. Royal Aeron. Soc.*, vol. LXII, 1958, p. 151.

16 Jamison, R. R., "The Ramjet Engine," *Interavia*, vol. XIII, 1958, p. 955.

17 Jamison, R. R., "Ram-Jets," *J. Royal Aeron. Soc.*, vol. LXI, 1957, p. 407.

18 Propulsion Chemistry Division, Lewis Flight Propulsion Laboratory, NACA, "Basic Considerations in the Combustion of Hydrocarbon Fuels with Air," NACA Rep. 1300, 1957.

19 Zucrow, M. J., "Aircraft and Missile Propulsion," vols. I and II, John Wiley and Sons, Inc., N. Y., 1958.

20 Lancaster, O. E., Ed., "Jet Propulsion Engines," vol. XII, Princeton University Press, 1959.

21 Bondariak, M. M. and Il'iashenko, S. M., "Ramjet Engines," State Publishing House of the Defense Industry, Moscow, 1958.

22 The Johns Hopkins University, Applied Physics Laboratory, W. G. Berl, Ed., "Ramjet Technology," to be published in 1960.

23 The Combustion Institute, "Sixth Symposium (Int.) on Combustion," Reinhold Publishing Corp., N. Y., 1957.

24 The Combustion Institute, "Seventh Symposium (Int.) on Combustion," Butterworths Scientific Pub., London, 1959.

25 AGARD, NATO, "Selected Combustion Problems, II," Butterworths Scientific Pub., London, 1956.

26 AGARD, NATO, "Combustion Researches and Reviews," AGARDograph no. 15, Butterworths Scientific Pub., London, 1957.

27 Spalding, D. B., "Some Fundamentals of Combustion," Academic Press, N. Y., 1955.

28 Lewis, B. and von Elbe, G., "Combustion, Flames, and Explosions of Gases," Academic Press, N. Y., 1951, revised edition in press.

29 Fristrom, R. M., Westenberg, A. A. and Berl, W. G., "Flame Structure, Its Measurement and Interpretation," to be published in 1960.

30 Gaydon, A. G., "The Spectroscopy of Flames," John Wiley and Sons, N. Y., 1957.

31 Weiss, M. A. and Worsham, G. H., "Atomization in High Velocity Airstreams," ARS Journal, vol. 29, no. 4, April 1959, pp. 252–259.

32 Agoston, G. A., Wise, H. and Rosser, W. A., "Dynamic Factors Affecting the Combustion of Liquid Spheres," in "Sixth Symposium (Int.) on Combustion," Reinhold Publishing Corp., N. Y., 1957, p. 708.

33 Miesse, C. C., "On the Combustion of a Liquid Fuel Spray," in

"Sixth Symposium (Int.) on Combustion," Reinhold Publishing Corp., N. Y., 1957, pp. 732, 735.

34 Foster, H. H. and Ingebo, R. D., "Evaporation of JP-5 Fuel Sprays in Air Streams," NACA RM E55K02, 1956.

35 Bolt, J. A. and Saad, M. A., "Combustion Rates of Freely Falling Fuel Drops in a Hot Atmosphere," in "Sixth Symposium (Int.) on Combustion," Reinhold Publishing Corp., N. Y., 1957, p. 717.

36 Marble, F. E. and Zukoski, E. E., "Flame Holding by Bluff Bodies," presented at 12th Meeting AGARD Combustion and Propulsion Panel, Washington, D. C., Nov. 1957.

37 Mullins, B. P., *Fuel*, vol. 32, 1953, pp. 343, 363, 467, 481.

38 Weiss, M. A., Rohrer, J. C. and Longwell, J. P., "Some Effects of Fuel Reactivity and Heat Loss on Flame Stabilization," in "Sixth Symposium (Int.) on Combustion," Reinhold Publishing Corp., N. Y., 1957, p. 439.

39 Miller, R. E. "Some Factors Governing the Ignition Delay of a Gaseous Fuel," in "Seventh Symposium (Int.) on Combustion," Butterworths Scientific Pub., London, 1959, p. 417.

40 Wright, F. H., "Bluff-Body Flame Stabilization," Progress Rep. no. 20-327. Jet Prop. Lab., Calif. Inst. Tech., 1958.

41 Spalding, D. B., "Some Fundamentals of Combustion," Academic Press, N. Y., 1955, p. 185.

42 Longwell, J. P. and Weiss, M. A., "High Temperature Reaction Rates in Hydrocarbon Combustion," *Ind. Eng. Chem.*, vol. 47, 1955, p. 1634.

43 Longwell, J. P., Frost, E. E. and Weiss, M. A., "Flame Stability in Bluff Body Recirculation Zones," *Ind. Eng. Chem.*, vol. 45, 1953, p. 1629.

44 Avery, W. H. and Hart, R. W., "Combustor Performance with Instantaneous Mixing," *Ind. Eng. Chem.*, vol. 45, 1953, p. 1634.

45 Weiss, M. A., Lang, R. J. and Longwell, J. P., "Combustion Rates in Spherical Reactors," *Ind. Eng. Chem.*, vol. 50, 1958, p. 257.

46 Hottel, H. C., Williams, G. C. and Baker, M. L., "Combustion Studies in a Stirred Reactor," in "Sixth Symposium (Int.) on Combustion," Reinhold Publishing Corp., N. Y., 1957, p. 398.

47 Williams, G. C., "Seventh Symposium (Int.) on Combustion," Butterworths Scientific Pub., London, 1959, p. 633.

48 Khramtsov, V. A., "Investigation of Pressure Effect on the Parameters of Turbulence and on Turbulent Burning," in "Seventh Symposium (Int.) on Combustion," Butterworths Scientific Pub., London, 1959, p. 609.

49 Hottel, H. A., Marion, C. P. and Jensen, J. P., "Flame Stabilization in Volatile Fuel Sprays," in "Sixth Symposium (Int.) on Combustion," Reinhold Publishing Corp., N. Y., 1957, p. 451.

50 Bowditch, F. W., "Some Effects of Turbulence on Combustion," in "Fourth Symposium (Int.) on Combustion," William & Wilkins Co., Baltimore, 1953, p. 675.

51 Scurlock, A. C., "Flame Stabilization and Propagation in High-Velocity Gas Streams," Meteor Rep. 19, Fuels Res. Lab., MIT, 1948.

52 Grover, J. H., Fales, E. N. and Scurlock, A. C., "Turbulent Flame Studies in a Two-Dimensional Open Burner," ARS JOURNAL, vol. 29, no. 4, April 1959, pp. 275–283.

53 Blackshear, P. L., Jr., "The Growth of Disturbances in a Flame-Generated Shear Region," in "Sixth Symposium (Int.) on Combustion," Reinhold Publishing Corp., N. Y., 1957, p. 512.

54 Fristrom, R. M. and Westenberg, A. A., "Flame Zone Studies IV—Microstructure and Material Transport in a Laminar Propane-Air Flame Front," *Combustion and Flame*, vol. 1, 1957, p. 217.

55 Fristrom, R. M. et al., private communication.

56 Walker, R. E. and Westenberg, A. A., "Molecular Diffusion Studies in Gases at High Temperature," *J. Chem. Phys.*, vol. 29, 1958, pp. 1139 and 1147; vol. 31, 1959, p. 519.

57 Sargent, W. H. and Gross, R. A., "A Detonation Wave Hypersonic Ramjet," Fairchild Engine Div., Fairchild Engine & Airplane Corp., Deer Park, N. Y., AFOSR TN 59 589, ASTIA AD 216 811, June 1959.

58 Agoston, G. A., Noon, A. W. and Witherly, T. D., "Experimental Study of a Reversed Jet Flameholder," *Combustion and Flame*, vol. II, 1958, p. 333.

59 Shepherd, D. G., "Flame Stabilization by Means of Annular Fluid Jets," in "Sixth Symposium (Int.) on Combustion," Reinhold Publishing Corp., N. Y., 1957, p. 472.

60 Bertin, J. H. and Salmon, B. J., "Study of the Aerodynamic Process of Combustion," presented at 12th Meeting of AGARD Combustion and Propulsion Panel, Washington, D. C., Nov. 18–26, 1957.

61 Huellmantel, L. W., Ziemer, R. W. and Cambel, A. B., "Stabilization of Premixed Propane-Air Flames in Recessed Ducts," JET PROPULSION, vol. 27, no. 1, Jan. 1957, pp. 31–34.

62 Unterberg, W., "Heating Problems in Ramjet Tailpipes," JET PROPULSION, vol. 27, no. 5, May 1957, pp. 514–521, 541.

63 Olson, W. T. and Setze, P. C., "Some Combustion Problems of High-Energy Fuels for Aircraft," in "Seventh Symposium (Int.) on Combustion," Butterworths Scientific Pub., London, 1959, p. 833.

64 Olsen, H. L. et al., "The Determination of Flame Speed of Pentaborane-Oxygen-Nitrogen Mixtures," Appl. Phys. Lab., Johns Hopkins Univ., CM-888, 1956.

65 Berl, W. G. and Renich, W., "The Combustion of Boron Hydrides," Appl. Phys. Lab., Johns Hopkins Univ., CM-942, 1958.

66 Breisacher, P., Dembrow, D. and Berl, W. G., "Flame Front Structures of Lean Diborane-Air and Diborane-Hydrocarbon-Air Mixtures," in "Seventh Symposium (Int.) on Combustion," Butterworths Scientific Pub., London, 1959, p. 894.

67 Marsel, J. and Kramer, L., "Spontaneous Ignition Properties of Metal Alkyls," in "Seventh Symposium (Int.) on Combustion," Butterworths Scientific Pub., London, 1959, p. 906.

68 Fletcher, E., Foster, H. and Straight, D., "The Use of Aluminum Borohydride and Aluminum Borohydride-Hydrocarbon Mixtures as a Source of Ignition for Combustors," presented at Amer. Chem. Soc. Meeting, Boston, April 5–10, 1959.

69 Wegener, P. P., "Study of Supersonic Flow with Chemical Reactions. II," Prog. Rep. no. 20-370, Jet Prop Lab., Calif. Inst. Tech., 1958.

70 Weber, R. J. and MacKay, J. S., "An Analysis of Ramjet Engines Using Supersonic Combustion," NACA Tech. Note 4386, 1958.

71 Dunlap, R., Brehm, R. L. and Nicholls, J. A., "A Preliminary Study of the Application of Steady-State Detonative Combustion to a Reaction Engine," JET PROPULSION, vol. 28, no. 7, July 1958, pp. 451–456.

72 Roy, M., *Comptes Rendus de l'Academie des Sciences*, Feb. 1, 1946, Paris.

73 Nicholls, J. A., Dabora, E. K. and Gealer, R. L., "Studies in Connection with Stabilized Gaseous Detonation Waves," in "Seventh Symposium (Int.) on Combustion," Butterworths Scientific Pub., London, 1959, p. 766; *see also* Nicholls, J. A., "Stabilized Gaseous Detonation Waves," ARS JOURNAL, vol. 29, no. 8, Aug. 1959, pp. 607–608.

74 Gross, R. A., "Research on Supersonic Combustion," ARS JOURNAL, vol. 29, no. 1, Jan. 1959, pp. 63–64.

75 Gross, R. A., "Exploratory Studies of Combustion in Supersonic Flow. I. Plane Detonation Waves. II. Oblique Detonation Waves," AFOSR TN 59 587, ASTIA AD 216 789; Chinitz, W. and Gross, R. A., "III. Chemical Reactions in a Supersonic Boundary Layer. IV. Supersonic Flame Stabilization," Project Squid, Contract no. NR 1858(25) NR-098-032, June 1959. (Parts I and II are expected to be published in *Combustion and Flame*.)

76 Hirschfelder, J. O. and Curtiss, C. F., "Theory of Detonations. I—Irreversible Unimolecular Reaction"; Linder, B., Curtiss, C. F. and Hirschfelder, J. O., "II—Reversible Unimolecular Reaction," *J. Chem. Phys.*, vol. 28, 1958, p. 1130.

77 Pinkel, I. I., Serafini, J. S. and Gregg, J. L., "Pressure Distribution and Aerodynamic Coefficients Associated with Heat Addition to Supersonic Air Stream Adjacent to Two-Dimensional Supersonic Wing," NACA RM E51K26, 1952.

78 Dorsch, R. G., Serafini, J. S., Fletcher, E. A. and Pinkel, I. I., "Experimental Investigation of Aerodynamic Effects of External Combustion in Airstream Below Two-Dimensional Supersonic Wing at Mach 2.5 and 3.0," NASA Memo 1-11-59E, 1959.

79 Luidens, R. W. and Flaherty, R. J., "Analysis and Interpretation of Supersonic Underwing Heat Addition," NASA Memo 3-17-59E, 1959.

80 Dorsch, R. G., Serafini, J. S. and Fletcher, E. A., "Exploratory Investigation of Aerodynamic Effects of External Combustion of Aluminum Borohydride in Airstream Adjacent to Flat Plate in Mach 2.46 Tunnel," NACA RM E57E16, 1957.

81 Fletcher, E. A., Dorsch, R. G. and Allen, H., Jr., "Combustion of Highly Reactive Fuels in Supersonic Airstream," presented at Amer. Chem. Soc. Meeting, Boston, April 5–10, 1959.

Theory of Particle Combustion at High Pressures

D. B. SPALDING[1]

Imperial College
London, England

Conventional theories of particle combustion become inaccurate when the gas pressure rises, and are completely useless above the critical pressure. The paper discusses the transient effects, neglected in conventional theories, which dominate the burning process at high pressures. A quantitative theory is presented, valid for these conditions, of the time variations of flame radius, burning rate and combustion efficiency.

IN CONSIDERING the influence of droplet vaporization on the performance of gasturbine, ramjet or rocket combustion chambers, it is customary to calculate the burning time of a droplet and to compare this time with the residence time of the droplet in the chamber. Various formulas are available for the burning time (1,2,3)[2]; they have in common the assumption that the process is quasi-steady, i.e., that the transient processes in the gas can be neglected.[3] The predicted burning times have been found to agree well, in the main, with the results of laboratory-scale experiments on single droplets (2,3,6 to 10), most of which have been carried out at atmospheric pressure.

Despite the good service which the quasi-steady formulas have given, their validity and utility are doubtful at the high pressures prevailing in current jet engines. There are two reasons: Firstly, as the pressure approaches the critical pressure of the injected fuel, the latent heat of vaporization decreases to zero; the quasi-steady formulas correspondingly predict a vaporization rate which rises to infinity. Secondly, and irrespective of changes to the latent heat, the mass of gas in the region influenced by the droplet increases steadily with pressure; its heat capacity therefore also increases, rendering illegitimate the neglect of the transient term in the energy equation. Kumagai and Isoda (11) have pointed out that the observed ratio of flame diameter to droplet diameter, even at atmospheric pressure, suggests the influence of transient processes.

The transient burning of a particle has been considered by Summerfield (30) in connection with his theory of the burning of composite solid propellants. The present paper was stimulated by, and may be regarded as an extension of, Summerfield's approach.

Contents of the Present Paper

The present paper attempts to predict the burning rates of fuel particles in a way which is valid at high pressures, whether or not the phase boundary has completely disappeared.

First we state the differential equations which express the conservation and transport of matter and of energy when all the diffusivities are equal. The latter assumption permits reaction kinetic considerations to be eliminated. The appropriate boundary condition for a phase interface is also stated.

Then the quasi-steady theory is reviewed. It is shown that this is not even a first-order approximation to the transient problem. A new theory is therefore derived which, when the property variations are neglected, gives an explicit formula for the burning time which is valid for particles at high pressures, when the gas state is not too near stoichiometric.

Differential Equations

General conservation and flux laws

We shall use the formulation of (1), generalized to the unsteady state. Other treatments of a similar nature may be found in (13 to 23).

The conservation and flux laws of the chemical element α in a single-phase fluid mixture are expressible through the equation

$$\vec{G}\cdot(\nabla n_\alpha) - \nabla\left[\sum_j n_{\alpha,j} D_j \rho\,(\nabla m_j)\right] = -\rho\,\frac{\partial n_\alpha}{\partial t} \qquad [1]$$

where

$\vec{G}$ = vector mass velocity of mixture, lbm/ft² hr
$n_{\alpha,j}$ = mass of chemical element α per unit mass of chemical compound j
$n_\alpha = \sum_j n_{\alpha,j} m_j$
= mass of chemical element α per unit mass of local mixture
m_j = mass of chemical compound j per unit mass of local mixture
D_j = local diffusion coefficient of chemical element j in mixture, ft²/hr
ρ = local mixture density, lbm/ft³
t = time, hr
$\sum_j$ = summation over all chemical compounds which are present

The first law of thermodynamics and the Fourier heat conduction law may be expressed, for a fluid in which thermal radiation and the kinetic energy of the mean motion are negligible, through the equation

$$\vec{G}\cdot(\nabla h) - \nabla\left[\sum_j h_j D_j \rho(\nabla m_j)\right] - \nabla[k(\nabla T)] = -\rho\,\frac{\partial h}{\partial t} + \frac{\partial p}{\partial t} \qquad [2]$$

Received Jan. 1959.

[1] Professor of Heat Transfer, Department of Mechanical Engineering.

[2] Numbers in parentheses indicate References at end of paper.

[3] Agafanova, Gurevich and Paleev (4) claim that the originator of the theory was Varshavskii (5); the present author has not had an opportunity to see the latter publication.

where

h_j = local partial enthalpy of chemical compound j, Btu/lbm
h = $\sum_j h_j m_j$
= local specific enthalpy of mixture, Btu/lbm
k = local thermal conductivity of mixture, Btu/ft hr F
T = local mixture temperature, F
p = local pressure, Btu/ft³

Simplified conservation and flux laws

If we assume that all the diffusion coefficients are equal at any particular point in the fluid, we may drop the suffix j to D_j; then Equation [1] simplifies to

$$\vec{G}\cdot(\nabla n_\alpha) - \nabla[D\rho(\nabla n_\alpha)] = -\rho(\partial n_\alpha/\partial t) \qquad [3]$$

One such differential equation can be written for each chemical element.

If we assume, in addition, that $D\rho = k/c$, where c is equal to the local mixture specific heat at constant pressure, and if the variation of pressure with time can be neglected, Equation [2] reduces to

$$\vec{G}\cdot(\nabla h) - \nabla(D\rho\Delta h) = -\rho(\partial h/\partial t) \qquad [4]$$

A mixing theorem

Equations [3 and 4] differ only in their respective dependent variables. If the boundary conditions of the two equations appropriate to a particular flow are also similar, the solutions of the equations are bound to be similar: n_α and h must be linearly related.

In particular, in a "two-stream" situation in which the whole of the fluid under consideration results from the mixing of two streams in a region with adiabatic impervious walls, it is easy to show that the linear relation between n_α and h is precisely the same as that which holds for an adiabatic steady-flow mixing chamber. For concreteness, we will regard the two streams as consisting of pure fuel and of pure oxidant.

The last conclusion permits us to ascribe to each mixture particle a "fuel fraction" f which is related to n_α and to h by

$$f = \frac{n_\alpha - n_{\alpha,O}}{n_{\alpha,F} - n_{\alpha,O}} = \frac{h - h_O}{h_F - h_F} \qquad [5]$$

where suffixes O and F refer to the oxidant and fuel streams. The quantity $f/(1-f)$ is equal to the ratio of the mass rates of fuel and oxidant into a steady-flow adiabatic mixing chamber if the outgoing stream is to have the properties n_α and h.

Equation [5] may be substituted in Equations [3] or [4] to yield

$$\vec{G}\cdot(\nabla f) - \nabla[D\rho(\nabla f)] = -\rho(\partial f/\partial t) \qquad [6]$$

This equation will be used extensively later.

The Mass Transfer Boundary Condition

Equations [3, 4 and 6] hold for a region of uniform phase. At the boundaries of such a region we have, as is shown in (1)

$$\dot{m}'' = \frac{(D\rho)_S(\partial P/\partial y)_S}{P_S - P_T} \qquad [7]$$

where

$\dot{m}''$ = component of $\vec{G}$ normal to phase boundary, directed into fluid phase under consideration, lbm/ft²hr
y = distance normal to phase boundary, in same direction, ft
P = n_α, h, f or any fluid property obeying a similar equation
S = state of the fluid under consideration immediately adjacent the phase boundary
T = value of the property in the "transferred substance," i.e., in a fictitious stream which is entirely equivalent in its effect on the fluid under consideration to all the material and heat fluxes across the phase boundary

When the quantities P_S and P_T are uniform and constant for all parts of the phase boundary, it is convenient to follow (1) by defining a new variable b through

$$b \equiv P/(P_S - P_T) \qquad [8]$$

The differential equation and boundary condition then take the form

$$\vec{G}\cdot(\nabla b) - \nabla[D\rho(\nabla b)] = -\rho(\partial b/\partial t) \qquad [9]$$

and

$$\dot{m}'' = (D\rho)_S(\partial b/\partial y)_S \qquad [10]$$

Equations [9 and 10] will be used extensively. We therefore note already two particularly important forms of Equation [8] valid for the case when the transferred substance is fuel:

1 If the property P is the fuel fraction f, clearly $f_T = 1$. There results

$$b = f/(f_S - 1) \qquad [11]$$

2 If we choose the zero of enthalpy so that unburned fuel, products and inerts have zero enthalpy in the gas phase at state S, and if, as is true for burning volatile fuels, no unburned oxidant is present at the surface, it is possible to replace $h_S - h_T$ by Q, this quantity being the heat transfer from the gas to the surface per unit mass transfer (Btu/lbm). Q is, of course, often equal to the latent heat of vaporization. Equation [8] then takes the form

$$b = h/Q \qquad [12]$$

Quasi-Steady Theory

The System Considered

Fig. 1 shows a spherical particle, for example a fuel droplet, in a large gas reservoir. The gas is at rest except for a radial motion occasioned by the mass transfer outward from the particle. Often there will be a spherical flame surrounding the particle (at the radius where $f = f_{\text{stoich}}$, the stoichiometric fuel-oxidant ratio), but we need not consider this at the moment. The assumption of spherical symmetry is known to be well-justified when the droplet is very small.

It will be supposed that the rate of change of droplet radius is so slow (later the meaning of "slow" will be analyzed quantitatively), that the $\partial/\partial t$ terms can be omitted from the equations. The process is therefore treated as quasi-steady. The first application of this assumption to droplet vaporization appears to have been made by Fuchs (12).

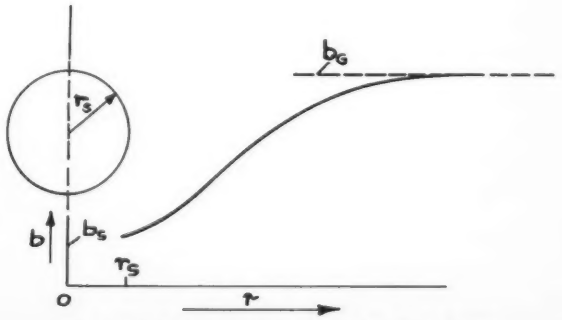

Fig. 1 Conditions adjacent to burning fuel droplet

Equations

Writing the partial differential equation of conservation [9] for this case in spherical coordinates, we obtain the ordinary differential equation

$$\frac{1}{r^2}\frac{d}{dr}\left(D\rho\, r^2 \frac{db}{dr}\right) - \dot{m}'' \cdot \frac{r_S^2}{r^2}\frac{db}{dr} = 0 \qquad [13]$$

where

r = radius
r_S = radius of particle surface
$\dot{m}''$ = mass transfer rate at the surface

The boundary condition [10] takes the form

$$r = r_S: \quad \dot{m}'' = \left(D\rho \frac{db}{dr}\right)_S \qquad [14]$$

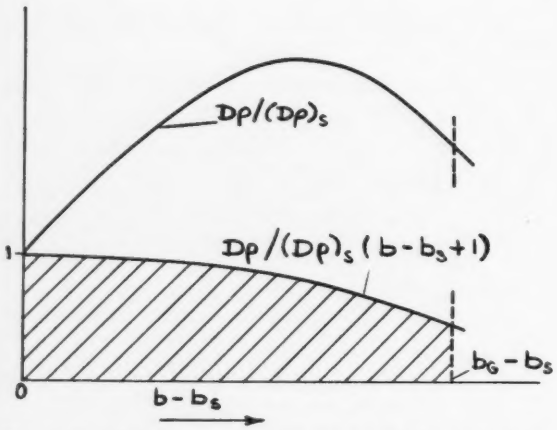

Fig. 2 Determination of burning rate when $D\rho$ depends on temperature and composition

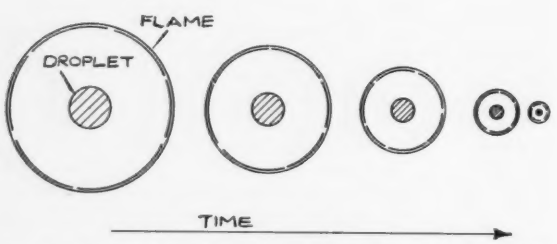

Fig. 3a Appearance of burning droplet: Quasi-steady theory

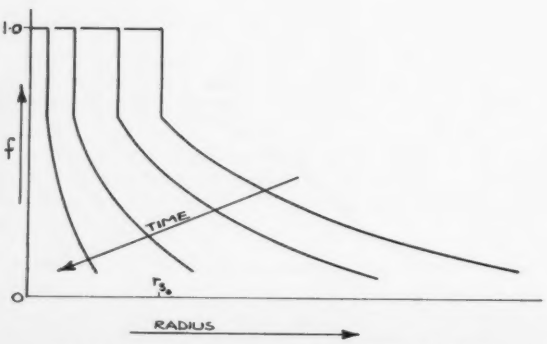

Fig. 3b Fuel fraction profiles: Quasi-steady theory

and in addition we have

$$r = r_S: \quad b = b_S \text{ (gas in contact with the surface)} \qquad [15]$$

$$r = \infty: \quad b = b_G \text{ (gas in the reservoir)} \qquad [16]$$

If the gas can be taken as in thermodynamic equilibrium at all points, $D\rho$ is a known function of b, which may have some such form as that of Fig. 2; the maximum value occurs in the neighborhood of the flame where the temperature is highest. It is known that departures from equilibrium are always small if the flame stays alight (14, 24).

Solution for Burning Rate

Equation [13], with boundary conditions [14, 15 and 16], is easily solved. The burning rate is then obtained from

$$\frac{\dot{m}'' r_S}{(D\rho)_S} = \int_{b_S}^{b_G} \frac{D\rho}{(D\rho)_S} \cdot \frac{db}{(b - b_S + 1)} \qquad [17]$$

which may be evaluated by quadrature; the integral represents the area shaded in Fig. 2.

It is often convenient to express [17] in terms of a mean value of $D\rho$, namely $(D\rho)_m$, and the "transfer number" B, defined by

$$B \equiv b_G - b_S \qquad [18]$$

Then Equation [17] becomes

$$\dot{m}'' r_S/(D\rho)_m = \ln(1 + B) \qquad [19]$$

The mean value of $D\rho$ must therefore be chosen so that

$$(D\rho)_m = \frac{\int_{b_S}^{b_G} \frac{D\rho\, db}{(b - b_S + 1)}}{\ln(1 + B)} \qquad [20]$$

Evaluation of burning rate

Equation [19] can be evaluated, in any particular case, by insertion of the appropriate values for b_G and b_S, in which b can be a dimensionless measure of either composition or enthalpy. The difference B commonly has values of the order of 5 for liquid fuel combustion. Reference (25) contains discussion of the expressions for B which are useful in particular circumstances. In certain cases the exact determination of b_S presents difficulties. Reference (26) describes a method of doing this graphically on an enthalpy-composition chart; this matter will therefore not be discussed further here.

Solution for Burning Time

We now note that the transfer of mass from the particle to the gas phase causes a diminution in the particle radius in accordance with

$$\frac{-dr_S}{dt} = \frac{\dot{m}''}{\rho_p} \qquad [21]$$

where ρ_p is the particle density, which is assumed much greater than the gas density.

If it can be assumed that B and $(D\rho)_m$ are independent of time, it is an easy matter to combine Equations [19 and 21], to integrate, and so to obtain the time for complete disappearance of the particle t_b. We find

$$t_b = r_{S_0}^2 \rho_p / 2(D\rho)_m \ln(1 + B) \qquad [22]$$

where r_{S_0} is the particle radius at time zero.

The variation of flame appearance with time may also be deduced from the equations. It is illustrated in Fig. 3a for comparison with the alternative predictions of the transient theory (Fig. 5b).

Burning time of a liquid close to the critical pressure

Equation [22] shows that the burning time of a particle of given size and density decreases to zero as B increases to infinity. Now B can be written $(h_G - h_S)/Q$; and in many cases Q is equal to the latent heat of vaporization of the fuel. As the critical pressure is approached, the latent heat tends to zero. So the burning time tends to zero also. Comforting though this conclusion is, it must be subjected to examination before acceptance.

Influence of the Neglected Transient Term

Although the burning-rate law (Eq. [19]) has been frequently confirmed experimentally (2, 3, 6 to 10), some of the implications of the quasi-steady theory are entirely incorrect. This fact is illustrated by Fig. 3b, which shows the variation of the fuel fraction f which follows from the solution for b with Equation [11]: Within the fuel particle itself, $f = 1$; at the phase boundary there is a discontinuity in f, which falls off gradually to zero as the radius increases.

The quasi-steady theory leads to the conclusion that f depends on the ratio r/r_S alone, i.e., that all the f profiles are similar. This means that since r_S decreases with time, so does the width of the profile. Now since in evaluating f we take no account of whether the fuel is burned or unburned, it is clear that the area under the f profile is a measure of the amount of fuel in the original fuel particle; the vanishing of this area as time proceeds therefore contravenes the law of conservation of matter.

This unsatisfactory feature results from the neglect of the transient term in the derivation of Equation [13] from Equation [9]. This term becomes increasingly important (because of the multiplier ρ) as the pressure increases. In order to examine its influence, we now abandon the quasi-steady assumption.

Transient Combustion of a Single Fuel Particle

Outline

In this section a fresh approach is made to the prediction of the burning rate of fuel particles introduced into an oxidant gas. The quasi-steady assumption is abandoned, and also its corollary that the rate of burning is identical with the rate of vaporization. This latter assumption is obviously useless when the phase boundary has ceased to exist.

The new theory has two main parts. In the first, the variation of fuel fraction with position and time is established. This part makes use of a result from the theory of unsteady heat conduction. In the second part, the distinction is made between the fuel fraction and the mass fraction of unburned fuel; knowledge of the stoichiometry of the reaction then permits the first part of the theory to be used for the prediction of how the burning rate varies with time. The total time of burning is found incidentally.

High speed computing machinery is needed to integrate the equations when full account is taken of the variation of the gas properties with temperature. This has not been done so far. However, the case of uniform properties is easy to evaluate analytically, and gives information which is adequate for present purposes. This is the case which is discussed below.

The main result is a new formula for burning time (Eq. [34]), which should be used in preference to Equation [22] at high pressures.

Uniform-Property Solution for Fuel Fraction Distribution

Differential equation and boundary conditions

Since we are now not particularly concerned with the phase boundary, there is no advantage in using the variable b. Instead the fuel fraction f will be considered. The corresponding conservation Equation [6], for uniform properties and spherical symmetry, becomes

$$\rho \frac{\partial f}{\partial t} - D\rho \cdot \frac{1}{r^2} \frac{\partial}{\partial r}\left(r^2 \frac{\partial f}{\partial r}\right) = 0 \qquad [23]$$

Here the convection term $\vec{G} \cdot \nabla f$ has disappeared, because, with the initial fuel density assumed equal to the (uniform) gas density, $\vec{G}$ is zero throughout. This follows from consideration of mass conservation.

The boundary condition at large radius is

$$r = \infty : f = f_G \qquad [24]$$

where it has been assumed, for generality, that the surrounding gas already contains a certain amount of fuel.

Another boundary condition is given by the fact that the total amount of fuel in the system is constant. This will be expressed by

$$\int_0^\infty 4\pi r^2 (f - f_G)\, \rho\, dr = W_f(1 - f_G) \qquad [25]$$

where W_f is the mass of fuel injected at time zero symmetrically about the point $r = 0$.[4]

In addition, there are initial conditions (f as function of r at $t = 0$) which state how the fuel is distributed at the moment of injection. The initial condition will be discussed later.

A particular solution

A well-known result of heat conduction theory concerns the distribution of temperature in an infinite solid after a sudden transfer of a finite amount of heat at a point in the solid. This can be used in the present problem. We obtain for the fuel fraction resulting from sudden injection of the quantity W_f of fuel at $r = 0$

$$f - f_G = \frac{W_f(1 - f_G)}{\rho(4\pi Dt)^{3/2}} \cdot e^{-r^2/4Dt} \qquad [26]$$

which is a solution to [23, 26 and 25], as may be verified.

Fitting the initial conditions

The starting condition of most practical interest is that in which the injected fuel is in the form of a sphere, of radius r_{S_0}, in which $f = 1$, surrounded by as yet undiluted oxidant gas, in which $f = f_G$. The corresponding solution for the subsequent fuel distribution can be obtained from Equation [26] by summing the effects of an infinite number of infinitesimal fuel sources, of appropriate magnitude and uniformly distributed over the sphere of radius r_{S_0}.

However it is easy to show that, for times of the order of r_{S0}^2/D and greater, the fuel distribution is practically the same whether the initial source is concentrated at a point or is finite. We shall therefore use Equation [26] without further integration, and shall substitute

$$W_f = \frac{4}{3}\pi r_{S_0}^3 \rho_p \qquad [27]$$

where ρ_p is the initial fuel sphere density, allowed here (and here only) to differ from that of the surrounding gas. Of course the use of Equation [26] is unrealistic at short times, because it then implies f values greater than unity, which are physically impossible.

In this way we simultaneously sidestep the difficulty that the differential Equation [23] does not hold at the phase

[4] The $(1 - f_G)$ term arises because the fuel, immediately on injection, comprises a volume in which $f = 1$; it is the part of this *in excess of* the average fuel fraction f_G which diffuses out.

boundary (if present), where there is a discontinuity in f. The simplifications which are being made are thus diametrically opposed to those of the quasi-steady theory; the present theory may be expected to become exact at just those conditions where the quasi-steady theory is inaccurate.

Fig. 4 shows some successive distributions of f according to Equation [26]. The contrast with Fig. 3b is obvious.

Variation of Flame Radius With Time: Burning Time

In order to proceed further, it is necessary to make the assumption that the gas is everywhere in thermodynamic equilibrium. Then knowledge of the local value of f completely specifies the local gas state, including its temperature, the degree of dissociation, etc.

Stoichiometric considerations

As an example, a fuel is considered which is capable of reacting with the oxidant in only one way, and in which dissociation is negligible. This means that at any point it is possible to have either unburned fuel or unburned oxidant, but not both, and that the mass fraction of unburned fuel m_f is given by

$$m_f = (f - f_{st})/(1 - f_{st}) \qquad [28]$$

where f_{st} is the stoichiometric fuel fraction, and $f > f_{st}$. If $f \leqslant f_{st}$, $m_f = 0$.

Flame radius

The flame is a surface separating the fuel-rich region from the oxidant-rich region, characterized by $f = f_{st}$. Its position may be determined by substituting this value in Equation [26]. The flame is evidently a sphere concentric with the injection point. If its radius is r_{st}, we have

$$\frac{r_{st}^2}{4Dt} = \ln\left[\frac{W_f\,(1 - f_G)}{(f_{st} - f_G)\rho(4\pi Dt)^{3/2}}\right] \qquad [29]$$

This equation permits the flame radius to be evaluated as a function of time. For ease of computation we introduce ϕ, the dimensionless flame radius, and θ, the dimensionless time, defined respectively by

$$\phi \equiv \frac{r_{st}}{[W_f(1 - f_G)/\rho(f_{st} - f_G)]^{1/3}} \qquad [30]$$

$$\theta \equiv \frac{4\pi Dt}{[W_f(1 - f_G)/\rho(f_{st} - f_G)]^{2/3}} \qquad [31]$$

Then Equation [29] becomes

$$\phi = [-(3/2\pi)\theta \ln \theta]^{1/2} \qquad [32]$$

This function is plotted in Fig. 5a. It shows that the flame radius is zero at the moment of injection, increases to a maximum at $\theta = 0.368$, and then diminishes to zero. This is illustrated by the sketches in Fig. 5b. Since the maximum value of ϕ is 0.419, the maximum radius attained by the flame is

$$r_{st_{max}} = 0.419[W_f(1 - f_G)/\rho(f_{st} - f_G)]^{1/3} \qquad [33]$$

This quantity therefore increases in proportion to the cube root of the injected mass and inversely as the cube root of the difference between the stoichiometric fuel fraction and the fuel fraction in the gas reservoir. If the latter gas consists of stoichiometric combustion products, the flame is infinitely far from the point of injection.

Because the fuel is not really injected at a point, Equation [32] is in error for small θ.

Time for complete combustion

One of the most important implications of Fig. 5a is that the flame radius diminishes to zero when $\theta = 1$. This time marks the instant at which all the injected fuel has finally been burned. The time for complete combustion t_b is therefore

$$t_b = \frac{[W_f(1 - f_G)/\rho(f_{st} - f_G)]^{2/3}}{4\pi D} \qquad [34]$$

So the time of burning increases as the two-thirds power of the injected mass, and as the minus two-thirds power of the difference $f_{st} - f_G$. In particular it appears that, if the gas reservoir consists of stoichiometric combustion product ($f_G = f_{st}$), the burning time is infinite; this occurs because, of course, there is no free oxidant in this case.

Variation of Burning Rate With Time

The region within the flame contains unburned fuel. Equations [28 and 26] may be combined to enable the quantity

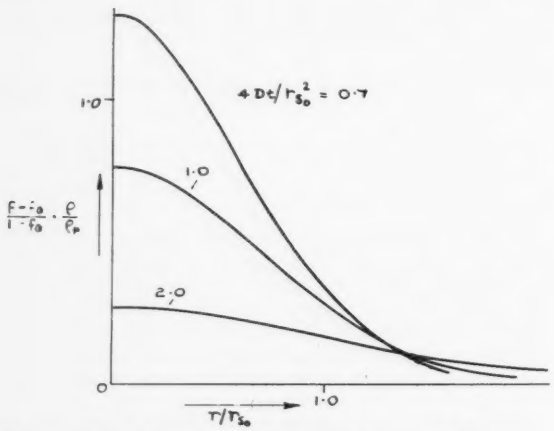

Fig. 4 Successive fuel fraction distributions: Point-source theory

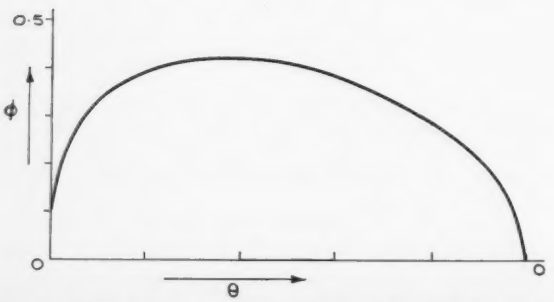

Fig. 5a Flame radius vs. time (Eq. [32]). θ varies from 0 to 1.0

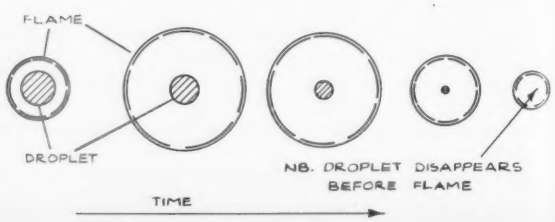

Fig. 5b Appearance of burning droplet: Transient theory

of this fuel to be evaluated. Then the efficiency of combustion η can be related to time and other variables.

If η is defined as unity minus the ratio of the fuel remaining unburned to the injected fuel quantity, we have

$$1 - \eta \equiv \frac{\int_0^{r_{st}} 4\pi r^2 \rho m_f \, dr}{W_f} \qquad [35]$$

Introducing Equations [28 and 26], Equation [35] becomes

$$1 - \eta = \frac{\int_0^{r_{st}} 4\pi r^2 \rho \left\{ f_G - f_{st} + [W_f(1 - f_G)/\rho(4\pi Dt)^{3/2}] e^{-r^2/4Dt} \right\} dr}{W_f(1 - f_{st})} \qquad [36]$$

After some rearrangement, this equation reduces to

$$\frac{(1 - \eta)(1 - f_{st})}{(1 - f_G)} = erf\left[\left(-\frac{3}{2}\ln\theta\right)^{1/2}\right] - \left(\frac{6}{\pi}\right)^{1/2} \theta^{3/2}[(-\ln\theta)^{1/2} + (-\ln\theta)^{3/2}] \qquad [37]$$

where θ is once again the dimensionless time coordinate defined by Equation [31]. $(1 - \eta)(1 - f_{st})/(1 - f_G)$ is plotted vs. θ in Fig. 6.

Examination of Fig. 6 shows that the proportion of unburned fuel diminishes to zero at $\theta = 1$, which agrees with the conclusion about the burning time. At $\theta = 0$, $(1 - \eta)(1 - f_{st}) = 1$; this signifies that the inefficiency of combustion can be greater than 100 per cent. This conclusion is of course unrealistic, and arises from the use of the point-source formula Equation [26] without further integration; for this formula leads to f values on the axis which exceed unity at small θ, and so to *negative* oxidant fractions. It seems wisest to use only the right-hand part of Fig. 6, for practical calculations, and to imagine the left-hand branch to consist of a horizontal line at height $(1 - f_{st})/(1 - f_G)$.

The burning rate is obtained by differentiating Equation [37]. We obtain

$$\frac{(1 - f_{st})\, d\eta}{(1 - f_G)\, d\theta} = \left(\frac{27}{2}\right)^{1/2} \theta^{1/2}(-\ln\theta)^{3/2} \qquad [38]$$

This function is also plotted in Fig. 6. It is seen to have a maximum at $\theta = 0.0498$, which in many cases will be in the "unrealistic" period.

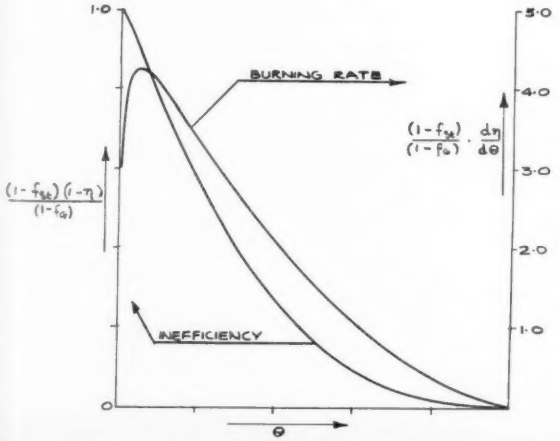

Fig. 6 Unburned fuel proportion and burning rate. θ varies from 0 to 1.0

Discussion

Comparison of Present and Quasi-Steady Theories

Comparison of flame behavior

Figs. 3a and 5b illustrate qualitatively the differing predictions of the two theories. According to the quasi-steady theory, the flame shrinks steadily in proportion to the droplet radius[5]; according to the transient theory, it increases at first and then decreases. Experimental data are available showing that, even at atmospheric pressure, droplet flames exhibit the latter behavior rather than the former (11). However, if the droplet is introduced at a temperature lower than its wet-bulb temperature, the initial value of B is less than the final value; then even the quasi-steady theory will predict an initial increase of flame size while the droplet is heating up. These data cannot therefore be taken as confirming the importance of transient effects in the gas phase, although they certainly indicate their importance in the liquid phase.

Comparison of burning times

In order to compare the burning time predicted by the quasi-steady theory $(t_b)_{q.s.}$ with that of the present (point-source) solution $(t_b)_{p.s.}$, Equations [22, 27 and 34] will be combined. We obtain

$$\frac{(t_b)_{q.s.}}{(t_b)_{p.s.}} = 2.82\left(\frac{\rho_p}{\rho}\right)^{1/3} \frac{(f_{st} - f_G)^{2/3}/(1 - f_G)^{2/3}}{\ln(1 + B)} \qquad [39]$$

Evidently, if this fraction is much greater than unity, the quasi-steady formula [22] should be used for burning time; if it is much smaller than unity, the transient formula [34] should be used. When the fraction is of the order of unity, both formulas will underestimate the burning time; in the absence of an analysis of the "mixed" regime, it is probably wisest to take the sum of $(t_b)_{q.s.}$ and $(t_b)_{p.s.}$ as the burning time. The corresponding formula for t_b is therefore

$$t_b = \left[1 + 2.82\left(\frac{\rho_p}{\rho}\right)^{1/3} \frac{(f_{st} - f_G)^{2/3}/(1 - f_G)^{2/3}}{\ln(1 + B)}\right] \times \frac{\{W_f(1 - f_G)/\rho(f_{st} - f_G)\}^{2/3}}{4\pi D} \qquad [40]$$

Example

To fix ideas, we consider a liquid oxygen droplet burning with kerosene at 40-atm pressure in a rocket motor with $f_G = 0.25$ (fuel rich). For these propellants we have $f_{st} = 0.226$. Other data required are: $\rho_p/\rho = 382$, $B = 134.2$.

Replacing f by $1 - f$ in Equation [39] (since an oxidant particle is in question), the ratio of burning times can now be determined; it is 0.88. So here the two predicted burning times are of the same order of magnitude for the oxidant. For the fuel, of course, the transient formula *must* be used, since kerosene has a critical point below 40 atm.

Influence of pressure

The density ratio of particle to gas appears in Equation [39] and causes the burning time ratio to decrease as the pressure

[5] Using the quasi-steady theory, and Equations [11 and 27], it is easy to show that the flame radius r_{st} is given by

$$r_{st} = \frac{\left(\frac{3}{4\pi} \cdot \frac{W_f}{\rho_p}\right)^{1/3}\left[1 - \frac{2t \cdot (D\rho)_m \ln(1 + B)}{r_{s0}^2\, \rho_p}\right]^{1/2}}{1 - \frac{\ln\left[1 + \frac{B(1 - f_{st}) + (f_G - f_{st})}{1 - f_G}\right]}{\ln(1 + B)}}$$

rises, with fixed particle density; for ρ is proportional to pressure. The point-source formula is therefore the one to use at high pressures.

There is another effect of pressure, however. As has been pointed out above, B tends to infinity as the critical pressure is approached, because the latent heat of vaporization vanishes. This effect causes the fraction in Equation [39], which reappears in Equation [40], to diminish still more. Once again it is the transient terms which dominate the solution.

The transport property $D\rho$ is practically independent of pressure for gases. To show the effect of pressure on the burning time predicted by the point-source solution, we rearrange Equation [34] to give

$$t_b = \frac{\rho^{1/3}[W_f(1 - f_G)/(f_{st} - f_G)]^{2/3}}{4\pi\, D\rho} \qquad [41]$$

Since ρ is proportional to pressure, Equation [41] shows that the burning time of a particle of fixed mass increases in proportion to the cube root of the pressure. This throws light on the increasing relevance of the transient terms in the equation from a different point of view, for the quasi-steady prediction of burning time is independent of pressure and is bound to be increasingly in error as the pressure rises.

Influence of f_G

In most engines, fuel particles are injected into gases containing an appreciable proportion of combustion products; in rockets for example, $f_{st} - f_G$ may be of the order of 0.1. Now it is easy to prove that such a dilution of the oxidant gas has very little effect on the value of the transfer number B, and so still less on $\ln(1 + B)$. It follows that dilution of oxidant gas by combustion products decreases the ratio in Equation [39] and again makes the burning time nearer to that predicted by the present theory.

Influence of particle size

In one respect the quasi-steady and transient formulas agree: The burning time is proportional to the square of the diameter of the injected particle, i.e., to $(W_f)^{2/3}$. So fine subdivision of the injected fuel is important for fast burning, whichever formula is appropriate.

Influence of Approximations Made During the Analysis

It should be noted that the analysis leading to the new burning time formula [34] involves a number of departures from reality. These include:

1 In the differential equations of conservation, the main relevant assumption is that all chemical substances possess identical diffusion coefficients.

2 Thermodynamic equilibrium has been supposed to prevail throughout.

3 This equilibrium assumption has been supposed to imply that unburned fuel and oxidant cannot have finite concentrations at the same point; dissociation and the possibility of more than one set of reaction products have been neglected.

4 D and ρ have been assumed uniform throughout the gas.

5 The injection of a fuel particle of finite size has been simulated by an instantaneous point source of fuel.

6 The mutual influence of neighboring droplets has been neglected.

We will discuss the influence of each of these assumptions in turn:

1 This assumption is necessary and usual. It involves only a small departure from reality unless very heavy or very light molecules are present.

2 This assumption probably accords well with reality in rocket motors owing to the rapid chemical reaction rates pertaining to high pressures and temperatures.

3 This assumption represents too crude a picture. In rocket motors, for example, the addition of further fuel to a stoichiometric fuel-oxidant mixture *would* cause further reaction. However the present assumption has the advantage of clarity and approximate correctness.

4 and 5 These assumptions are certainly incorrect, and cause the theoretical predictions for the early stage of burning to be in error; they have much less effect at larger times. The assumptions can be removed without difficulty if sufficient computing effort is available to permit numerical solution of the nonsimplified equations.

6 This neglect, together with assumption 3, is responsible for the implication that no burning takes place if f_G is already equal to f_{st}. In reality of course, fuel particles can burn under these conditions because oxidant particles are present within a finite distance. This matter has been analyzed by the author and will be reported elsewhere.

Conclusions

The quasi-steady formula for the burning time of a fuel (or oxidant) particle underestimates the burning time when the pressure is large, the transfer number becomes high and the gas condition approaches the stoichiometric.

The recommended formula for the burning time of a fuel particle, irrespective of conditions, is Equation [40]. This is valid far above and far below the initial point; its validity when both terms are of the same order requires further examination.

The burning time increases the nearer to stoichiometric is the fuel-oxidant ratio of the atmosphere surrounding the particle.

It will be necessary to re-examine, in the light of the present theory, the conclusions drawn from studies of the role of particle burning in the performance of liquid fuel rocket motors (27 to 29). Although the present theory agrees with the earlier ones in showing that fine fuel subdivision is favorable, it shows that the important propellant properties may be considerably different from those which have previously attracted attention.

Acknowledgment

This paper arose out of an examination of Summerfield's theory (30) of the burning of solid composite propellants. Using dimensional arguments, and considering *only* transient processes, Summerfield deduced the result that the burning time of a particle is proportional to the square of the particle diameter, divided by the diffusion coefficient, and hence increases as the cube root of the pressure; Equation [34] is thus a more complete version of Summerfield's result.

The author is grateful to Miss M. P. Steele for carrying out the computations and plotting the curves.

Nomenclature

b	=	dimensionless generalized mass transfer variable
B	=	$(\equiv b_O - b_S)$, transfer number
c	=	specific heat at constant pressure
D	=	diffusion coefficient
f	=	fuel fraction (mass of fuel, whether burned or not, in unit mass of mixture)
h	=	enthalpy
k	=	thermal conductivity
m_j	=	mass fraction of chemical compound j in mixture
n_α	=	mass fraction of chemical element α in mixture
$n_{\alpha,j}$	=	mass of element α in unit mass of compound j
p	=	pressure
P	=	general conserved property
Q	=	heat transfer from gas per unit mass changing phase
r	=	radius
t	=	time

T = temperature
$\dot{m}''$ = mass flow rate per unit area through phase boundary
$\vec{G}$ = mass flow rate vector
W = injected mass
η = efficiency of combustion
$\theta \equiv 4\pi Dt/[W_f(1 - f_G)/\rho(f_{st} - f_G)]^{2/3}$
ρ = density
$\phi \equiv r_{st}/[W_f(1 - F_G)/\rho(F_{st} - F_G)]^{1/3}$

Subscripts

α = chemical element
b = complete burning
f = fuel (unburned)
F = fuel reservoir
G = gas reservoir
j = chemical compound
m = mixture, mean
O = oxidant
p = injected particle
$p.s.$ = point-source theory
$q.s.$ = quasi-steady theory
S = gas in equilibrium with surface
S_0 = initial surface
st = stoichiometric
T = transferred substance

References

1 Spalding, D. B., "Fourth Symposium on Combustion," Williams and Wilkins, Baltimore, 1953, p. 854. *See also* "Combustion of Liquid Fuel in a Gas Stream," *Fuel*, vol. 29, 1950, p. 25; and "Combustion of Fuel Particles," *Fuel*, vol. 30, 1951, p. 121, for early treatments of this problem.

2 Hottel, H. C., Williams, G. C. and Simpson, H. C., "Fifth Symposium on Combustion," Reinhold Publishing Corp., New York, 1955, p. 101.

3 Goldsmith, M. and Penner, S. S., "On the Burning of Single Drops of Fuel in an Oxidizing Atmosphere," JET PROPULSION, vol. 24, 1954, pp. 245–251.

4 Agafanova, F. A., Gurevich, M. A. and Paleev, I. I., "Theory of Burning of a Liquid Fuel Drop," *Soviet Physics, Tech. Phys.*, vol. 2, 1958, p. 1689.

5 Varshavskii, G. A., "Burning of a Liquid Fuel Drop" (Diffusion Theory), 1945 (*sic.* see reference 4).

6 Godsave, G. A. E., "Fourth Symposium on Combustion," Williams and Wilkins, Baltimore, 1953, p. 818.

7 Kumagai, S. and Kimura, I., "Combustion of Fuel Droplets," *Science of Machine*, vol. 3, 1951, pp. 431–434.

8 Kumagai, S. and Isoda, H., "Experimental Study on Evaporation and Combustion of Fuel Droplet," *Science of Machine*, vol. 4, 1952. pp. 337–342.

9 Kobayasi, K., "Fifth Symposium on Combustion," Reinhold Publishing Corp., New York, 1955, p. 141.

10 Bolt, J. A. and Saad, M. A., "Sixth Symposium on Combustion," Reinhold Publishing Corp., New York, 1957, p. 717.

11 Kumagai, S. and Isoda, H., "Sixth Symposium on Combustion," Reinhold Publishing Corp., New York, 1957, p. 726.

12 Fuchs, N., *Phys. Zeitschr. USSR*, vol. 6, 1934, p. 224. (Title of paper not available.)

13 Shvab, V. A., "Relation Between the Temperature and Velocity Fields of the Flame of a Gas Burner," *Gos. Energ. izd.* M-L, 1948.

14 Zeldovich, Y. B., "On the Theory of Combustion of Initially Unmixed Gases," NACA TM 1296, 1951; *also Zh. Tekh. Fiz.*, vol. 19, 1949, p. 1199.

15 Browne, W. G. and Powell, H. N., "A Principle of Mixing Similarity and Its Application to Inhomogeneous Combustion," Aircraft Gas Turbine Div., General Electric Co., Cincinnati, Rep. R 56AGT266, May 22, 1956.

16 Lees, L., "Combustion and Propulsion Third AGARD Colloquium," Pergamon Press Ltd., London, 1958, p. 451.

17 Bromberg, R. and Lipkis, R. P., "Heat Transfer in Boundary Layers With Chemical Reactions Due to Mass Addition," JET PROPULSION, vol. 28, no. 10, Oct. 1958, pp. 668–674.

18 Emmons, H. W., "The Film Combustion of Liquid Fuel," *Z. Angew. Math. Mech.*, vol. 36, 1956, p. 60.

19 Emmons, H. W., "Theoretical Aerothermodynamics," 1958 Heat Transfer and Fluid Mechanics Inst., Stanford Univ. Press, Stanford, Calif.

20 Hartnett, J. P. and Eckert, E. R. G., "Mass Transfer Cooling With Combustion in a Laminar Boundary Layer," 1958 Heat Transfer and Fluid Mechanics Inst., Stanford Univ. Press, Stanford, Calif.

21 Sutton, G. W., "Seventh Symposium on Combustion," Butterworths Scientific Pub., London, 1958, p. 539.

22 Coffin, K. P. and Brokaw, R. S., "A General System for Calculating Burning Rates of Particles and Drops and Comparison of Calculated Rates for Carbon, Boron, Magnesium and Iso-octane," NACA TN 3929, 1957.

23 Merk, H. J., "The Macroscopic Equations for Simultaneous Heat and Mass Transfer in Isotropic, Continuous and Closed Systems," *Appl. Sci. Res.*, Section A, vol. 8, p. 73.

24 Spalding, D. B., "A Theory of the Extinction of Diffusion Flames," *Fuel*, vol. 33, July, 1954, p. 255.

25 Spalding, D. B., "Some Fundamentals of Combustion," Butterworths Scientific Pub., London, 1955, p. 96.

26 Spalding, D. B. and Tyler, R. D., "Graphical Representation of Thermodynamic Properties of Reacting Two-Phase Mixtures," International Union Pure and Appl. Chem./I. Mech. Engrs. Joint Conference, 1957, paper 1, session 4.

27 Priem, R. J., "Propellant Vaporization as a Criterion for Rocket Engine Design; Calculations of the Length to Vaporize a Single n-Heptane Drop," NACA TN 3985, 1957.

28 Spalding, D. B., "Combustion in Liquid-Fuel Rocket Motors," *Aeron. Quart.*, vol. 10, 1959, p. 1.

29 Mayer, E., "Vaporization Rate Limited Combustion in Bipropellant Rocket Chambers," ARS JOURNAL, vol. 29, no. 7, July 1959, pp. 505–513.

30 Summerfield, M., "Theory of Burning of a Composite Solid Propellant," ARS preprint, 1958.

Vaporization of Propellants in Rocket Engines

RICHARD J. PRIEM[1] and MARCUS F. HEIDMANN[1]

NASA,
Lewis Flight Propulsion Laboratory
Cleveland, Ohio

The theory and equations required to calculate the vaporization rates in a rocket engine, based on a model considering propellant vaporization as the rate controlling combustion process, are presented. Included in the model are changes in combustion gas velocity, droplet velocity, temperature and mass. The vaporization rates of heptane, ammonia, hydrazine, liquid fluorine and liquid oxygen sprays were computed for various log probability distributions and mass median drop sizes of the spray. The rates were also calculated for an engine operating with various injection velocities, final gas velocities, initial propellant temperatures and chamber pressures. The calculations of the per cent of propellant vaporized are correlated with an effective chamber length. The correlated results show that the percent of propellant vaporized can be increased either by decreasing the mass median drop size and the initial drop velocity or by increasing the chamber length, chamber pressure, final gas velocity and initial fuel temperature. A method of analysis that relates experimental rocket engine performance to the quantity of liquid propellant vaporized is also presented. With this method experimental engine performance results are compared with the calculations. The comparison suggests that incomplete vaporization is responsible for combustor inefficiency. Experimental results agree with the calculations for sprays having a geometric standard deviation of 2.3 and a mass median drop radius of 70 to 240 microns, depending on the type of injector.

THE LARGE number of different phenomena that can have a fundamental role in the combustion within a liquid propellant rocket engine makes it difficult to determine and study the controlling process. Some of these phenomena, as given in (1 and 2),[2] are atomization, heating, vaporization, liquid and gaseous diffusion, combustion of droplets, and liquid or gas phase reaction. The consideration of all of these phenomena results in a large number of similarity parameters (1 to 4) that should be used in designing and scaling rocket engines.

The inherent complexity of the problem, when all the phenomena are considered, make it desirable to simplify the problem. Simplification is obtained by neglecting those processes that require only a small time or distance in the chamber, and by considering only the phenomena that require the greatest time or distance. Recent studies (5 to 9) show that the atomization, heating, gaseous diffusion and gas phase reaction require only a small fraction of the rocket chamber length under normal operation. Liquid diffusion and reaction are only encountered with premixing rocket injectors using certain hypergolic propellants, as nitric acid, with some fuels. Therefore, vaporization and combustion of droplets remain to be evaluated. The results reported in (10) indicate that vaporization rate equations evaluate both the vaporization and the combustion of droplets. The results of an analytical study of the importance of propellant vaporization rates on rocket engine combustor efficiency are reported herein.

Of the various techniques (11 to 14) for determining vaporization rates, the one given in (14) seemed most applicable to the conditions encountered in rocket engines. This technique permits consideration of the heating period of the drop, unidirectional diffusion and the effect of mass transfer on heat transfer. Furthermore, the results of the technique are in good agreement with the experimental results of single-drop investigations over a wide range of conditions that approach those encountered in rocket engines (9, 15 and 16). Therefore, this technique (14) was used to calculate the vaporization rates of sprays by using a model which assumes that the vaporization of the propellants is the rate controlling step in rocket engine combustion. The analysis also assumes one-dimensional steady-state flow with no interaction between drops and no shattering of drops. Many combustor parameters were varied to show how they affected the combustion chamber length required to vaporize the propellant. The calculations were made for five propellants: Heptane, ammonia, hydrazine, liquid oxygen and liquid fluorine. From these results a general correlation was developed to adequately cover the range of parameters studied.

By assuming that droplet evaporation is the rate limiting step in rocket combustion, the performance of a propellant combination can be either correlated or predicted from calculated vaporization rates. This was done for the heptane-liquid oxygen system. The experimental performance of one injector was correlated over a wide range of operating conditions, and the performance of six different injectors was predicted and compared with experimental values.

Theory

The calculation technique was based on applying known steady-state mass, momentum and heat transfer equations to droplets vaporizing in a rocket engine. The first order differential equations were set up using the model shown in Fig. 1 for a single drop.

A liquid droplet is shown at position x and at a small increment later in time $\Delta\theta$ and distance Δx. During this increment the drop velocity v changes by a small amount Δv. In this same increment, the gas velocity u changes by Δu. The drop velocity would start at the injection velocity and either slow down or speed up, as determined by the drag on the drop. The gas velocity is zero at the injector and increases

Presented at the ARS 13th Annual Meeting, New York, N. Y., Nov. 17–21, 1958.

[1] Aeronautical Research Scientist.

[2] Numbers in parentheses indicate References at end of paper.

downstream as the propellants vaporize and burn. While the drop is moving through the increment, heat is transferred to the liquid surface at a constant rate q_v, and mass is being transferred from the surface at a constant rate w; oxidant is added to burn the vaporizing fuel (or vice versa) instantaneously at stoichiometric conditions. During the increment, the mass and the radius of the drop change from m_1 to m_2 and r_1 to r_2, respectively, while the temperature T_l changes by ΔT_l.

The equations used to determine the mass transfer rate are:

$$w = A_s K p \alpha \quad [1]$$

$$Nu_M = \frac{2rK}{DM/\bar{R}T} = 2 + 0.6\, Sc^{1/3} Re^{1/2} \quad [2]$$

$$\alpha = \frac{P}{p} \ln \frac{P}{P - p} \quad [3]$$

The Ranz and Marshall (17) correlation (Eq. [2]) was used for the Nusselt number Nu_M, since a heat transfer and mass transfer correlation had been determined therein under conditions involving simultaneous heat and mass transfer. Also, the nature of their investigation was similar to that studied in this paper, although the maximum temperatures and pressures were not as high as those used in this investigation. The mass transfer equation included the α term to account for unidirectional diffusion in the theory presented in (14 and 18). The α factor is always greater than 1 and ranged between 1 and 3 in these calculations.

The rate of heat transfer to the liquid surface is obtained from the following equations

$$q_v = A_s h (T_g - T_l) Z \quad [4]$$

$$Nu_H = h2r/k = 2 + 0.6\, Pr^{1/3} Re^{1/2} \quad [5]$$

$$Z = z/(e^z - 1) \quad [6]$$

$$z = w c_{p,\,f}/h A_s \quad [7]$$

The Ranz and Marshall (17) correlation for the heat transfer Nusselt number Nu_H was used for the same reasons given for mass transfer. The heat transfer included the Z term to account for the sensible heat taken up by the diffusing vapor as required in the theory presented in (14 and 19). The value of Z is always less than 1 and ranged between 1 and 0.05 in these calculations.

The change in drop temperature is determined by

$$\frac{dT_l}{d\theta} = \frac{q_l}{m c_{p,\,l}} \quad [8]$$

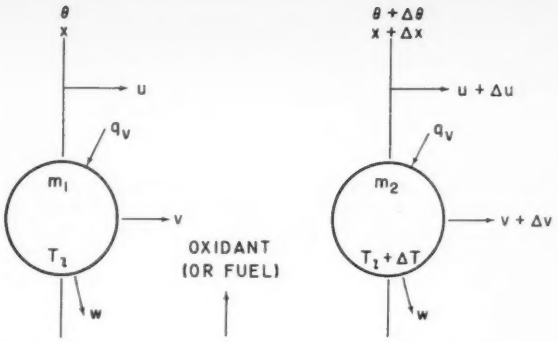

Fig. 1 Schematic model of fuel or oxidant drops vaporizing in rocket engine

where

$$q_l = q_v - w\lambda \quad [9]$$

The drop velocity was calculated from equations for aerodynamic drag

$$\frac{mdv}{d\theta} = -C_D A_c \rho \frac{U^2}{2} \quad [10]$$

The drag coefficient obtained by Ingebo (20) was used as it was determined for evaporating sprays over a Reynolds number range of 6 to 400

$$C_D = 27\, Re^{-0.84} \quad [11]$$

No correction was added for the effect of mass or heat transfer on the drag coefficient. The equation was also used for Reynolds number as large as 2000.

The gas velocity equation is derived from the assumption that stoichiometric reaction follows instantaneously after evaporation; thus the gas phase consists only of reaction products. Therefore, gas velocity, developed by mass addition at constant temperature and pressure, is directly proportional to the fraction of propellant evaporated and is given by Equation [12], which was derived in (21) for a single drop and in (22) for sprays

$$\frac{u}{u_{fin}} = 1 - \sum n_i m_i / \sum n_i m_{i,\,0} \quad [12]$$

Table 1 Range of conditions used for calculations

Initial drop temperature, R					Mass median drop radius, in.	Geometric standard deviation	Initial drop velocity, in./sec	Final gas velocity, in./sec	Chamber pressure, lb/in.²
Heptane	Ammonia	Hydrazine	Oxygen	Fluorine					
400	300	...	...	...	0.003	2.3	1200	9600	300
500[a]	400[a]	500[a]	140[a]	140[a]	0.003[a]	2.3[a]	1200[a]	9600[a]	300[a]
					0.001	2.3	1200	9600	300
					0.003	2.3	600	9600	300
							1200	2400	300
								9600	150
								9600	600
								19,200	300
							2400	9600	300
					0.009	2.3	1200	9600	300
700	500	700	220	220	0.003	2.3	1200	9600	300

[a] Conditions used for calculations presented in Figs. 3 to 6.

For calculation purposes the propellant was assumed to be in five groups of drop sizes, which were arbitrarily selected to correspond to a log-probability distribution as described in (23) by

$$\frac{dR}{dr} = \frac{a}{r} \exp\left\{-\frac{1}{2}\left[\frac{\ln (r/M_{g,M})}{\ln \sigma_g}\right]^2\right\} \qquad [13]$$

The five sizes were chosen from the log probability distribution as those equal to 10, 30, 50, 70 and 90 per cent of the mass in drops smaller than the drop radius. The number of drops in each group was so chosen that each group had 20 per cent of the total mass. Plots of the distribution obtained by this method and from Equation [13] are shown in Fig. 2 for a geometric standard deviation σ_g of 2.3. The geometric standard deviation is a spray characteristic where 68.23 per cent of the mass is in the drop size range between $M_{g,M}/\sigma_g$ and $\sigma_g M_{g,M}$.

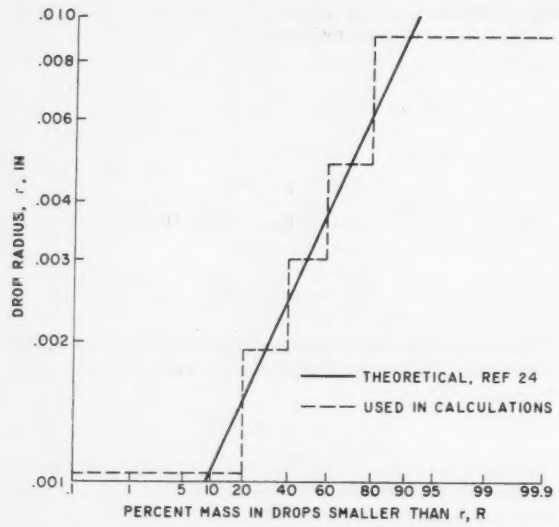

Fig. 2 Drop size mass distribution for standard deviation of 2.3

The vaporization equations were solved numerically by an iterative procedure to obtain the per cent of propellants vaporized in various chamber lengths. Table 1 shows the spray conditions as well as the design and operating parameters used in the calculations. Physical properties used in the calculations for the various propellants are given in the appendix of (24).

The relation between combustor efficiency η_c (characteristic exhaust velocity efficiency) and per cent of propellants vaporized was obtained by considering the exhaust to be a mixture of oxidant drops, fuel drops and gaseous combustion products. The gaseous combustion products were assumed to be in thermodynamic equilibrium, and the volume and kinetic energy of the drops were assumed to be negligible. Efficiency is then related to vaporized propellant by the following equation, derived in (25)

$$(\eta_c) = \frac{(c_{th}^*)_{O/\mathfrak{F}}}{(c_{th}^*)_{O/F}} \left(\frac{\mathcal{O}\dot{w}_o + \mathfrak{F}\dot{w}_f}{\dot{w}_o + \dot{w}_f}\right) \qquad [14]$$

Results and Discussion

Analytical Results

The results of the vaporization calculations are droplet histories, examples of which are shown in Figs. 3 to 6 for the various propellants. The conditions for which these calculations were performed are indicated by asterisks in Table 1. The calculated temperatures of the mass median drops are shown in Fig. 3. With all propellants, the temperature of the droplet rises to within 1 degree of a constant temperature (wet bulb) in less than one tenth of the distance required to vaporize the drop.

Typical histories of the per cent of propellant vaporized for various propellants are shown in Fig. 4 for the mass median

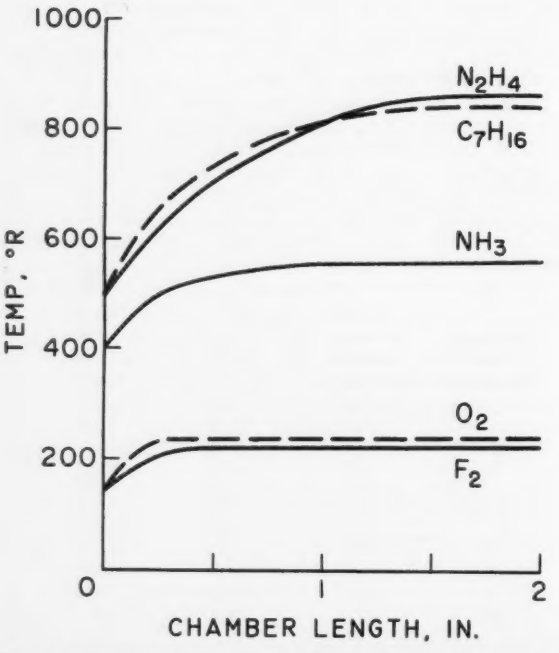

Fig. 3 Typical droplet temperature histories for various propellants. [Conditions used in calculations given by (a) in Table 1]

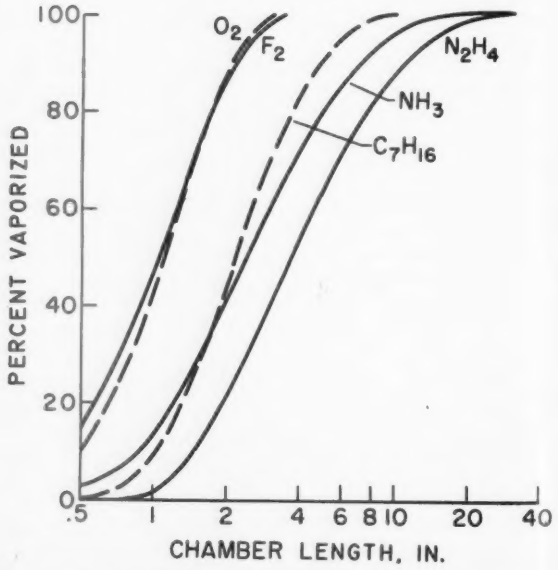

Fig. 4 Typical droplet mass histories as shown by per cent vaporized for various propellants. [Conditions used in calculations given by (a) in Table 1]

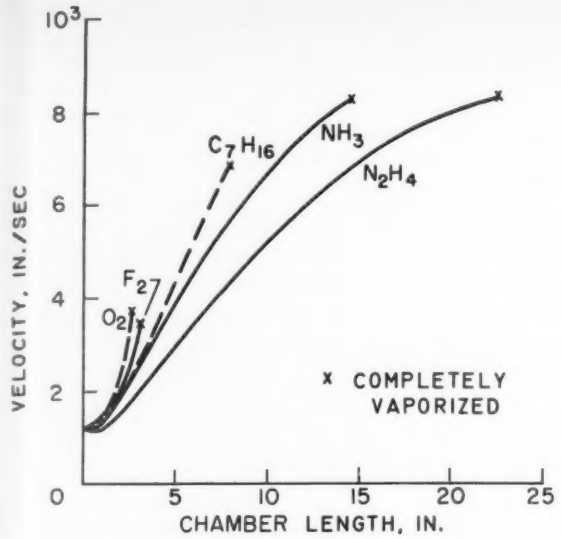

Fig. 5 Droplet velocity histories for various propellants. [Conditions used in calculations given by ([a]) in Table 1]

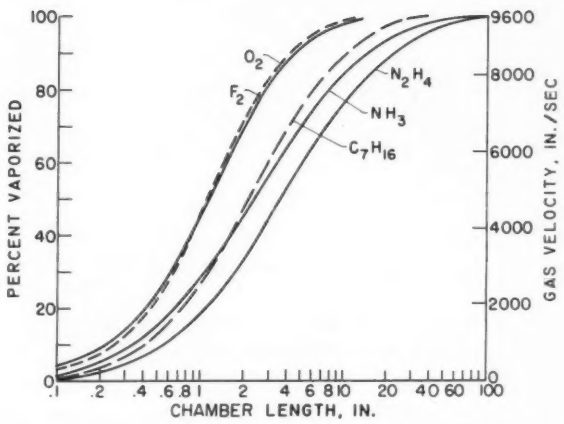

Fig. 6 Typical average mass histories, as shown by per cent vaporized. [Conditions used in calculation given by ([a]) in Table 1]

drops. The curves are similar for all propellants. The oxidants—oxygen and fluorine—vaporize in shorter lengths than the fuels—heptane, ammonia and hydrazine; the length increases in the order listed.

Drop velocity histories of the mass median drops are given in Fig. 5. The drop velocity first decreases because of the drag produced by the low gas velocity. After reaching a minimum, the drop velocity is increased because of increasing gas velocity.

Per cent of total mass vaporized is shown in Fig. 6. Since the per cent of mass vaporized (for all drops) is proportional to the gas velocity (Eq. [12]), the gas velocity is also shown in this figure. The per cent vaporized in a given length was greatest with oxygen and fluorine and decreased with heptane, ammonia and hydrazine, in that order. Comparison of the per cent of the mass median drops vaporized (Fig. 4) with the total mass vaporized (Fig. 6) shows that with heptane the mass median drops are completely vaporized in 9 in., but that only 88 per cent of the total mass is vaporized in that length. This difference is due to the large drops that are only partially vaporized. It is the large drops in the spray, therefore, that reduce combustor efficiency. Curves showing the effect of various operating parameters on the per cent vaporized for single heptane drops may be found in (21). The effect of changing the propellant spray characteristics is given in (22).

The relation between per cent fuel and oxidant vaporized and combustor efficiency, as determined from Equation [14], is shown in Fig. 7 for heptane and oxygen. For equal fractions of fuel and oxidant vaporized, the combustor efficiency is equal to the per cent vaporized. Each value of efficiency, however, may be obtained with various relations between the per cent oxidant and fuel vaporized. Additional curves relating performance to propellant vaporized for various mixture ratios can be found in (25) for hydrogen-fluorine, hydrogen-oxygen, ammonia-fluorine and JP-4-oxygen propellant combinations.

Correlation of Analytical Results

Vaporization histories similar to those in Figs. 3 to 6 were obtained for heptane, ammonia, hydrazine, oxygen and fluorine as listed in Table 1. A range in chamber pressure of 150 to 600 psi, median drop radius of 0.001 to 0.009 in., droplet velocity of 600 to 2400 in. per sec, and gas velocity of 2400 to 19,200 in. per sec was covered. An attempt was made to fit the results for each propellant over these ranges of conditions to a single curve, usable for engine design. The correlation of results was accomplished by modifying chamber length with a correction factor to obtain an effective chamber length

$$\text{Effective length} = LP^{0.66}u_{fin}{}^{0.40}\,1.9 \times 10^{-5}/(1 - T_r)^{0.40}M_g{}_{.M}{}^{1.45}v_0{}^{0.75} \quad [15]$$

A plot of the per cent mass unvaporized as a function of effective length for heptane sprays with a distribution of 2.3 is shown in Fig. 8. The log-log plot is used in Fig. 8 and in

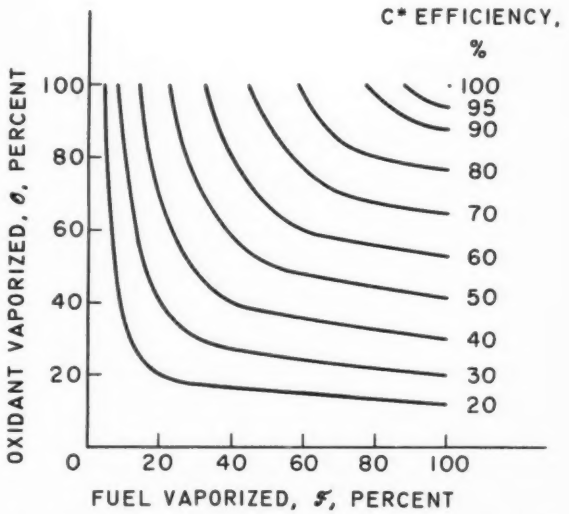

Fig. 7 Percentages of vaporized fuel and oxidant required to maintain a given C^* efficiency. Propellants, heptane and oxygen; oxidant-fuel weight ratio, 2.2

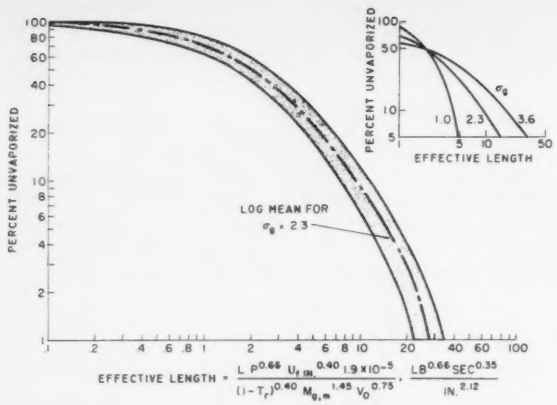

Fig. 8 Correlated results for all combustor conditions with heptane sprays

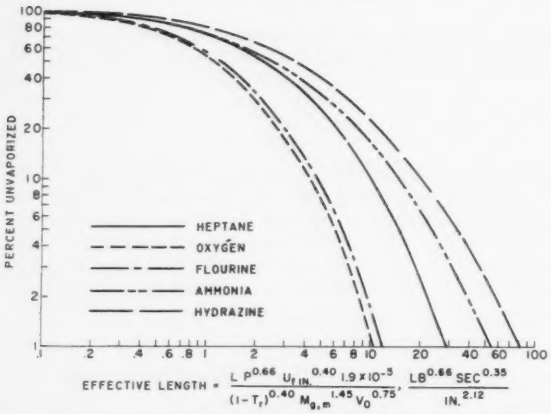

Fig. 9 Correlated results for all combustor conditions with various propellant sprays which have a particular distribution. (Standard deviation of 2.3)

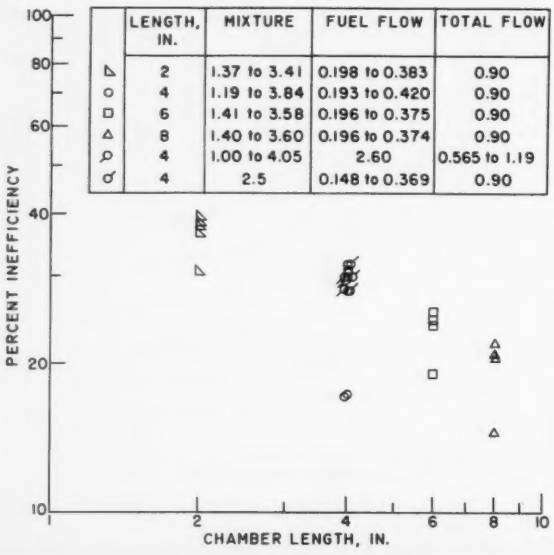

Fig. 10 Combustor efficiency for various chamber lengths and flow conditions

subsequent figures to obtain better resolution in the 90 to 100 per cent vaporized region. The combustor length required to vaporize a given percentage propellant increases with increasing drop size and injection velocity, and with decreasing gas velocity and chamber pressure. The spread in effective length required to vaporize a given per cent of propellant for various conditions was approximately ±20 per cent about the log mean curve.

The spray distribution of 2.3 used to obtain Fig. 8 and subsequent figures corresponds to that observed in (6) for an impinging-jet injector. The effect of using a different distribution is illustrated in Fig. 8. Additional calculations can be found in (24).

The correlation of per cent of mass unvaporized with effective length for various propellants is shown in Fig. 9. Only the log mean curve is shown. The spread in effective length for various conditions was always less than ±20 per cent for all propellants. The curves for fluorine and oxygen are almost identical with the effective lengths required to vaporize a given percentage of propellant increasing in order with heptane, ammonia and hydrazine.

Correlation of Combustor Data

The correction factor to obtain an effective length (Eq. [15]) may also be used in the correlation of experimental combustor data. Experimental heptane-oxygen combustor efficiencies for a given injector, in which propellant flows, mixture ratios, chamber pressure and chamber length were varied, are shown in Fig. 10. The injector used two impinging jets of heptane to produce a sheet and was similar to that used in (6). The liquid oxygen was finely atomized by using very small injector orifices and, therefore, could be assumed to be completely vaporized in the shortest chamber investigated. The plot of combustor efficiency against chamber length (Fig. 10) shows that a wide variation in efficiency was obtained with the various conditions. Converting combustor efficiency to per cent fuel vaporized by use of Equation [14] resulted in the correlation of the data as shown in Fig. 11. Modifying the chamber length by the correction factor to obtain an effective length (Eq. [15]) produces the curve of per cent of fuel vaporized against effective length shown in Fig. 12. The absolute value of the results agrees with the correlated analytical results shown by the shaded area in Fig. 12. The spread in the data was less than that of the correlated results. The mean drop size $M_{g,M}$ for the various data points was calculated from the following equation obtained from (6)

$$D_j/M_{g,M} = 1.12\sqrt{D_j V_j} + 0.108\, D_j |V_g - V_j| \qquad [16]$$

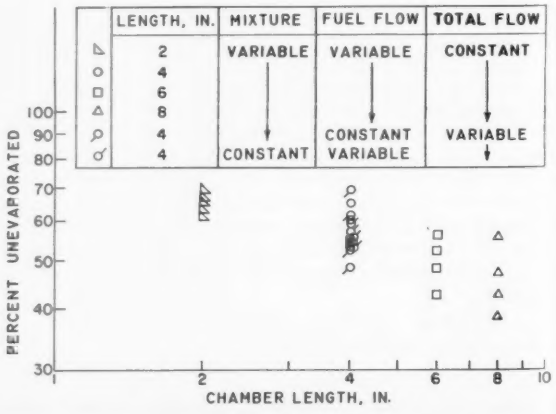

Fig. 11 Propellant vaporized for various chamber lengths and flow conditions

Table 2 Drop sizes produced by various injector types

Injector type	Mass mean radius, μ	Mass mean radius, ref. 6
jets	240	...
sheets	95	92
triplet	70	...

In this equation the diameter of the jet D_j and the jet velocity V_j are directly calculated from the experimental conditions. However, the gas velocity V_g cannot be determined in this manner. This velocity increases from zero at the injector face to the final velocity at the point where all the heptane is evaporated. An average value of 1200 in. per sec was assumed for this calculation. This velocity corresponds to the velocity attained about one quarter of the way down the chamber, or it could be the velocity perturbations produced by small pressure fluctuations.

The comparison of correlated experimental and analytical results on the basis of propellant vaporization exhibits excellent agreement for an injector where cold-flow studies have established drop sizes. All variations in experimental performance with different operating conditions are predicted analytically by changes in the vaporization rate as a result of changes in operating conditions. The variations are a function of the difference in drop size, injection velocity, chamber pressure and final gas velocity produced with different operating conditions.

Predicted Combustor Efficiency

The analytical results are also sufficient to predict combustor efficiency for various injection techniques. Experimental heptane-oxygen combustor efficiencies of six injectors with chamber lengths of 2, 4 and 8 in. at an oxidant to fuel weight ratio of 2.5 have been presented in (26).

The combustor efficiencies for these injectors in a given chamber length may be predicted from a knowledge of the drop sizes, the injection velocity and the initial temperature of both the oxygen and heptane, as well as environmental conditions of chamber pressure and final gas velocity. These parameters specify an effective chamber length as expressed by Equation [15]. The injectors used in (26) differ primarily in the drop size produced by the various atomization methods. The effective length can be determined for each injector by assuming that the same drop size was produced with oxygen and heptane for each method of atomization and by assuming a drop size for each method, as shown in Table 2. The only

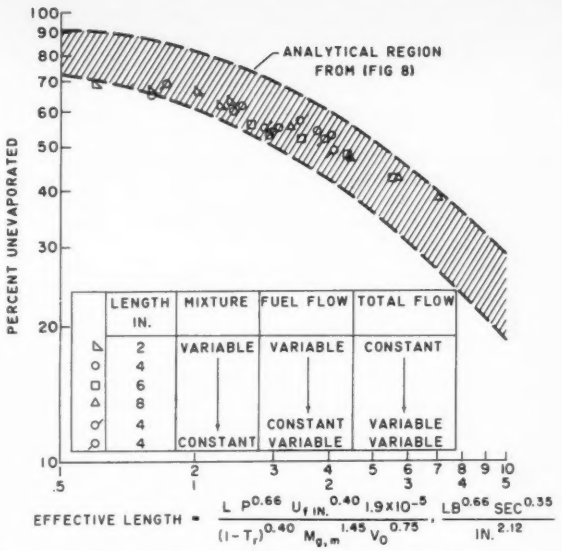

Fig. 12 Comparison of experimental and analytical results for various chamber lengths and flow conditions

check on drop size is with the sheets or impinging-jet atomizer, where the size agrees with that obtained by Equation [16]. The velocity of the gas into which the propellant is injected again was assumed to be 1200 in. per sec.

A summary of the analysis to predict the combustion efficiency of the various tests made in (26) is given in Table 3. The combustor variables are given along with the effective lengths calculated for each propellant. From these effective lengths, the per cent of each propellant vaporized was taken from Fig. 9.

In all cases where the atomization technique was the same for both propellants, somewhat more oxygen was vaporized than heptane, although the difference was not great. From these percentages vaporized, the combustor efficiency was determined by using Fig. 7. The predicted results are compared with the experimental results in the last two columns of Table 3. The calculated and experimental values agree within ±4 efficiency units, which is within the accuracy of the analytical correlations.

The comparison of experimental and calculated efficiencies in Table 3 also shows that there is a wide variation between per cent of oxidant or fuel vaporized and combustor efficiency. To obtain high efficiency, both propellants should be

Table 3 Comparison of experimental and calculated performances

Injector type		Chamber length,	Calculated results: Oxidant		Fuel			Experimental[a]
Oxidant	Fuel	in.	Effective length	Per cent vaporized	Effective length	Per cent vaporized	η_c	η_c
jets	jets (wide)	8	1.08	50	1.43	38	41	41
jets	jets (close)	8	1.15	52	1.22	33	44	47
sheets	jets	8	5.1	93	1.22	33	55	51
jet	sheets	8	1.27	56	5.65	78	64	68
sheets	sheets	2	2.10	73	2.15	50	65	68
		4	3.22	85	3.33	63	77	76
		8	5.5	94	5.05	75	85	82
triplet	triplet	2	3.22	85	3.33	63	79	81
		4	5.1	93	5.25	76	83	82
		8	7.4	97	8.00	86	90	88

[a] Ref. 26.

vaporized. However, it is possible to obtain an efficiency that is higher than the per cent fuel vaporized if the oxidant is almost completely vaporized, or higher than the per cent oxidant vaporized if the fuel is almost completely vaporized. The results of the comparison also indicate that better atomization of the propellants is responsible for the higher efficiency obtained with the triplet injector. Additional studies on drop sizes produced by various injector techniques are still required to either verify or disprove this point. Such data would also be valuable as an aid in engine designing.

Summary of Results

Calculations were made to determine the vaporization rates of sprays in a rocket engine for five different propellants. The calculated results show that the combustor length required to vaporize a given high percentage of propellants is the shortest with oxygen and increases in order for fluorine, heptane, ammonia and hydrazine. The combustor length required to vaporize a given percentage of propellants decreases with decreasing drop size and injection velocity, and with increasing gas velocity and chamber pressure.

Comparisons of experimental and calculated results showed excellent agreement for injector types where the drop size could be calculated. Variations in engine performance with various operating conditions were explained by determining the relation between performance and the per cent of propellants vaporized. The results indicate that combustor efficiency can be predicted from a model based on propellant vaporization as the rate controlling combustion process.

Nomenclature

A_c = cross-sectional area of drop, in.^{2}
A_s = surface area of drop, in.^{2}
a = constant for mass distribution, dimensionless
C_D = coefficient of drag for sphere, dimensionless
c_p = specific heat at constant pressure, Btu/(lb) (F)
c^* = characteristic exhaust velocity, fps
D = diffusion coefficient, in.^{2}/sec
D_j = jet diameter, in.
e = Naperian base
$\mathfrak{F}$ = fuel vaporized, per cent
h = heat transfer coefficient, Btu/(in.^{2}) (sec) (F)
K = coefficient of mass transfer, sec^{-1}
k = thermal conductivity, Btu/(in.) (sec) (F)
L = chamber length, in.
M = molecular weight of propellant, lb/mole
$M_{g,M}$ = mass median drop radius, in.
m = mass of drop, lb
Nu_H = Nusselt number for heat transfer, dimensionless
Nu_M = Nusselt number for mass transfer, dimensionless
n = number of drops of a particular size
$\mathcal{O}$ = oxidant vaporized, per cent
P = total pressure in chamber, psi
p = vapor pressure of liquid, psi
Pr = Prandtl number, dimensionless
q_l = sensible heating rate of drop, Btu/sec
q_v = heat transfer rate to surface of drop, Btu/sec
R = per cent of mass in drop smaller than r
$\bar{R}$ = universal gas constant, lb/(mole) (F)
Re = Reynolds number, dimensionless
r = radius of drop, in.
Sc = Schmidt number, dimensionless
T = temperature, R
T_c = critical temperature of propellant, R
T_r = reduced initial propellant temperature, $T_{l,0}/T_c$
$\bar{T}$ = mean temperature in boundary, R
U = velocity difference between gas and drop, in./sec
u = velocity of gas in chamber, in./sec
u_{fin} = final velocity, in./sec
V_g = gas velocity, in./sec
V_j = jet velocity, in./sec
v = droplet velocity, in./sec
w = vaporization rate, lb/sec
$\dot{w}_o$ = oxidant weight flow, lb/sec
$\dot{w}_f$ = fuel weight flow, lb/sec
x = axial position in chamber, in.
Z = correction factor for heat transfer, dimensionless
α = correction factor for mass transfer, dimensionless
η_c = characteristic velocity efficiency, per cent of theoretical
θ = time, sec
λ = latent heat of vaporization, Btu/lb
ρ = density, lb/in.^{3}
σ_g = geometric standard deviation, dimensionless

Subscripts

f = vapor
g = gas
i = ith size drops
l = liquid
O/F = oxidant-fuel weight ratio, $\dot{w}_o/\dot{w}_f$
$\mathcal{O}/\mathfrak{F}$ = ratio of vaporized oxidant to vaporized fuel weight flow, $\mathcal{O}\dot{w}_o/F\dot{w}_f$
th = theoretical
0 = beginning of time

References

1 Ross, C. C., "Scaling of Liquid Fuel Rocket Combustion Chambers. II—Transport Phenomena; Ignition, Altitude Behaviour and Scaling of Aeroengines," AGARD Selected Combustion Problems, Butterworths Sci. Pub., 1956, pp. 444–456.

2 Crocco, L., "Considerations on the Problem of Scaling Rocket Motors. II—Transport Phenomena; Ignition, Altitude Behaviour and Scaling of Aeroengines," AGARD Selected Combustion Problems, Butterworths Sci. Pub., 1956, pp. 457–468.

3 Penner, S. S. and Datner, P. P., "Combustion in Liquid-Fuel Rocket Engines," in "Fifth Symposium (Int.) on Combustion," Reinhold Pub. Corp., 1955, pp. 11–29.

4 Penner, S. S., "Rational Scaling Procedures for Liquid-Fuel Rocket Engines," JET PROPULSION, vol. 27, no. 2, Feb. 1957, pp. 156–161.

5 Heidmann, M. F., Priem, R. J. and Humphrey, J. C., "A Study of Sprays Formed by Two Impinging Jets," NACA TN 3835, 1957. (Supersedes NACA TN 2349.)

6 Ingebo, R. D., "Impinging-Jet-Injector Drop-Size Distributions in Airstreams Simulating Rocket-Combustor Velocity Conditions," NACA TN 4222, 1957.

7 Demetriades, S. T. and Aroeste, H., "Theoretical Studies on the Thermal Decomposition of Nitric Oxide in a Shock Tube," GALCIT, Tech. Rep. no. 3, June 1956. (Contract AF 18(603)-2.)

8 Bittker, D. A., "An Analytical Study of Gaseous Diffusion in Rocket Combustion," NACA TN (to be published).

9 El Wakil, M. M., Priem, R. J., Brikowski, H. J., Myers, P. S. and Uyehara, O. A., "Experimental and Calculated Temperature and Mass Histories of Vaporizing Fuel Drops," NACA TN 3490, 1956.

10 Agoston, G. A., Wise, H. and Rosser, W. A., "Dynamic Factors Affecting the Combustion of Liquid Spheres," Jet Prop. Lab., CIT, Prog. Rep. no. 20-291, Nov. 20, 1956. (Contract DA-04-495-ORD-18.)

11 Godsave, G. A. E., "Studies of the Combustion of Drops in a Fuel Spray—The Burning on Single Drops of Fuel," in "Fourth Symposium (Int.) on Combustion," The Williams and Wilkins Co., 1953, pp. 818-830.

12 Ingebo, R. D., "Vaporization Rates and Heat-Transfer Coefficients for Pure Liquid Drops," NACA TN 2368, 1951.

13 Penner, S. S., "On Maximum Evaporation Rates of Liquid Droplets in a Rocket Motor," JOURNAL OF THE AMERICAN ROCKET SOCIETY, vol. 23, no. 2, March-April 1953, pp. 85–88, 98.

14 El Wakil, M. M., Uyehara, O. A. and Myers, P. S., "A Theoretical Investigation of the Heating-Up Period of Injector Fuel Droplets Vaporizing in Air," NACA TN 3179, 1954.

15 Priem, R. J., Borman, G. L., El Wakil, M. M., Uyehara, O. A. and Myers, P. S., "Experimental and Calculated Histories of Vaporizing Fuel Drops," NACA TN 3988, 1957.

16 Borman, G. L., El Wakil, M. M., Uyehara, O. A. and Myers, P. S., "Reduced Graphs for Computing Histories of Vaporizing Fuel Drops and Drop Histories under Pressure," NACA TN (to be published).

17 Ranz, W. E. and Marshall, W. R., Jr., "Evaporation from Drops, Pt. I," *Chem. Eng. Prog.*, vol. 48, no. 3, March 1952, pp. 141–146.

18 Sherwood, T. K. and Pigford, R. L., "Absorption and Extraction," McGraw-Hill Book Co., Inc., 1952.

19 Priem, R. J., "Vaporization of Fuel Drops Including the Heating-Up Period," Ph.D. Thesis, Univ. of Wisconsin, 1955.

20 Ingebo, R. D., "Vaporization Rates and Drag Coefficients for Isooctane Sprays in Turbulent Air Streams," NACA TN 3265, 1954.

21 Priem, R. J., "Propellant Vaporization as a Criterion for Rocket Engine Design; Calculations of Chamber Length to Vaporize a Single n-Heptane Drop," NACA TN 3985, 1957.

22 Priem, R. J., "Propellant Vaporization as a Criterion for Rocket Engine Design; Calculations Using Various Log-Probability Distribution of Heptane Drops," NACA TN 4098, 1957.

23 Bevans, R. S., "Mathematical Expressions for Drop Size Distributions in Sprays," Conf. on Fuel Sprays, Univ. of Mich., March 30–31, 1949.

24 Priem, R. J., "Propellant Vaporization as a Criterion for Rocket-Engine Design; Calculation for Various Propellants," NACA TN 3883.

25 Priem, R. J. and Heidmann, M. F., "Propellant Vaporization as a Design Criterion for Rocket-Engine Combustion Chambers," NASA TR (to be published).

26 Heidmann, M. F. and Auble, C. M., "Injection Principles from Combustion Studies in a 200-Pound-Thrust Rocket Engine Using Liquid Oxygen and Heptane," NACA RM E55C22, 1955.

Composite Trajectories Yielding Maximum Coasting Apogee Velocity

STANLEY ROSS[1]

Lockheed Missile Systems Division
Palo Alto, Calif.

In the present paper, thrust direction (angle of attack) is optimized during the second of two adjacent satellite ascent stages. At second stage burnout, a coasting ellipse is to carry a third and final stage to some prescribed orbit height. We seek the thrust direction program which will maximize velocity at the apogee of this coasting arc. An expression for this program is obtained, and assumes a form noted in several previous papers. Supposing second stage thrust to be of constant magnitude, the equations of motion there are integrable in closed form. During this phase only, the Earth is assumed flat; aerodynamic effects are neglected beyond first stage burnout. Under these assumptions, determination of the optimum trajectory is reduced to a one-parameter iteration, readily effected by machine or hand calculation. Forms are derived for the second variation and also for the total variation. These expressions permit the investigation of conditions which insure mathematically optimum paths. Finally, a sample calculation is presented, using announced Vanguard data as parameters. Results for the optimum trajectory are obtained and compared with two non-optimal programs.

CURRENT problems of wide engineering interest very often involve not the design of totally radical systems to perform a new task, but rather the adaptation of those already in existence. We cite, as an example, the present use of large military rockets as satellite launching vehicles. The trajectory analyst often encounters fundamental difficulties in applying available booster stages to a job for which they were not designed. He may wish to program thrust or lift according to some preconceived optimizing relation, but practical limitations can narrowly restrict his choice. A typical dilemma arises, which furnishes the subject of this paper.

A certain long-range rocket is to carry some fixed final stage mass to a specified perigee injection altitude. Because of aerodynamic instabilities associated with any but the most insignificant angles of attack, the booster stage must ascend on a zero-lift trajectory, at least until detrimental effects become negligible. After a certain condition is reached, e.g., attainment of some given height, air density, time or dynamic pressure, the angle of attack (thrust angle) may be varied at will. Thrust magnitude is to be held constant, however, and may not be altered. Following booster engine burnout, the final stage is to ascend to the given injection height by means of a gravitational coasting ellipse. The final stage engine provides a velocity increment at coast apogee, sufficient to establish an orbit. Clearly, the smaller the velocity increment required, the greater the useful final stage payload which may be realized.[2] The problem, therefore, becomes that of choosing a thrust angle program during the latter portion of the boost (this latter portion we shall call the "second stage," as indeed may actually be the case), so that maximum velocity be attained at the coasting apogee.

The notion of partial optimization of a composite ascent path was mentioned by Perkins (3)[3] and also by Fried (4). Their results, along with those of a number of other authors (2–5) arose in the consideration of optimum thrust direction programs for a flat, airless Earth. The model thus established indicates a thrust angle program whose expression is quite simple. Furthermore, for constant thrust, the equations of motion during optimized powered flight are integrable in closed form and are easily adaptable to rapid calculation procedures. The main drawback, of course, is due to the neglect of drag forces and Earth's curvature; the inclusion of these (6, 7) renders the problem intractable. Here, we propose to use an exact analysis for the first boost stage, and also for the coasting phase. The second stage is to make use of the preceding simplifying assumptions. This composite method combines ease of computation with a close adherence to physical reality.

Equations of Motion

Referred to a fixed rectilinear coordinate system located at the point of second stage ignition (the "staging point"), the equations of motion for an ascent rocket, treated as a point mass, are (see Fig. 1)

$$\phi_1 \equiv \ddot{x} - (T/m)\cos\alpha = 0 \qquad [1]$$

$$\phi_2 \equiv \ddot{y} + g - (T/m)\sin\alpha = 0 \qquad [2]$$

where x and y are the rectilinear position coordinates. Second stage motion is assumed to occur over a flat, airless Earth, and under the influence of a constant gravitational acceleration g.[4] T is a constant; $m(t) = m_0 - \dot{m}_0 t$, where m_0 and $\dot{m}_0$ are given constants, and t denotes time. α is the angle of attack (thrust angle), referred to the x-axis.

Presented at the ARS 13th Annual Meeting, New York, N. Y., Nov. 17–21, 1958.

[1] Senior Scientist. Member ARS.

[2] We assume, as a convenience, that fuel and hardware in the third stage are interchangeable, supposedly possessing average densities which are equal.

[3] Numbers in parentheses indicate References at end of paper.

[4] See Fried, B. D., "Corrections to 'Comments on the Powered Flight Trajectory of a Satellite,'" JET PROPULSION, vol. 28, no. 5, May 1958, pp. 342–343. The author of the note discusses flat Earth assumptions. He concludes that these approximations are valid, providing that distance covered during this phase is small compared to the Earth's radius R_e, and that $t_b - t_0$ is much less than 9.5 min, which we assume to be the case here.

As a matter of fact, the following bounds on burnout condition errors can be shown to hold

$$-1/2[\omega(t_b - t_0)]^2\dot{x}_b \leq (\bar{\dot{x}}_b - \dot{x}_b) \leq -1/2[\omega(t_b - t_0)]^2\dot{x}_0$$

$$[\omega(t_b - t_0)]^2\dot{y}_0 \leq (\bar{\dot{y}}_b - \dot{y}_b) \leq [\omega(t_b - t_0)]^2\dot{y}_b$$

$$1/3[\omega^2(t_b - t_0)^3]\dot{y}_0 \leq (\bar{y}_b - y_b) \leq 1/3[\omega^2(t_t - t_0)^3]\dot{y}_b$$

where the quantities with a bar superscript are corrected values obtained by perturbing Equations [1] and [2] with terms of order $1/R_e$ in the gravitational force expansion. Here, $R_e\omega^2 = g$, and we assume $\ddot{y} \geq 0$ in (t_0, t_b).

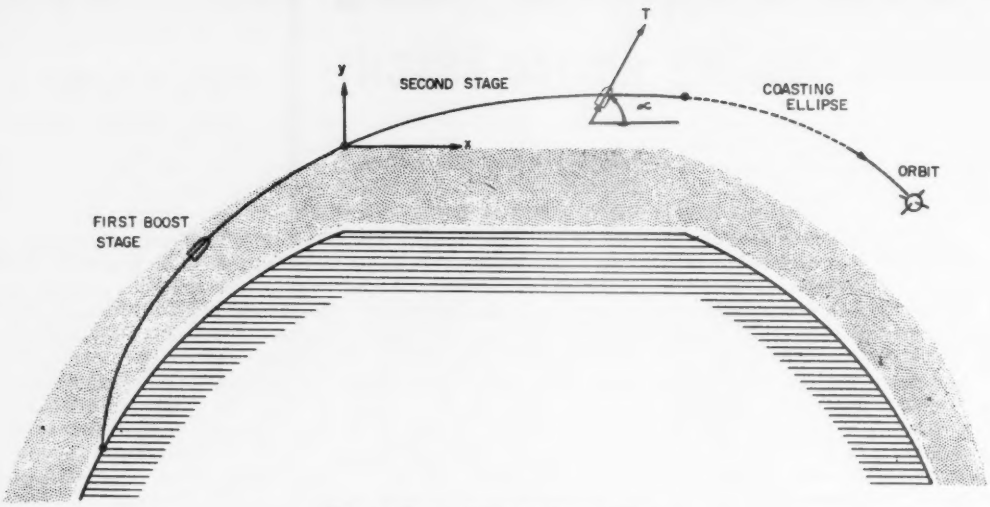

Fig. 1 Nomenclature and conventions

Zero-lift trajectory characteristics for the first boost stage are assumed known, and these may include drag and Earth curvature effects, if so desired. For the present problem we suppose that staging occurs after a given time t_0 of first stage flight. The velocity components, height and mass at staging then are known functions of some first stage parameter, such as y_0, the staging height. This one-parameter set of burnout values provides initial conditions for the second stage motion, which is to be optimized. At second stage burnout, an inverse-square gravitational field is assumed, and the burnout conditions here completely determine an ellipse whose apogee is interpreted to be the orbital injection height.

The Variational Problem

Maximizing tangential velocity at a coast apogee of given radial distance from the Earth's center is equivalent to maximizing angular momentum at that distance. And since the coasting ellipse preserves angular momentum, this is, in turn, equivalent to maximizing angular momentum at second stage burnout. Because of the assumption that $(1/R_e)(x_b - x_0)$ is negligible, this latter quantity may be written as

$$M_b \doteq (R_e + y_b)\dot{x}_b \qquad [3]$$

where R_e is the length of a radius vector from Earth's center to the x,y origin. $\dot{y}_b$ and $\dot{x}_b$ are burnout values, referred to the coordinate system of the previous section.

Since the coasting ellipse also preserves total energy, we have

$$E = \frac{\dot{x}_b^2 + \dot{y}_b^2}{2} - \frac{g_0 R_e^2}{(R_e + y_b)} = \frac{M_b^2}{2(R_e + y_a)^2} - \frac{g_0 R_e^2}{(R_e + y_a)} \qquad [4]$$

$(R_e + y_a)$ is the specified orbital injection height.

Mathematically speaking, the problem is to find that function $\alpha(t)$ which maximizes expression [4] subject to conditions [1, 2 and 4], where $(R_e + y_a)$ and the first stage burnout characteristics are known. This problem is treated within the framework of the variational calculus, and an analysis is presented in the Appendix. We describe here the principal results, and a computational scheme to be employed in the solution.

Discussion of the Analytical Results

In support of the conclusions of (2 to 5), we find the optimal thrust angle program to be characterized by the expression

$$\tan \alpha = b - at \qquad [5]$$

where a and b are constants to be determined. Equations [1 and 2] which must also be satisfied, add four more constants to be found, making a total of six.

On the other hand, we have the parameter-varied set of two staging values $\dot{x}_0(y_0)$ and $\dot{y}_0(y_0)$, plus the value of y_0 itself. Two relations at burnout are afforded by the energy equation [4] and the burnout transversality condition (Eq. [A-20])

$$\left.\frac{\tan \alpha}{\tan \theta}\right|_{t_b} = \frac{a + a_{1b}}{a_{2b} + a_{1b}} \qquad [6]$$

where $a_{1b} = -\dot{x}_b/(R_e + y_b)$, and $a_{2b} = -g/\dot{x}_b$.[5]

Finally, the sixth condition is given by the staging transversality relation for a fixed staging time t_0 (Eq. [A-24])

$$a = \left[\frac{d\dot{x}_0}{dy_0} + b\,\frac{d\dot{y}_0}{dy_0}\right]_{y_0} \qquad [7]$$

which guarantees that the complete solution is stationary over all neighboring choices for first as well as second stage trajectories.

The solution is therefore determined in principle, and presumably is calculable for any choice of orbit height. However, the transcendental nature of the equations defining a solution precludes any direct approach. It proves more expedient to plot orbit height as a function of starting conditions, and to extract the required result by interpolation. For every choice of y_0 there will result a corresponding orbit height $(R_e + y_a)$, and an apogee velocity V_a, which will be maximum for that height. We propose to calculate $(R_e + y_a)$ and V_a as functions of y_0, and to select from these curves the desired values. The one-guess calculation proceeds as follows. Choose

[5] Referring to Equation [6], it can be shown that a_{1b} is the optimal thrust-angle turning rate for maximum burnout momentum, neglecting the energy consideration [4]; conversely, a_{2b} is the optimal turning rate for maximum burnout energy, if momentum considerations are neglected (2).

a value for y_0. Next, guess the value of $b = \tan \alpha_0$. The corresponding value of a is obtained from Equation [7], since the derivatives involved are assumed known, at least numerically, if not analytically. For the value of y_0 selected, $\dot{x}_0$ and $\dot{y}_0$ are also known. Now the integrated equations of motion are used (2,4)

$$\dot{x}_b = \dot{x}_0 + \hat{c} \cos \alpha_k \ln \frac{\tan [(\alpha_0 - \alpha_k)/2]}{\tan [(\alpha_b - \alpha_k)/2]} \qquad [8a]$$

$$\dot{y}_b = [\dot{y}_0 - g(t_b - t_0)] + \hat{c} \left\{ \sin \alpha_k \ln \frac{\tan [(\alpha_0 - \alpha_k)/2]}{\tan [(\alpha_b - \alpha_k)/2]} + \ln \frac{\tan [(\alpha_0 + \pi/2)/2]}{\tan [(\alpha_b + \pi/2)/2]} \right\} \qquad [8b]$$

$$(R_e + y_b) = [(R_e + y_0) + \dot{y}_0(t_b - t_0) - \frac{1}{2} g(t_b - t_0)^2] - \frac{\hat{c}}{\dot{m}_0} m_b \left\{ \sin \alpha_k \ln \frac{\tan [(\alpha_0 - \alpha_k)/2]}{\tan [(\alpha_b - \alpha_k)/2]} + \ln \frac{\tan [(\alpha_0 + \pi/2)/2]}{\tan [(\alpha_b + \pi/2)/2]} \right\} - \frac{\hat{c}}{a} [\sec \alpha_b - \sec \alpha_0] \qquad [8c]$$

c is the effective exhaust velocity, considered constant in the vacuum we have assumed. $\alpha_k = \tan^{-1} [a(m_0/\dot{m}_0) + b]$, and is interpreted as being that thrust angle which would finally result, were the entire second stage mass to be burned as fuel.[6] $\dot{x}_b$, $\dot{y}_b$ and y_b obtained here must satisfy Equation [6]. If this is not the case, guess another value for b and repeat the calculations until Equation [6] is satisfied. The correct values of $\dot{x}_b$, $\dot{y}_b$ and y_b thus found are used to evaluate M_b in Equation [3] and $(R_e + y_a)$ in Equation [4]. Finally, V_a is obtained from the momentum equation

$$M_b \doteq (R_e + y_a) V_a = M_a \qquad [9]$$

$(R_e + y_a)$ and V_a are plotted against y_0 first, and then against each other, so that coast apogee velocity may be obtained directly for any given injection height. The scheme is quite simple, and very rapid if an automatic computer is used. Even by hand, a few hours labor will usually suffice for the calculations.

Second Variation and the Question of Maximality

In consequence of the results derived in the Appendix, we find (Eq. [A-29])

$$\left[1 - (1 - \rho^2) \frac{\tan \alpha_b}{\tan \theta_b}\right] \frac{\delta^2 M_b}{R_e + y_b} = \left\{ \left(\frac{d^2 \dot{x}_0}{dy_0^2} + \frac{d^2 \dot{y}_0}{dy_0^2} \right) \frac{\delta y_0^2}{2!} - \frac{1}{2!} \int_{t_0}^{t_b} \frac{T}{m} \sec \alpha \, \delta\alpha^2 \, dt \right\} - \left\{ \dot{x}_b + \frac{\tan \alpha_b}{2\dot{y}_b^3} [E^2 + (\dot{x}_b^2 - \dot{y}_b^2)\dot{y}_b^2] \right\} \frac{\delta y_b^2}{(R_e + y_b)^2} \qquad [10]$$

By Equation [9], since $(R_e + y_a)$ is fixed, $\delta M_b = \delta V_a = 0$, and $\delta^2 M_b = (R_e + y_a)\delta^2 V_a$. Equation [10] reduces to

$$\left[1 - (1 - \rho^2) \frac{\tan \alpha_b}{\tan \theta_b}\right] \delta^2 V_a \doteq \frac{\rho}{2!} \left\{ \left(\frac{d^2 \dot{x}_0}{dy_0^2} + b \frac{d^2 \dot{y}_0}{dy_0^2} \right) \delta y_0^2 - \int_{t_0}^{t_b} \frac{T}{m} \sec \alpha \, \delta\alpha^2 \, dt \right\} - \left\{ \dot{x}_b + \frac{\tan \alpha_b}{2\dot{y}_b^3} [E^2 + (\dot{x}_b^2 - \dot{y}_b^2)\dot{y}_b^2] \right\} \frac{\delta y_b^2}{(R_e + y_a)(R_e + y_b)} \qquad [11]$$

Total velocity increment due to optimizing stems from three factors. The first represents a contribution from staging point errors, resulting from non-optimal use of the initial booster stage. The second term arises when a non-optimal second stage thrust direction program is employed. Finally, the last term is due to a difference in coasting arc lengths between the optimal and any comparison path.

For the range of values considered here

$$\rho^2 = (R_e + y_b)/(R_e + y_a)^2 \sim 1$$

and the term $(1 - \rho^2)(\tan \alpha_b/\tan \theta_b)$ is negligible in comparison with unity. The coefficient of $\delta^2 V_a$ is positive then, and the question of maximality of V_a reduces to determining the sign of the right-hand side of Equation [11]. If this latter quantity is negative, V_a is mathematically a local maximum and the trajectory is to be considered optimal.

From physical considerations, the integral term

$$- \int_{t_0}^{t_b} \frac{T}{m} \sec \alpha \, \delta\alpha^2 \, dt$$

in Equation [11] must be negative. We therefore conclude that the condition

$$\left[\frac{d^2 \dot{x}_0}{dy_0^2} + b \frac{d^2 \dot{y}_0}{dy_0^2} \right] \frac{\delta y_0^2}{2!} - \left\{ \dot{x}_b + \frac{\tan \alpha_b}{2\dot{y}_b^3} [E^2 + (\dot{x}_b^2 - \dot{y}_b^2)\dot{y}_b^2] \right\} \frac{\delta y_b^2}{(R_e + y_b)^2} < 0 \qquad [12]$$

is sufficient for a maximum V_a. Inclusion of the first bracketed term in condition [12] guarantees a compound maximum, implying that the entire trajectory, containing both boost phases plus the coasting arc, is the optimal solution.

Furthermore, let us now suppose

$$\left[\frac{d^2 \dot{x}_0}{dy_0^2} + b \frac{d^2 \dot{y}_0}{dy_0^2} \right]$$

to be negative. Rough numerical calculations seem to indicate that the assumption is justified for several existing boosters, and there seems good cause for its acceptance. With this conjecture valid, the condition

$$\left\{ \dot{x}_b + \frac{\tan \alpha_b}{2\dot{y}_b^3} [E^2 + (\dot{x}_b^2 - \dot{y}_b^2)\dot{y}_b^2] \right\} > 0 \qquad [13]$$

becomes sufficient for a maximum. The inequality holds if

$$(\dot{x}_b^2 - \dot{y}_b^2) > 0$$

and also

$$\tan \alpha_b / \tan \theta_b > 0$$

[6] We omit consideration of the infinite accelerations which would theoretically be produced with a vanishing mass.

both of which seem to be the case in most physically sensible instances.

Total Variation; Direct Comparison With Non-Optimal Programs

Consider Equations [1 and 2] for the special case when they define motion along the optimal trajectory. Let us adjoin to them the multipliers λ_1 and λ_2 of the Appendix, and integrate the sum $\lambda_1\phi_1 + \lambda_2\phi_2$. There results

$$-ay - \dot{x} - \dot{y}\tan\alpha\Big|_{t_0}^{t_b} = \int_{t_0}^{t_b}\frac{T}{m}\sec\alpha\,dt \qquad [14]$$

Now consider Equations [1 and 2] when they define any admissible comparison trajectory (variables on this path are denoted by the superscript tilde, $\sim$). We again adjoin λ_1 and λ_2, add and integrate

$$-a\tilde{y} - \tilde{\dot{x}} - \tilde{\dot{y}}\tan\alpha\Big|_{t_0}^{t_1} = \int_{t_0}^{t_b}\frac{T}{m}\,(\cos\tilde{\alpha} + \tan\alpha\sin\tilde{\alpha})dt \qquad [15]$$

By subtracting Equation [14] from Equation [15], we find

$$a\Delta y + \Delta\dot{x} + \Delta\dot{y}\tan\alpha\Big|_{t_b} = a\Delta y + \Delta\dot{x} + b\Delta\dot{y}\Big|_{t_0} - \int_{t_0}^{t_b}\frac{T}{m}\sec\alpha[1 - \cos\Delta\alpha]dt \qquad [16]$$

where

$$(\tilde{y} - y) = \Delta y = \delta y + \delta^2 y + \ldots$$

and similarly for the other variables.[7] $\Delta(\ )$ is the total variation, and refers to the actual numerical difference between optimal and non-optimal paths.

Since

$$\Delta(uv) = (u + \Delta u)\Delta v + v\Delta u$$

and

$$\Delta\left(\frac{1}{u}\right) = -\frac{\Delta u}{u(u + \Delta u)}$$

Equations [3 and 4] provide (after considerable manipulation) the relations

$$\Delta\dot{x}_b = \frac{M_b - \dot{x}_b\Delta y_b}{[(R_e + y_b) + \Delta y_b]} \qquad [17]$$

$$\Delta\dot{y}_b = \frac{\Delta y_b}{\dot{y}_b(R_e + y_b)}\left[\dot{x}_b^2 - \frac{g_0R_e^2}{R_e + y_b}\right] + \frac{\dot{x}_b\Delta M_b}{\dot{y}_b(R_e + y_b)}(\rho^2 - 1) + \frac{\Delta M_b^2}{2\dot{y}_b(R_e + y_b)^2} - \frac{\Delta y_b^2}{\dot{y}_b(R_e + y_b)}\left[\left(\frac{3\dot{x}_b^2}{2} - \frac{g_0R_e^2}{R_e + y_b}\right) + \frac{1}{2\dot{y}_b^2}\left(\dot{x}_b^2 - \frac{g_0R_e^2}{R_e + y_b}\right)^2\right] \qquad [18]$$

Here we have assumed that terms

$$\mathcal{O}\left[\left(\frac{\Delta y_b}{R_e + y_b}\right)^3\right],\ \mathcal{O}\left[\left(\frac{\Delta\dot{x}_b}{R_e + y_b}\right)^3\right]$$

etc. are negligible.

Equations [17 and 18] inserted into Equation [16] produce

$$\frac{1}{2\dot{x}_b}\frac{\tan\alpha_b}{\tan\theta_b}(\rho^2 - 1)\Delta V_a^2 + \rho\left[1 - (1 - \rho^2)\frac{\tan\alpha_b}{\tan\theta_b}\right]\Delta V_a = \rho^2\left\{[a\Delta y_0 + \Delta\dot{x}_0 + b\Delta\dot{y}_0] - \int_{t_0}^{t_b}\frac{T}{m}\sec\alpha[1 - \cos\Delta\alpha]dt\right\} - \left\{\dot{x}_b + \frac{\tan\alpha_b}{2\dot{y}_b^3}[E^2 + (\dot{x}_b^2 - \dot{y}_b^2)\dot{y}_b^2]\right\}\frac{\Delta y_b^2}{(R_e + y_a)^2} \qquad [19]$$

[7] Equation [16] for the total variation may also be obtained by writing each successive variation of $\lambda_1\phi_1 + \lambda_2\phi_2$, and forming the infinite sum.

The first bracketed term on the right-hand side of Equation [19] may be written as

$$[a\Delta y_0 + \Delta\dot{x}_0 + b\Delta\dot{y}_0] = \left(\frac{d^2\dot{x}_0}{dy_0^2} + b\frac{d^2\dot{y}_0}{dy_0^2}\right)\frac{\Delta y_0^2}{2!} + \left(\frac{d^3\dot{x}_0}{dy_0^3} + b\frac{d^3\dot{y}_0}{dy_0^3}\right)\frac{\Delta y_0^3}{3!} + \ldots$$

by virtue of the staging relations $\dot{x}_0 = \dot{x}_0(y_0)$, $\dot{y}_0 = \dot{y}_0(y_0)$ and the staging transversality condition [7].

It is interesting to compare expression [11] for the second variation of V_a with Equation [19] for the total variation including terms $\mathcal{O}[\Delta y_b^2/(R_e + y_b)^2]$. The apparent discrepancy between the two equations represented by

$$\frac{1}{2\dot{x}_b}\frac{\tan\alpha_b}{\tan\theta_b}(\rho^2 - 1)\Delta V_a^2$$

disappears when higher order variations are considered. At any rate, this latter term seems to be dispensable, considering that both $(\rho^2 - 1)$ and $|\Delta V_a|/2\rho\dot{x}_b$ are usually quite small in magnitude. For $|\Delta\alpha|$ small compared to 1 radian and terms

$$\mathcal{O}\left(\frac{d^3\dot{x}_0}{dy_0^2}, \frac{d^3\dot{y}_0}{dy_0^3}\right)$$

negligible, we may write $\delta\alpha \to \Delta\alpha$, $\delta y_0 \to \Delta y_0$, $\delta y_b \to \Delta y_b$. Both formulas then agree entirely, i.e., $\delta^2 V_a = \Delta V_a$. For practical purposes the second variation (Eq. [11]) provides a good approximation to the total variation when each $\delta(\ )$ is replaced by the corresponding $\Delta(\ )$.

When $|\Delta\alpha| \ll 1$ radian, the integral term in Equation [19] may be written

$$-\int_{t_0}^{t_b}\frac{T}{m}\sec\alpha[1 - \cos\Delta\alpha]dt \doteq -\frac{\dot{x}_b - \dot{x}_0}{2}\sec^2\alpha_t\,\epsilon[(\Delta\alpha^2)]$$

where $\alpha_0 \geq \alpha_t \geq \alpha_b$. $\epsilon[(\Delta\alpha^2)]$ is the mean-square value of $\Delta\alpha$, for any given non-optimal program, weighted rather strongly toward t_b by the term $\ddot{x} = (T/m)\cos\alpha$, which increases rapidly with time. Because of this factor, relatively little penalty is suffered if a small, finite time be required in practice to adjust the pitch angle immediately after staging. Generally speaking, a non-optimum program which steadily approaches the neighborhood of the optimum is a favorable substitute; zero-lift programs seem to fall into this category, which apparently explains their effectiveness (2).

Illustrative Example

A convenient example is furnished by the Vanguard satellite launching vehicle, formerly in use for IGY research. The rocket is composed of three stages; the first two are sequential boost phases of the type under discussion. After a coasting period which carries the final stage to its apogee, a third rocket supplies the necessary velocity increment to establish an orbit. According to publicly released nominal data,[8] the following constants were used

$$m_0 = 149 \text{ sl.} \qquad m_b = 37.3 \text{ sl.} \qquad t_b = 129.5 \text{ sec} \qquad \bar{c} = 8694 \text{ fps}$$

Staging data were available only for a single trajectory; these are

$$y_0 = 1.9 \times 10^5 \text{ ft} \qquad \dot{x}_0 = \dot{y}_0 = 3889 \text{ fps}$$

Since parameter-varied staging information was unavailable, the following two assumptions were applied and seemed accurate enough for present purposes:

1 $\dot{x}_0 + \dot{y}_0 = \text{const} = 2(3889)$, for all staging points in the vicinity of the known one.

2 Total energy is assumed invariant for all staging points in the vicinity of the known one.

Using these assumptions, reasonable expressions were obtainable for the derivatives appearing in Equation [7]. The results are plotted in Fig. 2, where flight with the optimum second stage program is compared with two non-optimal cases, zero lift and constant thrust direction. The same first stage trajectory family and identical second stage approximations were used for all three curves. With the two foregoing approximations valid, the term

$$\left[\frac{d^2\dot{x}_0}{dy_0^2} + b\,\frac{d^2\dot{y}_0}{dy_0^2}\right]$$

mentioned in the previous section, is always negative.

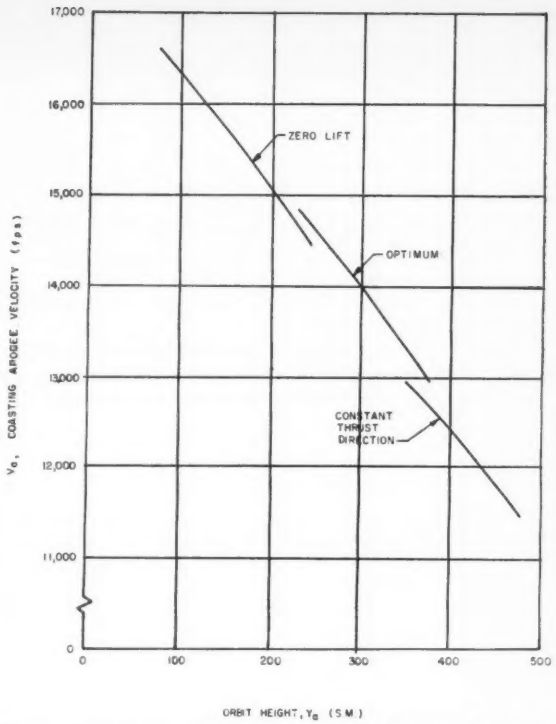

Fig. 2 Coasting apogee velocity vs. orbital injection height for different thrust programs

Appendix

The variational method is applied, with customary notations, in the following manner (8). From Equations [1 and 2]

$$\delta\phi_1 \equiv \delta\ddot{x} + (T/m)\sin\alpha\,\delta\alpha = 0 \qquad \text{[A-1]}$$

$$\delta\phi_2 \equiv \delta\ddot{y} - (T/m)\cos\alpha\,\delta\alpha = 0 \qquad \text{[A-2]}$$

Multiplier functions $\lambda_1(t)$ and $\lambda_2(t)$ are introduced, and the product $F_1 = \lambda_1\phi_1 + \lambda_2\phi_2 = 0$ is formed. The quantities λ_1 and λ_2 are as yet undetermined in form, and subject only to the restriction that each be piecewise continuous between t_0 and t_b, the staging and burnout times. Now F_1 is integrated between t_0 and t_b

$$0 = \int_{t_0}^{t_b} F_1\,dt = \int_{t_0}^{t_b}\left\{\lambda_1\delta\ddot{x} + \lambda_2\delta\ddot{y} + \frac{T}{m}\left[\lambda_1\sin\alpha - \lambda_2\cos\alpha\right]\delta\alpha\right\}dt \qquad \text{[A-3]}$$

The terms $\lambda_1\delta\ddot{x}$ and $\lambda_2\delta\ddot{y}$ are each integrated twice by parts. We find

$$\int_{t_0}^{t_b}\lambda_1\delta\ddot{x}\,dt = \lambda_1\delta\dot{x} - \dot{\lambda}_1\delta x\Big|_{t_0}^{t_b} + \int_{t_0}^{t_b}\ddot{\lambda}_1\delta x\,dt$$

$$\int_{t_0}^{t_b}\lambda_2\delta\ddot{y}\,dt = \lambda_2\delta\dot{y} - \dot{\lambda}_2\delta y\Big|_{t_0}^{t_b} + \int_{t_0}^{t_b}\ddot{\lambda}_2\delta y\,dt$$

Equation [A-3] becomes

$$\lambda_1\delta\dot{x} + \dot{\lambda}_2\delta y - \lambda_1\delta\dot{x} - \lambda_2\delta\dot{y}\Big|_{t_0}^{t_b} = \int_{t_0}^{t_b}\left\{\ddot{\lambda}_1\delta x + \ddot{\lambda}_2\delta y + \frac{T}{m}\left[\lambda_1\sin\alpha - \lambda_2\cos\alpha\right]\delta\alpha\right\}dt \qquad \text{[A-4]}$$

Now we choose

$$\ddot{\lambda}_1 = 0 \qquad \text{[A-5]}$$

$$\ddot{\lambda}_2 = 0 \qquad \text{[A-6]}$$

Equation [A-4] must hold for any values of δx, δy, $\delta\dot{x}$, $\delta\dot{y}$ at each limit, in particular, when all eight of these values are zero. Therefore

$$0 = \int_{t_0}^{t_b}\frac{T}{m}\left[\lambda_1\sin\alpha - \lambda_2\cos\alpha\right]\delta\alpha\,dt \qquad \text{[A-7]}$$

must hold.

However, of the three variables δx, δy, $\delta\alpha$ appearing in Equations [A-1 and A-2], one may be considered independent—say $\delta\alpha$. If $\delta\alpha$ is arbitrary, the Fundamental Lemma (8) applied to Equation [A-7] guarantees that

$$\lambda_1\sin\alpha - \lambda_2\cos\alpha \equiv 0$$

or

$$\tan\alpha = \lambda_2/\lambda_1 \qquad \text{[A-8]}$$

in (t_0, t_b).

We have the particularly simple solutions to Equations [A-5 and A-6]

$$\lambda_2 = b - at \qquad \text{[A-9]}$$

$$\lambda_1 = d + ct \qquad \text{[A-10]}$$

from which Equation [A-8] shows

$$\tan\alpha = (b - at)/(d + ct) \qquad \text{[A-11]}$$

[8] I am indebted to S. B. Kramer of Lockheed MSD for these figures.

to be the optimal program. This result is to be found in (2–5).

Returning to Equation [A-4] in its general form, we have

$$\lambda_1\delta x + \lambda_2\delta y - \lambda_1\delta\dot{x} - \lambda_2\delta\dot{y}\Big|_{t_b} = \lambda_1\delta x + \lambda_2\delta y - \lambda_1\delta\dot{x} - \lambda_2\delta\dot{y}\Big|_{t_0} \quad [A\text{-}12]$$

Equation [A-12] must hold for any and all values of either side, so that each side must be identically zero. Consider the left-hand side

$$\lambda_1\delta x + \lambda_2\delta y - \lambda_1\delta\dot{x} - \lambda_2\delta\dot{y}\Big|_{t_b} = 0 \quad [A\text{-}13]$$

We have, however, at point t_b the two relations Equations [3 and 4]. Since M_b is to be a maximum, $\delta M_b = 0$, and the first variations of these expressions may be written as

$$\delta M_b = 0 = (R_e + y_b)\delta\dot{x}_b + \dot{x}_b\delta y_b \quad [A\text{-}14]$$

$$\delta E = 0 = \dot{x}_b\delta\dot{x}_b + \dot{y}_b\delta\dot{y}_b + \frac{g_0R_e^2}{(R_e + y_b)^2}\,\delta y_b \quad [A\text{-}15]$$

From Equations [A-14 and A-15] we have

$$\delta\dot{x}_b = -\frac{\dot{x}_b}{(R_e + y_b)}\,\delta y_b \quad [A\text{-}16]$$

$$\delta\dot{y}_b = \frac{1}{\dot{y}_b(R_e + y_b)}\left[\dot{x}_b^2 - \frac{g_0R^2}{(R_e + y_b)}\right]\delta y_b \quad [A\text{-}17]$$

Inserting these latter two relations into Equation [A-13], it becomes

$$\left[\frac{\lambda_{2b}}{\dot{y}_b(R_e + y_b)}\left(\dot{x}_b^2 - \frac{g_0R_e^2}{R_e + y_b}\right) - \left(\lambda_{2b} + \lambda_{1b}\frac{\dot{x}_b}{R_e + y_b}\right)\right]\delta y_b - \lambda_{1b}\delta x_b = 0 \quad [A\text{-}18]$$

δx_b and δy_b are arbitrary, so that we find

$$\lambda_{1b} = c = 0 \quad [A\text{-}19]$$

$$-\frac{a}{d} + \frac{\dot{x}_b}{R_e + y_b} = \frac{\tan\alpha_b}{\dot{y}_b(R_e + y_b)}\left(\dot{x}_b^2 - \frac{g_0R_e^2}{R_e + y_b}\right) \quad [A\text{-}20]$$

Equations [A-5 and A-6] are homogeneous in λ_1 and λ_2 and their derivatives, we may assign any arbitrary value to either multiplier at any point in (t_0, t_b). We choose $\lambda_{10} = d = 1$.

Now let us return to Equation [A-12]. The right-hand side is

$$\lambda_2\delta y - \delta\dot{x} - \lambda_2\delta\dot{y}\Big|_{t_0} = 0 \quad [A\text{-}21]$$

Note here that the operator $\delta(\ )$ refers to changes from one comparison arc to another at a constant time t. However, the staging time t_0 may itself vary from one first stage arc to another, depending upon the particular staging condition chosen. In the general case then, the complete displacement resulting from following the staging point from one arc to a neighboring one is

$$d(\ ) = \delta(\ ) + [(d/dt)(\ )]_{t_0}dt_0 \quad [A\text{-}22]$$

Therefore Equation [A-21] is rewritten as

$$[\lambda_2 dy - d\dot{x} - \lambda_2 d\dot{y}]_{t_0} - [\dot{\lambda}_2\dot{y} - \ddot{x} - \lambda_2\ddot{y}]_{t_0}dt_0 \quad [A\text{-}23]$$

However, under the assumption of the problem at hand that t_0 be fixed, Equation [A-23] becomes

$$\dot{\lambda}_{20} - \frac{d\dot{x}_0}{dy_0} - \lambda_{20}\frac{d\dot{y}_0}{dy_0} = 0 \quad [A\text{-}24]$$

The second variation of M_b is now evaluated. We form

$$F_2 \equiv \lambda_1\delta^2\phi_1 + \lambda_2\delta^2\phi_2 \equiv \delta^2\ddot{x} + \lambda_2\delta^2\ddot{y} + \frac{1}{2!}\cdot\frac{T}{m}\sec\alpha\,\delta\alpha^2 \equiv 0$$

where λ_1 and λ_2 are defined as previously. Performing integrations analogous to those of Equation [A-3] ff., we obtain

$$\dot{\lambda}_2\delta^2 y - \delta^2\dot{x} - \lambda_2\delta^2\dot{y}\Big|_{t_0}^{t_b} = \frac{1}{2!}\int_{t_0}^{t_b}\frac{T}{m}\sec\alpha\,\delta\alpha^2 dt \quad [A\text{-}25]$$

which reduces to

$$\delta^2\dot{x}_b + \lambda_{2b}\delta^2\dot{y}_b = \dot{\lambda}_{2b}\delta^2 y_b + \left[\left(\frac{d^2\dot{x}_0}{dy_0^2} + b\,\frac{d^2\dot{y}_0}{dy_0^2}\right)\frac{\delta y_0^2}{2!} - \frac{1}{2!}\int_{t_0}^{t_b}\frac{T}{m}\sec\alpha\,\delta\alpha^2 dt\right] \quad [A\text{-}26]$$

Likewise, the second variations of Equations [3 and 4] are found (using Eqs. [A-16 and A-17]) to be

$$\delta^2 M_b - (R_e + y_b)\delta^2\dot{x}_b = \dot{x}_b\delta^2 y_b - \frac{\dot{x}_b}{R_e + y_0}\,\delta y_0^2 \quad [A\text{-}27]$$

$$\frac{M_b}{R_e + y_a}\,\delta^2 M_b - \dot{x}_b\delta^2\dot{x}_b - \dot{y}_b\delta^2\dot{y}_b = \frac{g_0R_e^2}{(R_e + y_b)^2}\,\delta^2 y_b + \frac{1}{2(R_e + y_b)^2}\left[\dot{x}_b^2 + \frac{1}{\dot{y}_b^2}\left(\dot{x}_b^2 - \frac{g_0R_e^2}{R_e + y_b}\right)^2 - \frac{2g_0R_e^2}{R_e + y_b}\right]\delta y_b^2 \quad [A\text{-}28]$$

Equations [A-26, A-27 and A-28] are solved for $\delta^2 M_b$

$$\left[1 - (1 - \rho^2)\frac{\tan\alpha_b}{\tan\theta_b}\right]\frac{\delta^2 M_b}{R_e + y_b} = \left\{\left(\frac{d^2\dot{x}_0}{dy_0^2} + b\,\frac{d^2\dot{y}_0}{dy_0^2}\right)\frac{\delta y_0^2}{2!} - \frac{1}{2!}\int_{t_0}^{t_b}\frac{T}{m}\sec\alpha\,\delta\alpha^2 dt\right\} - \left\{\dot{x}_b + \frac{\tan\alpha_b}{2\dot{y}_b^3}\,[E^2 + (\dot{x}_b^2 - \dot{y}_b^2)\dot{y}_b^2]\right\}\frac{\delta y_b^2}{(R_e + y_a)(R_e + y_b)} \quad [A\text{-}29]$$

where $\tan\theta_b = \dot{y}_b/\dot{x}_b$ and $\rho = (R_e + y_b)/(R_e + y_a)$.

Acknowledgment

I should like to thank Dr. John V. Breakwell of Lockheed MSD for his valuable and most helpful comments, which smoothed many a rough spot from the analysis. The numerical calculations were performed by David Hunter and Stanley Blacker of Lockheed MSD, for whose aid I am also deeply grateful.

References

1 Lawden, D. F., "Optimum Launching of a Rocket into an Orbit About the Earth," *Astronautica Acta*, vol. 1, fasc. 4, 1955.

2 Lawden, D. F., "Optimal Programming of Rocket Thrust Direction," *Astronautica Acta*, vol. 1, fasc. 1, 1955.

3 Perkins, F., "Flight Mechanics of Ascending Satellite Vehicles," JET PROPULSION, vol. 26, no. 5, 1956.

4 Fried, B. D., "Powered Flight Trajectory of a Satellite," JET PROPULSION, vol. 27, no. 6, June 1957.

5 Okhotsimsky, D. E. and Enyeyev, T. M., "Certain Variational Problems Connected with the Launching of an Artifical Earth Satellite," *Usp. Fiz. Nauk*, vol. LXIII, no. 1a, Sept. 1957 (in Russian); *also J. Brit. Interplan. Soc.*, vol. 16, no. 5, Jan.-Feb. 1958.

6 Foy, W. H., Jr., "Steering of an Ascent Rocket for Maximum Cutoff Velocity," Amer. Astronaut. Soc. preprint 57-14, Jan. 1958.

7 Edelbaum, T. N., "Comments on the Powered Flight Trajectory of a Satellite," JET PROPULSION, vol. 27, no. 12, Dec. 1957.

8 Bolza, O., "Lectures on the Calculus of Variations," Stechert-Hafner, Inc., New York, 1946.

Earth-Period (24-Hr) Satellites

J. H. HUTCHESON[1]

Rand Corp.
Santa Monica, Calif.

An Earth-period satellite is a satellite which has an orbital period of revolution exactly equal to the Earth's period of rotation on its axis (i.e., one sidereal day). As originally conceived, the term implies an idealized equatorial and circular orbit where no relative motion exists between the Earth and satellite. This paper discusses the type of relative motion which will exist in a practical case where the orbital plane is inclined, the motion is elliptical, and perturbations due to the moon, sun and Earth's oblateness are considered. Several illustrations are given showing the effect of various different orbital parameters (using exaggerated values) on the satellite ground track. Some possible practical uses are mentioned, and it is suggested that the use of an inclined orbit may have some merit for observation purposes.

THE MENTION of an Earth-period or 24-hr satellite immediately brings to mind the often discussed and much publicized vision of some type of vehicle which will remain suspended over a point on the Earth's equator as if connected to some form of "sky hook." This is possible if the following conditions can be met:

1 The orbital plane is exactly coincident with the Earth's equatorial plane.

2 The orbit is exactly circular.

3 The altitude is 22,240 miles, corresponding to a period exactly equal to the Earth's rotating about its axis (i.e., one sidereal day).

4 The satellite is not subjected to perturbing forces which might alter its path.

These conditions would be impossible to establish with perfect precision, which brings up the question of what happens in the imperfect or general case applying to all Earth-period satellites.

Let us assume that the satellite period is perfectly equal to one sidereal day. This assumption defines the semimajor axis of the elliptical orbit, or the radius in the circular case, as equal to 6.61 Earth radii (see Appendix A). The period, being a function of only the semimajor axis, depends on the initial conditions of velocity magnitude and attitude at launch. The remaining orbital parameters depend on velocity magnitude and orientation, altitude, position and time of launch. The first question of interest is the relative ground track, which is described by a line between the Earth's center and the satellite, intersecting the Earth's surface. Six orbital elements define the position of any satellite in space at any time. Since in the present case we are interested only in the relative motion of the satellite with respect to some arbitrary point on the Earth's surface at any arbitrary time, two of these elements, defining space orientation and time of passage, may be ignored. The four remaining elements which will define the relative motion and time are:

P = period ($23^h56^m\,4.091^s$)
e = eccentricity of the elliptical orbit
i = angle of inclination of the orbital plane with the Earth's equatorial plane
w = angular longitude of perigee measured from the line of nodes

(For the "sky hook," $e = 0$, $i = 0$, and w is meaningless.)

Inclined Circular Orbit ($e = 0$, $i \neq 0$)

Now consider a case where the orbit is circular; the period is equal to one sidereal day; the orbital plane is inclined at some angle i to the Earth's equatorial plane; and no perturbing forces exist. That is:

$P = 23^h56^m\,4.091^s$
a = 26,200 statute miles
$e = 0$

By a simple transformation of spherical coordinates (given in Appendix A) the relative Earth motion, or ground track, of the satellite may be described by the deviation in longitude and latitude from a reference point on the equator. Since the period is the same as the Earth's rotational period, the satellite must return to the same point from which it started over the Earth at the end of one period. For convenience, the latitude and longitude of this point may be taken as the reference. A plot of the deviation from the equinoctial reference point is shown in Fig. 1 for several values of i. The ground tracks representing the relative motion are shown to be "figure eight" paths over the Earth's surface. The lobes of the "eight" shrink to a point for $i = 0$, and expand to occupy an entire hemisphere for a polar orbit.

Fig. 2 shows a plot of the maximum longitudinal deviation as a function of inclination angle i for a circular orbit.

Elliptical Orbits

The ground tracks of elliptical orbits are not so easily visualized as in the preceding case, since two additional parameters shape the apparent path (P and i having been assumed). These are: Eccentricity e and angular longitude of perigee w, measured from the ascending node. In Fig. 3, Ω defines the line of nodes, w is the angular longitude of perigee, v is the angular displacement of the satellite from perigee at time t (i.e., time is assumed to start from perigee crossing), and u is the angular displacement measured from the line of nodes. It is convenient to take the Earth meridian at perigee crossing as a reference, corresponding to $t = 0$.

The general effect of eccentricity variation is to bend or distort the lobes of the basic figure eight pattern, as shown in Fig. 4. For these cases, the line of apsides has been chosen to lie in the equatorial plane, i.e., $w = 0$. Since north-south symmetry exists, only one lobe (north or south) is shown, for clarity.

The effect of rotating the line of apsides (i.e., the angular longitude of perigee w) is to cause a displacement in latitude of the crossover or nodal point as illustrated in Fig. 5. The dashed curve shows that the nodal point is shifted from the reference perigee meridian and the equatorial plane in a similar figure eight locus as w is varied.

Received Sept. 17, 1958.
[1] Engineer, Electronics Department.

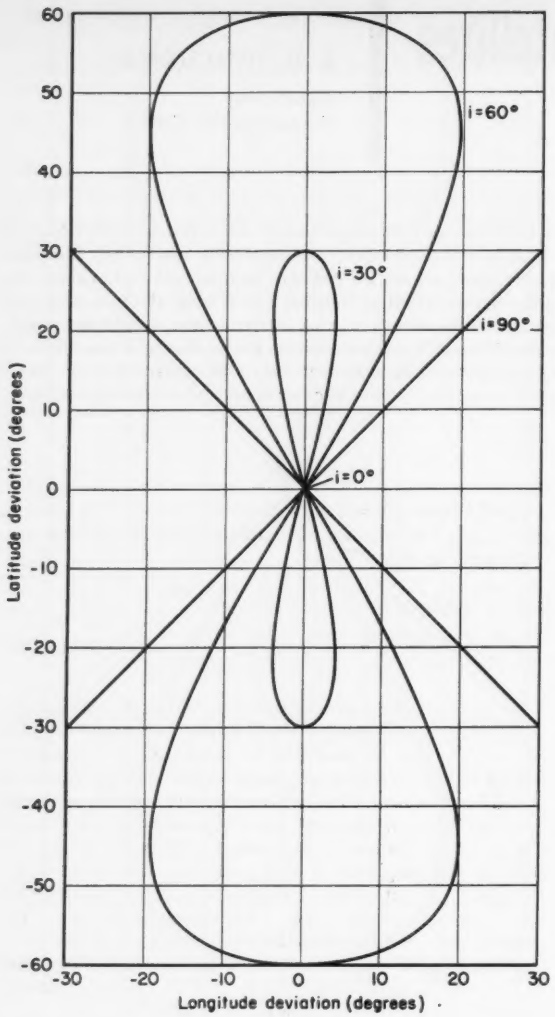

Fig. 1 Effect of inclination variation

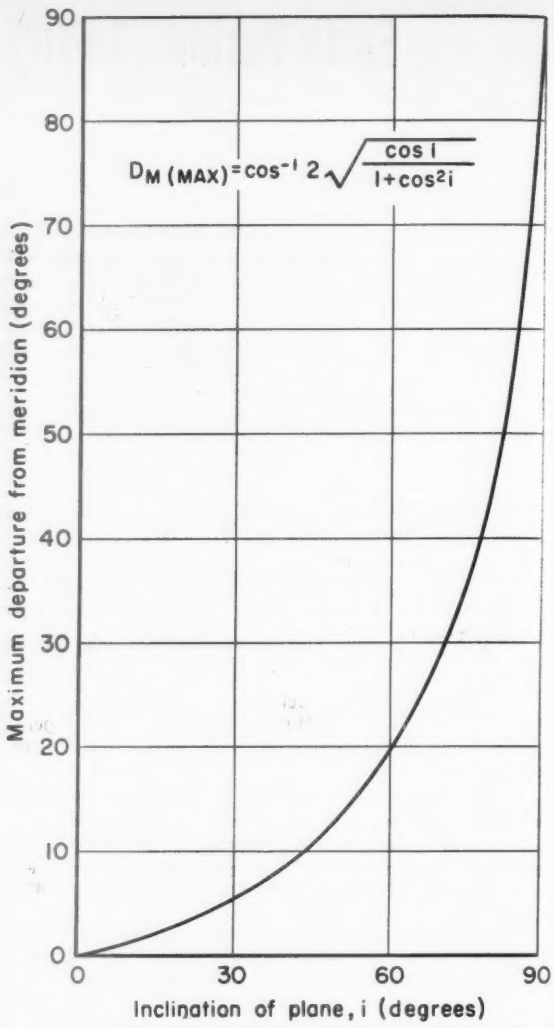

Fig. 2 Maximum departure from meridian for circular orbit ($e = 0$)

Perturbing Forces

In the preceding case, no perturbing forces have been assumed. Because a 24-hr satellite is at a distance from the Earth of 6.61 Earth radii, the gravitational pull of the moon and sun may be expected to be more significant than with lower altitude satellites. However, the more significant perturbing force is still that due to the oblateness of the Earth.

The effect of atmospheric drag has been assumed to be negligible. The sun and moon will exert an attraction on both the Earth and the satellite. Thus, both will accelerate toward the sun and moon. The difference between the acceleration of the Earth and the acceleration of the satellite is the disturbing acceleration which perturbs the orbit. In Appendix B, the disturbing accelerations due to the sun, the moon and the Earth's oblateness have been calculated using a first-order approximation. For a low altitude satellite, the disturbing forces are about the same as the tidal forces exerted on the Earth, but the disturbing acceleration on a 24-hr satellite due to the sun is about 200 times as great as this tidal acceleration. Similarly, the moon will cause an acceleration 230 times greater. These perturbations will cause the plane of the orbit to regress and the path to depart from circularity or ellipticity. In the worst case, where the Earth, satellite, moon and sun are in line, or in conjunction, this departure will be about 3600 ft. The combined regression rate due to sun and moon is 1.44×10^{-9} radian per sec, resulting in one revolution of the orbital plane about the ecliptic in 139 years. The maximum regression rate due to the Earth's oblateness will be 2.74×10^{-9} radians per sec about the celestial pole, which, when added to the rate due to the sun and moon, will result in approximately one revolution of the orbital plane in 49 years, or 7.5 deg per year. This is a worst-case value, since the period will be greater for higher inclination angles owing to the variation of the rate due to the Earth's oblateness with $\cos i$.

Summarizing, the effects of perturbations on a 24-hr satellite are quite small relative to those encountered by a low altitude satellite. The most significant result of these perturbations will be to cause a westward drift of the ground track of the order of 7.5 deg per year. In theory, this drift might be removed by lowering the period to slightly less than a sidereal day, creating a counteracting eastward drift.

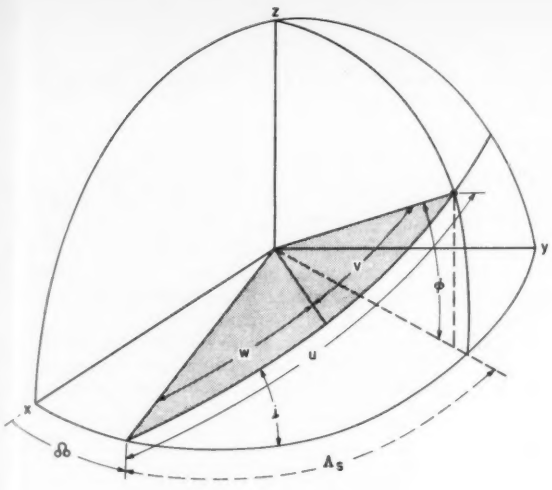

u = w + v
w = Angular longitude of perigee
v = Angular displacement of satellite from perigee at any time, t
u = Angular displacement of satellite from line of nodes

Fig. 3 Spherical coordinate system

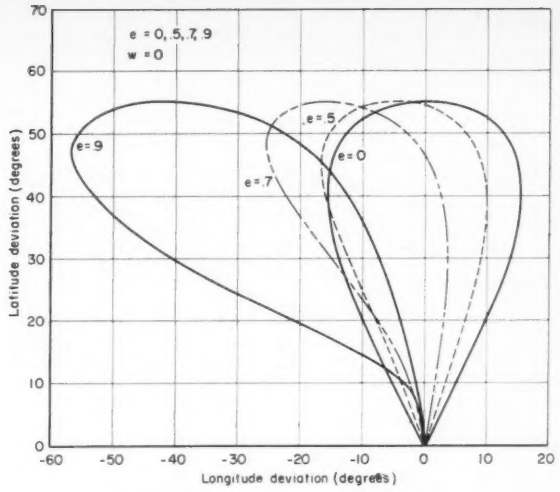

Fig. 4 Effect of eccentricity variation

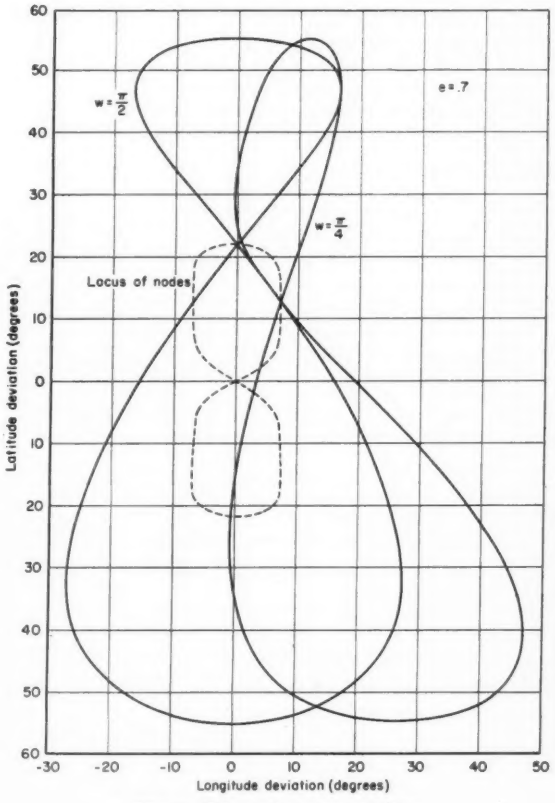

Fig. 5 Effect of perigee rotation

Possible Applications

By definition, a 24-hr satellite is a satellite selected to minimize relative motion with respect to the Earth As we have seen, this motion may be nearly zero for the equatorial orbit, or may range over an entire hemisphere for the 90-deg inclined polar orbit. The zenith positions of all are confined to one hemisphere of the Earth. The equatorial-plane satellite will only be within line-of-sight for points on the Earth within a globular sector ±81.3 deg latitude and ±81.3 deg longitude (relative to the satellite meridian); whereas the polar satellite will be within line-of-sight of almost every point on the Earth for at least one time during the period. This implies that for observation purposes, an inclined orbit might be more desirable due to its figure eight wandering ground track. By properly phasing two or more satellites, the northern (or southern) latitudes and, in particular, the polar regions may be kept under constant observance. This, of course, is not possible with the equatorial orbit, because of the 81.3-deg limitation.

For purposes of communication, it would seem that the equatorial orbit is more desirable in order to minimize the Earth-antenna pointing and tracking problem.

The ability of an optical sensor, such as TV or photography, to resolve ground detail at high altitudes depends greatly upon the contrasting luminosities and background. Because of reflection and light scattering from layer discontinuities above the tropopause, the brightness and contrast of ground areas will be veiled by the higher level returned light. However, due to the low atmospheric density, there is no reason to believe this effect would be any worse for a 22,000-mile orbit than for a 500-mile orbit. Accordingly, sufficient aperture and focal length should provide comparable ability to resolve ground detail.

At 22,200 miles altitude, 100 ft on the Earth will subtend an angular arc of about 0.1615 sec. The use of Dawes' empirical criterion for aperture and resolution results in a required optical aperture of 28 in. to resolve two points separated by this distance. In terms of wave length, this aperture is roughly 1.42×10^6 λ. Accordingly, for the same 100-ft resolution, an infrared sensor would need an aperture of 112 in., and a 3-cm radar would require 42.6 km. For higher values of resolvable angular arc, the required aperture is inversely proportional.

These values are given to suggest the practical limitations involved in any application for detailed ground area observation. Such large aperture sizes may not be required to detect point sources of light (or heat). In that case, detection will depend upon the intensity of the point source, upon background contrast and upon the square of the aperture.

Appendix A[2]

Semimajor Axis of Orbit

$$a = \left(\frac{k}{2\pi} P\right)^{2/3} = 6.61 \text{ Earth radii}$$

where

$k = 0.0743651$
$P = 1436.067$ min

Circular Orbit ($e = 0$, $i \neq 0$)

Let n equal the Earth's angular rotation rate about its axis. Then $n = 2\pi/P$ (where $P = 25^h\ 56^m\ 4.091^s$). For a circular orbit, the angular rate $\dot{u}$ (see Fig. 3), is constant and by definition

$$\dot{u} = n = 2\pi/P$$

and

$$u = nt \qquad [1]$$

Now, assuming a spherical coordinate system as shown in Fig. 3, where

ϕ = angle between r and the projection of r on the Earth's equatorial plane
r = radius vector from the center of the Earth to the satellite
Λ_s = angle measured in equatorial plane between the line of nodes and the projection of r on the equatorial plane

Then, by trigonometry

$$\cos \Lambda_s = \cos u/\cos \phi$$
$$\Lambda_s = \cos^{-1} \cos u/\cos \phi$$
$$\sin \phi = \sin u \sin i$$
$$\cos \phi = \sqrt{1 - \sin^2 u \sin^2 i}$$
$$\Lambda_s = \cos^{-1} \cos u/\sqrt{1 - \sin^2 u \sin^2 i}$$

Designating the angle in the Earth's equatorial plane through which a meridian moves in a time t as $\Lambda_E = nt$, then the longitudinal deviation D_M of the satellite from any given Earth reference meridian is

$$D_M = \Lambda_E - \Lambda_s = nt - \cos^{-1} \cos (nt)/\sqrt{1 - \sin^2 (u) \sin^2 i} \qquad [2]$$

where, from Equation [1], $u = (nt)$.

By trigonometry, the deviation in latitude is given by

$$D_L = \phi = \sin^{-1} \sin u \sin i \qquad [3]$$

For $e = 0$

$$\phi = \sin^{-1} \sin (nt) \sin i$$

Differentiating Equation [2] with respect to (nt) and setting it equal to zero, a maximum occurs when

$$\sin \Lambda_E = \pm \sqrt{1/(1 + \cos i)}$$

and

$$D_{max} = \cos^{-1} 2 \sqrt{\cos i/(1 + \cos i)^2} \qquad [4]$$

Elliptical Orbit

The analysis is essentially the same as in the circular case, see (1),[3] except that instead of $u = nt$

$$u = w + v = w + \tan^{-1}(\sqrt{1 - e^2} \sin E)/(\cos E - e) \qquad [5]$$

where E is the eccentric anomaly defined by Kepler's equation

$$E - e \sin E = nt$$

Therefore, Equations [2 and 3] are the same except that u is given by Equation [5].

Appendix B

The following approximations have been given by Lyman Spitzer Jr. (2), and are based on the methods of Hill (3), Brown (4) and Brouwer (5). They assume atmospheric drag is negligible, the satellite orbit is nearly circular, and perturbations due to other planets are insignificant. In the following examples, the maximum values of the perturbing effects are calculated to a first-order approximation.

Assuming that the Earth, satellite and the sun (or moon) are in conjunction and that an x-axis is taken along a line joining the three bodies, the acceleration of the satellite relative to the Earth is given by

$$\ddot{x} = \frac{GM_E}{R^2} - \frac{GM_s}{(R_s - R)^2} + \frac{GM_s}{R_s^2}$$

where

R = distance between Earth's center and satellite
R_s = distance between sun and Earth
M_E = mass of the Earth
M_s = mass of the sun
G_M = gravitational constant

The disturbing acceleration is the sum of the last two terms. Designating ψ as the ratio of the disturbing acceleration to the Earth's acceleration, and expanding $(R_s - R)^2$

$$\psi \cong 2 \frac{M_s}{M_e} \left(\frac{R}{R_s}\right)^3 \left(1 + \frac{3R}{2R_s}\right)$$

(neglecting the higher order terms).

Substituting numbers

$$M_s = 1.98 \times 10^{33} \text{ gm}$$
$$M_e = 5.97 \times 10^{27} \text{ gm}$$
$$R = 26{,}200 \text{ miles}$$
$$R_s = 9.3 \times 10^7 \text{ miles}$$

and for the moon

$$R_M = 2.39 \times 10^5 \text{ miles}$$
$$M_M = 7.32 \times 10^{25} \text{ gm}$$
$$\psi \text{ (24-hr satellite)} = 1.48 \times 10^{-5} \text{ (sun)}$$
$$= 3.72 \times 10^{-5} \text{ (moon)}$$
$$\psi \text{ (500-mile satellite)} = 0.73 \times 10^{-7} \text{ (sun)}$$
$$= 1.6 \times 10^{-7} \text{ (moon)}$$

an approximation to G. W. Hill's equation for departure from circularity p is given by

$$p_{max} = (1/2)R\psi = 1024 \text{ ft (sun)}$$
$$= 2575 \text{ ft (moon)}$$

At conjunction of Earth satellite, moon and sun

$$p_{max} \cong 3600 \text{ ft}$$

The regression rate of the line of nodes referred to the ecliptic plane and the ecliptic pole is given by

$$\dot{\Omega} = \frac{3}{8} \psi n = 4.05 \times 10^{-10} \text{ (sun)} \qquad \left(n = \frac{2\pi}{p}\right)$$
$$= 10.2 \times 10^{-10} \text{ (moon)}$$

$$\text{Total} = 14.25 \times 10^{-10} \text{ radians/sec (at conjunction)}$$

The regression of the line of nodes due to the Earth's oblateness referred to the equatorial plane and the celestial pole is approximated by

$$\dot{\Omega} \cong \frac{na^2}{R^2} \left[\frac{3(C - A)}{2M_e a^2}\right]$$

[2] The reader is referred to reference (1) for explanation of astronomical terms and notation used herein.

[3] Numbers in parentheses indicate References at end of paper.

where

$$3(C - A)/2M_e a^2 = 1.64 \times 10^{-3}$$

by measurement, and a = mean radius of the Earth. Accordingly

$$\dot{\Omega} = 2.73 \times 10^{-9} \text{ radians/sec}$$

due to the Earth's oblateness. The regression of the line of nodes due to the sun and moon has been calculated for the ecliptic plane. This regression rate referred to the equatorial plane is then

$$\dot{\Omega} = 1.425 \times 10^{-9} \cos 23.5 \text{ deg} = 1.31 \times 10^{-9} \text{ radians/sec}$$

The total regression rate for small inclinations is then 4.04×10^{-9} radians per sec or one revolution in 49 years.

References

1 Moulton, F. R., "An Introduction to Celestial Mechanics," second ed., Macmillan Co., Inc., New York, 1914, pp. 140–160.
2 Spitzer, L., Jr., "Perturbations of a Satellite Orbit," *J. Brit. Interplanet. Soc.* vol. 9, no. 3, May 1950.
3 Hill, G. W., "Collected Works, Memoir No. 32." *also Amer. J. Math.*, vol. 1, 1878, pp. 5, 129, 245.
4 Brown "An Introductory Treatise on the Lunar Theory," Cambridge Univ. Press, 1896, p. 130.
5 Brouwer, *Astronom. J.*, vol. 51, 1946, p. 223.

Dynamic Analysis of a Nuclear Rocket Engine System

BERNARD R. FELIX[1] and RICHARD J. BOHL[2]

Rocketdyne Division, North American Aviation, Inc. Canoga Park, Calif.

An important consideration in the design of an operational nuclear engine is that of the engine dynamic performance and control. Chemical systems have generally been designed for fixed calibration rather than automatic control of performance. Nuclear reactors have usually been designed to be sufficiently sluggish so that manual control is feasible. This paper will indicate that neither approach is suitable for a nuclear rocket engine system. A typical solid structured heat exchanger-type nuclear engine is described together with nonlinear dynamic equations describing its characteristics. Distributed parameter effects in the heat transfer processes are presented, and methods of simulation are discussed. The analysis, together with considerations of nuclear vehicle applications, is used to develop system dynamic performance criteria.

DURING the last 10 years several authors have considered the application of nuclear energy to propulsion systems for space missions. Although a number of exotic propulsion schemes have been proposed, most of the reported work has been concerned with the more straightforward approach of solid structured heat exchanger systems (1,2).[3] Since such systems are intrinsically temperature limited, low molecular weight working fluids, such as hydrogen, have generally been considered (3,4) for high performance.

It has been shown that the nuclear rocket engine offers a substantial performance advantage over chemical systems; however, many engineering and operational problems must be solved if this advantage is to be realized. McGrath (5) has pointed out the need for a systematic development plan in order to achieve this goal. An extensive subsystem development program must precede engine hot firing, because of the hazardous and perhaps infrequent nature of nuclear engine hot firings. However, experience with more conventional systems has shown that many component problems arise from the system environment and require solution both by real and simulated system operation. In order to accomplish simulated system operation, it is necessary to properly model system characteristics. The simulation hardware may consist of mechanical, hydraulic or electronic models; however, in all cases a realistic mathematical system model must exist in order to permit transformation of real system characteristics into a simulator performance specification.

The purpose of this paper is to present one such mathematical model which has been used to study system dynamic and control characteristics with an electronic analog computer. System operational and control problem areas which have been developed during the study are discussed.

System Operational and Control Requirements

Applications

In order to determine some of the problem areas which must be considered in the design of nuclear rocket systems, it is advantageous to speculate on possible applications of nuclear vehicles. Table 1 illustrates vehicle performance requirements for typical missions. The two lower specific impulse values (I_s = 300 sec and I_s = 400 sec) are in the range discussed by Tormey (6) for the more energetic chemical propellants. The higher values are in the range calculated by Rosenblum (4) for possible nuclear working fluids. Evidently, Earth orbits can be achieved with a single-stage nuclear vehicle, but for longer journeys one might eject the booster after reaching orbital or escape velocities. However, for less energetic space maneuvers, such as lunar capture, one would probably not wish to discard a nuclear engine after

Presented at the ARS 13th Annual Meeting, New York, N. Y., Nov. 17–21, 1958.

[1] Formerly Supervisor, Advance Design Section.
[2] Research Engineer, Advance Design Section.
[3] Numbers in parentheses indicate References at end of paper.

Table 1 Ideal mass ratio requirements for space maneuvers, $v = gI_s \ln R$

Maneuver	Ideal velocity increment (15), fps	Average specific impulse, sec				
		300	400	800	1200	1600
enter 350 mile Earth orbit	27,000	16.4	8.13	2.85	2.015	1.692
enter lunar transfer	10,000	2.82	2.18	1.476	1.295	1.215
lunar capture and landing	19,100	2.57	2.02	1.425	1.266	1.194
enter Mars transfer	11,600	3.32	2.46	1.57	1.35	1.253
Mars capture	6125	1.89	1.61	1.27	1.172	1.127
minimum energy to Mars orbit and return to Earth orbit	63,500	710	104	11.6	5.16	3.42

every firing. Not only would such operations be expensive, but also inefficient from an overall vehicle performance standpoint, since the heavy nuclear engine would not be used to its full capability.

From these considerations, it is clear that for some types of missions, it is desirable to be able to start the engine in space and cool the reactor after firing. Proper functioning of propellant pumps also requires close control of propellant physical properties on extended journeys.

Engine Operation

In order to typify the operation of a nuclear engine, consider the possible operating sequence described here.

Initial Reactor Startup. After the reactor is critical, its power must be increased by many decades before a temperature rise is felt. In the range of low neutron flux levels, stabilizing feedback reactivities are absent, and one would proceed slowly with startup over an interval of perhaps 10 min. For example, to increase power by 10 decades from source strength on a reactor period (e-folding time) of 20 sec, about 8 min is required. The reactivity required is a relatively safe value of 30 cents (7). During this time neutron level indications are required; however, the control rod position could be manually adjusted for booster and manned applications.

Reactor Warmup. As the reactor approaches the rated power range, a period of a minute or more is required for the fuel elements to reach the operating temperature. The exact time would be fixed by reactor thermal time constants and thermal stress criteria. Neutron detectors (ion chambers) would supply signals for the reactor warmup rate control, and reactor temperature indications would initiate the controlled engine transition phase of operation.

Engine Transition. As the core nears mainstage temperature, coolant must be supplied. The turbopump would be started at a low power condition, perhaps from a chemical gas generator. After propellant values are opened, the reactor power would be programmed to mainstage in close synchronization with the propellant flow. To conserve the propellant, this would be done as quickly as would be practical. During this transient and most critical period of reactor operations, accurate and reliable neutron level, propellant flow and temperature indications are required for control.

Mainstage Operation. After achieving rated power, steady-state operation will not be immediately achieved due to long term thermal transients in the structure, fuel burnup, poison buildup, etc. Depending on the relative values of component tolerances and internal feedback effects, automatic control may be required during mainstage operation, but this system may be very simple compared to that of the startup period. Mainstage duration is less than I_s in seconds because for a constant thrust, Earth takeoff vehicle, burning time (t_b) is given by (8)

$$t_b = \left(\frac{R-1}{R}\right)\left(\frac{I_s}{F/W}\right)$$

As shown in Table 1, mainstage will last for less than 10 or 20 min. Longer burning times occur if the engine is a sustainer type, which does not overcome the full force of gravity.

Cutoff. Engine thrust decay or cutoff requirements depend on the type of mission. However, fission fragment afterheat defines the procedure of reactor shutdown, because by inserting all of the control elements, immediate neutron level depletion is impossible due to background radiation. An Earth takeoff, with booster ejection after reaching some prescribed velocity, requires a rapid thrust decay for separation. Hence propellant flow rate must be reduced to zero, and the fission fragment afterheat will vaporize the engine in a few thermal lag times. The second and more difficult form of cutoff, if one desires to re-use a nuclear engine, requires propellant to continuously cool the reactor until power is sufficiently low so that another form of cooling, such as thermal radiation, can be employed. In order to conserve propellant, it would be desirable to throttle the propellant flow so as to keep the exit temperature as high as practical. In the latter case, the expellant would not entirely be a weight penalty, since thrust would be generated which might be used for vernier trajectory correction.

Control Requirements

From these general considerations, some of the control hardware requirements may be outlined.

Instrumentation. In order to assure satisfactory engine operation during start, mainstage and cutoff, transducers are required to independently measure the following variables: Neutron level (power), temperature and reactor flow rate. Obviously, many other measurements are also required in a development program.

Control Computers. An integrated engine control system requires a control computer which accepts and properly operates on the subsystem performance information in such a way as to satisfactorily synchronize component operation.

Final Control Elements. In our example, the control computer generates signals to properly position the following subsystem control elements:

1 Reactivity control elements. These might be moving poison rods, or flows of poison or moderating fluids within the reactor.

2 Turbine control valve. The gross buildup of propellant flow is here determined by programming the pump input power.

3 Main propellant values. Initial priming of the propellant passages (with which may be associated a positive reactivity insertion) as well as the proper switching from warmup to transition is controlled by the main propellant valves downstream of the pump.

The requirement that the hardware must operate reliably in an environment of high nuclear radiation and heat generation poses several novel design problems with even the simplest of controls components.

System Representation

Engine Concept

An illustrative nuclear engine system schematic, such as has been discussed by Rosenblum et al. (4) and McGrath (5) is typified in Fig. 1. It is similar in concept to a chemical engine except that the combustion chamber is replaced by a nuclear reactor. The working fluid, stored in a low pressure tank to save weight, is pumped to high pressures and initially used to regeneratively cool various engine components which

are heated due to the absorption of thermal and nuclear radiation fluxes. The fluid then enters the reactor heating channels and finally exhausts at supersonic velocities through a conventional de Laval nozzle. A portion of the heated working fluid is either bled off from the main stream or passed through a separate heating region in order to provide hot gases to power the turbopump. A summary of lumped parameter equations used to describe these processes is shown in Table 2.

Reactor Neutronics

The configuration of a solid structured, gas cooled reactor suitable for rocket propulsion will generally be established from heat transfer and structural design considerations. However, if the thrust level is low, then reactor criticality also must be considered. The steady-state design concept used depends strongly on the performance requirements; hence, many trial and error designs are required before the final concept is evolved. Fortunately, the kinetic features of the fission process are sufficiently similar in many reactors so that a fairly simple model produces useful results.

The speed with which a reactor can change power level is determined primarily by the magnitude of reactivity changes produced by temperature, density, control poisons, and by the yield and decay constants of certain fission fragments which during decay emit "delayed" neutrons. The delayed neutrons permit power changes sufficiently slow to achieve control.

The reactor kinetic equations include the neutron-level equation (7)

$$\frac{dN}{dt} = \frac{\rho - 1}{l}\beta N + \sum_{i=1}^{n} \lambda_i C_i + S$$

and the precursor concentration equation

$$\frac{\partial C_i}{\partial t} = \frac{\beta_i N}{l} - \lambda_i C_i + D\frac{\partial^2 C_i}{\partial y^2} \quad (10)$$

rate of change of concentration = production rate − radioactive decay + diffusion loss

These equations imply the following assumptions:

1 The rate of change of neutron level is the sum of the increase of prompt neutrons produced in fission and the buildup of delayed neutron emission from fission product decay.

Table 2 System equations

I NEUTRONICS

1. $N = \frac{1}{S}\left[(\rho - 1)\frac{\beta N}{l} + \sum_i \lambda_i C_i\right]$

2-7. $C_i = \frac{1}{1+S/\lambda_i}\frac{\beta_i}{\beta}\lambda_i\left[N - \left(\frac{2}{a}\sqrt{\frac{D}{\lambda_i}}\tanh\sqrt{\frac{D}{\lambda_i}}\frac{a}{2}\right)\left(\frac{1+S/\omega_2}{(1+S/\omega_1)(1+S/\omega_3)}\right)N\right]$

8. $P = P_r - \gamma_T(T_p - T_{p_0}) + \gamma_a(M_R - M_{R_0})$

9. $\dot{Q}_v = (N_v \sigma_f V E_f)N$

II HEAT TRANSFER (ONE LUMPED PARAMETER SECTION)

10. $\dot{M}_1 C_p (T_2 - T_1) + \frac{M_1 C_p}{2}\frac{d}{dt}(T_1 + T_2) = \dot{Q}_s A_{HS}$

11. $\dot{Q}_s = h(T_w - 0.5T_1 - 0.5T_2)$

12. $T_p = T_{p_0} + \frac{1}{d_w C_w S}\left[\dot{Q}_v - \frac{2}{b}\dot{Q}_s\right]$

13. $T_w = T_p - \frac{b}{6K}\frac{\dot{Q}_s}{1 + \frac{TS}{10}}$

III REACTOR — THRUST CHAMBER PRESSURES

14. $P_2 = \frac{\dot{M}_1 C^*}{(1+T_c S) g A_t}$; $C^* = f(T_2)$

15. $P_1 = P_2 + \frac{\dot{M}_1^2 R}{2gA_F^2}\left[\frac{T_2}{P_2} - \frac{T_1}{P_1} + \frac{fL}{m}\left(\frac{T_2+T_1}{P_2+P_1}\right)\right] + \frac{L_R S \dot{M}_1}{gA_F}$

16. $M_R = \frac{V_R}{R}\left(\frac{P_2+P_1}{T_2+T_1}\right)$

IV FEED SYSTEM

PUMP

17. $\dot{M}_p = \dot{M}_1 + \dot{M}_T$

18. $P_p = P_s + d_p K_1 N_p^2 + K_2 \dot{M}_p N_p + K_3 \frac{\dot{M}_p^2}{d_p}$

19. $L_p = d_p K_4 N_p^2 + K_5 \dot{M}_p N_p + K_6 \frac{\dot{M}_p^2}{d_p}$

HOT GAS VALVE ; TURBINE

20. $\dot{M}_T = \frac{A_{TN} P_T}{C_T^*} = \frac{g A_{TN} P_p}{C_T^*}\left[F\left(\frac{A_{HG}}{A_{TN}}\right)\right]$

21. $L_T = \frac{\dot{M}_T}{2g}(K_7 r_1 C - K_8 r_1^2 N_T)$

22. $C = \sqrt{2g C_{pT} T_T\left[1 - (P_{ss}/P_1)^{\frac{\gamma-1}{\gamma}}\right]}$

23. $\left(\frac{P_{ss}}{P_T}\right)^{\frac{\gamma-1}{\gamma}} = f(\dot{M}_T) = \text{CONSTANT IF SONIC}$

POWER BALANCE

24. $(I_p + GR^2 I_T) N_p = \frac{1}{S}\left[GRL_T - L_p\right]$

MAIN PROPELLANT LINE PRESSURE DROP

25. $\dot{M}_p = A_R\sqrt{2 d_p g\left(P_b - P_1 - \frac{R_1 \dot{M}_p^2}{d_p} - L_L S \dot{M}_p\right)}$

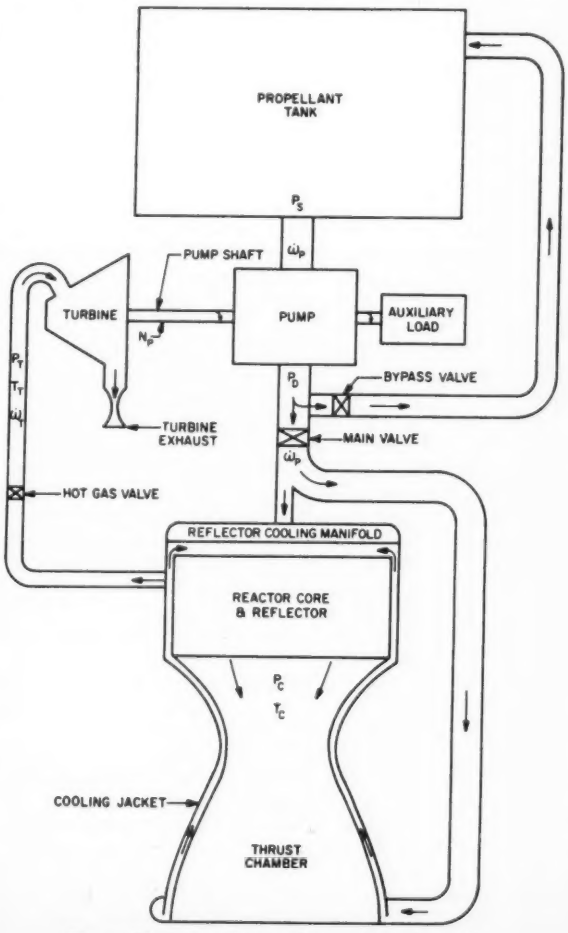

Fig. 1 Nuclear rocket engine system schematic

2 The spatial distribution of power is independent of time; only the amplitude changes.

3 Neutrons may be assigned averaged properties, and delayed neutrons have the same properties as those produced directly in fission. If the delayed neutron parameters are adjusted to the energy spectrum of a particular reactor, the latter assumption need not be made.

4 A fraction of the delayed neutron precursors diffuse from the fuel elements at elevated temperatures and are immediately swept out by the propellant stream.

Power transients are of principal interest in many dynamic studies, since temperature changes are relatively slow. Thus, it is instructive to consider the case where the diffusion "constant" D is either constant or varies slowly with time.

Then, taking the Laplace transform of the precursor concentration equation with the initial conditions equal to zero

$$\frac{d^2C_i(y, S)}{dy^2} - \frac{\lambda_i + S}{D} C_i(y, S) = -\frac{\beta_i N(S)}{l}$$

The solution is

$$C_i(y, S) = \frac{\beta_i N(S)}{(\lambda_i + S)l} + C_3 \exp\left(\sqrt{\frac{S + \lambda_i}{D}}\, y\right) + C_4 \exp\left(-\sqrt{\frac{S + \lambda_i}{D}}\, y\right)$$

At the boundary, the concentration is zero (9). Thus

$$C_i(y, S) = \frac{\beta_i N(S)}{l(S + \lambda_i)} \times \left[1 - \frac{\exp\left(\sqrt{\frac{S + \lambda_i}{D}}\, y\right) + \exp\left(-\sqrt{\frac{S + \lambda_i}{D}}\, y\right)}{\frac{1}{2}\cosh\left(\sqrt{\frac{S + \lambda_i}{D}}\, \frac{a}{2}\right)}\right]$$

Averaging the precursor concentration over the region

$$\bar{C}_i(S) = \frac{\beta_i N(S)}{l(\lambda_i + S)}\left[1 - \frac{2}{a}\sqrt{\frac{D}{S + \lambda_i}} \tanh\left(\sqrt{\frac{S + \lambda_i}{D}}\, \frac{a}{2}\right)\right]$$

Although this transcendental form is not suitable for electronic analog simulation work, its exact frequency response plots can be obtained by digital computer techniques. The results can then be approximated by a series of lag-lead-lag approximations which converge faster than a direct application of finite difference methods.

Feedback Effects of Reactivity

The variable principally used for the discussion of neutron kinetics is the reactivity. In the present definition it has the units of dollars, where 1 dollar represents the fraction of neutrons arising from fission product decay. Essentially, it measures the excess of neutrons produced over that required to maintain a chain reaction. As long as the reactivity is less than 1 dollar, changes of neutron level can be brought about sufficiently slow (since it is necessary to wait for precursor decay) to achieve control. If the net reactivity input to the reactor exceeds 1 dollar, the power will rise very rapidly, and controller response requirements become unreasonable. Hence, it is necessary to limit rapid changes to less than this value.

Origin of Reactivity Changes

In addition to the precursor loss, reactivity changes arise from four principal phenomena in a nuclear engine.

Control Elements. These may be in the conventional form of movable neutron absorbing materials (boron or cadmium) or fissionable or moderating material. Other possibilities include injection of poison into the working fluid, variation of the reflector and circulation of poison material in the core.

Gross Temperature Changes in Moderating Material. Changes in moderator temperatures affect criticality by modifying the neutron energy spectrum, thereby altering fission cross sections. Due to the high temperatures required in a nuclear rocket reactor, this effect is of major importance during startup.

Propellant Density Changes in Core and Structure. Three of the possible nuclear working fluids which have been considered (4) are rich in hydrogen, a good neutron moderator. In the liquid state, hydrogen, ammonia and water have hydrogen atomic densities differing only by a factor of 2 or 3. Since light water moderated reactors may be critical at sizes as small as 12 in. (10), it is clear that the introduction of small amounts of dense propellant into a nuclear rocket reactor, which may be undermoderated to conserve weight (2), can have an important reactivity contribution.

Thermal Expansion and Pressure Effects on Reactor Geometry. Neutron leakage from the reactor boundary is altered by changes in geometry, thus altering criticality.

These reactivity effects are summarized as linear coefficients in Equation [8] of Table 2. In general, the effects are nonlinear and must be evaluated from multigroup reactor calculations or critical experiments. Even then, the values cannot be sufficiently well relied upon to predict a reactivity vs. time curve which would yield a proper power buildup at start. Hence, the programming of an automatic power control system is required to automatically define the proper reactivity sequence.

Heat Transfer

The difference between chemical and nuclear engines is most strikingly illustrated by the distributed parameter effects of heat transfer. In a chemical engine, energy is imparted to the propellant gases in times measured in milliseconds (8). The dynamic effect is frequently neglected or only crudely approximated in controls analysis studies, since it is of high frequency compared to many control element responses. In a nuclear engine, on the other hand, energy transfer to the propellant may take place over a region of several feet (4). Thus, in order to obtain a temperature rise in the propellant gases, it is necessary to wait until a large mass of solid material has warmed. Although large and rapid reactivity changes may cause violent power surges to occur under malfunction conditions, damage to the reactor fuel elements generally will be associated with the resulting temperature rise. Assuming a reactor can be designed to possess a negative temperature coefficient, then an important parameter in stability and control is the thermal lag times of the fuel elements, that is, the time required for temperatures to reach 63 per cent of equilibrium values after a step change in power. In deriving this parameter, the following assumptions are employed:

1 Fuel element thermal conductivity is constant in time.

2 One-dimensional heat transfer, that is, temperature gradients are small except in the direction of heat flow to the propellant.

3 Uniform heat generation in the radial direction.

4 Single phase, turbulent and subsonic flow of propellant through the reactor core.

The following basic equations are thereby implied: Fuel element heat transfer and enthalpy storage (11)

$$K_M \frac{\partial^2 T}{\partial y^2} - d_M C_M \frac{\partial T}{\partial t} = -\dot{Q}_v$$

Coolant heat transfer and enthalpy storage (12)

$$\frac{\dot{M}_r}{A_F} C_p \frac{\partial T_g}{\partial y} + d_g C_p \frac{\partial T_g}{\partial t} = \frac{h}{m}(T_w - T_g)$$

Coolant mass storage (12)

$$\frac{\partial}{\partial x}\left(\frac{\dot{M}_r}{A_F}\right) + \frac{\partial d_g}{\partial t} = 0$$

Coolant pressure drop and inertia (12)

$$\frac{\partial}{\partial x}\left(P + \frac{\dot{M}_r^2}{g d_g A_F^2}\right) + \frac{2f\dot{M}_r^2}{g d_g m A_F^2} = -\frac{1}{g}\frac{\partial}{\partial t}\left(\frac{\dot{M}_r}{A_F}\right)$$

Gas law (12)

$$P = d_g R_g Z T_g$$

In order to eliminate the space dimension in the fuel element heat transfer and enthalpy storage equation and render it more suitable for simulation studies, the technique of iterated Laplace transform will be employed. To simplify the treatment, initial conditions are neglected; this is equivalent to taking perturbations about a steady state. Transforming the time domain

$$\frac{d^2T(y, S)}{dy^2} - \frac{d_M C_M}{K_M} ST(y, S) = -\frac{\dot{Q}_v(S)}{K_M}$$

Since heat generation is independent of y, the solution is

$$T(y, S) = \frac{\dot{Q}_v(S)}{d_M C_M S} + C_1 \exp\left(\sqrt{\alpha S}\, y\right) + C_2 \exp\left(\sqrt{\alpha S}\, y\right)$$

where

$$\alpha = d_M C_M / K_M$$

Assuming boundary conditions of heat fluxes $\dot{Q}_{s1}$ and $\dot{Q}_{s2}$ leaving the surface $y = 0$ and $y = b$ respectively, then

$$\dot{Q}_{s1}/K_M = C_1\sqrt{\alpha S} - C_2\sqrt{\alpha S}$$

$$\dot{Q}_{s2}/K_M = -C_1\sqrt{\alpha S}\exp\left(\sqrt{\alpha S}\, b\right) + C_2\sqrt{\alpha S}\exp\left(-\sqrt{\alpha S}\, b\right)$$

Solving simultaneously and integrating over y to obtain the average element temperatures

$$\bar{T}(S) = \frac{1}{d_M C_M S}\left[\dot{Q}_v - b^{-1}(\dot{Q}_{s1} + \dot{Q}_{s2})\right]$$

The wall temperatures are then given by

$$T_{w1} = \bar{T} - \frac{b}{3K_M}\left(H_1\dot{Q}_{s1} - \frac{H_2}{2}\dot{Q}_{s2}\right)$$

$$T_{w2} = \bar{T} - \frac{b}{3K_M}\left(-\frac{H_2}{2}\dot{Q}_{s1} + H_1\dot{Q}_{s2}\right)$$

where

$$H_1 = (3/\tau S)\left[\sqrt{\tau S}\coth\left(\sqrt{\tau S}\right) - 1\right]$$

and

$$H_2 = (6/\tau S)\left[1 - \sqrt{\tau S}\,\mathrm{csch}\left(\sqrt{\tau S}\right)\right]$$

Both transfer function gains are unity at low frequencies and they begin dropping at $10/\tau$ radians per sec, where

$$\tau = d_M C_M b^2 / K_M$$

For example: Taking $b = 0.1$ in., which is in the range suggested by Levoy and Newgard (2), then for graphite

$$\tau = 0.2 \text{ sec}$$

As a later example shows, the overall thermal time constants may be appreciably greater than this value; these transcendental transfer functions may be set equal to unity in some cases.

Since the coolant heat transfer and pressure drop and gas law equations are nonlinear, it is not possible to separate the space dimension; hence, one must use finite difference techniques in treating the axial temperature distribution. If the steady-state temperature distribution is known, it is frequently possible to obtain a method (such as logarithmic averaging) which converges more rapidly; however, the arithmetic averaging of properties in a region has been found suitable for dynamic studies. Here, the partial space derivatives are replaced by finite differences, and time derivatives are taken on average properties. For this reason, the simplified, lumped parameter equations of Table 2 represent only one increment into which the reactor is mathematically separated. In general, several regions are required to satisfactorily represent the distributed parameter heat transfer effects.

In order to obtain an order of magnitude estimate of the overall thermal time constant, we use Equations [10 to 13] of Table 2 to obtain a linearized relationship between perturbations in reactor power level and temperature. The effect of fuel element temperature gradient in Equation [13] is also neglected. Perturbing Equations [10 to 13], we have

$$\delta T_2 = \delta T_1 + (T_2 - T_1)\frac{\delta\dot{Q}_s}{\dot{Q}_s} - (T_2 - T_1)\frac{\delta\dot{M}_R}{\dot{M}_R}$$

$$\frac{\delta\dot{Q}_s}{\dot{Q}_s} = \left(\frac{T_p}{T_p - 0.5T_2 - 0.5T_1}\right)\left(\frac{\delta T_p}{T_p} - 0.5\frac{\delta T_2}{T_2} - 0.5\frac{\delta T_1}{T_1}\right)$$

$$\frac{\delta T_p}{T_p} = \frac{1}{S}\left(\frac{\dot{Q}_v}{d_M C_M T_p}\right)\left(\frac{\delta\dot{Q}_v}{\dot{Q}_v} - \frac{\delta\dot{Q}_s}{\dot{Q}_s}\right)$$

Solving simultaneously

$$\frac{\delta T_p}{T_p} = \left[\left(\frac{T_p - T_1}{T_p}\right)\frac{\delta\dot{Q}_v}{\dot{Q}_v} - \left(\frac{T_p - T_1}{2T_p}\right)\frac{\delta\dot{M}_R}{\dot{M}_R} + \frac{\delta T_1}{T_1}\right]\Big/(1 + \tau_p S)$$

where

$$\tau_p = \frac{d_M C_M (T_p - T_1)}{\dot{Q}_v}$$

This response is that of a simple lag; that is, temperatures reach 63 per cent of final steady-state values at τ_p seconds after a step change in power.

Taking, for example, a graphite element at 4000 F and a power density of 100 megawatt/ft³ which is in the range mentioned by Levoy and Newgard (2), then the thermal lag one might expect is

$$\tau_p = \frac{(103)(0.5)(4000)(1055)}{10^8} = 2.2 \text{ sec}$$

By comparison, the Calder Hall power reactor (2) operates at 11.5 kw/ft³ and $T_p - T_1 = 353$ F which yields

$$\tau_p = 1330 \text{ sec} \approx 22 \text{ min}$$

The need for automatic control in operating a nuclear engine thereby becomes obvious: In 20 min a human operator can easily (and reliably) set operating temperature, but in a few seconds, only a go-no-go type decision is possible. If the reactor design possesses a negative temperature coefficient, then a system this fast will normally be very stable at mainstage due to rapid negative reactivity changes caused by temperature variations; however, since the thermal time constant is inversely proportional to power, the temperature feedback needed for stability will be slow and therefore ineffective at low power levels.

Feed System

The basic feed system components illustrated in Fig. 1 are the pump, turbine, hot gas throttle valve and main propellant control valves. Normally, the latter valves are required only to properly synchronize initial flow buildup. At rated power, the hot gas valve could be used as a thrust regulating device, if desired. The principal dynamic effects to be considered have been discussed by Smith (14) and by Gore and Carroll (16) and will be only briefly outlined here.

The pump is assumed to obey the affinity laws, and empirical or theoretical data are used to obtain the effect of flow variations. The turbine nozzles are assumed choked, and only one turbine stage is represented by the equations of Table 2. If the turbine has more than one stage, one may

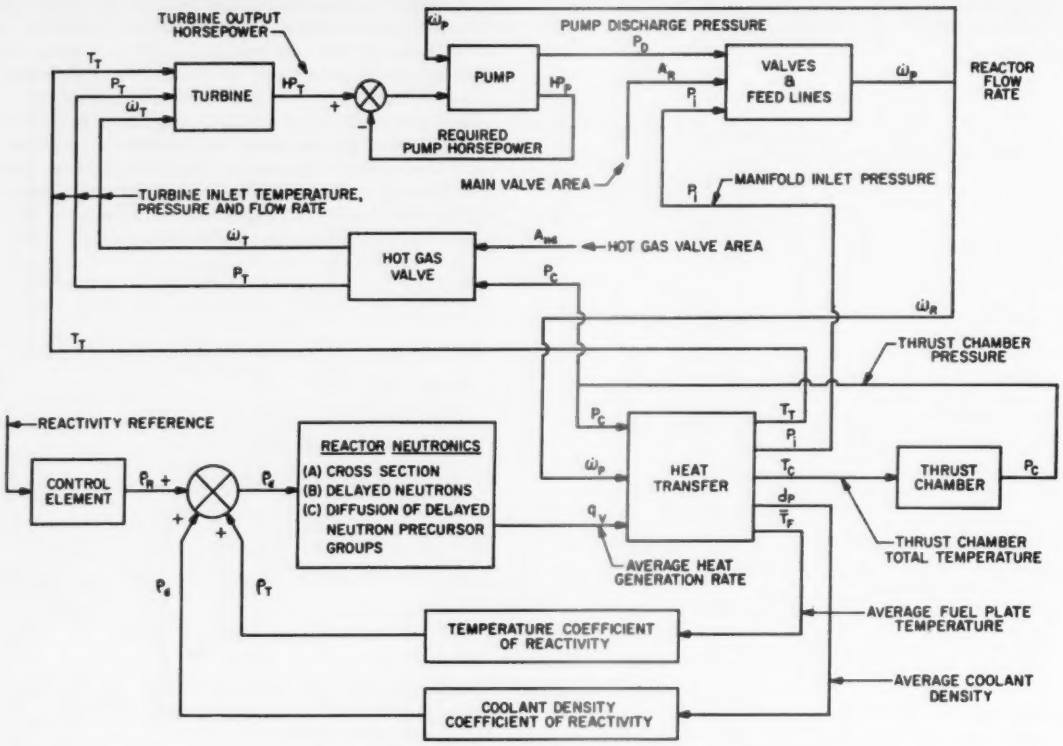

Fig. 2 Nuclear rocket engine system block diagram

either use several sets of equations or obtain an empirical map to show the effects of speed, temperature and flow on performance. The basic low frequency feed system time constant is associated with the rotary moment of inertia of turbopump moving parts. Other high frequency effects arise from the fluid line inertias and the gas compressibility effects. A feed system analog mechanization diagram is shown in Fig. 7.

Since these phenomena are fluid mechanical in nature, it is clear that the overall feed system response may be made sufficiently fast as to be dynamically decoupled from the reactor thermal response. An example of the application of control synthesis techniques to improving feed system response is shown in the root locus construction (17) of Fig. 4. For generality, the response is nondimensionalized in terms of the turbopump break frequency. The controller possibilities include:

1 Proportional, in which case the steady-state error will be large for gain values low enough to avoid instability due to high frequency poles.

2 Integral, in which case the steady-state error is zero, but little improvement in dynamic performance is possible without oscillatory response due to high frequency poles.

3 Integral with lead compensation. Here, zero steady-state error is obtained, and the effect of anticipation is a considerable improvement in the dynamic response.

Interactions

The system block diagram of Fig. 2 illustrates some of the basic subsystem interaction problems. The basic feature of system response is that the reactor power level is not uniquely determined by the propellant flow. In a chemical rocket, suitable orificing of propellant supply lines to obtain proper propellant flow rates automatically fixes thrust. In a nuclear rocket engine, power perturbations effect both reactor and feed system operation due to temperature changes thereby produced. Increased temperatures will result in a rise of turbine output horsepower, if not controlled. This rise will eventually be felt back at the reactor due to increase pump flow rate, with a resulting decrease in reactor temperature. Hence, the feedback loop of temperature through the feed system should be stable if the temperature coefficient predominates. However, if the positive reactivity effect due to propellant density changes is large, an increase of reactor power may feed through the turbopump to produce an increased amount of propellant in the reactor, which in turn raises power farther. Thus, if the density coefficient is large, not only does the system become much more sensitive to disturbances, but also the possibility of overall system instability exists. The need for designing a nuclear rocket reactor to be both insensitive to density changes and to minimize the amount of propellant in the core is thus apparent.

Control Loops

In view of the preceding discussion, it is clear that two distinct control loops must be considered. The intrinsic speed with which the reactor power and the propellant flow can respond requires that these two parameters be automatically controlled at least during the dangerous period of engine transition. Temperature changes take place relatively slowly with respect to the speed of response of these two loops. Hence it is possible to consider pre-setting the desired maximum values of power and flow before each run. The main-stage tolerance situation will then dictate whether a rather slow and simple automatic adjustment of temperatures is

needed during flight, or if a short preflight calibration test will suffice.

Conclusions

Considerations of nuclear engine applications and operational requirements indicate the need for advanced control methods if satisfactory and safe engine performance is to be obtained. To achieve the high degree of component reliability required to permit a realistic engine development program to succeed, extensive controls and other component testing under simulated system operation is required. This paper has presented a mathematical model which can be used to generate a simple, but useful, electronic simulation of system dynamic characteristics.

Appendix
Example of Simulation and Servo Analysis Techniques in Studying System Response

Simulation of Kinetics Equations

A useful mathematical technique which permits transformation of equations into scaled form suitable for electronic simulation and simultaneously allows application of linearized servo analysis tools to the system, is that of nondimensional, nonlinear perturbation. Consider the basic neutronic kinetic equations without precursor loss

$$\dot{N} = (\rho - 1)(\beta N/l) + \sum_{i=1}^{6} \lambda_i C_i$$

$$\dot{C}_i = (\beta_i N/l) - \lambda_i C_i$$

Let $N = N_0(1 + n/100)$ and $C_i = C_{i0}(1 + C_i/100)$, and replace ρ by $\rho/100$ where the new reactivity is in cents (or volts on an analog computer). The nominal steady-state values are related by

$$C_{i0} = \beta_i N_0/l\lambda_i$$

Then, the perturbed equations are

$$n = \left[\frac{1}{1 + (l/\beta)S}\right]\left(\rho + \frac{\rho n}{100} + \sum_{i=1}^{6} \frac{\beta_i}{\beta} C_i\right)$$

$$C_i = \frac{n}{1 + S/\lambda_i}$$

The values of the delayed neutron parameters have been discussed by Keepin (13) and are summarized in Table 3 for U^{235}.

Form of Open Loop Neutronics Transfer Function

Elimination of the nonlinear term in the previous equation permits a linearized transfer function to be formed by simultaneous solution of the seven equations. For simplicity, consider only one delayed group with suitable averaged properties. Then

$$n = \left[\frac{1}{1 + (l/\beta)S}\right]\left(\rho + \frac{n}{1 + S/\bar{\lambda}}\right)$$

Table 3 Delayed neutron parameters (10)

Delayed group	Half life $\tau_{1/2}$, sec	Relative yield β_i/β	Decay constant $\lambda_i = 0.693/\tau_{1/2}$
1	54.3	0.036	0.0128
2	21.7	0.210	0.0319
3	5.87	0.192	0.118
4	2.18	0.409	0.318
5	0.46	0.135	1.51
6	0.13	0.018	5.33

The transfer function is then

$$\frac{n}{\rho} = \left(\frac{\beta\bar{\lambda}}{\beta + l\bar{\lambda}}\right)\left\{\frac{1 + S/\bar{\lambda}}{S\left[1 + \left(\frac{l}{\beta + l\bar{\lambda}}\right)S\right]}\right\}$$

The response is basically integral, modified by a lead-lag term. With six delayed groups, there would be six lead-lag terms.

In order to evaluate a suitable averaged decay constant $\bar{\lambda}$, one method is to make the integral gains equal (7); then

$$\frac{1}{\bar{\lambda}} = \sum_{i=1}^{6} \frac{\beta_i}{\lambda_i}\beta^{-1} = \frac{1}{0.0805} = 12.4 \text{ sec}$$

Example of Response

As an example, consider a prompt lag $l/\beta = 0.01$ sec, and a negative temperature coefficient of -5 cents per per cent temperature change. The simplified, one-group neutron transfer function is then

$$\frac{n}{\rho} = \frac{0.0805}{S}\frac{(1 + S/0.0805)}{(1 + S/100)}$$

These values have been chosen for convenience (a 0.01-μf capacitor and a $\times 5$ amplifier input were available), however, they are in the range considered representative by Schultz. With the previous estimate of a 2-sec thermal lag time (break frequency 0.5 radian/sec) the open loop transfer function becomes

$$\frac{\rho_T}{\rho} = \frac{0.4025}{S}\frac{(1 + S/0.0805)}{(1 + S/0.5)(1 + S/100)}$$

The closed loop response becomes clear from root locus consideration. At low loop gains, the integrating pole moves to the first zero at 0.08 radian per sec, thus stabilizing the system and yielding a flat response below the thermal lag frequency. The heat transfer and prompt lag poles at 0.5 and 100 radians per sec move together and eventually break away from the real axis at high gains with oscillatory response. Normally, this situation would only be obtained in water moderated reactors in which the negative coefficient of reactivity due to density changes is very large. For a nuclear rocket reactor, this oscillatory condition might be obtained if delayed neutron loss were sufficiently high.

For our example the heat transfer pole simply moves to higher frequencies yielding the following approximate closed loop response to external reactivity changes

$$\frac{\theta}{\rho} = \frac{0.2(1 + S/0.0805)}{(1 + S/0.069)(1 + S/3.04)(1 + S/97)}$$

$$\frac{n}{\rho} = \frac{0.2(1 + S/0.5)(1 + S/0.0805)}{(1 + S/0.069)(1 + S/3.04)(1 + S/97)}$$

These transfer functions are shown in the form of frequency response plots in Fig. 3. The typical lead-lag response of power to reactivity is evident from the figure. At frequencies below the thermal lag frequency, the response is flat, but when disturbances are inserted at frequencies above the thermal lag frequency, the gain goes up as the stabilizing effect of the thermal lag disappears. The gain difference between low and high frequency response is closely associated with the temperature coefficient, thus providing a convenient experimental method for measuring the latter quantity.

The effect of nonlinearities on response is evident in the analog computer results of Fig. 5. These results were obtained using the mechanization diagram of Fig. 6 and the previous data. For simplicity, the section representing precursor loss was omitted. At low reactivity inputs, the response is linear and as expected; however, as large positive reactivities are inserted, very large power surges occur before the tempera-

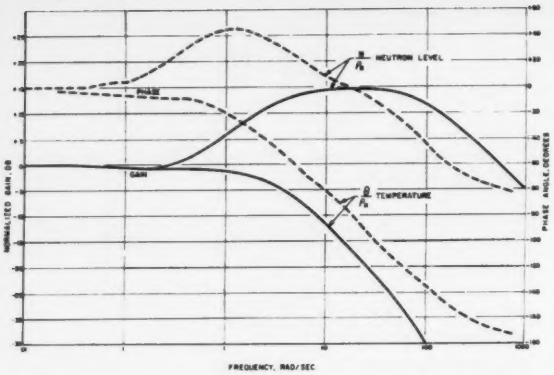

Fig. 3 Reactor frequency response with temperature feedback

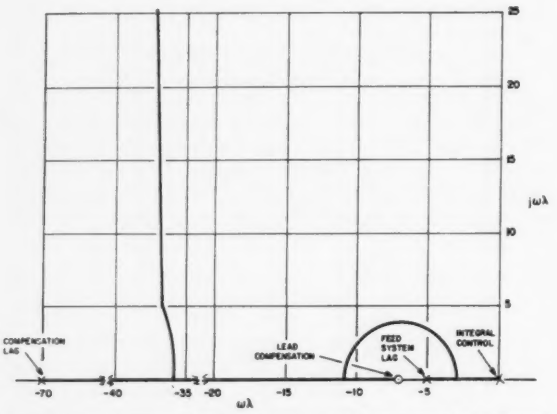

Fig. 4 Feed system bode plot with lead compensated integral control

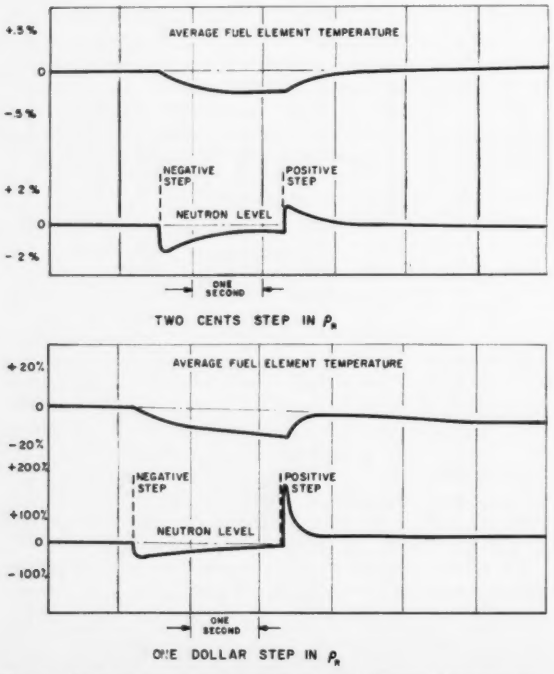

Fig. 5 Reactor power and average fuel element temperature response to step inputs of reference reactivity

ture feedback can become effective. Although it appears that the existence of a negative temperature coefficient will eventually stabilize these power excursions, it is clear that they are undesirable from the point of view of other components. Hence, reactivity must be closely controlled to guard against any sudden, large changes.

Acknowledgment

The authors wish to acknowledge the valuable contributions made to this study by R. F. Searle and R. E. George. Acknowledgment is also made to R. K. Seferian for valuable advice on analog computing technique. The authors are also indebted to R. Matulenko for his constructive criticisms and technical contributions.

Nomenclature

A_{HS} = reactor heat transfer area, in.^{2}
A_T = nozzle throat area, in.^{2}
A_F = reactor flow area, in.^{2}
A_{HG} = hot gas valve effective area, in.^{2}
A_{TN} = turbine nozzle throat area, in.^{2}
A_R = main valve effective area, in.^{2}
b = fuel element thickness, in.
a = characteristic length for diffusion, in.
C = turbine nozzle spouting velocity, ips
C^* = nozzle characteristic velocity, ips
C^*_T = turbine characteristic velocity, ips
C_i = ith group precursor concentration
C_{PT} = specific heat of turbine working fluid, Btu/lb R
C_p = specific heat of propellant, Btu/lb R
C_M = specific heat of fuel element, Btu/lb R
d_g = reactor coolant density, lb/in.^{3}
d_p = propellant density, lb/in.^{3}
d_M = fuel element density, lb/in.^{3}
D = precursor diffusion coefficient, cm^2/sec
E_f = energy yield per fission, Btu/fission
F = vehicle thrust, lb
f = friction factor
GR = gear ratio
g = acceleration due to gravity, in./sec^2
h = heat transfer coefficient, Btu/R in.^{2} sec
I_p = effective pump inertia, lb-in.-sec^2
I_s = specific impulse, sec
I_T = effective turbine inertia, lb-in.-sec^2
K_1 = coefficient in pump H-Q curve fit, sec^2/in.
K_2 = coefficient in pump H-Q curve fit, sec^2/in.^{2}
K_3 = coefficient in pump H-Q curve fit, sec^2/in.^{5}
K_4 = coefficient in pump torque curve, sec.^{2}/in.^{4}
K_5 = coefficient in pump torque curve, in.-sec.^{2}
K_6 = coefficient in pump torque curve, sec^2/in.^{2}
K_7, K_8 = coefficients in turbine efficiency curve fit
K_M = fuel element thermal conductivity, Btu/in. R sec
L_L = main propellant line inertness, sec^2/in.^{2}
L_T = turbine torque, in.-lb
L_p = required pump output torque, in.-lb
L = length of lumped parameter reactor section, in.
l = effective neutron lifetime, sec
m = hydraulic radius, in.
M_R = mass of propellant in reactor, lb
M_{R0} = nominal propellant mass in reactor, lb
$\dot{M}_r$ = reactor weight flow rate, lb/sec
$\dot{M}_p$ = pump mass flow rate, lb/sec
$\dot{M}_T$ = turbine mass flow rate, lb/sec
N_0 = density of fissionable atoms, atom/in.^{3}
N = neutron density, neutron/in.^{3}
N_p = pump speed, radian/sec
N_T = turbine speed, radian/sec
P_1 = reactor inlet pressure, psia
P_2 = reactor outlet pressure, psia
P_D = pump discharge pressure, psia
P_S = pump suction pressure, psia
P_T = turbine inlet pressure, psia
P_{ex} = turbine exhaust pressure, psia
P_y = bootstrap sensing pressure, psia
$\dot{Q}_s$ = fuel element surface heat flux, Btu/in.^{2} sec

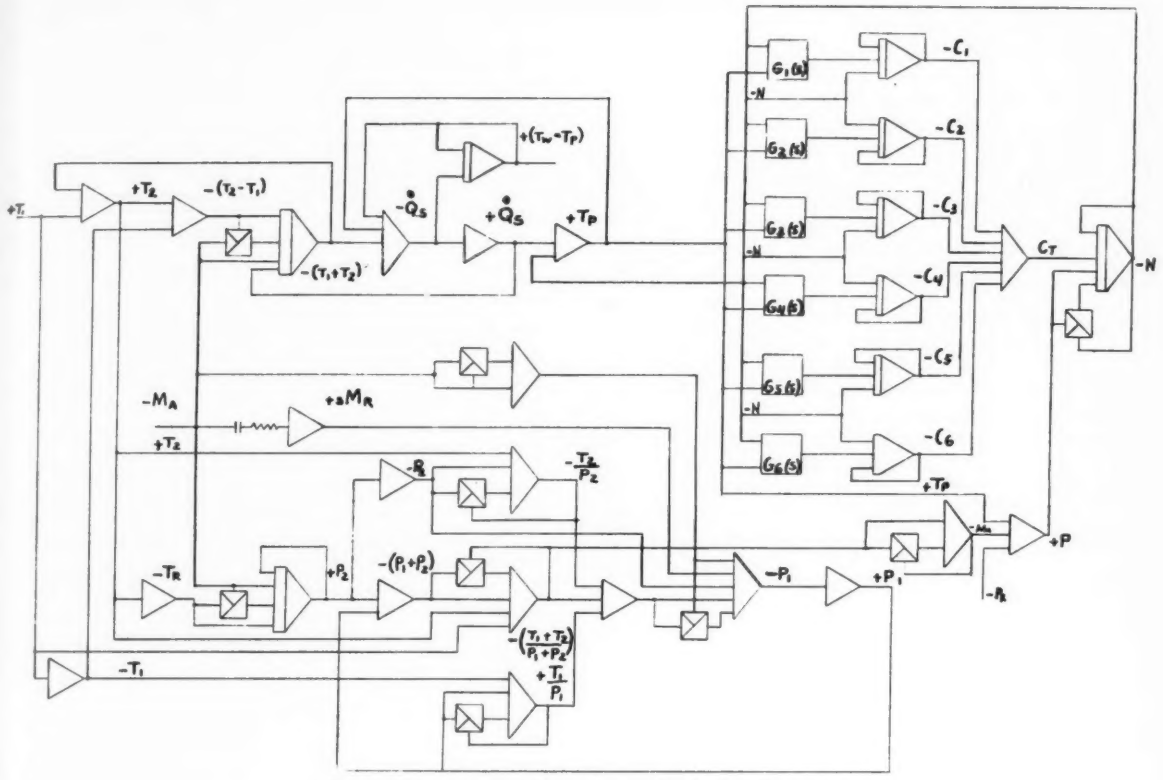

Fig. 6 Reactor neutronics analog mechanization diagram

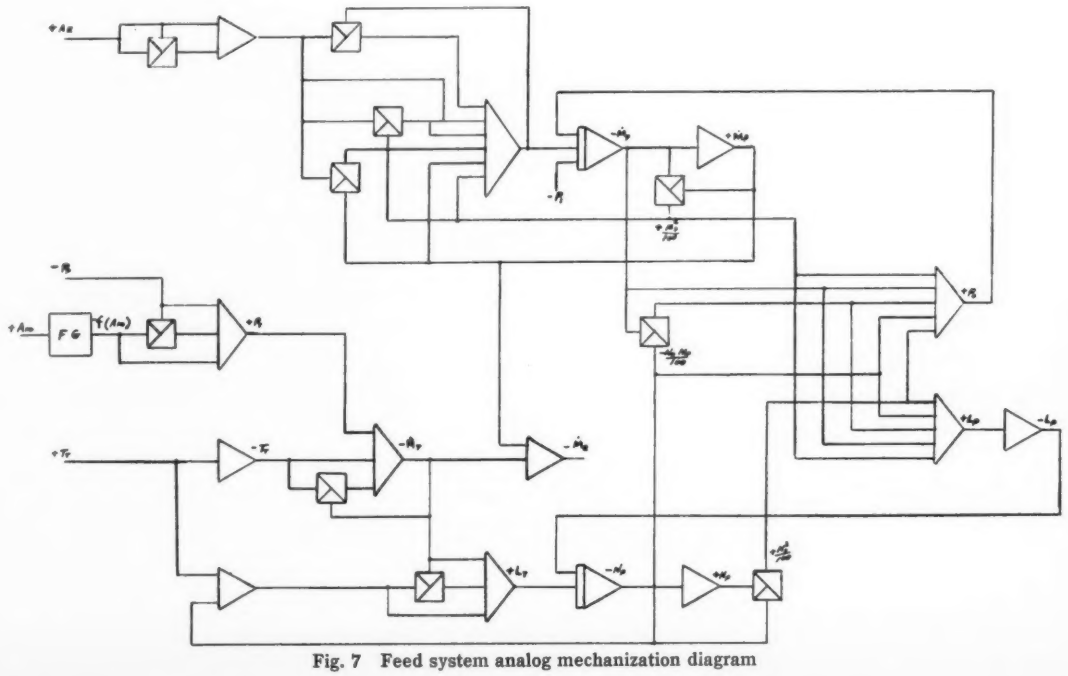

Fig. 7 Feed system analog mechanization diagram

$\dot{Q}_v$ = reactor heat generation rate, Btu/in.^{3} sec
r_T = turbine radius, in.
R_L = effective resistance of main propellant line, sec^2/in.^{5}
R = vehicle mass ratio
R_g = gas constant, Btu/lb R
S = Laplace variable, sec^{-1}
T_g = gas temperature
T_p = fuel element temperature, R
T_{pe} = nominal fuel element temperature, R
T_1 = propellant temperature at reactor inlet, R
T_2 = propellant temperature at reactor outlet, R
T_w = fuel element wall temperature, R
T_T = turbine inlet temperature, R
v = average neutron velocity, in./sec
V_R = reactor flow volume, in.^{3}
W = vehicle weight, lb
β = total delayed neutron yield
β_i = neutron yield of the ith precursor group
γ_T = temperature coefficient of reactivity, dollar/R
γ_d = propellant mass coefficient of reactivity, dollar/lb
γ = specific heat ratio
σ_f = fission cross section, barns
τ = fuel element temperature distribution lag, sec
τ_c = thrust chamber storage lag, sec
ρ_R = reference reactivity, dollar
ρ = reactivity, dollar
λ_i = ith precursor decay constant, sec^{-1}

References

1 Grey, T., "Nuclear Rockets," *Nucleonics*, vol. 16, July 1958, pp. 62–65.
2 Levoy, M. M. and Newgard, J. J., "Rocket Reactor Design," *Nucleonics*, vol. 16, July 1958, pp. 66–68.
3 Bussard, R. W. and Delauer, R. D., "Nuclear Rocket Propulsion," McGraw-Hill Book Co., Inc., New York, 1958.
4 Rosenblum, M. H., Rinehart, W. T. and Thompson, T. L., "Rocket Propulsion with Nuclear Energy," ARS preprint 559-57.
5 McGrath, T. F., "A Development Approach for Nuclear Rocket Engines," ARS preprint 594-58.
6 Tormey, J. F., "Liquid Rocket Propellants—Is There an Energy Limit," *Ind. and Engng. Chem.*, vol. 49, Sept. 1957, pp. 1339–1343.
7 Schultz, M. A., "Control of Nuclear Reactors and Power Plants," McGraw-Hill Book Co., Inc., New York, 1955.
8 Sutton, G. P., "Rocket Propulsion Elements," John Wiley & Sons, Inc., London, 1956, p. 193.
9 Barrer, R. M., "Diffusion in and Through Solids," Cambridge University Press, New York, 1951.
10 "The Reactor Handbook," USAEC, May 1955, vol. 2, p. 1033.
11 Carslaw, H. S. and Jaeger, J. C., "Conduction of Heat in Solids," Oxford University Press, New York, 1947.
12 Binder, R. C., "Advanced Fluid Dynamics and Fluid Machinery," Prentice-Hall, Inc., New York, 1951, pp. 29, 67–88.
13 Keepin, G. R., "Progress in Nuclear Energy," McGraw-Hill Book Co., Inc., 1956, chap. 7.
14 Smith, B. N., "Perturbation Analysis of Low Frequency Rocket Engine Dynamics on an Analog Computer," JET PROPULSION, vol. 26, 1956, p. 40.
15 Ehricke, K., "Survey of Instrumental Vehicles for Space Research," Table I in "Astronautical and Space-Medical Research with Automatic Satellites," Monograph No. 2, Franklin Institute of Pennsylvania, June 1956.
16 Gore, M. R. and Carroll, J. J., "Dynamics of a Variable-Thrust, Pump-Fed, Bi-propellant, Liquid Rocket Engine System," ARS preprint 299-56.
17 Truxal, John G., "Control System Synthesis," McGraw-Hill Book Co., Inc., New York, 1955, pp. 223–276.

ARS SOLID PROPELLANTS CONFERENCE

January 28–29, 1960

Princeton University, Princeton, N. J.

Thrust and Vector Control
Unstable Burning
Grain Design

Combustion, Gas Kinetics and Ignition
Interrelations of Nozzle Geometry and Nozzle Performance

Technical Notes

Applicability of Euler's Dynamical Equations to Rocket Motion[1]

JAMES W. ELLIS[2] and CHARLES W. McARTHUR[3]

Florida State University, Tallahassee, Fla.

Let S denote a system of particles, such as a rocket, where angular momentum is transferred from the system by mass particles leaving the system. Rosser and associates have shown that the moment of the exterior forces acting on S is equal to the time rate of change of the moment of momentum of S plus the rate at which the particles that are leaving S are transferring moment of momentum out of S, with all angular momenta being taken about the center of mass of S. From this principle, a set of equations for the rotational motion of a rocket with varying moments of inertia and center of mass is derived. This set of equations is a generalization of the standard Euler dynamical equations. The new terms which appear in them are seen to be negligible only under certain conditions. The set of equations reduces to the standard Euler dynamical equations when the mass and center of mass of the rocket are constant.

A NUMBER of mathematical studies of the rotational motion of rockets are based on Euler's dynamical equations. These equations have been derived for rigid bodies with constant moments of inertia about principal axes. Inasmuch as the moments of inertia of a rocket vary as its fuel burns, the question arises as to what extent the use of the Euler dynamical equations is justified in studies of rocket motion. Jarmolow (1)[4] claims to give "a heuristic proof of the applicability of these equations." Using a principle of mechanics stated and proved by Rosser (2) and associates we derive, under assumptions given below, equations which are a generalization of the standard Euler dynamical equations. Conditions under which the new terms which appear in them may be neglected are discussed in the conclusion.

Assumptions and Notation

We will discuss the equations of motion of a rocket which is losing mass through k openings in its base. The following simplifying assumptions will be made:

1 The ejected particles are not given any angular velocity relative to the rocket.

2 The system of openings through which the particles are ejected lies in a plane perpendicular to the longitudinal axis, and has $2n$-gonal rotational symmetry about that axis for some $n \geq 2$. Symmetrically placed openings will be assumed to lose mass at equal rates.

3 The center of mass will be considered to always lie on the longitudinal axis of the rocket.

4 All the mass leaving through an opening will be considered as leaving through its center.

The unit vectors $\bar{x}_1$, $\bar{x}_2$, $\bar{x}_3$, will denote a right-handed orthogonal coordinate system, fixed in the rocket, with $\bar{x}_1$ along the longitudinal axis and directed forward, and $\bar{x}_2$, $\bar{x}_3$ in the plane perpendicular to this axis through the center of mass. In addition, the following symbols will be used:

$\bar{B} = -B\bar{x}_1$ = the vector from the center of mass to C

C = the center of symmetry of the system of openings in the base. (C is the intersection of the base with the longitudinal axis)

$\bar{h}$ = angular momentum of the rocket about its center of mass

$[\bar{h}]'_{\text{body}}$ = time derivative of $\bar{h}$ with respect to the system $\bar{x}_1, \bar{x}_2, \bar{x}_3$

$[\bar{h}]'_{\text{space}}$ = time derivative of $\bar{h}$ with respect to an inertial system

I_i = magnitude of moment of inertia about the $\bar{x}_i$ axis, $i = 1, 2, 3$ (note that $I_2 = I_3$)

k_i = radius of gyration of rocket about $\bar{x}_i$ axis, $i = 1, 2, 3$ ($k_2 = k_3$)

M = mass of rocket and contents at time t

m = mass of particles which have left the rocket by time t

m_i = mass of those particles lost through the ith opening at the instant t

$q^2 = \left(\sum_{i=1}^{k} m_i r_i^2\right) \Big/ \left(\sum_{i=1}^{k} m_i\right)$

$\bar{r}_i$ = vector from C to the center of the ith opening

$\bar{T} = \sum_{i=1}^{3} T_i \bar{x}_i$ = sum of the exterior torques (about the center of mass) acting on the rocket

$\bar{w} = \sum_{i=1}^{3} w_i \bar{x}_i$ = angular velocity of the rocket, or of the moving axes, with respect to an inertial system

$\bar{Z}$ = the rate at which angular momentum is being transferred out of the system by loss of particles

Generalized Euler Equations

Rosser (2) and associates prove that

$$\bar{T} = [\bar{h}]'_{\text{space}} + \bar{Z} \qquad [1]$$

Since $\bar{x}_1$, $\bar{x}_2$, $\bar{x}_3$ are principal axes of inertia, it follows that

$$\bar{h} = I_1 w_1 \bar{x}_1 + I_2 w_2 \bar{x}_2 + I_2 w_3 \bar{x}_3 \qquad [2]$$

From our assumptions it follows that

$$\bar{Z} = \dot{m} q^2 w_1 \bar{x}_1 + \dot{m}(B^2 + \tfrac{1}{2}q^2)(w_2 \bar{x}_2 + w_3 \bar{x}_3) \qquad [3]$$

It is well-known that

$$[\bar{h}]'_{\text{space}} = [\bar{h}]'_{\text{body}} + \bar{w} \times \bar{h} \qquad [4]$$

Received April 1, 1959.

[1] This work was supported by the U. S. Air Force under Contract no. AF 08(616)-79.

[2] Associate Professor of Mathematics. Present address: Louisiana State University, New Orleans, La.

[3] Associate Professor of Mathematics.

[4] Numbers in parentheses indicate References at end of paper.

EDITOR'S NOTE: The Technical Notes and Technical Comments sections of ARS JOURNAL are open to short manuscripts describing new developments or offering comments on papers previously published. Such manuscripts are usually published without editorial review within a few months of the date of receipt. Requirements as to style are the same as for regular contributions (see masthead page).

Also, we have

$$\dot{I}_j = (Mk_j^2)^{\cdot} = -\dot{m}k_j^2 + M(k_j^2)^{\cdot} \qquad [5]$$

$j = 1, 2, 3$ since $\dot{M} = -\dot{m}$.

Using Equations [2, 3, 4 and 5], Equation [1] yields the following system of coordinate equations

$$\begin{aligned}
&I_1\dot{w}_1 + (I_3 - I_2)w_2w_3 + \dot{m}(q^2 - k_1^2)w_1 + M(k_1^2)^{\cdot}w_1 = T_1\\
&I_2\dot{w}_2 + (I_1 - I_3)w_3w_1 + \dot{m}(B^2 + \tfrac{1}{2}q^2 - k_2^2)w_2 + M(k_2^2)^{\cdot}w_2 = T_2\\
&I_3\dot{w}_3 + (I_2 - I_1)w_1w_2 + \dot{m}(B^2 + \tfrac{1}{2}q^2 - k_2^2)w_3 + M(k_2^2)^{\cdot}w_3 = T_3
\end{aligned} \qquad [6]$$

Rosser (2) has derived these equations in the special case $w_2 = w_3 = 0$ and with the openings equidistant from the center of mass.

Conclusions

Equations [6] differ from the standard Euler equations for nonvarying inertia

$$\begin{aligned}
I_1\dot{w}_1 + (I_3 - I_2)w_2w_3 &= T_1\\
I_2\dot{w}_2 + (I_1 - I_3)w_3w_1 &= T_2\\
I_3\dot{w}_3 + (I_2 - I_1)w_1w_2 &= T_3
\end{aligned} \qquad [7]$$

by the addition of the terms $\dot{m}(q^2 - k_1^2)w_1 + M(k_1^2)^{\cdot}w_1$, $\dot{m}(B^2 + \frac{1}{2}q^2 - k_2^2)w_2 + M(k_2^2)^{\cdot}w_2$ and $\dot{m}(B^2 + q^2 - \frac{1}{2}k_2^2)w_3 + M(k_2^2)^{\cdot}w_3$, respectively. These are the terms disregarded by Jarmolow (1). We note that making these terms negligible becomes a design problem. If the radii of gyration change slowly then the terms $M(k_j^2)^{\cdot}w_j, j = 1, 2, 3$ may be neglected. If, in addition, the rocket is so constructed that q^2 is near k_1^2, and $B^2 + \frac{1}{2}q^2$ is near k_2^2, these terms may be virtually neglected and the standard Euler Equations [7] used in place of the more complex set [6].

In the usual case, in which the direction of $\bar{w}$ is close to that of the longitudinal axis, only the first of these requirements (that q^2 be near k_1^2) is really relevant, due to the smallness of w_2 and w_3.

References

1 Jarmolow, K., "Dynamics of a Spinning Rocket with Varying Inertia and Applied Moment," *J. Appl. Phys.* vol. 28, pt. 1, 1957, pp. 308–313.

2 Rosser, J. B., Newton, R. R. and Gross, G. L., "Mathematical Theory of Rocket Flight," McGraw-Hill Book Co., Inc., New York, 1947, p. 15 and Appendix 2.

Some Extensions of the Hohmann Transfer Maneuver

T. N. EDELBAUM[1]

United Aircraft Corp., East Hartford, Conn.

IN 1925, Hohmann demonstrated (1)[2] that tangential impulses at the apsides of a cotangential transfer orbit minimize the fuel consumption for transfer between coplanar circular orbits. It has since been recognized that such maneuvers also minimize fuel consumption for transfer from a circular orbit to coplanar orbits which satisfy any desired functional relationship between energy and angular momentum and which have any desired orientation. Examples of these functional relationships are fixed energy (or major axis or period), fixed angular momentum (or latus rectum), fixed apogee or perigee radii, and fixed eccentricity and major axis.

In determining what combinations of tangential apsidal impulses are optimum for any given problem, it has been customary to consider only one- or two-impulse maneuvers. It is the purpose of this note to point out some examples of two- and three-impulse maneuvers which are more economical of fuel (or characteristic velocity) than the corresponding one- and two-impulse maneuvers.

The first example is a comparison of the classic Hohmann transfer and a three-impulse transfer between circular orbits. For orbits which are more than 12 times larger (or smaller) than the original orbit, fuel can be saved by transferring beyond the final orbit, applying a retrothrust at the apogee of this ellipse and entering the final orbit at the

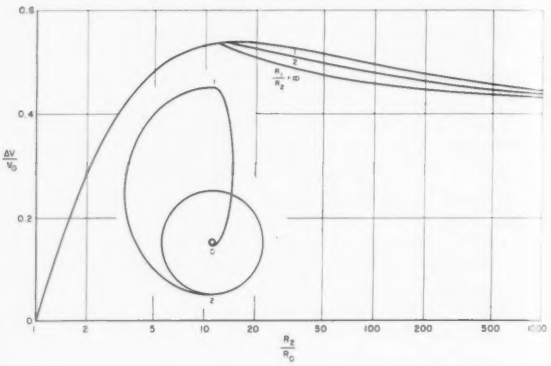

Fig. 1 Characteristic velocity requirements for transfer between distant circular orbits

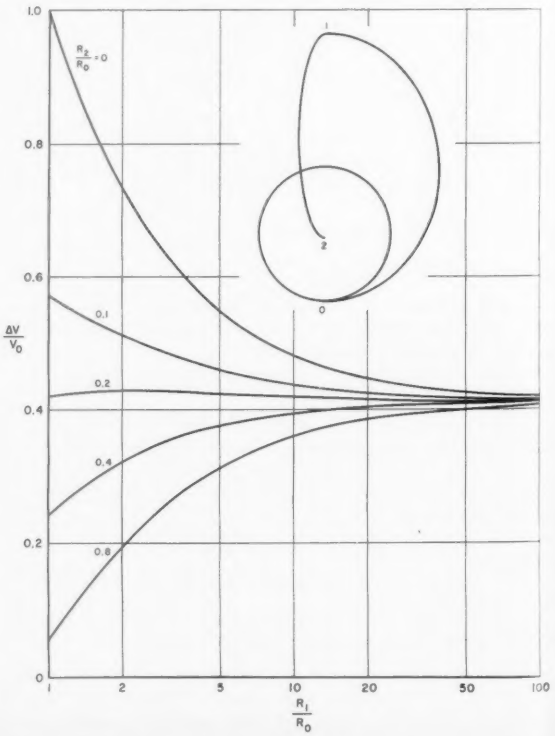

Fig. 2 Characteristic velocity requirements for a solar probe

Received June 9, 1959.

[1] Research Engineer, Research Laboratories. Member ARS.

[2] Numbers in parentheses indicate References at end of paper.

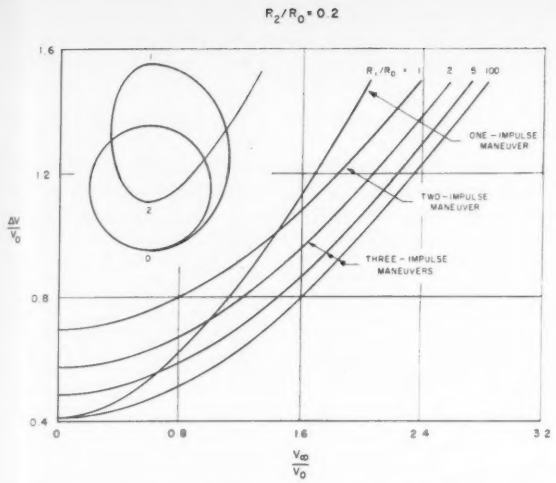

Fig. 3 Characteristic velocity requirements for hyberbolic escape

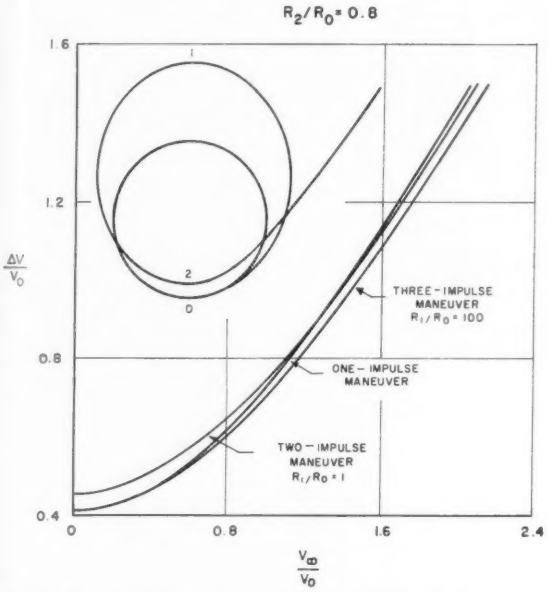

Fig. 4 Characteristic velocity requirements for hyberbolic escape

perigee of a second transfer ellipse. The further away the apogee of the transfer ellipses, the greater is the fuel saving. The absolute minimum fuel consumption necessitates escaping to infinity along a parabola, using an infinitesimal impulse at infinity to cause the vehicle to return along a new parabola which is tangent to the final orbit, and entering the final orbit at the perigee of this parabola. A sketch of this maneuver and its characteristic velocity savings are shown in Fig. 1. As the maximum possible savings in characteristic velocity are only about 8 per cent, the resultant fuel saving probably does not justify the added time and complexity of such a maneuver. However the next example represents a case where the fuel savings are so large that they more than justify the additional time and complexity.

This example represents a solar probe in which it is desired to come as close as possible to the sun to sample its atmosphere. It is possible to approach the sun to within one tenth to one hundredth of an astronomical unit (A.U.) before the probe melts. However this is a formidable propulsion problem. The conventional method of impacting the sun is to apply a large enough retrothrust to completely stop the vehicle in its motion around the sun. This requires a characteristic velocity of about 100,000 fps, more than twice as much as is required to escape the solar system. This propulsion requirement can be greatly reduced by first applying a forward thrust to transfer beyond the Earth's orbit and stopping the vehicle at the aphelion of the resulting ellipse. Fig. 2 shows this path, and the characteristic velocities required to transfer from the Earth's orbit to within various distances of the sun as a function of the aphelion distance of the transfer ellipses. The two-impulse maneuver is optimum for approaching to less than 0.2 A.U. For closer approaches, the characteristic velocity is a monotonically decreasing function of the maximum excursion from the sun. Even going out only to the orbit of Mars produces appreciable savings in characteristic velocity.

The third, and most complicated, example is concerned with maximizing the energy of hyperbolic orbits so as to maximize velocity at infinity. Lawden (2) has analyzed a two-impulse maneuver for this case. However a three-impulse maneuver can provide appreciable savings over both the one- and two-impulse cases. The maneuver consists of first going outside the original orbit with a forward thrust, passing inside the original orbit with a retrothrust at apogee, and finally escaping with a forward thrust at the perigee of the second transfer ellipse. In general, this maneuver will be limited by a minimum attainable orbital radius. Figs. 3 and 4 represent two typical cases, minimum radii of two tenths and eight tenths times the original orbital radius. In each case the velocity at infinity is plotted vs. the characteristic velocity, for various maximum excursions. The figures show that it is always possible to save fuel with this maneuver by going out far enough initially. The magnitude of the fuel saving depends upon how closely the origin can be approached. The theoretical optimum represents escaping to infinity along a parabola, using an infinitesimal impulse to fall back to the origin, and using another infinitesimal impulse at the origin to obtain any desired velocity at infinity. By closely approaching this optimum it is possible to obtain very large velocities at infinity with characteristic velocities only slightly greater than that needed for escape.

References

1 Hohmann, W., "Die Erreichbarkeit der Himmelskorper," R. Oldenbourg, Munich, 1925.

2 Lawden, D. F., "Escape to Infinity from Circular Orbits," *J. Brit. Interplanet. Soc.*, vol. 12, 1953, p. 68.

Comparison of Minimum Energy Paths and Apogee Designation Paths

WAYNE TEMPELMAN[1]

Convair Div., General Dynamics Corp., San Diego, Calif.

A comparison of minimum energy paths and apogee designation paths reveals that for distances greater than three times the injection distance there is little difference. Distances less than twice the injection distance reveal significant differences. For minimum energy paths, corresponding to each velocity there is a reachable en-

Received June 11, 1959.

[1] Research Engineer, Operations Analysis Group, Astronautics. Member ARS.

velope in space which constitutes an ellipse. Also, constant injection angles are found to be represented in space by straight lines, equally spaced, originating from the initial point.

THE ANALYSIS is based on the usual simplified two-body assumptions. The formulas that are not derived are easily derived from a number of sources.[2] All distances are dimensionless, with the initial distance being unity.

Minimum Energy Paths

The locus of points representing the far focus is obtained by noting that the apogee angle is between the initial line and the major axis, and that the linear eccentricity extends to the far focus (see Fig. 2)

$$\tan \theta_A = \frac{\alpha\beta}{1 - \beta^2} = \frac{x}{y}$$

$$2c = \frac{2[\alpha^2\beta^2 + (\beta^2 - 1)^2]^{1/2}}{2 - V_0^2} = [x^2 + y^2]^{1/2}$$

[2] Singer, S. F. and Wentworth, R. C., "A Method for Calculating Impact Points of Ballistic Rockets: Convenient Representations," JET PROPULSION, vol. 28, 1958, pp. 684–687.

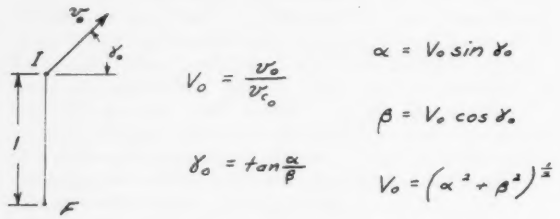

Fig. 1 Injection conditions

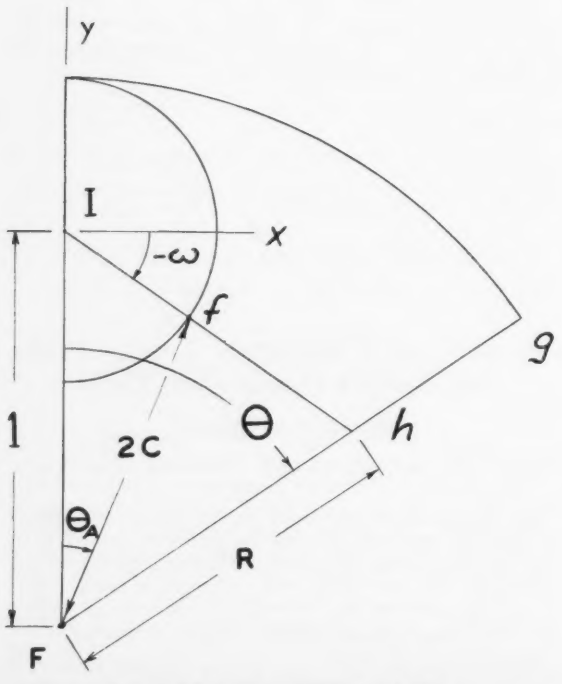

Fig. 2 Minimum energy path notation

Therefore

$$x = \frac{2\alpha\beta}{2 - V_0^2} \qquad y = \frac{2(1 - \beta^2)}{2 - V_0^2} \qquad [1]$$

This is a circle with origin at $R = 1, \theta = 0$ deg, and a radius of $V_0^2/(2 - V_0^2)$.

Considering that for an ellipse the distance from a focus to a point on the ellipse plus the distance from the point to the other focus equals the major axis, the maximizing of R for a give θ occurs when $gh = fh$. Considering Fig. 2

$$fh = gF - R = hI - fI$$

or

$$1 + \frac{V_0^2}{2 - V_0^2} - R = (R^2 - 2R \cos \theta + 1)^{1/2} - \frac{V_0^2}{2 - V_0^2}$$

which reduces to

$$R = \frac{4V_0^2/(4 - V_0^4)}{1 - \cos \theta\,(2 - V_0^2)/(2 + V_0^2)} \qquad [2]$$

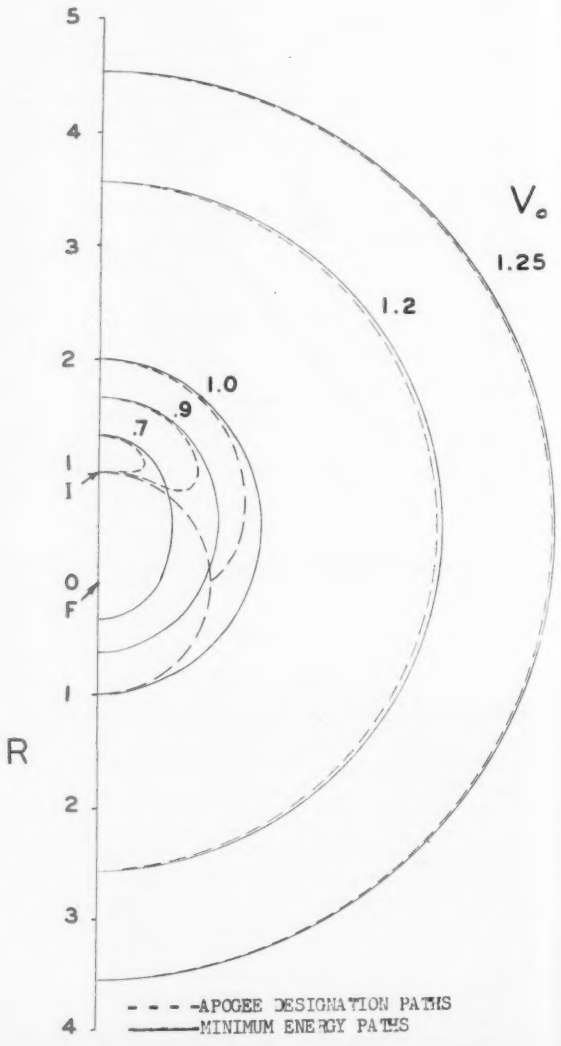

Fig. 3 Reachable envelopes

The envelope of reachable points in R, θ space for a given velocity is therefore an ellipse with $c = \frac{1}{2}$, putting the origin of the ellipse at $R = \frac{1}{2}$, $\theta = 0$ deg (see Fig. 3). The axes are

$$a = \frac{2 + V_0^2}{2(2 - V_0^2)} \qquad b = \frac{2^{1/2} V_0}{2 - V_0^2} \qquad [3]$$

Considering the equation of line fI, the velocity components can be found using Equation [1], which lead to the injection angle

$$y - 1 = \frac{R \cos\theta - 1}{R \sin\theta} x$$

$$\alpha = \frac{R \cos\theta - 1 + (R^2 - 2R \cos\theta + 1)^{1/2}}{[R(1 + \cos\theta)(R^2 - 2R \cos\theta + 1)^{1/2}]^{1/2}}$$

$$\beta = \frac{[R(1 - \cos\theta)]^{1/2}}{(R^2 - 2R \cos\theta + 1)^{1/4}}$$

$$\gamma_0 = \tan^{-1} \frac{R \cos\theta - 1 + (R^2 - 2R \cos\theta + 1)^{1/2}}{R \sin\theta}$$

..... [4]

Equations [4] result in a plot of straight lines in R, θ space for a constant γ_0, originating from $R = 1, \theta = 0$ deg (see Fig. 4). The proof involves proving that the relation between the injection angle and the angle ω (see Fig. 2). is given by

$$\omega = 2\gamma_0 - 90 \text{ deg} \qquad [5]$$

The relation $\omega = f(R, \theta)$ is found from Fig. 2

$$\omega = \sin [(R \cos\theta - 1)/(R^2 - 2R \cos\theta + 1)^{1/2}] \qquad [6]$$

Using trigonometry

$$\sin (2\gamma_0 - 90 \text{ deg}) = -(1 - \tan^2 \gamma_0)/(1 + \tan^2 \gamma_0) \qquad [7]$$

By inserting Equations [4] into Equation [7], [6] is seen to be true, proving Equation [5].

The formulas given in Equations [2 and 4] can be applied for $R = 1$ (the solution for this special case can be obtained directly by maximizing the apogee angle) with the results

$$\theta = \cos^{-1} \frac{4 - 4V_0^2 - V_0^4}{(2 - V_0^2)^2}$$

$$V_0 = \left[\frac{2\{\cos\theta - 1 + [2(1 - \cos\theta)]^{1/2}\}}{1 + \cos\theta} \right]^{1/2}$$

$$\alpha = V_0 \left(\frac{1 - V_0^2}{2 - V_0^2} \right)^{1/2}$$

$$\beta = \frac{V_0}{(2 - V_0^2)^{1/2}}$$

$$\gamma_0 = \tan^{-1}(1 - V_0^2)^{1/2}$$

$$e = (1 - V_0^2)^{1/2}$$

$$a = \frac{1}{2 - V_0^2}$$

Apogee Designation Paths

The general conic section formula can be written for the apogee point and the injection point (R and θ refer to the coordinates of the apogee point)

$$R = \frac{a(1 - e^2)}{1 - e} \qquad 1 = \frac{a(1 - e^2)}{1 - e \cos\theta} \qquad [8]$$

The eccentricity and semimajor axis are derived from Equations [8]

$$e = \frac{R - 1}{R - \cos\theta} \qquad a = \frac{R(R - \cos\theta)}{2R - \cos\theta - 1}$$

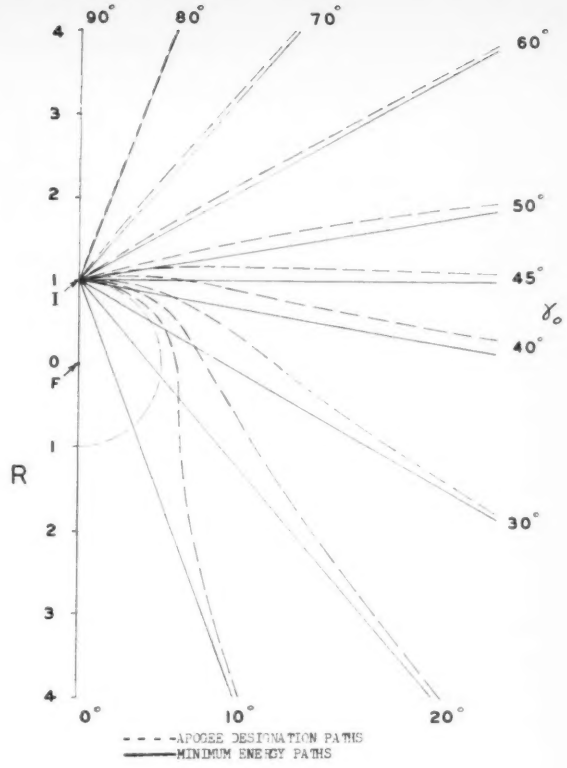

Fig. 4 Injection angles

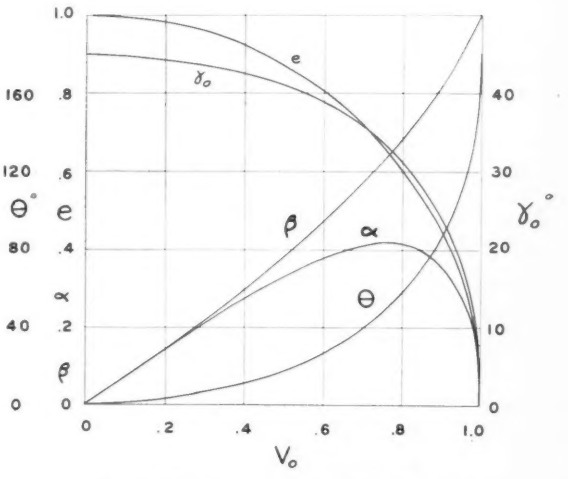

Fig. 5 Minimum energy paths for $R = 1$

The velocity components are obtained from the general relationships for the semilatus rectum and the semimajor axis

$$\beta = p^{1/2} = [a(1 - e^2)]^{1/2}$$

$$\alpha = (2 - \beta^2 - 1/a)^{1/2}$$

$$\beta = \left\{ \frac{R(R - \cos\theta)}{2R - 1 - \cos\theta} \left[1 - \left(\frac{R - 1}{R - \cos\theta} \right)^2 \right] \right\}^{1/2}$$

..... [9]

Table 1 Special conditions for $\theta = 0$, 90 and 180 deg

θ	Zero deg	90 deg (*MEP*)	90 deg (*ADP*)	180 deg
V_0	$\left[\frac{2(R-1)}{R}\right]^{1/2}$	$\left\{\frac{2[(R^2+1)^{1/2}-1]}{R}\right\}^{1/2}$	$\frac{(2R^2-2R+1)^{1/2}}{R}$	$\left(\frac{2R}{R+1}\right)^{1/2}$
α	$\left[\frac{2(R-1)}{R}\right]^{1/2}$	$\frac{(R^2+1)^{1/2}-1}{[R^2(R^2+1)]^{1/4}}$	$\frac{R-1}{R}$	0
β	0	$\frac{R^{1/2}}{(R^2+1)^{1/4}}$	1	$\left(\frac{2R}{R+1}\right)^{1/}$
γ_0	90	$\tan^{-1}\frac{(R^2+1)^{1/2}-1}{R}$	$\tan^{-1}\frac{R-1}{R}$	0
e	1	$\left[3-\frac{2(1+R)}{(1+R^2)^{1/2}}\right]^{1/2}$	$\frac{R-1}{R}$	$\frac{R-1}{R+1}$
a	$\frac{R}{2}$	$\frac{R}{2[1+R-(R_2+1)^{1/2}]}$	$\frac{R^2}{2R-1}$	$\frac{R+1}{2}$

$$\alpha = \left[2 - \left\{\frac{R(R-\cos\theta)}{2R-1-\cos\theta}\left[1-\left(\frac{R-1}{R-\cos\theta}\right)^2\right]\right\} - \frac{2R-1-\cos\theta}{R(R-\cos\theta)}\right]^{1/2} \quad [9]$$

The injection angle is

$$\gamma_0 = \tan^{-1}\left\{\frac{2 - \frac{R(R-\cos\theta)}{2R-\cos\theta-1}\left[1-\left(\frac{R-1}{R-\cos\theta}\right)^2\right] - \frac{2R-\cos\theta-1}{R(R-\cos\theta)}}{\frac{R(R-\cos\theta)}{2R-\cos\theta-1}\left[1-\left(\frac{R-1}{R-\cos\theta}\right)^2\right]}\right\}^{1/2}$$

The reachable envelope for a given velocity is found using Equations [8 and 9]

$$\cos\theta = \frac{R^2(2-V_0^2) - 2R + 1}{R(2-V_0^2) - 1}$$

It is seen from Figs. 3 and 4 that the solutions are identical for $\theta = 0$ and 180 deg. The results for these two cases along with $\theta = 90$ deg are summarized in Table 1.

Nomenclature

a	=	semimajor axis
b	=	semiminor axis
c	=	linear eccentricity
e	=	eccentricity
f	=	far focus
F	=	focus at center of attracting body
g, h	=	points (see Fig. 2)
I	=	injection point
p	=	semilatus rectum
R	=	distance
v	=	velocity
V	=	dimensionless velocity
α	=	dimensionless radial velocity
β	=	dimensionless normal velocity
γ	=	injection angle
θ	=	polar coordinate (measured from FI)
ω	=	angle (see Fig. 2)

Subscripts

A	=	apogee
ADP	=	apogee designation paths
c	=	circular
MEP	=	minimum energy paths
0	=	initial condition

New Ion Source for Propulsion of Space Vehicles

C. D. MOAK,[1] H. E. BANTA, J. W. JOHNSON and R. F. KING

Oak Ridge National Laboratory, Oak Ridge, Tenn.

SOME recent developmental work on high intensity ion sources for use in accelerators indicates that certain modifications of the duo-plasmatron source, originally described by von Ardenne in 1948 (1),[2] may prove to be well-adapted for low thrust, high specific impulse ion propulsion of satellites and space vehicles.

Fig. 1 shows the configuration of a small duo-plasmatron now being used at Oak Ridge National Laboratory (2). Originally built for 10-milliamp proton service, this source has delivered up to the 50-milliamp capability of the power supply used in the tests. Throughout this current range, the source can deliver up to 100 amp of protons per cm^2 of exit aperture area, in agreement with figures taken by von Ardenne for a proton current of 1 amp. Power consumption is only 400 w,

Received June 18, 1959.

[1] Presently on one year assignment AERE, Harwell, England.

[2] Numbers in parentheses indicate References at end of paper.

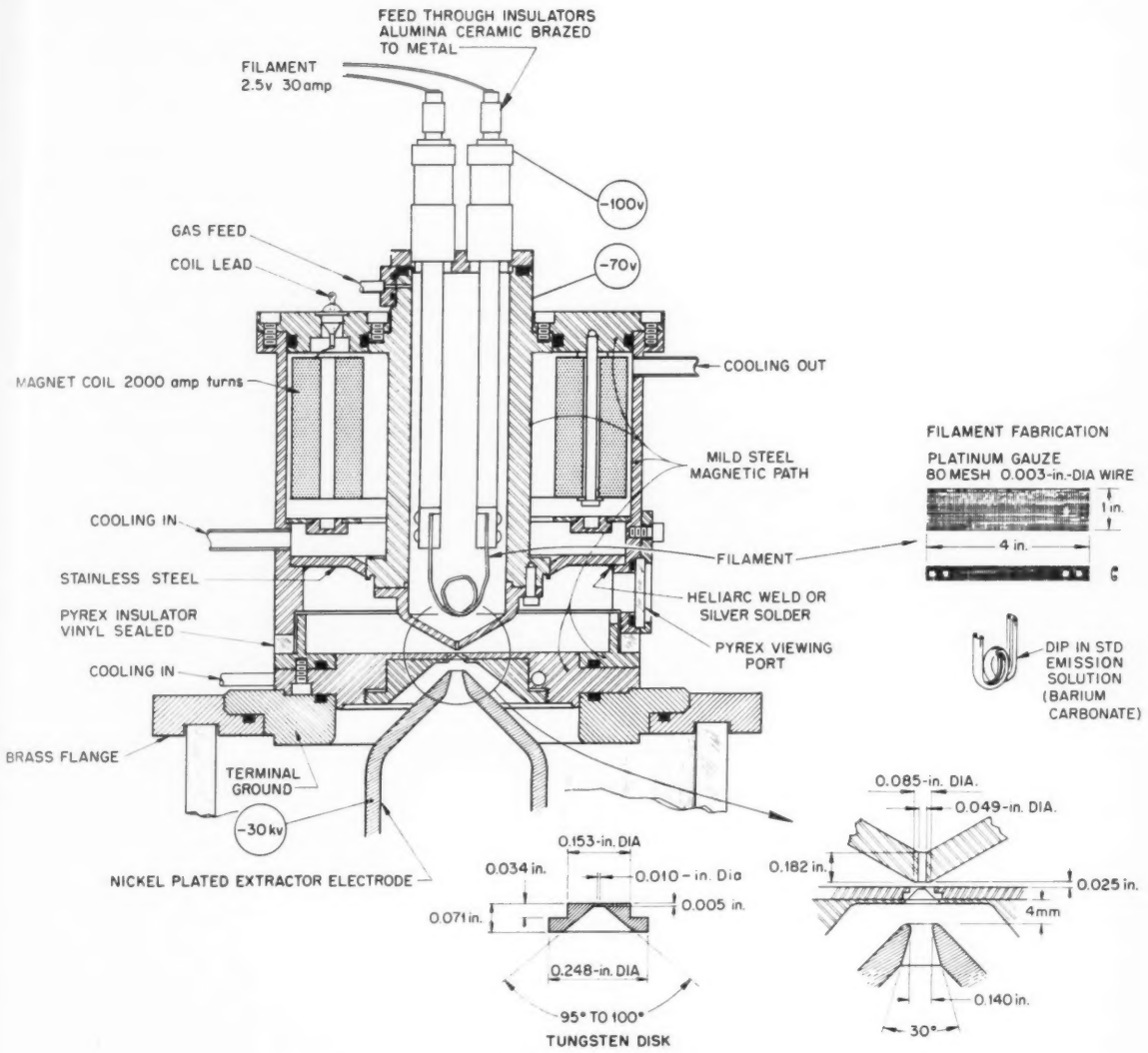

Fig. 1 Duo-plasmatron ion source

and gas efficiency is very nearly unity. For one or more amperes of protons at accelerator voltages of 10 kv or more, beam power would constitute 96 per cent of the total power consumption of the propulsion system. Total source weight is approximately 5 lb.

It has been shown (3) that optimization of the propulsion system design calls for a choice of exhaust velocities which makes most efficient use of the power supply and propellant loads. In some cases the design calls for programmed exhaust velocity (4). In most instances the use of heavy ions with accelerator voltage of some tens of kilovolts is dictated. The use of light ions would dictate very low accelerator voltage and such short gap spacings as to make the accelerator rather small and fragile. Experience with He and N_2 as feed gases indicate that no great difficulty should be experienced with heavy-ion operation of the duo-plasmatron. The problems to be encountered with space charge neutralization and beam expansion should be no different with this than with any other source of ions for this type of service.

Clearly, the weight of the accelerator can be small compared to that of the power supply and propellant loads so that power supply weight now becomes the most important item to be minimized. Even with power sources presently available it appears that several applications of ion propulsion are now feasible.

References

1 von Ardenne, M., "Tabellen der Elektronenphysik Ionenphysik und Ubermikroskopie," Deutscher Verlag der Wissenschaften, Berlin, 1956.

2 Moak, C. D., Banta, H. E., Thurston, J. N., Johnson, J. W., and King, R. F., "A Duo-Plasmatron Ion Source for Use in Accelerators," *Rev. Sci. Instr.*, vol. 30, no. 8, 1959, pp. 694–700.

3 Preston-Thomas, H., "A Note on 'A Nuclear Electric Propulsion System,'" *J. Brit. Interplanet. Soc.*, vol. 16, 1958, p. 508.

4 Irving, J. H. and Blum, E. K., "Comparative Performance of Ballistic and Low-Thrust Vehicles for Flight to Mars," Space Technology Laboratories report (unpublished).

Solubility of Air, N_2 and O_2 in n-Propyl Nitrate

ADOLPH B. AMSTER[1] and JOSEPH B. LEVY[2]

U. S. Naval Ordnance Laboratory, Silver Spring, Md.

The presence of bubbles is known to sensitize liquid propellants. The magnitude of the effect is determined by the composition of the gas in the bubble; this in turn depends upon the solubility of various gases in the liquid. This paper presents data for the solubility, at ambient temperature, of air, N_2 and O_2 in n-propyl nitrate. Abnormal solubility of oxygen and the consequences thereof are noted.

Received June 18, 1959.

[1] Supervisory Chemist, Physical Chemistry Division. Member ARS.

[2] Present address: Atlantic Research Corp., Alexandria, Va.

THE SOLUBILITY of different gases in n-propyl nitrate (NPN) could conceivably be an important factor in the determination of the safest ways to use this propellant. If, for example, in its use a pressurization by some gas were to be followed by depressurization, the evolution of gas in the form of bubbles or foam would constitute a potential hazard (1, 2).[3] The degree of such gas evolution depends in part on the gas solubility; such data seemed to be lacking at present.

Procedure

An apparatus has been completed with which a study of the solubility in NPN has been made of various gases at pressures below 1 atm and at ambient temperature. The equipment has been adapted from that described elsewhere (3).

The apparatus is shown in Fig. 1. In operation a weighed quantity of NPN is put into the flask F. Dissolved gases are removed by alternately freezing and thawing the NPN, and pumping on the frozen material until a constant residual pressure is noted. With stopcocks 2, 3 and 4 open, gas is admitted to 1 until the desired pressure P is reached; 2 and 3 are closed, and F is shaken vigorously enough so that the liquid within is turbulent. Work elsewhere (4) has shown that a negligible quantity of gas dissolves prior to shaking. The change in level of the mercury in capillary C indicates the change in pressure within that section confined by the flask and flexible spiral up to stopcock 2 and mercury level L (in the widest part of the bulb). The volume of this section V is known,[4] and it is a relatively simple matter to calculate the solubility of the gas. The final expression for doing this is

$$S_p = V'\Delta P/WRT$$

[3] Numbers in parentheses indicate References at end of paper.

[4] See (3) for the method of obtaining V.

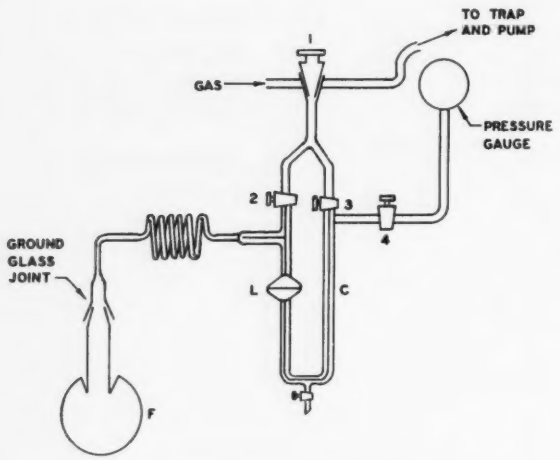

Fig. 1 Gas solubility apparatus

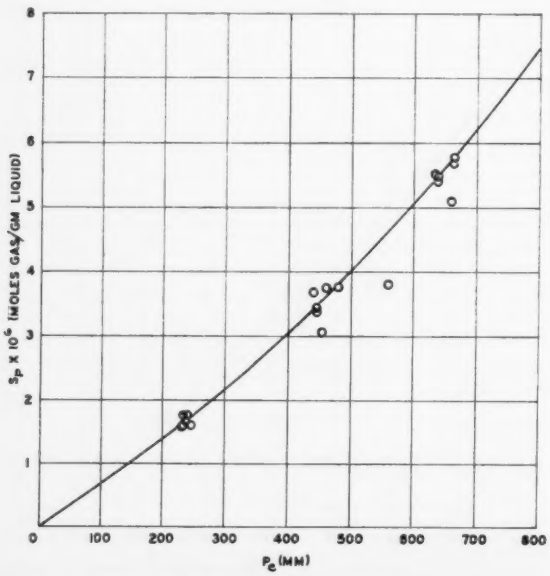

Fig. 2 Solubility of air in n-propyl nitrate

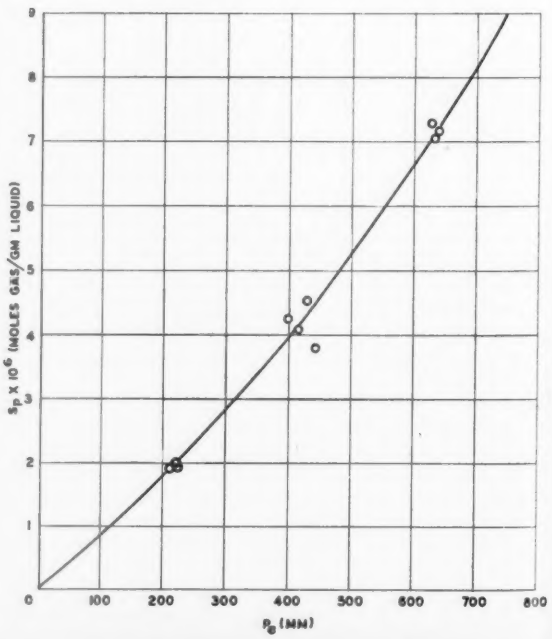

Fig. 3 Solubility of oxygen in n-propyl nitrate

where

S_p = moles gas absorbed per gm. NPN at equilibrium pressure P_e
V' = total volume V minus volume of NPN
P_e = total pressure at equilibrium minus NPN vapor pressure
ΔP = pressure change during equilibration
W = weight of NPN used
R = gas constant
T = absolute temperature

In our calculations we have used values for the density and vapor pressure of NPN given by Thomson (5).

Results

The solubilities of air, oxygen and nitrogen in NPN have been studied at room temperature and over a pressure range of approximately 200 mm to 1 atm.

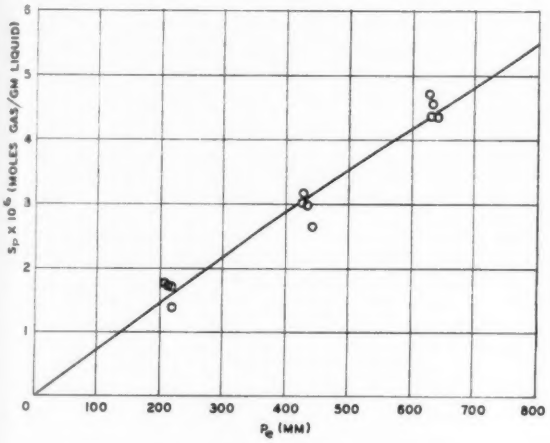

Fig. 4 Solubility of nitrogen in n-propyl nitrate

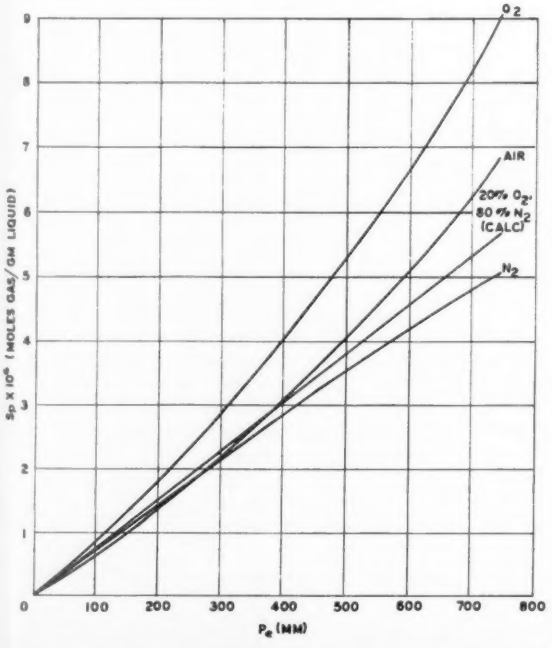

Fig. 5 Comparison of solubilities of air, O_2 and N_2 in n-propyl nitrate

Technical grades of oxygen and of water-pumped nitrogen were used. The gases, assaying better than 99.5 per cent purity, were passed through a drying tube before being admitted to the system. The air was similarly dried.

Results are plotted in Figs. 2, 3 and 4 as S_p vs. P_e.

A least-squares treatment of the data has given the following equations

$$\text{air} \quad S_p = 5.787 \times 10^{-9} P_e + 4.265 \times 10^{-12} P_e^2$$
$$\text{nitrogen} \quad S_p = 7.371 \times 10^{-9} P_e - 7.277 \times 10^{-13} P_e^2$$
$$\text{oxygen} \quad S_p = 7.515 \times 10^{-9} P_e + 6.012 \times 10^{-12} P_e^2$$

The resultant curves are superimposed on the data in Figs. 2, 3 and 4 and are collected in Fig. 5 where they may be compared with each other. In addition, there is a curve for a hypothetical mixture consisting of 80 per cent nitrogen and 20 per cent oxygen. This is predicted from the solubility of each gas at its own partial pressure.

Significance of Results

It is seen that the oxygen solubility is significantly greater than that of nitrogen. Furthermore, the solubility of air is greater than that predicted on the basis of the oxygen and nitrogen data. The higher solubility of oxygen indicates an unusual, but not unexpected, interaction between it and NPN. A possible interpretation of the abnormal air solubility might be that the dissolved air is enriched in oxygen, at the expense of the nitrogen. This is further supported by the apparently linear behavior of the nitrogen which indicates, for this gas, no interaction with the solvent.

If it is true, as seems to be the case, that nonideal absorption occurs, then it should be borne in mind that the data presented here for air are dependent upon the final gas to liquid ratio as well as the equilibrium pressure. This restriction does not apply to nitrogen and oxygen.

A consequence of this phenomenon is that bubbles formed by the release of pressure during the pumping of NPN are apt to be significantly enriched in oxygen. This would, of course, present a distinct hazard. This same unexpected solubility phenomenon is observed with water. At atmospheric pressure air dissolved in water is about 34 per cent oxygen (6). It must be strongly recommended in the absence of contradictory information, that an inert gas be used when pumping the liquid NPN.

References

1 Mead, G. A., "Compression Sensitivity of Monopropellants," ARS JOURNAL, vol. 29, no. 3, March 1959, pp. 192–198.

2 Lawrence, R. W. and Knight, W. P., "Improvements in the Operating Characteristics of n-Propyl Nitrate," ARS JOURNAL, vol. 29, no. 1, Jan. 1959, pp. 29–32.

3 Levy, J. B., Taft, R. W., Jr., Aaron, D. and Hammett, L. P., "Rates and Temperature Coefficients in the Hydration of Two Gaseous Pentenes by Dilute Aqueous Nitric Acid," *J. Amer. Chem. Soc.*, vol. 75, 1953, p. 3955.

4 Taft, R. W., Jr., Purlee, E. L. and Riesz, P., "A Method for Determining the Distribution Constant for a Substance between the Gas Phase and a Condensed Phase," *J. Amer. Chem. Soc.*, vol. 77, 1955, p. 899.

5 Thomson, G. W., "Some Properties of Normal Propyl Nitrate," Ethyl Corp. Research and Engineering Dept., RM-124, Dec. 17, 1954.

6 International Critical Tables, Vol. III, McGraw-Hill, 1928, p. 258.

Magnetogasdynamic Flow Regimes

CHING-SHI LIU[1] and ALI BULENT CAMBEL[2]

Northwestern University, Evanston, Ill.

The prediction of plasma flow subject to a magnetic field is of considerable interest to the engineer designing mag-

Received June 5, 1959.

[1] Graduate Assistant in Mechanical Engineering.

[2] Professor and Chairman of Mechanical Engineering. Fellow ARS.

netogasdynamics devices. In this note we evaluate some flow parameters for certain simple cases and delineate the associated flow regimes.

THREE dimensionless parameters are commonly used in magnetogasdynamics. These are the magnetic Reynolds number (1),[3] the Hartmann number (1) and the Lundquist number (2), and are defined respectively as follows

$$Rem = VL\nu_m^{-1/2} \quad [1]$$

$$Ha = \sigma^{1/2}HL\mu\eta^{-1/2} \quad [2]$$

$$Lu = \sigma HL\mu^{3/2}\rho^{-1/2} \quad [3]$$

In addition to these dimensionless parameters at least two others should be considered because they conveniently define the flow conditions. Both of them are based on the Alfvén wave propagation velocity V_A.

In our hypothetical model we assume that the plasma is described by the thermal equation of state $p = \rho RT$. It is also predicated that the electrical conductivity of the plasma $\sigma \to \infty$, and that the permeability $\mu = 1$. Finally, we consider steady, one-dimensional, continuum flow. Thus, if the plasma flow is in the x-direction and a homogeneous magnetic field H_0 is applied in the z-direction, then an electric current flowing in the y-direction is produced. This in turn produces a variable magnetic field H' in the direction of flow. Alfvén (3) has shown that the magnetic disturbances propagate with the Alfvén velocity V_A defined as

$$V_A = \frac{H_0}{\rho^{1/2}} = \frac{B_0}{\rho^{1/2}} \quad [4]$$

It has been shown by deHoffmann and Teller (4) and by Dungey (5) that the speed a_M with which small disturbances in magnetogasdynamic systems propagate is given by

$$a_M = a + V_A \quad [5]$$

We therefore suggest in this note that a magnetic Mach number M_M be defined as

$$M_M = V/(a + V_A) \quad [6]$$

An associated magnetic Mach angle α_M may then be defined as

$$\sin^{-1}\alpha_M = 1/M_M \quad [7]$$

It follows that for the same plasma flow with and without a magnetic field, the Mach numbers and Mach angles are

$$M_M < M \quad [8]$$

$$\alpha_M > \alpha \quad [9]$$

Simple laboratory experiments can be conceived, to verify Equations [8 and 9]. This would also make possible the convenient measurement of the speed of small disturbances in magnetogasdynamics.

For studies in astrophysics, Cowling (1) has used the S-ratio which we shall call the Cowling number C defined as

$$C = \frac{V_A^2}{V^2} = \frac{B_0^2}{\rho V^2} \quad [10]$$

In Equation [10], the numerator represents the energy associated with the propagation of a magnetic disturbance, and the denominator represents the kinetic energy of the fluid. In effect, C is analogous to $1/M^2$ which is used extensively by aeronautical engineers. It seems more consistent, however, to write the ratio $1/\sqrt{C}$. We shall do so, and in honor of the eminent engineer Theodore von Kármán, we shall call this parameter the Kármán number K.[4] Thus

$$K = \frac{V\sqrt{\rho}}{B_0} = \frac{V}{V_A} \quad [11]$$

It is evident from Equation [11] that the Kármán number is an indication of the magnetic field dissipation. The applications of this in the analysis of magneto-aerodynamic devices are obvious. Thus, if $K < 1$, the disturbances in the field are propagated as magnetohydrodynamic waves without producing any appreciable changes in the field. On the other hand, when $K > 1$, the magnetic disturbances produce distortions at such a rapid rate that they cannot be dissipated as magnetogasdynamic waves. Therefore, we conclude that magnetogasdynamic problems are of engineering interest when K is small.

Logarithmic differentiation of Equation [11] gives

$$\frac{dK}{K} = \frac{dV}{V} + \frac{1}{2}\frac{d\rho}{\rho} - \frac{dB_0}{B_0} \quad [12]$$

It follows that particularly at high velocities the Kármán number is a measure of the density and thus of the compressibility.

The logarithmic differential of the Mach number is (see for example (6))

$$\frac{dM}{M} = \frac{dV}{V} - \frac{1}{2}\frac{dT}{T} \quad [13]$$

If we combine Equations [12 and 13] and perform the algebraic manipulations, we arrive at an equation relating the Mach number and the Kármán number

$$\frac{2dM}{2M + (\gamma - 1)M^3} = \frac{dK}{K} - \frac{d\rho}{2\rho} \quad [14]$$

Equation [14] will be helpful in predicting the density variation in magnetogasdynamic flow. Thus we have compression when

$$\frac{2dM}{2M + (\gamma - 1)M^3} < \frac{dK}{K} \quad [15]$$

or

$$\frac{M}{[2 + (\gamma - 1)M^2]^{1/2}} < K \quad [16]$$

Similarly, expansion occurs when

$$\frac{2dM}{2M + (\gamma - 1)M^3} > \frac{dK}{K} \quad [17]$$

or when

$$\frac{M}{[2 + (\gamma - 1)M^2]^{1/2}} > K \quad [18]$$

In magnetogasdynamics, the continuity equation remains unchanged, but the momentum and the energy equations must be modified. (See for example (7).) Recalling the definition of the Alfvén wave propagation velocity, the energy equation for adiabatic flow becomes

$$V^2 + \frac{2}{\gamma - 1}a^2 + V_A^2 = \text{constant} \quad [19]$$

[3] Numbers in parentheses indicate References at end of paper.

[4] At the completion time of this note, it came to the authors' attention that in a lecture at Amsterdam (to be published in the Proceedings of the IX Annual Congress of the International Astronautical Federation; Lange and Springer), entitled "Magneto Fluid Dynamics in Relation to Space Flight Problems," Dr. von Kármán himself suggested the use of this parameter and designated it as the magnetic Mach number.

We can represent Equation [19] geometrically as in Fig. 1 in which several magnetogasdynamic regimes are recognized. Thus in regime A we have subsonic flow with no appreciable magnetic effects, whereas in regime B the flow is supersonic, though still without important magnetic effects. In regimes C and D the magnetogasdynamic phenomena are important. The flow in regime C is supersonic; in D it is subsonic.

In classical gasdynamics, the equations resulting from the various combinations of the mass and momentum equations are called the Rayleigh equations. Analogous magnetic Rayleigh equations may be derived by combining the classical continuity equation with the magnetogasdynamic momentum equation. If we do this, and use in the algebraic manipulations the equation of state for a perfect gas as well as the definitions of the Mach and Kármán numbers, we get the following magnetic Rayleigh equations

$$\frac{p_2}{p_1} = \frac{1 + \gamma M_1^2(1 + 1/2K_1^2)}{1 + \gamma M_2^2(1 + 1/2K_2^2)} \qquad [20]$$

$$\frac{T_2}{T_1} = \frac{M_2^2[1 + \gamma M_1^2(1 + 1/2K_1^2)]}{M_1^2[1 + \gamma M_2^2(1 + 1/2K_2^2)]} \qquad [21]$$

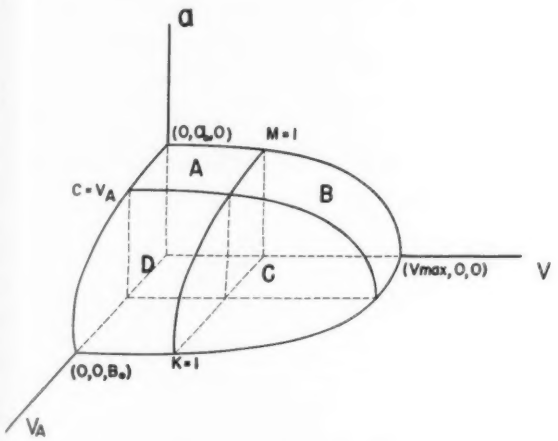

Fig. 1 Magnetogasdynamic flow regimes

$$S_2 - S_1 = \frac{\gamma R}{\gamma - 1} \ln \left\{ \frac{M_2^2}{M_1^2} \left[\frac{1 + \gamma M_1^2(1 + 1/2K_1^2)}{1 + \gamma M_2^2(1 + 1/2K_2^2)} \right]^{(\gamma+1)/\gamma} \right\} \qquad [22]$$

For the case when $K \to \infty$, there is no magnetogasdynamic effect, and the equations reduce to their usual counterparts in classical gasdynamics.

Nomenclature

a = acoustic velocity
a_M = magnetic acoustic velocity
B = magnetic field vector
C = S, Cowling number
H = magnetic intensity
Ha = Hartmann number
K = Kármán number
L = characteristic length
Lu = Lundquist number
M = Mach number
M_M = magnetic Mach number
p = pressure
Rem = magnetic Reynolds number
s = entropy
T = temperature
V = flow velocity
V_A = Alfvén velocity
α = Mach angle
α_M = magnetic Mach angle
γ = specific heat ratio
η = fluid dynamic viscosity
μ = permeability
ν_m = magnetic viscosity
ρ = density
σ = electrical conductivity

References

1 Cowling, T. G., "Magnetohydrodynamics," Interscience Publishers, Inc., New York, 1957.
2 Lundquist, S., "Studies in Magneto-hydrodynamics," *Arkiv fur Fysik*, vol. 5, no. 15, 1952, p. 297.
3 Alfvén, H., "Existence of Electromagetic-Hydrodynamic Waves," *Nature*, vol. 150, 1942, p. 405.
4 DeHoffmann, F. and Teller, E., "Magneto-Hydrodynamic Shocks," *Phys. Rev.*, vol. 80, 1950, p. 692.
5 Dungey, J. W., "Cosmic Electro-Dynamics," Cambridge University Press, London, 1958.
6 Cambel, A. B. and Jennings, B. H., "Gas Dynamics," McGraw-Hill Book Co., New York, 1958.
7 Resler, E. L. and Sears, W. R., "The Prospects of Magneto-Aerodynamics," *J. Aeron. Sci.*, vol. 25, no. 4, 1958, p. 235.

Technical Comments

Comment on "Generalized Trajectories for Free-Falling Bodies of High Drag" and "Vertical Re-Entry Into Earth's Atmosphere for Both Light and Heavy Bodies"

JERZY H. TEISSEYRE[1]

Technical University in Wroclaw, Wroclaw, Poland

IN THE April[2] and May[3] 1958 issues of JET PROPULSION, there appeared investigations concerning a free-falling body coming from very great height through the Earth's atmosphere. In such calculations, one tacitly assumes that the Earth's acceleration due to gravity is constant and equal to 9.81 m/sec² or 32.2 fps².

I shall discuss here a rapid method of calculation where the Earth's variable acceleration is taken into account and different drag coefficients can be inserted in the calculus. Moreover, the exponential density equation $\rho_x = \rho_0 e^{-kx}$ can be considered with variable coefficient k as is really the case. The atmospheric data assumed are given in Table 1 and also represented in Fig. 2.

Considering Fig. 1 and assuming the following nomenclature

- m = mass
- g = acceleration of gravity on the Earth's surface
- g_x = $g(R/R + x)^2$ acceleration of gravity at the height x above the Earth's surface
- v = velocity, m/sec
- ρ = air density, kGsec²/m⁴
- A = cross-sectional area of body, m²

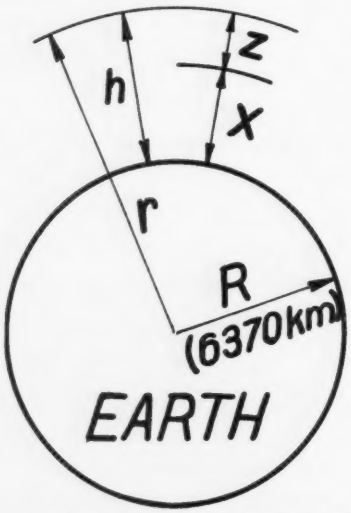

Fig. 1. Earth and the adopted designations

Table 1 Atmospheric data of free-falling bodies

Height, m × 10³	Ratio of density ρ_x/ρ_0
0	1
10	0.337
15	0.1625
20	0.0718
30.5*	1.43×10^{-2}
45.7	1.51×10^{-3}
61	2.90×10^{-4}
91.44	8.83×10^{-6}
122	3.50×10^{-7}
152.4	4.13×10^{-8}
185.3	6.16×10^{-9}
215.36	1.90×10^{-9}
243.84	5.90×10^{-10}
296.5	1.13×10^{-10}
370.64	1.70×10^{-11}

* The unequal numbers result from converting feet into meters.

C_d = drag coefficient = drag/$(1/2)\rho v^2 A$

we get the following equations of a vertically falling body

$$m\ddot{x} = -m \cdot g \left(\frac{R}{R+x}\right)^2 + D \qquad [1]$$

where $D = (1/2)\,\rho_x C_d A v^2$ is the force of drag. Thus

$$\ddot{x} = \frac{dv}{dt} = -g\left(\frac{R}{R+x}\right)^2 + \frac{D}{m} \qquad [2]$$

or

$$\ddot{x} = -g\left(\frac{R}{R+x}\right)^2 + E\,e^{-kx}\dot{x}^2 \qquad [3]$$

where constant

$$E = \frac{\rho_0}{2} C_d \frac{A}{m}$$

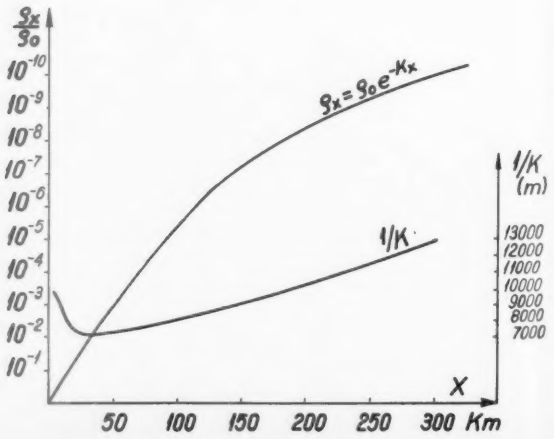

Fig. 2 Adopted characteristics of the atmosphere

Received April 27, 1959.

[1] Chairman, Polish Astronautical Society, Wroclaw.

[2] Turnacliff, R. D. and Hartnett, J. P., "Generalized Trajectories for Free-Falling Bodies of High Drag," JET PROPULSION, vol. 28, April 1958, pp. 263–266.

[3] Linnel, R. D., "Vertical Re-Entry Into the Earth's Atmosphere for Both Light and Heavy Bodies," JET PROPULSION, vol. 28. May 1958, pp. 329–330.

Table 2 Example of calculation

h, km	z, km	Δz, km	$2gR^2/(r-z)^2$	k, km	$2E \cdot e^{kz}/e^{hk} = 2G \cdot e^{kz}$	$2Ge^{kz} \cdot u$	du/dz	$u = v^2$, m/sec^2
100	0	0	19.017	1/8	0.00000933	0	19.017	0
95	5	5	19.04	1/7.9	0.00001327	1.261	17.78	95085
90	10	5	19.07	1/7.8	0.0000250	4.35	14.72	173985
85	15	5	19.10	1/7.7	0.0000380	9.415	9.685	247585
84	16	1	19.112	1/7.7	0.0000433	11.135	7.977	257270

Putting also $x = h - z$ (Fig. 1) we have: $e^{-kz} = e^{-hk} \cdot e^{zk}$, where h is the height from which the body begins to fall. At this height the velocity $v = \dot{z} = 0$. Putting $G = E \cdot e^{-hk}$ (which is variable, k being variable as well) we get

$$\ddot{z} = -g\left(\frac{R}{r-z}\right)^2 + Ge^{zk}\dot{z}^2 \qquad [4]$$

and since

$$\ddot{z} = \frac{dv}{dt} = \frac{dv}{dz} \cdot \frac{dz}{dt} = v\frac{dv}{dz} = \frac{1}{2}\frac{dv^2}{dz}$$

and putting $v^2 = u$, we get finally

$$\frac{du}{dz} - 2Ge^{kz} \cdot u + \frac{2gR^2}{(r-z)^2} = 0 \qquad [5]$$

This equation can be readily solved by step-by-step calculation if we know the initial conditions. Now the initial conditions are: $u = 0$ for $x = h$ or $z = 0$. So we have for initial conditions $du/dz + 2gR^2/r^2 = 0$, from which du/dz can be calculated, and for an assumed Δz (say of 5 km) the value of $u_{\Delta z} = (du/dz)\,\Delta z$ can be obtained. Putting this $u_{\Delta z}$ into Equation [5] and assuming again a certain Δz, we find another value of du/dz and also another $u_{\Delta z} = u$. For purposes of quick calculation, Table 2 is useful. From Table 2 one can also calculate the accelerations of the falling body and the time of fall.

Figs. 3 and 4 show the results of the calculations for two different bodies: One of a very large drag and small mass, (a parachute), with $2E = \rho_0 (C_d A/m) = 2.5|m^{-1}|$, and the second one for a small drag and large mass (a missile), with $2E = 3 \times 10^{-3}|m^{-1}|$. The cases of medial values $2E = 0.003$, 0.3 and 1 have been also considered.

The balance of energy of the falling body is given by the equation

$$\text{energy} = g_z(h-z) + \frac{1}{2}v_z^2 + E\int_h^{h-z} \varphi_z v_z^2 dz \text{ (per unit of mass)} \qquad [6]$$

where $\varphi_z = e^{kz} \cdot e^{-hk}$. The first term gives us the potential energy, the second term kinetic energy, and the third one represents the work necessary to overcome the drag of the body.

The condition of constant energy (d energy $= 0$) gives us

$$-gdz + vdv + E\varphi_z v_z^2 dz = 0 \qquad [7]$$

from which we can get the increase of speed per unit of trajectory.

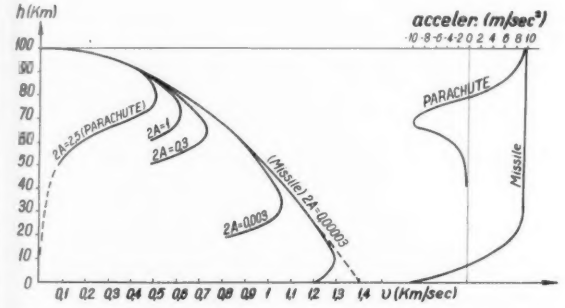

Fig. 3 Speed and acceleration of falling bodies (parachute and missile)

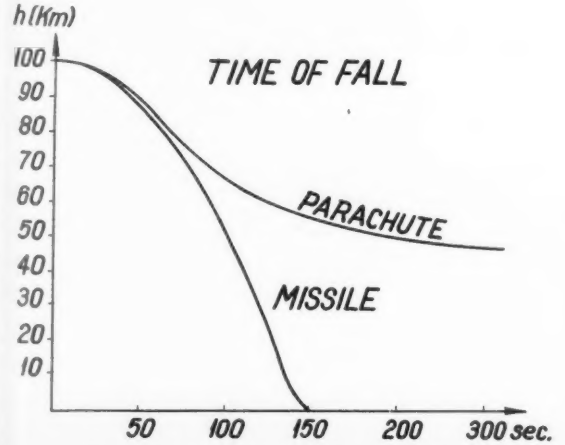

Fig. 4 Time of fall for parachute and missile

Comments on "Recent Advances in Cryogenic Engineering"

S. L. BRAGG[1]

Rolls Royce Ltd., Derby, England

I WOULD like to comment on the article "Recent Advances in Cryogenic Engineering" by Robert B. Jacobs which appeared in the April 1959 issue of ARS JOURNAL, and in particular to disagree with Dr. Jacobs' statement on page 249 that "Dynamic pressure measurement (in a cryogenic liquid) offers no difficulty if the transducer temperature is known."

It appears to be normal practice in cryogenic engineering to keep transducers at ambient temperature so that an accurate calibration may be maintained. Unless, therefore, a water-warmed diaphragm type of pickup (such as the Li-Liu) is used, it is necessary to connect the transducer to the tapping point by a pipe some 10-in. long. Under

Received June 9, 1959.

[1] Chief Performance Engineer, Rocket Engine Division. Member ARS.

steady conditions, this pipe will be full of vapor, except in the immediate vicinity of the tap.

If now the pressure in the main liquid line suddenly rises, liquid will flow into the tapping line, and the vapor there will be compressed. However, this compression will occur much more slowly than if it were a gas pressure that was being measured. This is because the volume inflow under a given pressure difference between main line and tapping is *inversely* proportional to the square root of the density. The response of the transducer, which records the pressure of the vapor, will therefore lag the pressure change of the liquid in the line. Finally, there may even be an uncomfortable overshoot, due to the momentum of the liquid in the tapping being suddenly arrested by the buffer of residual vapor at the transducer.

Thus, measurement of transient pressures in cryogenic liquids does produce an extra difficulty in that the response of a transducer which is not actually mounted at the tapping point will be considerably slower than it would be in either a completely gaseous or a completely liquid system.

Comments on "Recent Advances in Gaseous Detonation"

G. RIBAUD[1]

Faculté des Sciences, Paris, France

PAPERS by Döring and Schön (1)[2] concerning mixtures of CH_4-O_2 and C_2N_2-O_2 should be added to the bibliography given by Gross and Oppenheim in their recent article in this Journal (2). Döring and Schön avoided the theoretical errors in their calculations indicated by Gross and Oppenheim, and even though the authors of (1) used outdated thermodynamic values (3), their results are noteworthy. To my knowledge, these theoretical errors have up to now been avoided only by Manson (4), Döring and Schön (3), and Eisen, Gross and Rivlin (5).

In their discussion of non-Chapman-Jouguet detonations, Gross and Oppenheim indicated that the theory permitting prediction of the frequency of the spin, which is often visible in photographs of the waves and which characterizes their instability, was developed by Fay (6) and Chu (7). Actually, this theory had already been discussed by Manson (8). Fay cited Manson's work and noted some differences in the treatment of the phenomenon. However, Chu later showed that these differences were minor ones.

References

1 Schön, G. and Döring, W., *Zeitschrift für Elektrochemie*, vol. 54, 1950, p. 231.

2 Gross, R. A. and Oppenheim, A. K., "Recent Advances in Gaseous Detonation," ARS JOURNAL, vol. 29, no. 3, March 1959, pp. 173–179.

3 Zeise, H., *Zeitschrift für Elektrochemie*, vol. 48, 1942, p. 23.

4 Manson, N., *Comptes Rendus de l'Académie des Sciences*, Paris, vol. 218, 1944, p. 292; *see also* "Propagation des Détonations et des Déflagrations dans les Mélanges Gazeux," ONERA, Inst. Francais du Pétrole, 1947, English trans. ASTIA AD 132808.

5 Eisen, C., Gross, R. A. and Rivlin, T., "Theoretrical Calculation in Gaseous Detonation," Fairchild Engine Division, March 15, 1958; ASTIA AD 94173.

6 Fay, J., *J. Chem. Phys.*, vol 20, 1952, p. 942.

7 Chu, B. T., "Vibration in a Gaseous Column behind a Strong Detonation Wave," Proc. Gas Dynamics Symposium on Aerothermochemistry, Northwestern Univ., Aug. 1955, p. 95.

8 Manson, N., *Comptes Rendus de l'Académie des Sciences*, Paris, vol. 222, 1946, p. 46.

Received July 1, 1959.

[1] Professeur Honoraire à la Sorbonne, Membre de l' Institut.

[2] Numbers in parentheses indicate References at end of paper.

Simple Method of Estimating the Variation of Impact Points for Ballistic Missiles

SAMUEL W. FORDYCE[1]

Space Technology Laboratories, Inc., Los Angeles, Calif.

A PREVIOUS article[2] derived the following expression for the free flight range of a ballistic missile

$$S = 2R_E \sin^{-1}(Y_L^2 \sin 2\theta/2\epsilon) \quad [1]$$

where

R_E = radius of the Earth
Y_L = dimensionless velocity $\equiv \nu_L/\nu_c$
ν_L = cutoff speed of the missile
ν_c = orbital speed at the cutoff altitude (R_L from the Earth's center) $\equiv \sqrt{GM_E/R_L}$
GM_E = constant, 1.405×10^{16} ft^3 sec^{-2}
θ = angle between the velocity vector at cutoff and the local horizontal
ϵ = orbital eccentricity, given by

$$\epsilon = [1 - Y_L^2 \cos^2\theta(2 - Y_L^2)]^{1/2} \quad [2]$$

Suppose a small increment of velocity $\Delta\nu$ is added linearly to the velocity vector at cutoff. The revised cutoff speed is

$$\nu_L' = \nu_L + \Delta\nu \quad [3]$$

The dimensionless velocity becomes

$$Y_L' = Y_L + (\Delta\nu/\nu_c) \quad [4]$$

and since $Y_L >> \Delta\nu/\nu_c$, the revised orbital eccentricity is given approximately by

$$\epsilon' \approx \epsilon\left[1 - \frac{2\Delta\nu Y_L \cos^2\theta(1 - Y_L^2)}{\epsilon^2\nu_c}\right] \quad [5]$$

The revised angular range is given approximately by

$$\varphi' \approx 2\sin^{-1}(Y_L'^2 \sin 2\theta/2\epsilon') \quad [6]$$

Finally, the increment in surface range due to the small increment in velocity is approximated by the expression

$$\frac{\Delta S}{\Delta\nu} = \frac{2R_E Y_L \sin 2\theta}{\nu_c\epsilon(\cos\varphi/2)}\left[1 + \frac{Y_L^2\cos^2\theta(1 - Y_L^2)}{\epsilon^2}\right] \quad [7]$$

Received July 6, 1959.

[1] Member of the Technical Staff. Member ARS.

[2] Singer, S. F. and Wentworth, R. C., "A Method for Calculating Impact Points of Ballistic Rockets," JET PROPULSION, vol. 28, no. 10, 1958, pp. 684–687.

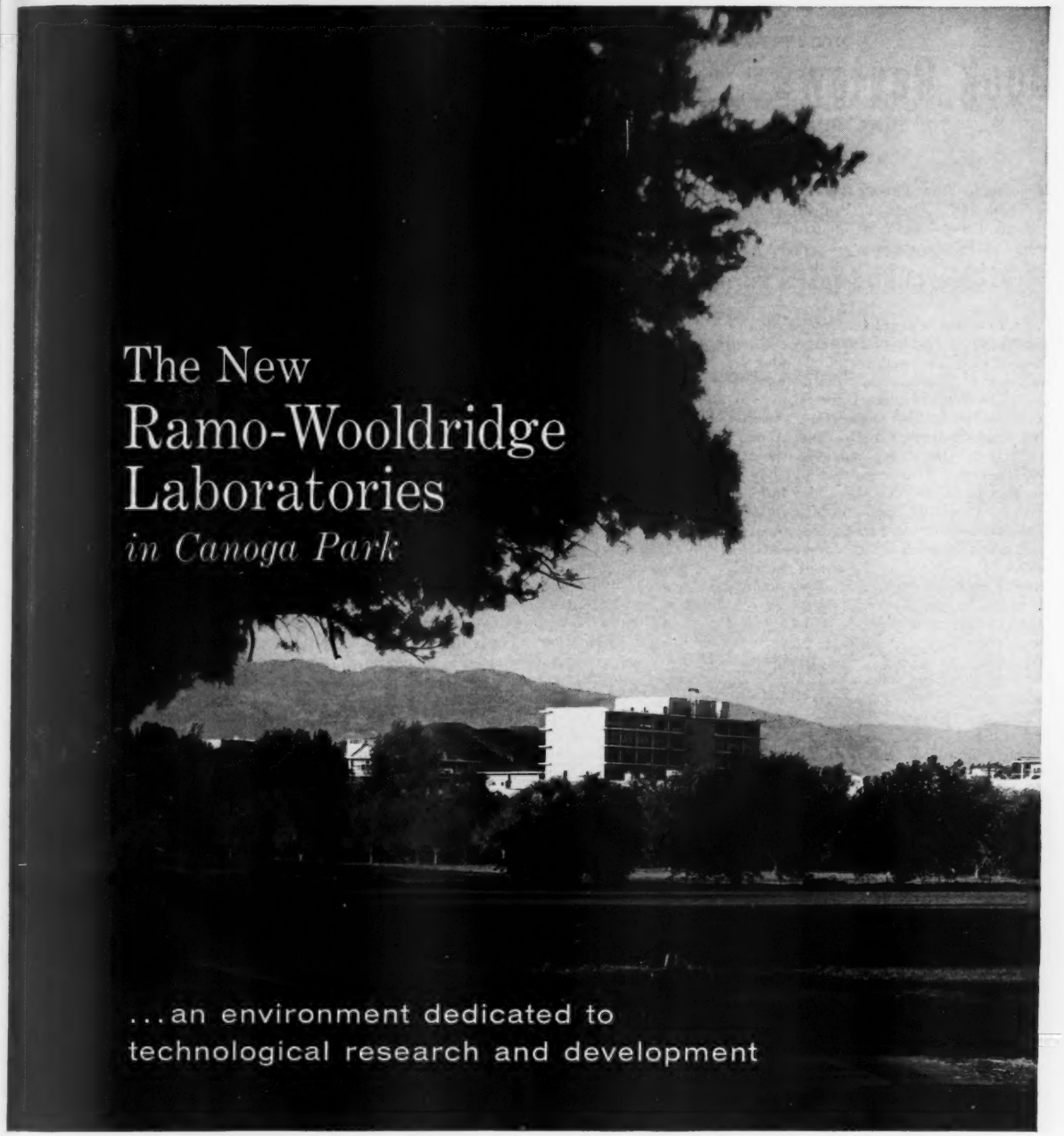

The new Ramo-Wooldridge Laboratories in Canoga Park, California, will provide an excellent environment for scientists and engineers engaged in technological research and development. Because of the high degree of scientific and engineering effort involved in Ramo-Wooldridge programs, technically trained people are assigned a more dominant role in the management of the organization than is customary.

The ninety-acre landscaped site, with modern buildings grouped around a central mall, contributes to the academic environment necessary for creative work. The new Laboratories will be the West Coast headquarters of Thompson Ramo Wooldridge Inc. as well as house the Ramo-Wooldridge division of TRW.

The Ramo-Wooldridge Laboratories are engaged in the broad fields of electronic systems technology, computers, and data processing. Outstanding opportunities exist for scientists and engineers.

For specific information on current openings write to Mr. D. L. Pyke.

THE RAMO-WOOLDRIDGE LABORATORIES

8433 FALLBROOK AVENUE, CANOGA PARK, CALIFORNIA

Book Reviews

Ali Bulent Cambel, Northwestern University, *Associate Editor*

Hypersonic Flow Theory, by Wallace D. Hayes and Ronald F. Probstein, Academic Press, New York, 1959, 464 + xiv pp. $11.50.

Reviewed by Arthur A. Kovitz
Northwestern University

This volume is the fifth in a series on applied mathematics and mechanics, editor-in-chief F. N. Frenkiel, prepared under the auspices of the Applied Physics Laboratory, The Johns Hopkins University. This reviewer has had occasion to use the first and third volumes, namely "Gas Dynamics," by K. Oswatitsch, and "Mathematical Theory of Compressible Fluid Flow," by R. von Mises. To those also familiar with the Oswatitsch and von Mises efforts, it should be quite clear that any companion volume must reach a high level of attainment. It is stated at the outset that this latest addition does so and excellently compliments its forerunners.

An outline of its contents should suggest the broad coverage that has been achieved. Beginning with small disturbance and Newtonian theory, constant density solutions for various shapes are discussed. The theory of thin shock layers followed by other methods for blunt body and locally supersonic flows receive individual chapters. The concluding three chapters deal with viscous effects, including interactions, molecule and rarefied gas flows.

The introductory chapter is not one to be skimmed lightly. After a few initial remarks on the "definition" of hypersonic flow, a section is devoted to the assumptions underlying inviscid hypersonic flow theory. Five fundamental assumptions are listed and discussed with respect to their use in particular theories. The remaining chapters on inviscid flow continually refer to these explicitly stated propositions as a basis for development of various analytical schemes. It is decidedly brought home to the reader that a clear grasp of the fundamentals is essential to his subsequent understanding of the remaining work.

The treatment in the remaining sections of the first chapter illustrates one of the leitmotifs of the following chapters on inviscid hypersonic flow. Wherever possible, existing theories applicable to perfect gases are formulated in terms of a general ideal (nonviscous) fluid. The normal shock is used to illustrate the behavior of the density ratio, and several interesting calculations are made to aid the reader in acquiring an understanding of its variations. Oswatitsch's result, that for a perfect gas the flow pattern becomes independent of free stream Mach number as this parameter becomes very large, is shown to be valid in a deeper sense for a general fluid. This is stated as a "Mach number independence principle." The first chapter is concluded with a brief discussion of real-fluid effects.

Small disturbance theory and hypersonic similitude are treated in the second chapter. A feature of this chapter is a concise, general description of the concept of similitude itself. Some early Russian work on small-disturbance theory is discussed.

Newtonian theory receives detailed, deep attention. It begins with a highly diverting excursion into the pertinent parts of "Principia Mathematica." The limitations of Newton's model are clearly pinpointed. Busemann's centrifugal correction to the sine-squared pressure formula is pointed out as an essential modification of the Newtonian flow model. Optimum shapes and shock layer structure in Newtonian theory are given treatments, some parts of which have not previously been reported in the literature.

A chapter on the constant density approximation is devoted to solutions for several simple bodies. Included are the wedge, cone, circular cylinder and sphere.

Thin shock layers are given a chapter of unique explanation. The senior author's artesian-well and shower-bath analogies are discussed in connection with the general problem of finding the shock shape, given the body shape. Several approximate methods of attack are outlined including successive approximations, constant-streamtube area, and inevitably, variable-streamtube area.

The last two chapters dealing with the ideal (nonviscous) fluid present numerical methods for treating blunt body and locally supersonic flows. Relaxation techniques, integral methods and the inverse approach are detailed for finding the shape and location of the detached bow shock given the body or vice versa. The method of characteristics is reviewed for a general fluid. Special attention is given to flows with equilibrium or frozen composition.

Two chapters are devoted to viscous flows and viscous interactions. The chapter on viscous flows is a comprehensive but highly condensed review of the intense efforts of the last five or six years to understand boundary layer flows with relaxation, diffusion and chemical reaction. The boundary layer equations are quoted in complete generality and transformed under Mangler and Howarth-Dorodnitsyn transformations as generalized recently by Lees. Similar laminar boundary layer solutions are described, and the limitations in finding them are pointed out.

The chapter on viscous interactions contains much of the second author's valuable contributions to the field in addition to what appears to be an excellent review. Much of the work done at Princeton University's Gas Dynamics Laboratory in the helium hypersonic wind tunnel is given well-deserved attention.

The final chapter is on free molecule and rarefied gas flows. It is suggested that the criterion for rarefied vs. continuum methods must be based on local flow conditions. A revised classification of flow regimes is presented that attempts to delineate more clearly the various regions, from continuum flow at high Reynolds number to free molecule flows at very low Reynolds number. Continuum solutions for rarefied gas flows are discussed after which free molecule transfer theory is outlined.

Two helpful organizational features of the book should be mentioned. First, the cited references are listed alphabetically according to author, with titles, in one section. Second, a symbol index is provided with the page number where the symbol first appeared.

It has already been remarked that one of the aims of the authors' presentation has been generality and completeness. Thus, the work takes on the character of a treatise, written in a sophisticated and terse style. As such, it can present comprehension difficulties to readers not too familiar with hypersonic flow. This volume is certainly not of a textbook nature. The subject is complex, and one must bring to it a rather well-rounded background in order to make good use of the presentation.

This reviewer has enjoyed encountering a book written by two authors well-prepared for the task of putting into one place the results of fairly recent research activity. The authors themselves have contributed significantly to the field. They write with a deep understanding of the present state of the art, and the certain knowledge that present research activity, their own included, will demand future books on hypersonic flow. However, the nature of the present volume makes it an important contribution to the contemporary scene as well as a book that will remain vital for many future years.

Some Problems in Chemical Kinetics and Reactivity, Vol. 2, by N. N. Semenov, translated from the Russian by Michael Boudart, Princeton University Press, Princeton, N. J., 1959, 330 pp. $4.50

Reviewed by S. S. Penner
California Institute of Technology

In the present volume, the following topics are treated: Competition between chain reactions and reactions between saturated molecules (including explicit discussion of such diverse topics as formation of NO from N_2 and O_2, decomposition of di-iodo-ethane and of alkyl bromides, cracking of hydrocarbons, etc.), thermal explosions, chain ignition (e.g., in the oxidation of phosphorus and of sulfur, ignition limits in the oxidation of phosphine, silane, etc.), chain ignition in H_2-O_2 mixtures, chain interactions including cold flame propagation in lean oxygen-carbon disulfide mixtures, and chain reactions with degenerate branching (e.g., oxidation of CH_4, H_2S, liquid-phase oxida-

NORELCO and CRYOGENICS

GAS PURIFICATION
GAS SEPARATION
AIR SEPARATION
CONVERSION OF GASEOUS O_2 and N_2 TO LIQUID PRODUCT
METAL TREATMENT
COLD CHAMBERS
LIQUID AIR PRODUCTION
LIQUID NITROGEN PRODUCTION
PRESERVATION OF BIOLOGICALS
COLD MACHINING
LOW TEMPERATURE PULVERIZATION
SHRINK FITTING

All of the applications listed—and more—stem from the one unit—THE NORELCO CRYOGENERATOR. Available in four different capacities, this remarkable unit consists of a single-stage refrigeration machine designed for operation in the range of minus 320 degrees F. to ambient temperatures. As a basic cryogenic tool, the cryogenerator is completely adaptable to a tremendous number of applications and is in fact being widely used by a host of manufacturers and laboratories throughout the country.

Since the operating principle is identical for all models, specific applications of each depend primarily on the capacity of the system rather than the form of equipment. The four models, designated A, B, C and D, have respective refrigeration capacities of 3,000, 12,000, 40,000 and 160,000 BTU/hr. at minus 320 degrees Fahrenheit.

"Packaged" units consisting of a Model Cryogenerator with special headers or accessory equipment are also available.

Research facilities at the Norelco Cryogenics Application Laboratory are available for consultation on industrial problems involving any low temperature application. Write today for illustrated brochures and complete technical information.

AIR LIQUEFIER — This unit liquefies air at atmospheric pressure — thereby insuring a contaminant-free product. Rate of production is 7½ liters per hour.

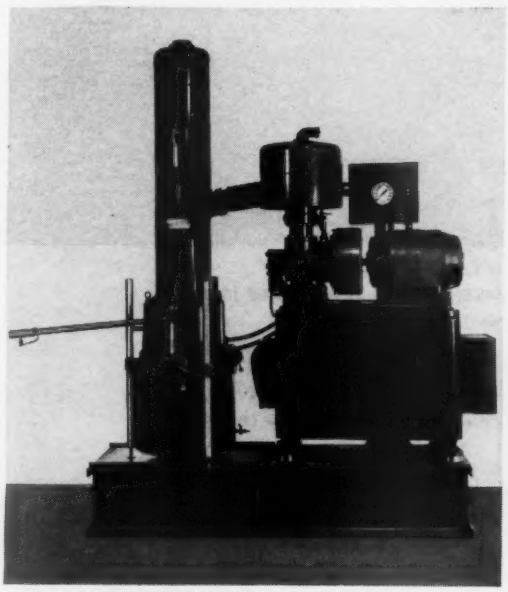

NITROGEN GENERATOR — Comprised of a Model A Cryogenerator acting as a nitrogen condenser and an atmospheric pressure separation column. Rate of production is 6 liters per hour over an uninterrupted period up to 200 hours.

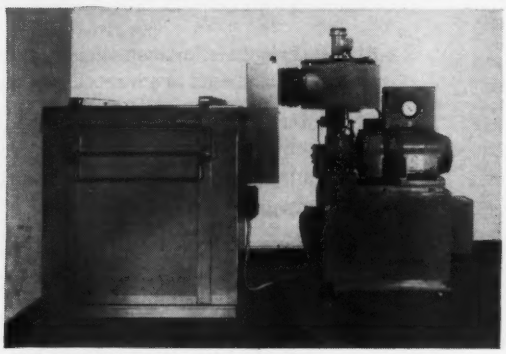

ENVIRONMENTAL CHAMBER — A specially insulated storage chest is used in conjunction with a Model A Cryogenerator. This permits the production and maintenance of temperatures down to minus 320 degrees F. for environmental testing.

Norelco ®
Serving Science and Industry

NORTH AMERICAN PHILIPS COMPANY, Inc.
CRYOGENICS DIVISION 100 Stevens Avenue, Mount Vernon, N. Y.

Explore new areas at IBM in

PHYSICS

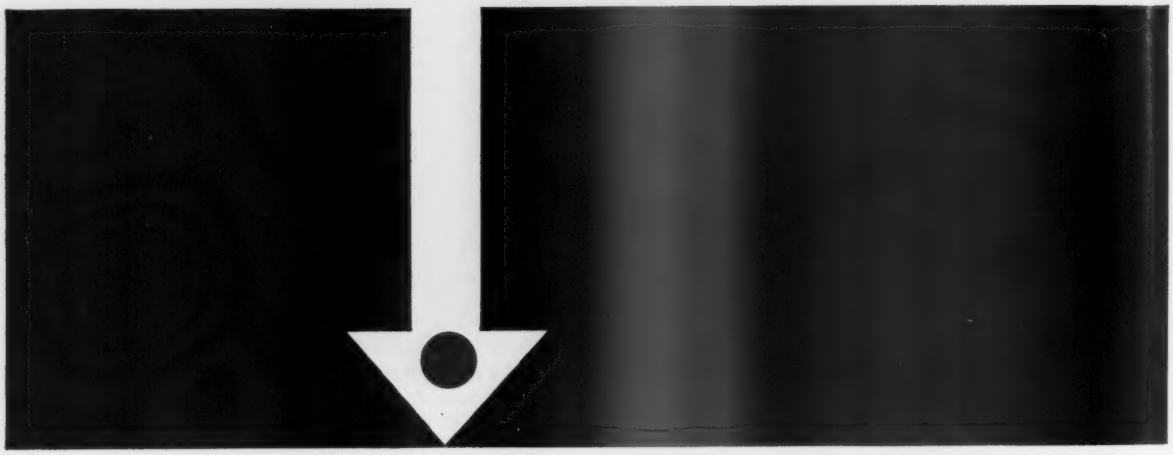

At IBM, scientists, mathematicians and engineers are currently engaged in many unique assignments in advanced physics. For example:

1. Photoelasticity is being studied to determine strain propagation as a function of time in solids. This work is designed to clarify laws governing impulse strain waves, as well as to determine dynamic stresses that exist in impact and other phenomena.
2. Fundamentals of the magnetic properties of materials are under study. The immediate interests are spin-wave investigations, particularly those relating to the switching times of remagnetization and spin-wave propagation in polycrystalline materials.
3. Optical techniques, with organic and inorganic thin films, are being used to examine the properties of absorption phenomena in surfaces and substrates.

You'll find a wide range and diversity of career areas at IBM. Advancement is rapid, due in part to the demands of a constantly expanding program of research and development, and in part to a long-continued record of promoting from within, based on individual merit and achievement. Depending on your field of interest and on your abilities, you may work alone or as a member of a small team. You'll be given all the specialized assistance you need.

CAREERS AVAILABLE IN THESE AREAS:

Acoustics
Aerodynamics
Astrophysics
Cryogenics
Inertial Control
Magnetics
Mathematics
Mechanics
Nuclear Physics
Optics
Semiconductors
Solid State

QUALIFICATIONS: B.S. or Advanced Degree in Physics, Electrical Engineering, Engineering Physics, or Mathematics—plus proven ability to assume a high degree of technical responsibility in your sphere of interest.

SOME ASSIGNMENTS NOW OPEN INCLUDE:

Investigation of theoretical device design and experimental proof of feasibility for ultrahigh-speed transistor; P-N junction technology; surface studies; optimization of semiconductor fabrication.

Creating techniques for solving boundary value problems, such as field theory of structures (Green's function methods, for example), or stress wave propagation in solids.

Study of flow and pressure distributions in hydrodynamic transients, to provide information for the development of a comprehensive theory of short duration (pulse), high Reynold's number fluid-flow systems.

Determining dynamic behavior of micromagnetic fields by applying low-level, high-frequency circuit knowledge for small, closely coupled circuits as a result of Hall effect studies.

Study of basic scientific phenomena in the field of energy conversion; design of experiments for the investigation of electrical discharge in various environments and investigation of distribution and loss of energy. The objective is to develop energy conversion techniques that exceed the limited performance and efficiency of existing conversion methods.

Physical-mathematical studies to determine how complex control problems may be solved with digital computers. Applications in missile systems and special-purpose computer systems.

Development of magnetic devices for use in logic switching and computer "memory." Experience in fundamentals of nonlinear magnetics necessary.

Write, outlining background and interests, to:
Mr. R. E. Rodgers, Dept. 572K
IBM Corporation
590 Madison Avenue,
New York 22, N.Y.

IBM®

INTERNATIONAL BUSINESS MACHINES CORPORATION

tion of hydrocarbons). Volume 2 contains brief appendixes dealing with the method of the activated complex (written by M. I. Temkin), quantum-mechanical calculations of the activation energy (written in collaboration with N. D. Sokolov), and selected additions to Volume 1 which were sent by the author to the translator after publication of Volume 1.

To the kineticist, the present volume constitutes an invaluable up-to-date compilation by the author who published a now classical treatise on chain reactions nearly 25 years ago; to the specialist in combustion or propulsion, the present work offers essential reference material in kinetics which, after suitable simplification, is sometimes useful in the quantitative description of combustion processes. Combustion theory per se is not considered in Semenov's book.

Ordinary Differential Equations, by Wilfred Kaplan, Addison-Wesley Publishing Co., Inc., Reading, Mass., 1958, 534 pp. $8.50.

Reviewed by E. A. Trabant
Purdue University

The first three chapters of the text are at an elementary level necessary for students beginning in differential equations. However, in these first three chapters material is included which contributes to the mathematical maturity of the student who has already had a brief introduction to differential equations—that is, existence theorems, step-by-step integration, one-to-one correspondence, concept of output and input, and superposition, etc.

The text is consistent with the form of introducing basic concepts and theory before a technique of solution. General theorems are stated; their importance and applications noted, but most proofs are delayed until the last chapter of the book which is titled "Fundamental Theory." An exception to this form is the chapter on phase-plane analysis where there is a good collection of stability theorems with proofs.

A chapter on numerical methods is included in which application of the methods to digital computers is mentioned. Analog computers are referred to, but no work or further discussion is presented.

The approach used in discussing linear independent equations in the chapter on linear equations of arbitrary order is excellent. Some may feel that the summary presented on complex functions and the Laplace transforms is too brief. However, the material included is sufficient for the purposes of the text.

A rather long and detailed treatment of simultaneous linear differential equations is made. An appendix here introduces vectors and the use of matrices.

The examples and exercises included throughout the text are fine, particularly those with physical interpretation and application.

The text will be useful to all those interested in the application of differential equations to engineering problems, particularly in the area of servomechanisms and automatic control. In addition, it pro-

vides a base for broadening the reader's mathematical horizons.

Recent Advances in the Engineering Sciences, Proceedings of Conference on Science and Technology for Deans of Engineering, Purdue University, McGraw-Hill Book Co., Inc., New York, 1958, 265 pp. $4.75.

Reviewed by CARL A. ANDERSON
Institute of Technology (Air University)

Although this book is made up of the proceedings of a conference held in September 1957, the topics covered are no less important today, two years later, than when originally presented. Certainly, engineering education is changing and growing to keep up with new developments in science and technology, but the changes and growth generally do not occur precipitately. Rather, they occur through an envolutionary process attended by considerable discussion, self-study and, perhaps, dissent on the part of engineering educators. This book can be a definite aid to these educators as they work to improve their curricula.

The conference was directed toward the problems of the engineering college administrators whose management duties often make it impossible for them to keep up-to-date on technical developments, but who are, nevertheless, responsible for curricular offerings. Each of the technical topics was covered in two parts: The first a survey of the state of the art in the field, and the second a discussion of how developments in the field might affect engineering education. With different speakers for each part, a certain amount of redundancy was evident in the papers. Even more redundancy would have been acceptable, however, if the post-presentation discussions could have been included in the book. The contributions of the administrators attending the meeting would probably have made quite valuable reading for their fellows and their co-workers. Unfortunately, as stated in the preface, it was not feasible to include the discussions in the book.

Seven technical fields were touched upon by 14 invited authorities in these fields. J. G. Truxal surveyed automation and automatic control, stressing the growing use of computers in control systems, the still new adaptive controllers, and the types of models used in control design. The companion piece by G. S. Brown was directed more toward engineering science in general and a possible reorganization of engineering education. Operations research and systems engineering were covered by H. H. Goode and D. G. Malcolm in papers which went a long way toward defining these new fields and locating them within the engineering spectrum. M. Tribus organized the subject of thermodynamics and pointed out the importance of modern studies of irreversible processes; N. A. Hall argued for a better grounding in thermodynamics for all engineers in order that they might better assimilate new ideas in their specialties. E. R. G. Eckert related the transport processes of mass, momentum and heat transfer with appropriate limitations and quite specifically outlined the problems for research. R. B. Bird agreed with Eckert in recommending that teaching of engineering be organized by basic concepts rather than specific applications. Bird emphasized use of his equations of change as a keystone to understanding the transport processes. S. McLain saw nuclear engineering as a broader field than did H. J. Gomberg, who kept it more to reactor work. Gomberg's hope for gaining better understanding of energy utilization from better understanding of the physical mechanism of nuclear energy release was interesting. In solid-state physics and engineering materials, J. E. Goldman and G. Murphy saw a science replacing an art in the development of materials. Goldman detailed specific technical advances, and Murphy detailed specific course requirements. The seventh technical field, computer development and application, was discussed by S. Alexander and J. P. Nash. Alexander emphasized data processing properties of computers. Nash saw a change in engineering education as a result of computers changing methods of engineering analysis.

R. W. Kettler developed an eighth area, administrative problems in engineering, in a paper "Recent Trends in the Cost of Engineering Education." He had several suggestions for meeting the problem of rising costs while maintaining the quality of engineering education.

As is evident from this listing, many areas of current engineering interest are covered in the book. The approach used is such that primary interest in its contents is to be expected from educators. It is certainly worth their time to consider the ideas presented. Many may argue that the unified organization of the engineering sciences which is obvious to the authority may be too difficult for the beginner, although this reviewer would have appreciated more of the unified approach as a student. For engineers out of the educational sphere, the book can serve as a good tool for broadening their understanding of modern technology, and, it is hoped, stimulate their interest in the engineering colleges from which their future co-workers must come.

New Patents

George F. McLaughlin, *Contributor*

Injector and method for fuel injection (2,881,588). W. H. Goss, Silver Spring, Md., assignor to the U. S. Navy.

In a ramjet-type guided missile, a fuel injector having a chambered windshield and an apertured strut. Fuel discharged from the windshield and strut against the airstream is mixed to produce a uniform combustible mixture.

Jet engine silencer (2,882,991). C. R. Killian, Hayesville, N. C.

A bulbous housing with a rear opening surrounding an exhaust tube. The inner surface of the housing is transversely corrugated to provide baffles for reflecting sound waves. A portion of the exhaust tube in the housing is spaced to form a low pass acoustical filter for attenuating the sound waves.

Low drag exhaust silencer (2,882,992). G. F. Hausmann, Glastonbury, Conn., assignor to United Aircraft Corp.

Outer casing forming a main passage for a jet exhaust. A central inner body terminates in a hollow conical member rotating within the casing. Small openings in the member emit fluid flow at a reduced noise level.

Silencer (2,882,993). K. T. Murty, Arlington, Texas, assignor to Chance Vought Aircraft, Inc.

Fluid flow conduit in an air conditioning system having a jet of air near sonic velocity. Equally spaced flat plates normal to the conduit longitudinal axis have orifices which are larger in number and size than those of the preceding plate, reducing the acoustical noise level in the system.

Powerplant incorporating a dynamic compressor (2,883,828). A. R. Howell, Farnborough, England, assignor to the British Government.

Rocket combustion chamber discharging into a hollow rotor with reaction nozzles positioned tangentially on the rotor blades. Reaction of gases from the nozzles drives a compressor mounted within a tubular main duct having a propulsion nozzle downstream.

Fuze (2,883,933). R. B. King, Altadena, Calif., assignor to the U. S. Navy.

Gas pressure from a rocket motor releases a firing pin to an armed position. A spring loaded acceleration responsive means intercepts a shutter separating the pin from the detonator to defer its movement for a limited time to the armed position.

EDITOR'S NOTE: Patents listed above were selected from the Official Gazette of the U.S. Patent Office. Printed copies of patents may be obtained from the Commissioner of Patents, Washington 25, D. C., at a cost of 25 cents each; design patents, 10 cents.

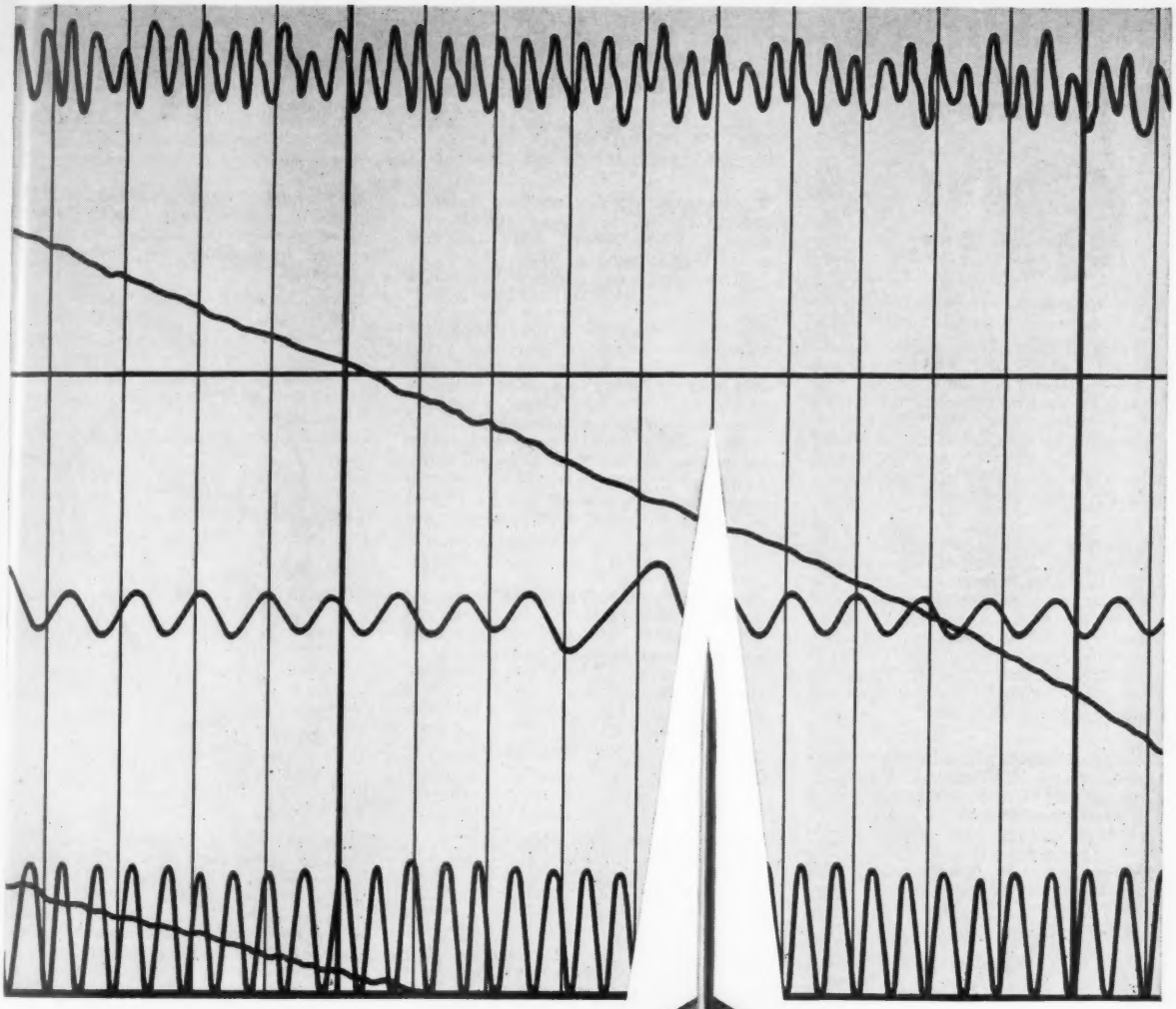

GET IT FAST, GET IT CLEAR ON LINO-WRIT 4

Du Pont Lino-Writ 4 is the fastest, toughest, whitest photorecording paper you can use. It accommodates writing speeds as high as 5000 cps at maximum amplitude; has exceptional exposing and processing latitude; its ultra-thin, all-rag stock has unusual wet or dry strength.

Our other outstanding papers include:

Lino-Writ 1. Orthochromatic paper designed for test requirements at lower writing speeds.

Lino-Writ 2. Moderately high-speed orthochromatic paper for use in intermediate speed recording requirements.

Lino-Writ 3. For high-frequency oscillographic traces without loss of detail.

These three papers are available in two types: Type B, standard-weight stock when greater opacity is required and Type W, a thin 100% all-rag stock.

Lino-Writ Rapid Processing Chemicals Kit is Du Pont's high-speed, low-odor formulation designed for rapid stabilization processing of all Du Pont photorecording papers.

For more information on our complete photorecording line, write: E. I. du Pont de Nemours & Co. (Inc.), Photo Products Department, 2430-A Nemours, Wilmington 98, Delaware. In Canada: Du Pont of Canada Limited, Toronto.

This advertisement was prepared exclusively by Phototypography.

Better Things for Better Living . . . *through Chemistry*

DU PONT
REG. U.S. PAT. OFF.

Vertical takeoff and landing apparatus (2,884,633). B. Stahmer, Ohaha, Neb.

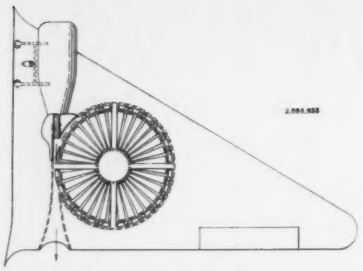

A pair of multibladed rotors set into the wing of an aircraft. Rotors are driven by the jet stream of a jet engine striking buckets on the rim. When the rotors are not operating, they close the circular opening in the wing, providing additional lift. Forward thrust is obtained during flight when the engines are mechanically moved to bypass the rotors.

Afterburner igniter (2,885,857). W. F. Hemlock, W. Hartford, Conn., assignor to the U. S. Air Force.

Pump housing with two chambers. Fuel is pumped from one chamber to the engine while fuel is supplied to the other. Reversing means then pumps fuel from the second chamber while fuel is supplied to the first chamber. Turbine discharge pressure controls the action.

Aircraft jet system with adjustable nozzle (2,886,262). P. J. Fletcher, Farnborough, England, assignor to Power Jets (Research and Development) Ltd.

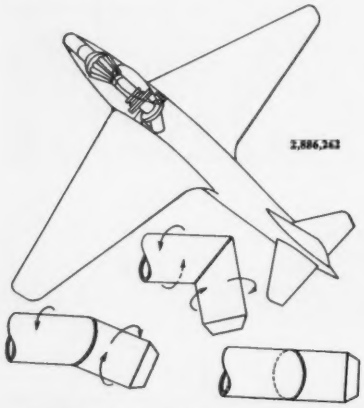

Nozzle for diverting a jet discharge smoothly from one direction to another. Jet can be diverted from rearward to downward to produce an upthrust for assisting takeoff or slow speed landing.

Sound absorbing housing (2,884,086). J. T. Welbourn, Pittsburgh, Pa.

Jet engine testing structure comprising spaced rows of perforated hollow cylinders containing loose granular material to absorb and deflect sound.

Fluid jet sustained and controlled aircraft (2,887,284). W. P. Perry, Trenton, N. J.

Air pressure fan mounted in a conveyance having a roof. Nozzles discharge air pressure across the opposite edges of areas of the roof surface to create a vortex surrounding and a vacuum within the areas to create lift.

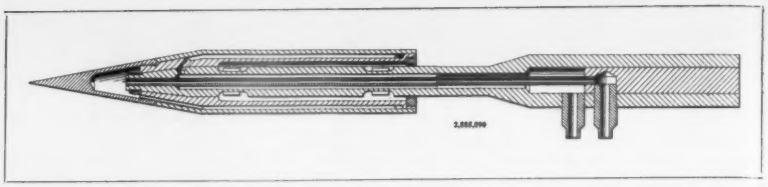

Water-cooled pitching moment balance (2,885,890). L. L. Liccini and R. H. Cornett, Silver Spring, Md., assignors to the U. S. Navy.

Strain-gage balance for a hypersonic wind tunnel in which air speeds of Mach 5 to 10 are reached. Cooling water passes through the balance to keep it at the temperature at which it was calibrated.

Windows for admitting solar radiation (2,888,007). H. Z. Tabor, Jerusalem, Israel, assignor to the State of Israel.

Solar trap with transparent plate having on the surface a number of lenses adapted to focus the solar radiation into an enclosed space where the foci of all lenses are located in one plane.

Method of preparing globular propellant powder (2,888,713). R. L. Cook and E. A. Andrew, Berkeley, Mo., assignors to Olin Mathieson Chemical Corp.

A lacquer of nitrocellulose subdivided into discrete particles in suspension in a nonsolvent liquid. Suspension is maintained under superatmospheric pressure sufficient to prevent boiling of the solvent for the nitrocellulose.

Partial pressure suit (2,886,027). J. P. Henry, Yellow Springs, Ohio, assignor to the U. S. Air Force.

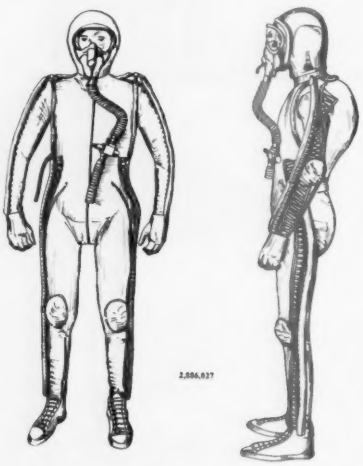

Suit supplying uniform all-over pressure to an aviator to balance the necessary rise in intrathoracic pressure applied by a special helmet, and to prevent blood pooling and plasma loss. Suit prevents dangerous shifts of liquids and gases within the body.

High altitude balloon for meteorological use (2,886,263). D. M. Ferguson, Marblehead, Mass., assignor to the U. S. Air Force.

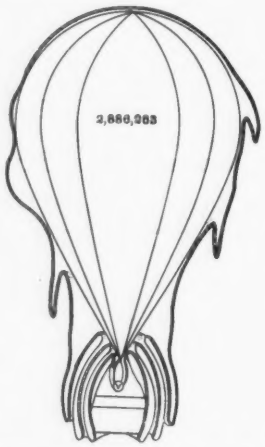

Inclusion of a relatively small inner balloon within the envelope of a high altitude balloon. Means between the envelopes permits gradual transfer of the initially-charged gas from the inflated inner envelope to the initially-deflated outer envelope during ascension.

Stall roll control for vertical takeoff airplane (2,886,264). D. B. Seager, Burbank, Calif., assignor to Lockheed Aircraft Corp.

Control for maintaining wing loading substantially symmetrical at high angles of attack at the threshold of a fully developed stall condition. Wing ports direct fluid onto the upper surface of the wing to establish a high lift critical angle of attack.

Technical Literature Digest——

M. H. Smith, *Associate Editor*
The James Forrestal Research Center, Princeton University

Jet Propulsion Engines

Advanced Propulsion Systems. A Preliminary Study, by H. F. Calcote, *Aerochem Res. Labs., Inc., Tech. Pub.* 6, July 1958, 91 pp.

Factors Influencing the Application of Unconventional Rocket Engine Systems, by George S. Gill and Leo Kusak, *SAE Preprint* 548, March 31–April 3, 1959, 15 pp.

A Graphical Solution for Solid-Propellant Motor Design, by Robert N. Witte, *Army Rocket and Guided Missile Agency, ARGMA Rep.* 6R15, Jan. 1959, 23 pp.

Thrust Magnitude Control of Solid Propellant Rocket Motors by Mechanical Means, by J. S. Gates and S. L. Pinto, *SAE Preprint* 59T, March 31–April 3, 1959, 19 pp.

Non-Air Breathing Auxiliary Powerplants, by D. L. Cochran, A. T. Biehl, D. R. Sawle, M. R. Gustavson and A. M. Taylor, *SAE Preprint* 53T March 31–April 3, 1959, 23 pp.

Optimum Exhaust Velocity Programming and Propulsion Efficiency, by Robert Fox, *J. Astron. Sci.*, vol. 6, no. 1, Spring 1959, pp. 13–16.

Combustion Instability in Liquid Propellant Rocket Motors, by David T. Harrje, *Princeton University, Dept. Aeron. Engng.*, Rep. 216x, May 1959, 20 pp.

Theoretical Studies of the Performance of Heat Engines Using Pressure Waves, by J. C. Logan Jr., *Cornell Aeronautical Laboratory Rep.* DD-799-A-1, Dec. 1954, 196 pp. (Declassified by authority of ONR: 429: CAP: III, June 3, 1959.)

Experimental Investigation of a Resonant Wave Engine, by A. Hettzberg and A. Russo, *Cornell Aeronautical Laboratory, Rep.* DD-799-a-2, Dec. 1954, 54 pp. (Declassified by authority of ONR: 429: CAP: III, June 3, 1959.)

Prospects for Thermoelectricity, by H. Gettings, *Missiles and Rockets,* June 22, 1959, pp. 29–31.

Rocket Turbines, by Otis E. Lancaster and Carlton J. Bates, *1958 Gas Turbine Report ASME,* 1959, 141 pp., pp. 66–75.

Nuclear Progress, by Richard P. Godwin and Edward Dennison, *1958 Gas Turbine Rep. ASME* 1959, 141 pp., pp. 134–141.

Rocket Thrust Termination Transients, by Howard C. Rodean, ARS JOURNAL, vol. 29, June 1959, pp. 406–409.

Suppression of Combustion Instability in the Plunger Jet Rocket Engine, by Herbert Shieber, ARS JOURNAL, vol. 29, June 1959, pp. 446–447.

Development of H_2O_2 Rocket Motors, by D. Hurden, *Raketentechnik und Raumfahrtforschung,* vol. 3, no. 1, Jan.–March 1959, pp. 9–13. (In German.)

EDITOR'S NOTE: Contributions from Professors E. R. G. Eckert, J. P. Hartnett, T. F. Irvine Jr. and P. J. Schneider of the Heat Transfer Laboratory, University of Minnesota, are gratefully acknowledged.

Aerodynamics of Jet Propelled Missiles

Slender Body of Revolution of Hypersonic Speeds—"An Approximation to the Determination of the Flow Field," by R. Capiaux, *General Research in Flight Sciences, Jan. 1958–Jan. 1959, vol. II, Fluid Mechanics, Inviscid Flows, Lockheed Aircraft Corp., Missiles and Space Division, Rep.* LMSD-48381, Jan. 1959, 163 pp., pp. 101–108.

A Linearized Method of Characteristics for Determining Body Aerodynamics Forces at Angle of Attack, by J. Der, *General Research in Flight Sciences, Jan. 1958–Jan. 1959, vol. II, Fluid Mechanics, Inviscid Flows, Lockheed Aircraft Corp., Missiles and Space Division, Rep.* LMSD-48381, Jan. 1959, pp. 109–138.

Use of Drag Modulation to Reduce Deceleration Loads During Atmospheric Entry, by Richard L. Phillips and Clarence B. Cohen, ARS JOURNAL, vol. 29, June 1959, pp. 414–422.

Effect of Thrust Termination Process Upon Range Dispersion of a Ballistic Missile, by Arnold J. Kelly, ARS JOURNAL, vol. 29, June 1959, pp. 432–440.

Theoretical and Experimental Analysis of a Cowling as a Means of a Drag Reduction for an Axisymmetric Center Body, by Marian Visich Jr. and Anthony Martelluci, ARS JOURNAL, vol. 29, June 1959, pp. 447–449.

Electrically Charged Bodies Moving in the Earth's Magnetic Field, by W. W. Fain and B. J. Greer, ARS JOURNAL, vol. 29, June 1959, pp. 451–453.

Fluid-Dynamic Properties of Some Simple Sharp and Blunt Nosed Shapes at Mach Numbers from 16 to 24 in Helium Flow, by Arthur Henderson Jr. and Patrick J. Johnston, *NASA Memo* 5-8-59L, June 1959, 63 pp.

Phugoid Motion of Hypervelocity Vehicles, by G. Breaux, *Symposium on High-Speed Aerodynamics and Structures, 3rd, San Diego, March 25–27, 1958 (Unclassified Papers),* vol. 3, pp. 11–16.

Aerodynamic Coefficients on Yawed Slender Bodies at Hypersonic Speeds, by L. Trilling and J. W. Clark, *Symposium on High-Speed Aerodynamics and Structures, 3rd, San Diego, March 25–27, 1958 (Unclassified Papers),* vol. 3, pp. 71–87.

Inviscid Hypersonic Flow Around Blunt Bodies, by Marcel Vinokur, *General Research in Flight Sciences, Jan. 1958–Jan. 1959, vol. II, Fluid Mechanics, Inviscid Flows, Lockheed Aircraft Corp., Missiles and Space Division, Rep.* LMSD 48381, Jan. 1959, pp. 1–39.

Supersonic Flow Around Blunt Bodies, an Extension of Van Dyke's Technique, by M. Vinokur and R. W. Sanders, *General Research in Flight Sciences, Jan. 1958–Jan. 1959, vol. II, Fluid Mechanics, Inviscid Flows, Lockheed Aircraft Corp., Missiles and Space Division, Rep.* LMSD 48381, Jan. 1959, pp. 40–56.

Surface Pressure Distribution on Blunt Bodies at Supersonic Speeds, by R. M.

RESEARCH
OPPORTUNITIES
In
SPACE
SCIENCES

The Space Technology Operations of Aeronutronic has immediate need for engineers and scientists who are interested in working in the stimulating and highly diversified field of space sciences. This West Coast division of Ford Motor Company has the newest facilities and most advanced equipment for carrying out highly technical work—challenging creative work that is exceptionally rewarding to qualified men.

Positions are at Aeronutronic's new $22 million Research Center, being completed at Newport Beach, Southern California. Here, overlooking famous Newport Harbor and the Pacific Ocean, relaxed California living can be enjoyed free of big-city congestion, yet most of the important cultural and educational centers are just a short drive away

AREAS OF INTEREST

VEHICLE TECHNOLOGY
- Aerodynamic design and testing
- Rocket Nozzle and re-entry materials
- High temperature chemical kinetics
- Combustion thermodynamics
- High temperature structural plastics and ceramics
- Advanced structures

SYSTEMS DEVELOPMENT
- Aerothermodynamics
- Re-entry programs
- High temperature heat transfer
- Penetration systems
- Hyper environmental test systems

ELECTRONICS AND ASTRO SCIENCES
- Astro navigation
- Space communications and communication satellites
- Instrumentation, telemetering and data reduction
- Space environmental physics
- Advanced techniques and system studies

Qualified applicants are invited to send resumes and inquiries to Mr. R. W. Speich, Aeronutronic, Dept. 19, Box 451, Newport Beach, California.

AERONUTRONIC
A Division of
FORD MOTOR COMPANY
Newport Beach
Santa Ana • Maywood, California

Mark, *General Research in Flight Sciences, Jan. 1958–Jan. 1959, vol. II, Fluid Mechanics, Inviscid Flows, Lockheed Aircraft Corp., Missiles and Space Division, Rep.* LMSD-48381, Jan. 1959, pp. 57–62.

An Extension of Second-Order Shock Expansion Theory, by R. Capiaux, *General Research in Flight Sciences, Jan. 1958–Jan. 1959, vol. II, Fluid Mechanics, Inviscid Flows, Lockheed Aircraft Corp., Missiles and Space Division, Rep.* LMSD-48381, Jan. 1959, pp. 63–99.

Variational Approach to the Re-Entry of a Ballistic Missile—Part I, by Angelo Miele and Carlos R. Cavoti, *Purdue University, School of Aeron. Engng., Rep.* A-59-1, Jan. 1959, 57 pp.

Surface Pressure Distribution at Hypersonic Speeds for Blunt Delta Wings at Angle of Attack, by Marcus O. Creager, *NASA Memo* 5-12-59 A, May 1959, 15 pp.

Aerodynamic Field Near the Stagnation Point of a Blunt Symmetrical Airfoil in Hypersonic Flow With Near Unity, by Aldo Muggia, *Torino, Politechnico Laboratorio di Meccanica Applicata, TN* 13 (*AFOSR TN* 59-339; *ASTIA AD* 213660), Feb. 1959, 15 pp.

The Motion of an Earth Satellite on Re-Entry to the Atmosphere, by T. Nonweiler, *Astronautica Acta,* vol. 5, no. 1, 1959, pp. 40–62.

Nose-Drag in Free Molecule Flow and Its Minimization, by H. S. Tan, *J. Aero/-Space Sci.,* vol. 26, June 1959, pp. 360–366.

Heat Transfer and Fluid Flow

Study of Supersonic Flows With Chemical Reactions, II: Supersonic Nozzle Flow with a Reacting Gas Mixture at High Reaction Concentration, by Peter P. Wegener, *Calif. Inst. Tech., Jet Prop. Lab. Progr. Rep.* 20-370, Dec. 1958, 29 pp.

Experimental Investigation of Coaxial Jet Mixing of Two Subsonic Streams at Various Temperature, Mach Number, and Diameter Ratios for Three Configurations, by Richard R. Burley and Lively Bryant, *NASA Memo* 12-21-58E, Feb. 1959, 29 pp.

An Introductory Discussion of Magnetohydrodynamics, by A. R. Kantrowitz and H. E. Petschek, *Avco Mfg. Corp., Avco Res. Lab. Div., Res. Rep.* 16, May 1957, 15 pp.

Supersonic Two-dimensional Magnetohydrodynamic Flow, by F. Fishman, J. Lothrop, R. Patrick and H. Petschek, *Avco Mfg. Corp., Avco Res. Lab. Div., Res. Rep.* 39, Feb. 1959, 49 pp.

On the Flow of Gases Under Free Molecular Conditions, by D. Roger Willis, *Princeton Univ., Dept. Aeron. Engng., Rep.* 442 (*AFOSR-TN*-58-1093; *ASTIA AD* 207594), Dec. 1958, 50 pp.

One Dimensional Compressible Flow Tables for a Perfect Gas in Mach Number Increment of 0.001 (k = 1.26), Isentropic Process, by C. Hoebich, *Army Rocket and Guided Missile Agency, Ordn. Missile Labs., Div. ARGMA, TN* 1H1N-1, Jan. 1959, 84 pp.

Adiabatic Wall Temperature Due to Mass Transfer Cooling With a Combustible Gas, by George W. Sutton, ARS JOURNAL, vol. 29, Feb. 1959, pp. 136–137.

Energy Transfer at a Chemically Reacting or Slip Interface, by Sinclaire M. Scala and George W. Sutton, ARS JOURNAL, vol. 29, Feb. 1959, pp. 141–143.

Effect of Unequal Wall Roughness on Flow Between Flat Plates, by H. N. McManus Jr., ARS JOURNAL, vol. 29, Feb. 1959, pp. 144–145.

Scale of Separation Phenomena in Liquids Under Conditions of Nearly Free Fall, by E. T. Benedikt, ARS JOURNAL, vol. 29, Feb. 1959, pp. 150–151.

Hypersonic Aerodynamics, Part I, by Wallace D. Hayes, ASTRONAUTICS, vol. 4, March 1959, pp. 24–25, 72, 74.

Arc-heated Plasma for Laboratory Hypersonics, by T. R. Hogness, ASTRONAUTICS, vol. 4, March 1959, pp. 40–42, 47.

On Initial Conditions in Hydromagnetics, by G. S. S. Ludford, *Cambridge Phil. Soc., Proc.,* vol. 55, Part 1, Jan. 1959, pp. 141–143.

An Investigation on Plasma in External Magnetic Fields, I: Steady State, by G. Schmidt, *Nuovo Cimento,* vol. 10, no. 1, Oct. 1, 1958, pp. 55–67.

An Investigation on Plasmas in External Magnetic Fields, II: Varying Fields, by G. Schmidt, *Nuovo Cimento,* vol. 10, no. 4, Nov. 16, 1958, pp. 659–674.

Statistical-Mechanical Theory of Transport in Fluids, by Hazime Mori, *Phys. Rev.,* vol. 112, Dec. 15, 1958, pp. 1829–1842.

Estimated Performance of Radial-flow Exit Nozzles for Air in Chemical Equilibrium, by Gerald W. Englert and Fred D. Kochendorfer, *NASA Memo* 1-5-59E, Feb. 1959, 53 pp.

Internal Performance of Two-dimensional Wedge Exhaust Nozzles, by William T. Beale and John H. Povolny, *NACA RM* E56K29b, Feb. 1957, 35 pp. (Declassified by authority of *NASA Pub. Announcement,* vol. 3, 2/4/59, p. 26).

Effect of Outer-Shell Design on Performance Characteristics of Convergent-plug Exhaust Nozzles, by H. George Krull and William T. Beale, *NACA RM* E54K22, April 1955, 18 pp. (Declassified by authority of *NASA Pub. Announcement,* vol. 3, 2/4/59, p. 22).

T-F Theory of Electron Emission in High-current Arcs, by T. H. Lee, *J. Appl. Phys.,* vol. 30, Feb. 1959, pp. 166–171.

An Application of Irreversible Thermodynamics to the Study of Diffusion, by Richard W. Laity, *J. Phys. Chem.,* vol. 63, Jan. 1959, pp. 80–82.

Hydromagnetic Equations for Two Isotopes in a Completely Ionized Gas, by Joseph Slepian, *Phys. Rev.,* vol. 112, Dec. 1, 1959, pp. 1441–1444.

Plasma Oscillations with Diffusion Velocity Space, by A. Lenard and Ira B. Bernstein, *Phys. Rev.,* vol. 112, Dec. 1, 1958, pp. 1456–1459.

Microwave Propagation in Hot Magneto-plasmas, by J. E. Drummond, *Phys. Rev.,* vol. 112, Dec. 1, 1958, pp. 1460–1464.

Transverse Plasma Waves and Plasma Vortices, by O. Buneman, *Phys. Rev.,* vol. 112, Dec. 1, 1958, pp. 1504–1512.

Microwave Emission from High-Temperature Plasmas, by David B. Beard, *Phys. Rev. Letters,* vol. 2, Feb. 1, 1959, pp. 81–82.

Fast Ion Heating, by Daryl Reagan, *Phys. Rev. Letters,* vol. 2, Feb. 1, 1959, pp. 82–83.

Spontaneously Growing Transverse Waves in a Plasma Due to an Anisotropic Velocity Distribution, by Erich S. Weibel, *Phys. Rev. Letters,* vol. 2, Feb. 1, 1959, pp. 83–84.

The Generalized Thermal Energy in Boundary Layer Type Flows with Chemical Reaction, by S. F. Shen, *Zeitschrift fur Angewandte Mathematik und Mechanik,* vol. 38, Nov.-Dec. 1959, pp. 431–436. (In English.)

Heat Transfer in Reacting Systems: I. Heat Transfer to N_2O_4 Gas under Turbulent Pipe Flow Conditions, by Walter F. Krieve and David M. Mason, *Calif. Inst. Tech., Jet Prop. Lab., Progr. Rep.* 20-366, Nov. 1958, 13 pp.

A Review of Two Phase Heat Transfer (1935–1957), by J. G Collier, *Gt. Brit., Atomic Energy Res. Estab., AERE* CE/R 2496, 1958, 93 pp.

Generation of Supersonic Dissociated and Ionized Non-equilibrium Streams, by D. E. Rosner and H. F. Calcote, *Aero-Chem. Res. Labs., Inc., TM*-10 (*AFOSR-TN*-58-1080; *ASTIA AD* 207590), Oct. 1958, 30 pp.

Rayleigh's Problem in Hydromagnetics: Impulse Motion of a Pole Piece, by G. S. S. Ludford, *Maryland Univ., Inst. for Fluid Dynamics and Appl. Math., TN* BN-151 (*AFOSR-TN*-58-1073; *ASTIA AD* 207242), Nov. 1958, 22 pp.

Sublimation in a Hypersonic Environment, by Sinclaire M. Scala, *Gen. Elec. Co., Missile and Space Vehicle Dept., Tech. Info. Series* R58SD289, 1958, 45 pp.

Gas Dynamic Mixing Processes; High Thrust through Jet Injection, by O. Lutz, *Wissenschaftlichen Geselischaft für Luftfahrt, Jahrbuch,* 1957, Braunschweig, Friedr. Vieweg & Sohn, 1959, pp. 374–380. (In German.)

Heat Transfer and Boundary Layer Formation in Sweated Materials, by E. Meyer-Hartwig, *Wissenschaftlichen Gesellschaft für Luftfahrt, Jahrbuch,* 1957, Braunschweig, Friedr. Vieweg & Sohn, 1958, pp. 439–468. (In German.)

Calculation of the Effective Ionization Potential in Plasmas, by H. Rother, *Ann. Phys.,* vol. 2, no. 5–6, 1958, pp. 326–338. (In German.)

Multiple Recording Manometer for Rapidly Changing Pressures in Flow Measurement, by Walter Wuest, *Arch. für Tech. Messen.,* no. 274, Nov. 1958, pp. 225–228. (In German.)

The Structure of a Hydromagnetic Shock in Steady Plane Motion, by G. S. S. Ludford, *J. Fluid Mech.,* vol. 5, Jan. 1959, pp. 67–80.

On the Structure of Jets from Highly Underexpanded Nozzles into Still Air, by T. C. Adamson Jr. and J. A. Nicolls, *Mich. Univ., Engng. Res. Inst., Rep.* 2397-5-F, Feb. 1958, 32 pp.

Hydromagnetic Instabilities of a Cylindrical Gas Discharge, II: Influence of Viscosity, by R. J. Taylor, *Gt. Brit., Atomic Energy Res. Estab., AERE* T/R 1888, 1958, 38, pp.

On the Surfaces of Discontinuity in the Magneto-fluid-dynamics, by L. G. Napolitano, *Aerotecnica,* vol. 38, Aug. 1958, pp. 210–220. (In Italian.)

Thermal Conductivity of Multicomponent Gas Mixtures, by Charles Muckenfuss and C. F. Curtiss, *J. Chem. Phys.,* vol. 29, Dec. 1958, pp. 1273–1277.

Statistical Mechanical Theory of the Thermal Conductivity of Binary Liquid Solutions, by Richard J. Bearman, *J. Chem. Phys.,* vol. 29, Dec. 1958, pp. 1278–1286.

Transport Processes in Binary Liquid Systems, by R. R. Irani and A. W. Adamson, *J. Phys. Chem.,* vol. 62, Dec. 1958, pp. 1517–1520.

On the Structure of Jets from Highly Underexpanded Nozzles into Still Air, by T. C. Adamson Jr., *J. Aero/Space Sci.,* vol. 26, Jan. 1959, pp. 16–24.

International Conference on the Condensed State of Simple Systems (The Liquid State), *Nuovo Cimento,* Supplement, 3d Quarter, no. 1, 1958, pp. 1–368.

Wave Theory of Heat Transfer in Film Boiling, by Yan Po Chang, *J. of Heat Transfer* (*ASME Trans.*) vol. 81, Series C, no. 1, Feb. 1959, pp. 1–12.

A Boundary-Layer Treatment of Laminar Film Condensation, by E. M. Sparrow and J. L. Gregg, *J. of Heat Transfer* (*ASME Trans.*), vol. 81, series C, no. 1, Feb. 1959, pp. 13–18.

Transient Heat Transfer for Laminar Forced Convection in the Thermal Entrance Region of Flat Ducts, by R. Siegel and E. M. Sparrow, *J. of Heat Transfer* (*ASME Trans.*), vol. 81, series C, no. 1, Feb. 1959, pp. 29–36.

Generalized Correlation of Boiling Heat Transfer, by S. Levy, *J. of Heat Transfer,* (*ASME Trans.*), vol. 81, series C, no. 1, Feb. 1959, pp. 37–42.

Heat Transfer to a Boiling Liquid-Mechanism and Correlations, by Kurt Engelberg-Forster and R. Grief, *J. of Heat Transfer* (*ASME Trans.*), vol. 81, series C, no. 1, Feb. 1959, pp. 43–53.

Transient Heat Conduction in Elliptical Plates and Cylinders, by E. T. Kirpatrick and W. F. Stokey, *J. of Heat Transfer* (*ASME Trans.*), vol. 81, series C, no. 1, Feb. 1959, pp. 54–60.

Free Convection, Forced Convection, and Acoustic Vibrations in a Constant Temperature Vertical Tube, by T. W. Jackson, W. B. Harrison and W. C. Boteler, *J. of Heat Transfer* (*ASME Trans.*), vol. 81, series C, no. 1, Feb. 1959, pp. 68–74.

Summary-Selected References on Gas Turbines, Regenerative Cycles, Rotary Regenerators, and Associated Heat Exchange and Pressure-Drop Information, by W. E. Hammond, *J. of Heat Transfer* (*ASME Trans.*), vol. 81, series C, no. 1, Feb. 1959, pp. 75–78.

Heat Transfer and Friction for Fluids Flowing Over Surfaces at High Temperatures and High Velocities, by R. G. Deissler and A. L. Loeffler, Jr., *J. of Heat Transfer* (*ASME Trans.*), vol. 81, series C, no. 1, Feb. 1959, pp. 89–94.

Thermal Relaxation in Gases: A New Method of Analysing the Experimental Data, by A. C. J. Johnson, *Phys. Soc., London, Proc.*, vol. 73, Feb. 1959, pp. 273–279.

Flow of Heat in a Composite Solid, by J. P. Newcomb, *Brit. J. of Appl. Phys.*, vol. 10, May 1959, pp. 204–205.

Theoretical Structure of Plasma Equations, by M. N. Rosenbluth and N. Rostoker, *Phys. Fluids,* vol. 2, Jan.–Feb. 1959, pp. 23–30.

Propagation of Disturbances at High Frequencies in Gases, Liquids, and Plasmas, by H. S. Green, *Phys. Fluids,* vol. 2, Jan.–Feb. 1959, pp. 31–39.

Experimental Demonstration of Hydromagnetic Waves in an Ionized Gas, by G. A. Sawyer, P. L. Scott and T. F. Stratton, *Phys. Fluids,* vol. 2, Jan.–Feb. 1959, pp. 47–51.

On the Confinement of a Plasma by Magnetostatic Fields, by Erich S. Weibel, *Phys. Fluids,* vol. 2, Jan.-Feb. 1959, pp. 52–56.

Magnetohydrodynamic Flow in a Shock Tube, by M. Mitchner, *Phys. Fluids,* vol. 2, Jan.-Feb. 1959, pp. 62–71.

Some Compression Waves in Plasma, by Daryl Reagan, *Phys. Fluids,* vol. 2, Jan.-Feb. 1959, pp. 93–94.

High-Current Ion Source, by Russell G. Meyerand Jr. and Sanborn C. Brown, *Rev. Sci. Instr.*, vol. 30, Feb. 1959, pp. 110–111.

Interested in Systems Engineering?

There are systems

...and systems

...and TOTAL systems in which the big bird and support equipment may rank only as a component.

This difference between systems can make a big difference in your career

IF YOU ARE QUALIFIED and interested in contributing to programs of "total" scope, it will be of value to you to investigate current opportunities with General Electric's DEFENSE SYSTEMS DEPT., whose work lies primarily in providing *total* solutions to large scale defense problems of the next 5, 10 and 20 years.

The work here lies almost entirely in the areas of systems engineering and systems management.

Inquire about these positions:

Guidance Equation Engineers
Systems Logistics Engineers
Electronic Systems Management Engineers
Operations Analysis Engineers
Systems Program Engineers
Data Processing Engineers
Systems Test Evaluation Engineers
Engineering Psychologists
Radar Equipment Engineers
Weapons Analysis Engineers
Weapons Systems Integration Engineers
Engineering Writers

Forward your confidential resume at an early date.
Whereas the growth potential is evident – both for DSD and the engineers who join us – the positions we fill during these early months will carry significant "ground-floor" benefits.
Write fully to Mr. E. A. Smith, Room 11-M

DSD DEFENSE SYSTEMS DEPARTMENT
A Department of the Defense Electronics Division

GENERAL ELECTRIC

300 South Geddes Street, Syracuse, N. Y.

Combustion, Fuels and Propellants

Burning Mechanism of Ammonium Perchlorate Propellants, by Martin Summerfield, G. S. Sutherland, M. J. Webb, H. J. Taback and K. P. Hall, *ARS Preprint* 737-58, Nov. 1958, 21 pp.

The Dependence of Linear Burning Rate upon Pressure for Ammonium Perchlorate-Polyester Resin Composite Solid Propellant, by Maurice J. Webb, *Princeton Univ., Dept. Aeron. Engng.*, (M.S. Thesis), May 1958, 10 figs., 40 pp.

Theoretical Combustion Performance of Several High-energy Fuels for Ramjet Engines, by Leonard K. Tower, Roland Breitwieser and Benson E. Gammon, *NACA Rep.* 1362, 1958, 18 pp.

Combustion of Various Highly Reactive Fuels in a 3.84 by 10-inch Mach 2 Wind Tunnel, by H. Allen Jr. and E. A. Fletcher, *NASA Memo* 1-15-59E, April 1959, 28 pp.

Analysis of Ammonium Nitrate III, Assay, by Eugene A. Burns, *Calif. Inst. Tech., Jet Prop. Lab., Progr. Rep.* 20-365, Sept. 2, 1958, 15 pp.

Some Thermal Stress Design Data for Rocket Grains, by M. L. Williams, ARS JOURNAL, vol. 29, April 1959, pp. 260–266.

Turbulent Flame Studies in a Two-Dimensional Open Burner, by J. H. Grover, E. N. Fales and A. C. Scurlock, ARS JOURNAL, vol. 29, April 1959, pp. 275–282.

Investigation of the Ignition of a Gas by an Electric Spark, by D. R. Lintin and E. R. Wooding, *Brit. J. Appl. Phys.*, vol. 10, April 1959, pp. 159–165.

The Heats of Combustion of Organic Compounds of Nitrogen, by F. W. Evans, D. M. Fairbrother and H. A. Skinner, *Trans., Faraday Soc.*, vol. 55, March 1959, pp. 399–403.

Burning Mechanism of Ammonium Perchlorate Propellants, by Martin Summerfield and George Sutherland, *Project Squid, Tech. Rep.* PR-87-P (*ASTIA AD* 207364), Dec. 1958, 30 pp. (Available only on microcards.)

Diffusion and Heterogeneous Reaction, II: The Catalytic Activity of Solids for Hydrogen Atom Recombinations, by Bernard J. Wood and Henry Wise, *Project Squid, Tech. Rep.* SRD-3-P (*ASTIA AD* 205533), Aug. 1958, 4 pp. (Available only on microcards.)

Thermal Decomposition of Some Group I, II, and III Metal Alkyls, by Louis Rosenblum, *NACA RM* E56L18, Feb. 1957, 22 pp. (Declassified from Confidential by authority of *NASA Pub. Ann.* 4, p. 23, 3/16/59).

Heterogeneous Flash Initiation of Thermal Reactions, by L. S. Nelson and J. L. Lundberg, *J. Phys. Chem.*, vol. 63, March 1959, pp. 433–436.

Cooperative Test Projects of the Joint Army-Navy-Air Force Panel on Analytical Chemistry of Solid Propellants, Part 6: Round Robin 10: Normal Methyl Violet Paper Stability Test; Round Robin 11: Flame Photo Meter for Sodium, Potassium and Calcium in Small Arms Propellant; Round Robin 12: Dibutylphthalate in Small Arms Propellant, by R. H. Pierson, *NOTS* 1937, Part 6, Feb. 1958, 82 pp.

Elastomeric-binder and Mechanical-property Requirements for Solid Propellants, by Thor L. Smith, *Calif. Inst. Tech., Jet Prop. Lab., Mem.* 20-178, 1959, 16 pp.

Analysis of Propyne-allene Mixtures, by C. M. Drew, S. R. Smith, A. Jensen, J. R. McNesby and A. S. Gordon, *NAVORD Rep.* 4913 (*NOTS* 1216), Oct. 1955. 13 pp. (Declassified from confidential by authority of NOTS ltr 75061 B.S.: AM Reg 75-53864, 17 Feb. 1959.)

Chemistry of Free Radicals Containing Oxygen, Part 2: Thermo-chemistry of the Hydroxyl and Hydroperoxyl Radicals, by P. Gray, *Trans., Faraday Soc.*, vol. 55, March 1959, pp. 408–417.

Patterns of Free Radical Reactivity, by C. H. Bamford, A. D. Jenkins and R. Johnston, *Trans., Faraday Soc.*, vol. 55, March 1959, pp. 418–432.

Studies in Bomb Calorimetry, X: Conditions for the Combustion of Solid and Liquid Fuels, by R. A. Mott and C. Parker, *Fuel*, vol. 38, April 1959, pp. 189–204.

Kinetics of Nitrogen Atom Recombination, by John T. Herron, J. L. Franklin, Paul Bradt and Vernon H. Dibeler, *J. Chem. Phys.*, vol. 30, April 1959, pp. 879–884.

A Method of Successive Approximations for Computing Combustion Equilibria on a High Speed Digital Computer, by D. S. Villars, *J. Phys. Chem.*, vol. 63, April 1959, pp. 521–530.

The Conservation Equations for Independent Coexistent Continua and for Multicomponent Reacting Gas Mixtures, by W. Nachbar, F. Williams and S. S. Penner, *Quart. Appl. Math.*, vol. 17, no. 1, April 1959, pp. 43–54.

A Note on Liquid and Solid Propellants for Rockets, by E. G. D. Andrews and A. W. T. Mottram, *J. Roy. Aeron. Soc.*, vol. 63, April 1959, p. 265.

Hydrolysis of Nitroguanidine and Nitroaminoguanidine, by William R. McBride, Ronald A. Henry and Sol Skolnik, *NAVORD Rep.* 2011 (*NOTS* 642), Jan. 1953, 41 pp. (Declassified from Confidential by authority of NOTS ltr 7606/-BJS: AM 75-54866, dtd 19 Feb. 1959.)

A Gravimetric Determination of Insoluble Impurities and Ash Impurities in Propellant-grade Cellulose Nitrate, by Aaron N. Fletcher, *NAVORD Rep.* 6444, Jan. 1958, 13 pp.

Cooperative Test Projects of the Joint Army-Navy-Air Force Panel on Analytical Chemistry of Solid Propellants, Part 5, Round Robin 9: Triacetin and Dioctylphthalate in OGK Propellant, by R. H. Pierson, *NOTS* 1937, 61 pp.

Results of Performance Calculations for N_2O_4-N_2H_4 Bipropellant System, by G. W. Elverum Jr. and S. Martinez Jr., *Calif. Inst. Tech., Jet Prop. Lab., Mem.* 20-174, July 1958, 56 pp.

Combustion in Liquid-fuel Rocket Motors, by D. B. Spalding, *Aeron. Quart.*, vol. 10, Feb. 1959, p. 1–27.

The Density of Solid Ozone, by A. G. Streng and A. V. Grosse, *J. Amer. Chem. Soc.*, vol. 81, Feb. 20, 1959, pp. 805–806.

Contribution to the Study of Flame Propagation in a Closed Tube, by G. Dalmai, *Inst. Franc. du Petrole, Rev. et Ann. des Combustibles Liquides*, vol. 13, Dec. 1958, pp. 1683–1724. (In French.)

Theory of Detonations, III: Ignition Temperature Approximation, by C. F. Curtiss, J. O. Hirschfelder and M. P. Barnett, *J. Chem. Phys.*, vol. 30, Feb. 1959, pp. 470–492.

High-temperature Gas Viscosities, II: Nitrogen, Nitric Oxide, Boron Trifluoride, Silicon Tetrafluoride, and Sulfur Hexafluoride, by C. P. Ellis and C. J. G. Raw, *J. Chem. Phys.*, vol. 30, Feb. 1959, pp. 574–576.

Gaseous Detonations, XII: Rotational Temperatures of the Hydroxyl Free Radicals, by G. B. Kistiakowsky and F. D. Tabbutt, *J. Chem. Phys.*, vol. 30, Feb. 1959, pp. 577–581.

The Mechanism of Deflagration of Pure Ammonium Perchlorate, by Raymond Friedman, Joseph B. Levy and Keith E. Rubmel, *Atlantic Res. Corp.* (*AFOSR TN*-59-173; *ASTIA AD* 211-313), Feb. 1959, 27 pp.

Recent Advances in Gaseous Detonation, by R. A. Gross and A. K. Oppenheim, ARS JOURNAL, vol. 29, March 1959, pp. 173–179.

Compression Sensitivity of Monopropellants, by G. A. Mead, ARS JOURNAL, vol. 29, March 1959, pp. 192–198.

Isothermal Compressibility of Liquid Oxygen and RP-1, by George T. Y. Chao, ARS JOURNAL, vol. 29, March 1959, pp. 199–203.

Effect of Initial Temperature on Flash Back of Laminar and Turbulent Burner Flames, by Burton Fine, *Ind. Engng. Chem.*, vol. 51, April 1959, pp. 564–566.

Predicting Burning Velocities of Lean Hydrocarbon Flames, by S. A. Weil, *Ind. Engng. Chem.*, vol. 51, April 1959, pp. 567–569.

Smoke Limits of Bunsen Burner Ethylene-Air Flames, by Joseph Grumer and M. E. Harris, *Ind. Engng. Chem.*, vol. 51, April 1959, pp. 570–574.

Determination of the Unreacted Hugoniot for Liquid TNT, by W. B. Garn, *J. Chem. Phys.*, vol. 30, March 1959, pp. 819–822.

Formation of Ozone From Atomic Oxygen at Low Temperatures, by R. A. Ruehrwein and J. S. Hashman, *J. Chem. Phys.*, vol. 30, March 1959, pp. 823–826.

Optical Method of Instantaneous Measurement of Flame Temperatures, by A. Moutet, C. Veret and L. Naudaud, *Recherche Aéronautique*, no. 68, Jan.-Feb. 1959, pp. 9–20. (In French.)

Analysis in Flight of Combustion Gases, by J. Fructus, *Recherche Aéronautique*, no. 68, Jan.-Feb. 1959, pp. 49–53. (In French.)

A Preliminary Investigation of Field-induced Ion Movement in Flame Gases and Its Applications, by K. G. Payne and F. J. Weinberg, *Proc., Royal Soc.*, vol. A 250, March 24, 1959, pp. 316–336.

The High-temperature Oxidation of Propane, by J. W. Falconer and J. H. Knox, *Proc., Royal Soc.*, vol. A 250, April 7, 1959, pp. 493–513.

RF Loss Through Rocket Flame Easy to Figure, by R. J. Schmeizer, *Space/-Aeron.*, vol. 31, April 1959, pp. 171–172.

Materials of Construction

Thermal Shock Resistance—a Design Parameter for Ceramic Radome Walls, by E. J. Luoma and E. B. Shand, *J. Aero/-Space Engng.* vol. 18, June 1958, pp. 43–47.

A Theory for the Ablation of Glassy Materials, by Hans A. Bethe and Mac. C. Adams, *J. Aero/Space Sci.*, vol. 26, June 1959, pp. 321–328.

Determination of Static Strength and Creep Buckling of Unstiffened Circular Cylinders Subjected to Bending at Elevated Temperatures, by Eldon E. Mathauser and Avraham Berkovits, *NASA Memo* 6-14-59L, June 1959, 18 pp., diagrs.

Telemetering Missile Data, by W. L. Keller, *Ordnance*, vol. 43, May-June 1959, p. 1004.

New Tungsten Know-How Widens Design Horizons, by Irwin Stambler,

Space/Aeronautics, vol. 32, July 1959, p. 48.

Refractory Ceramic Coatings, by David J. Larin and E. E. Mueller, *The Trend in Engineering*, vol. 11, April 1959, pp. 19–23.

Ceramic Materials for Nuclear Reactors, by Lavada A. Moudy and James I. Mueller, *The Trend in Engineering*, vol. 11, April 1959, pp. 28–31.

Criteria in the Selection of Materials for High Temperature Structures, by W. H. Steurer, *Symposium on High-Speed Aerodynamics and Structures, 3rd, San Diego, March* 25–27, 1958 (*Unclassified Papers*), vol. 1, pp. 179–227.

Ceramic Materials for Use in Hypersonic Aircraft, by John M. Nowak, *Symposium on High-Speed Aerodynamics and Structures, 3rd, San Diego, March* 25–27, 1958 (*Unclassified Papers*), vol. 1, pp. 229–252.

Thermal Properties of Nose Cone Materials, by I. V. Fieldhouse, J. I. Lang, A. N. Takata and T. E. Waterman, *Symposium on High-Speed Aerodynamics and Structures, 3rd, San Diego, March 25–27, 1958* (*Unclassified Papers*), vol. 1, pp. 253–276.

High Temperature Structures, by N. J. Hoff, *Symposium on High-Speed Aerodynamics and Structures, 3rd, San Diego, March 25–27, 1958* (*Unclassified Papers*), vol. 1, pp. 383–432.

A General Technique for Evaluating the RMAL Shock Characteristics of Materials Subjected to Temperature Gradients, by David Horwitz, *Symposium on High-Speed Aerodynamics and Structures, 3rd, San Diego, March 25–27, 1958* (*Unclassified Papers*), vol. 3, pp. 91–109.

Spaceflight

The Nature of Re-entry, by George E. Solomon, ASTRONAUTICS, vol. 4, March 1959, pp. 20–21, 98, 100.

Re-entry Heat Transfer, by Lester Lees, ASTRONAUTICS, vol. 4, March 1959, pp. 22–23, 60, 62, 65.

Planning a Re-entry and Recovery Test Program, by William R. Lucas and Myron E. Huston, ASTRONAUTICS, vol. 4, March 1959, pp. 30–31, 88.

Attitude Control of Space Vehicles, by M. Baron T. George, ASTRONAUTICS, vol. 4, March 1959, pp. 34–35, 106–107.

Communicating with the Hypersonic Vehicles, by Stephen G. Homic and Richard L. Phillips, ASTRONAUTICS, vol. 4, March 1959, pp. 36–37, 92, 94, 96, 98.

The Technology of Manned Return from Outer Space, by Hilliard W. Paige, *J. Franklin Inst.*, vol. 267, Feb. 1959, pp. 103–118.

Theory of the Effect of Drag on the Orbital Inclination of an Earth Satellite, by John P. Vinti, *J. Res., Nat. Bur. Standards*, vol. 62, Feb. 1959, pp. 79–88.

Vanguard I IGY Satellite (1958 Beta), by R. L. Easton and M. J. Votaw, *Rev. Sci. Instr.*, vol. 30, Feb. 1959, pp. 70–75.

Conduction Cuts Heating During Spacecraft Re-entry, by Carr B. Neel, *Space-Aeron.*, vol. 31, March 1959, pp. 42–45.

Accurate Position Data Needed for Space Course Changes, by E. V. Stearns and W. E. Frye, *Space-Aeron.*, vol. 31, March 1959, pp. 48–51.

Plasma Accelerator for Spacecraft Control (Design Progress), by Bernard Kovit, *Space-Aeron.*, vol. 31, March 1959, pp. 57–59.

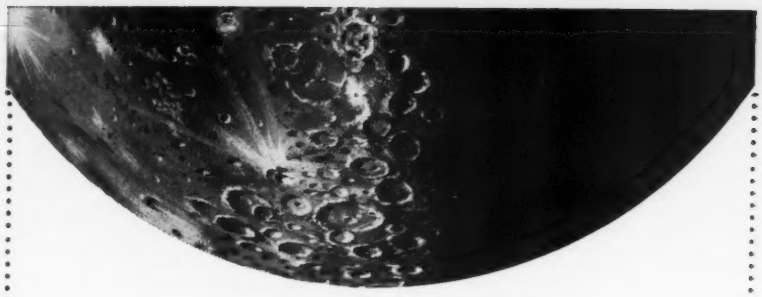

ROCKETDYNE

The Nation's Leader in Rocket Engines
Announces Limited Expansion in

RESEARCH

Some of the programs under study are:

The maximum specific impulse obtainable (compared to the classical infinite volume thrust chamber) for a rocket chamber which consists only of an injector and an exhaust nozzle.

Predicting the performance of a turbine operating with a gaseous working fluid which is still reacting and changing composition. The effect of boundary layer buildup, leading edge thickness, and radial flow on flow through supersonic turbine blades.

New methods of translating chemical energy into thrust, and how they will work in a rocket engine.

Types of fluid transport systems for rocket engines which offer simplicity, efficiency, and light weight. The fundamental parameters which govern the satisfactory operation of bearings and seals in corrosive propellant service.

Determine the separation point in an overexpended rocket nozzle as a function of nozzle divergence angle, and the applications of this phenomenon.

The dynamic interrelations of the various components of a rocket engine, and the control systems which best solve the problem of controlling a rocket engine.

Participation in these combined theoretical-experimental activities presents a stimulating challenge and involves project-oriented responsibility.

Qualifications include:
Advanced degree in Engineering
Advanced degree in Chemistry, Physics
BS degree supplemented by appropriate experience

For specific consideration of your background in Applied Research Write to:

Mr. Stanley Greenfield, Chief
Engineering Sciences Research
Dept. 596 A.R.
6633 Canoga Avenue, Canoga Park, Calif.

ROCKETDYNE

A DIVISION OF NORTH AMERICAN AVIATION, INC.

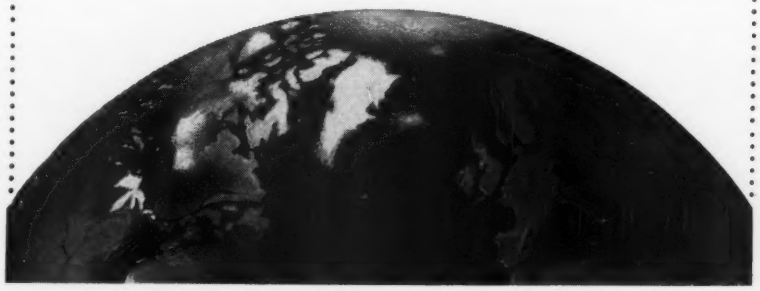

ROCKET CONTROLS ENGINEERS

1) For development and analytical design of valves and controls for rocket engine systems. Develop specification requirements for components covering design, test and development. Prepare data for proposals. BS in ME or AE and 3–7 years' experience with hydraulic pneumatic devices and systems.

2) For dynamic analysis of mechanical systems associated with rocket propulsion. Mathematical descriptions of controlled rocket components with regard to systems stability. Interpretation of designs for controlling rocket components. Analogue simulation of systems. Supervision of above areas. BS, ME or EE. Experience in servo systems analysis and techniques.

To arrange interview call collect, Niagara Falls BUtler 5-7851, or send resume to:

SUPERVISOR ENGINEERING EMPLOYMENT

BELL AIRCRAFT CORPORATION
BUFFALO 5, NEW YORK

TOP SPOTS FOR A TECHNICAL SPECIALIST AND TECHNICAL LEADER ON A NEW SPACE TEAM

Two excellent openings in Chance Vought's newly formed Astronautics Division.

Senior Specialist in Heat Transfer and Fluid Mechanics.

Advanced A.E., Ph.D. preferred. To supervise group in fields of heat transfer, pressure distribution analysis, ablation theory and general fluid mechanics. Requires knowledge of real gas effects, capability for training people, supervising company R & D, keeping abreast of technology.

Physics M.S. with Minor in Meteorology (and meteorological experience.)

To study physics of upper atmosphere, including compilation of data. Interpret data on atmospheric density, pressure, temperature and composition. Keep abreast of space probe and satellite data. Plan test programs. Recommend experimental work and conduct feasibility studies for weather satellite programs.

Write to:
Professional Placement Office
Dept. JP-8

CHANCE VOUGHT
DALLAS, TEXAS

Evaluating APU Systems for Spacecraft, by S. L. Sandelman and R. W. McJones, *Space-Aeron.*, vol. 31, March 1959, pp. 86, 88, 90, 92, 94, 97.

What Instruments for Space Crews?, by George W. Hoover, *Space-Aeron.*, vol. 31, March 1959, pp. 110, 112.

Biosatellite Decompression (nomographs), by Eugene B. Konecci, *Space-Aeron.*, vol. 31, March 1959, p. 117.

Space Communications, by F. W. Lehan and Leang P. Yeah, *Space-Aeron.*, vol. 31, March 1959, pp. 120–121.

Satellite Ascent Paths, by Charles L. Keller, *Sperry Engng. Rev.*, vol. 11, Dec. 1958, pp. 2–14.

Characteristic Velocity for Changing the Inclination of a Circular Orbit to the Equator, by Leonard Rider, ARS JOURNAL, vol. 29, Jan. 1959, pp. 48–49.

A Proposed Kepler Diagram, by Robert L. Sohn, ARS JOURNAL, vol. 29, Jan. 1959, pp. 51–54.

Is Newton's Law of Gravitation Really Universal?, by Fritz Zwicky, ASTRONAUTICS, vol. 4, Jan. 1959, pp. 18–19, 74, 76.

Interplanetary Probes: Three Problems, by Krafft Ehricke, ASTRONAUTICS, vol. 4, Jan. 1959, pp. 20–22, 42, 44, 46.

An Introduction to Space Navigation, by Manuel Fernandez, ASTRONAUTICS, vol. 4, Jan. 1959, pp. 23–25, 76.

Rocket Astronomy—Window into Space, by Herbert Friedman, ASTRONAUTICS, vol. 4, Jan. 1959, pp. 26–27, 69–70.

Mars—a World for Exploration, by Clyde W. Tombaugh, ASTRONAUTICS, vol. 4, Jan. 1959, pp. 30–31, 86–93.

Weather Reconnaissance by Satellites, by S. M. Greenfield and W. W. Kellogg, ASTRONAUTICS, vol. 4, Jan. 1959, pp. 32–33, 77–78.

The Earth Satellite Orbit, by Ballard B. Small, ASTRONAUTICS, vol. 4, Jan. 1959, pp. 40–41, 46, 48.

Re-Entry: Problems and Progress, by Coleman duP. Donaldson, ASTRONAUTICS, vol. 4, March 1959, pp. 38–39, 108.

Educational Opportunities in Astronautics, by Paul Sandorff, ASTRONAUTICS, vol. 4, April 1959, Part 2, pp. 2–6.

Preparing Man for Space Flight, by Carl C. Clark and James D. Hardy, ASTRONAUTICS, vol. 4, Feb. 1959, pp. 18–21, 88, 90.

Isolation, by George E. Ruff, ASTRONAUTICS, vol. 4, Feb. 1959, pp. 22–23, 110–111.

Aerodynamics for Space Flight, by E. P. Williams and Carl Gazley Jr., *Rand Corp.*, P-1256, Feb. 1958, 26 pp.

Space Vehicle Environment, by C. Gazley Jr., W. W. Kellogg and E. H. Vestine, *Rand Corp.*, P-1335, July 1958, 58 pp.

Internal Environment of Manned Space Vehicles, by S. H. Dole, *Rand Corp.*, P-1309, Feb. 1958, 23 pp.

Lunar Flight Dynamics, by R. W. Buchheim and H. A. Lieske, *Rand Corp.*, P-1453, Aug. 1958, 62 pp.

Lunar Base Planning Considerations, by R. D. Holbrook, *Rand Corp.*, P-1436, Feb. 1958, 24 pp.

On Lunar and Planetary Experiments, by S. M. Greenfield, *Rand Corp.*, P-1535, Oct. 1958, 9 pp.

Economic Considerations of Space Flight Ground Support Requirements, by M. A. Margolis and F. S. Pardee, *Rand Corp.*, P-1589, Jan. 1959, 17 pp.

Space Flight Gound Facilities Requirements Problems—Launching Facilities, by J. J. O'Sullivan, *Rand Corp.*, P-1431, Feb. 1958, 10 pp.

Lunar Instrument Carrier—Landing Factors, by H. A. Lang, *Rand Corp.*, RM-1725 (*ASTIA AD* 112403), June 1956, 36 pp.

Lunar Instrument Carrier—Attitude Stabilization, by R. W. Buchheim, *Rand Corp.*, RM-1730 (*ASTIA AD* 112402), June 1956, 22 pp.

Recovery of a Circum-lunar Instrument Carrier, by Carl Gazley Jr. and David J. Masson, *Rand Corp.*, P-1119, Aug. 1957, 20 pp.

Lunar Base Study Jury Report: Evaluation of an Experiment in Creative Design Conducted with College Students, by R. D. Holbrook, H. A. Lang and J. H. Huntzicker, *Rand Corp.*, RM-2174 (*ASTIA AD* 205422), Jan. 1958, 223 pp.

Outline of a Study of Extraterrestrial Base Design, by R. D. Holbrook, *Rand Corp.*, RM-2161 (*ASTIA AD* 156043), April 1958, 78 pp.

Space Flight Trajectories, Navigation and Maneuvers, by R. W. Buchheim, *Rand Corp.*, P-1387, May 1958, 45 pp.

Motion of a Small Body in Earth-Moon Space, by R. W. Buchheim, *Rand Corp.*, RM-1726 (*ASTIA AD* 123557), June 1956, 79 pp.

Circumlunar Trajectory Studies, by H. A. Lieske, *Rand Corp.*, P-1441, June 1958, 23 pp.

The Status and Improvement of Physical Constants Needed for Precision Trajectories, by Samuel Herrick, *Rand Corp.*, P-1559, Dec. 1958, 10 pp.

Russian Technical Articles*

Solution of the Basic Problems of Exterior Ballistics, by L. M. Vorob'ev, *PMM: J. Appl. Math. and Mech.*, vol. 22, no. 3, 1958, pp. 481–492.

On the Theory of Complicated Systems of Gyroscopic Stabilization, by A. Iu. Ishlinskii, *PMM: J. Appl. Math. and Mech.*, vol. 22, no. 3, 1958, pp. 493–512.

On the Stability of Motion of a Gyroscope on Gimbals, by V. V. Rumiantsev, *PMM: J. Appl. Math. and Mech.*, vol. 22, no. 3, 1958, pp. 513–520.

On a Gyroscope Mounted in Universal Suspension (on Gimbals), by N. G. Chetaev, *PMM: J. Appl. Math. and Mech.*, vol. 22, no. 3, 1958, pp. 521–532.

On a Class of Motions in Magneto-Hydromechanics, by V. N. Zhigulev, *PMM: J. Appl. Math. and Mech.*, vol. 22, nol 3, 1958, pp. 537–539.

On Gas Flow in Laval Nozzles, by O. S. Ryzhov, *PMM: J. Appl. Math. and Mech.*, vol. 22, no. 3, 1958, pp. 549–553.

Computation of a Laval Nozzle, by A. Sh. Dorfman, *PMM: J. Appl. Math. and Mech.*, vol. 22, no. 3, 1958, p. 554.

Analysis of Periodic Motions in Electrical Servomechanism Vibration Loop With Constant Disturbance, by I. N.

* The Editors of Technical Literature Digest are making a systematic search for pertinent Russian articles, both in the original Russian and in translated form. For the balance of 1959, these will appear in a separate section with this heading, mainly to draw the readers' attention to the new listing. After that, they will appear item by item under the proper subject headings.

Krutova, *Avtomatika i Telemekhanika*, vol. 20, no. 5, 1959, pp. 564–575. (In Russian.)

On the Invariance Principle in Automatic Control Combined Systems, by V. I. Dunaev, *Avtomatika i Telemekhanika*, vol. 20, no. 5, 1959, pp. 591–594. (In Russian.)

Electric Drive With Powder Clutch and Its Application in Automatic Control Systems, by G. G. Konovalov and Ya. I. Flid, *Avtomatika i Telemekhanika*, vol. 20, no. 5, 1959, pp. 657–662. (In Russian.)

Stabilizing Current L-C Devices, by B. E. Kubyshin and A. N. Miljakh, *Avtomatika i Telemekhanika*, vol. 20, no. 5, 1959, pp. 663–668. (In Russian.)

On a Stability Criterion for Nonlinear Control Systems, by Chang Szu-Ying, *Avtomatika i Telemekhanika*, vol. 20, no. 5, 1959, pp. 669–672. (In Russian.)

Concerning Absolute Stability of Certain Control Systems, by Yu S. Sobolev, *Avtomatika i Telemekhanika*, vol. 20, no. 4, 1959, pp. 401–405. (In Russian.)

Integral Estimate to Choose Optimum Parameters of Automatic Control Systems With Present Overshoot, by A. L. Tupitsyn, *Avtomatika i Telemekhanika*, vol. 20, no. 4, 1959, pp. 406–414. (In Russian.)

Application of Square Integral Estimate for Finding Optimum Parameters of Pilot With Rate Feedback, by V. D. Matytsin and V. A. Ryapolov, *Avtomatika i Telemekhanika*, vol. 20, no. 4, 1959, pp. 415–421. (In Russian.)

Dynamics of Electric Servomechanism Vibration Loop Under Free Oscillating Conditions, by I. N. Kritova, *Avtomatika i Telemekhanika*, vol. 20, no. 4, 1959, pp. 422–436. (In Russian.)

Compensation of Continuous Automatic Control System by Means of Delay Elements Filter, by Sin-min Van, *Avtomatika i Telemekhanika*, vol. 20, no. 4, 1959, pp. 437–446. (In Russian.)

Investigation of Pneumatic Jet Element Characteristics, by L. A. Zalmanzon and V. A. Semikova, *Avtomatika i Telemekhanika*, vol. 20, no. 4, 1959, pp. 447–467. (In Russian.)

Design Principles of Contactless Systems of Remote Control With Exponential Converters, by V. A. Il'in, *Avtomatika i Telemekhanika*, vol. 20, no. 4, 1959, pp. 468–472. (In Russian.)

Analysis of Operation of Pulse Magnetic Elements in Contactless Devices of Remote Control, by I. V. Prangishvili, *Avtomatika i Telemekhanika*, vol. 20, no 4, 1959, pp. 473–479. (In Russian.)

Concerning Stability of a Pulse Monitored Servosystem, by Ludvik Prouza, *Avtomatika i Telemekhanika*, vol. 20, no. 4, 1959, pp. 518–520. (In Russian.)

Analysis of Stability of Distributed Parameters Automatic Control Systems With Loss, by Ya. B. Kadymov, *Avtomatika i Telemekhanika*, vol. 20, no. 4, 1959, pp. 525–527. (In Russian.)

Bibliography on Automatic Control and Related Problems for 1956, *Avtomatika i Telemekhanika*, vol. 20, no. 4, 1959, pp. 528–532. (In Russian.)

Physical Phenomona That Occur When Bodies Compressed by Strong Shock Waves Expand in Vacuo, by Ia. B. Zel'dovich and Iu. P. Raizer, *Soviet Phys.-JETP*, vol. 35 (8), no. 6, June 1959, p. 980.

The Stability of Shock Waves in Magnetohydronamics, by S. I. Syrovatskii, *Soviet Phys.-JETP*, vol. 35 (8), no. 6, June 1959, p. 1024.

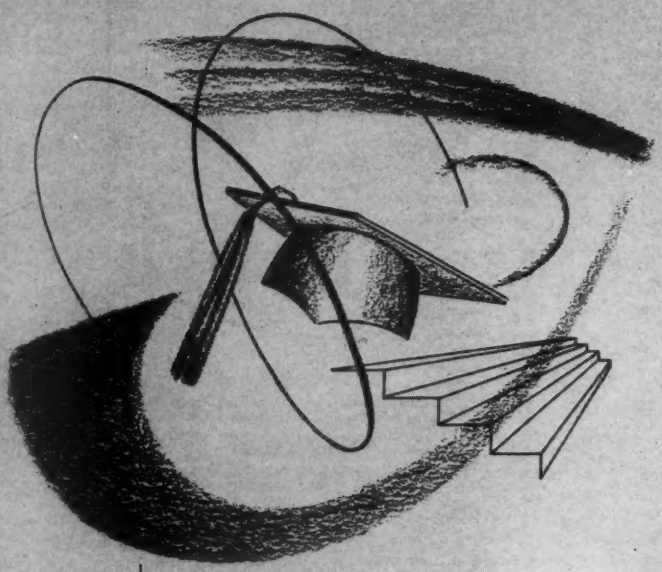

ADVANCED DEGREES

. . . another plus benefit at the Los Alamos Scientific Laboratory.

Graduate programs for advanced degrees in nuclear, mechanical and electrical engineering, chemistry, physics and mathematics are available to qualified employees of the Laboratory at the Los Alamos Graduate Center of the University of New Mexico. With tuition support from the Laboratory, employees may meet requirements for masters' degrees entirely in Los Alamos evening classes, and for Ph.D. degrees with courses at Los Alamos and a minimum of one academic year at the University of New Mexico campus. Frequently, research for dissertation may be done in the Laboratory with some of the world's finest facilities and equipment.

College graduates in engineering and science who want fascinating research assignments while continuing their advanced education may write to:

Director of
Personnel
Division 59-101

los alamos
scientific laboratory
OF THE UNIVERSITY OF CALIFORNIA
LOS ALAMOS, NEW MEXICO

SOUTHWEST
"Monoball"®
SELF-ALIGNING BEARINGS

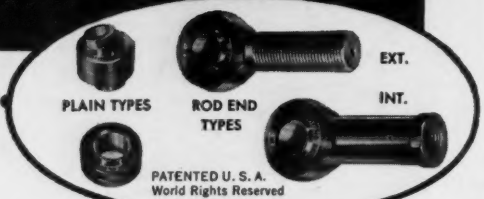

CHARACTERISTICS

	ANALYSIS	RECOMMENDED USE
1	Stainless Steel Ball and Race	For types operating under high temperature (800-1200 degrees F.).
2	Chrome Alloy Steel Ball and Race	For types operating under high radial ultimate loads (3000-893,000 lbs.).
3	Bronze Race and Chrome Steel Ball	For types operating under normal loads with minimum friction requirements.

Thousands in use. Backed by years of service life. Wide variety of Plain Types in bore sizes 3/16" to 6" Dia. Rod end types in similar size range with externally or internally threaded shanks. Our Engineers welcome an opportunity of studying individual requirements and prescribing a type or types which will serve under your demanding conditions. Southwest can design special types to fit individual specifications. As a result of thorough study of different operating conditions, various steel alloys have been used to meet specific needs. Write for Engineering Manual No. 551. Address Dept. ARS-59.

SOUTHWEST PRODUCTS CO.
1705 SO. MOUNTAIN AVE., MONROVIA, CALIFORNIA

RESEARCH ENGINEERS

IF YOU—

1. are experienced and interested in dynamic analysis and vibration engineering,
2. have M.S. or Ph.D. degree or equivalent in specific experience, and have United States citizenship,
3. desire to apply your knowledge to a wide variety of technically significant industrial and government problems,
4. would enjoy a permanent staff position ensured by multiple sponsorship,
5. would appreciate the opportunity to proceed with your graduate studies on a convenient basis while functioning as a full-time staff member,
6. enjoy working in communications and close professional contact with men from other scientific and engineering fields,
7. would like to join the staff of one of the largest independent research organizations in the world,

please contact:

E. P. Bloch

ARMOUR RESEARCH FOUNDATION
of Illinois Institute of Technology
10 West 35th Street
Chicago 16, Illinois

Index to Advertisers

AEROJET GENERAL CORP. ..... Back Cover
D'Arcy Advertising Co., Los Angeles, Calif.

AERONUTRONIC SYSTEMS, INC. 885
Honig-Cooper, Harrington & Miner, Los Angeles, Calif.

ALLIED CHEMICAL CORP., NITROGEN DIV. ..... 2nd Cover
G. M. Basford Co., New York, N. Y.

ARMOUR RESEARCH FOUNDATION OF ILLINOIS INSTITUTE OF TECHNOLOGY 892

BELL AIRCRAFT CORP. 890
The Rumrill Co., Inc., Buffalo, N. Y.

CHANCE VOUGHT AIRCRAFT, INC. 890
Tracy-Locke Co., Inc., Dallas, Texas

E. I. DUPONT DE NEMOURS & CO., INC. 883
N. W. Ayer & Son, Inc., Philadelphia, Pa.

EXCELCO DEVELOPMENT, INC. 815
Melvin F. Hall Advertising, Inc., Buffalo, N. Y.

GENERAL ELECTRIC CO., DEFENSE SYSTEMS DEPT. 887
Deutsch & Shea, Inc., New York, N. Y.

INTERNATIONAL BUSINESS MACHINES CORP. 880, 881
Benton & Bowles, Inc., New York, N. Y.

LOCKHEED AIRCRAFT CORP. 816, 817
Foote, Cone & Belding, Los Angeles, Calif.

LOS ALAMOS SCIENTIFIC LABORATORY 891
Ward Hicks Advertising, Albuquerque, N. Mex.

NORTH AMERICAN PHILIPS CO., INC. 879
Anders Associates, New York, N. Y.

RAMO-WOOLDRIDGE, A DIV. OF THOMPSON RAMO WOOLDRIDGE INC. 877
The McCarty Co., Los Angeles, Calif.

REPUBLIC AVIATION CORP. 813
Deutsch & Shea, Inc., New York, N. Y.

ROCKETDYNE, A DIV. OF NORTH AMERICAN AVIATION, INC. 889
Batten, Barton, Durstine & Osborn, Inc., Los Angeles, Calif.

SOUTHWEST PRODUCTS CO. 892
O. K. Fagan Advertising Agency, Los Angeles, Calif.

SPACE TECHNOLOGY LABORATORIES, INC. 818
Gaynor & Ducas, Inc., Beverly Hills, Calif.

WYMAN GORDON CO. ..... 3rd Cover
The Davis Press, Inc., Worcester, Mass